Biochemical and mass spectrometric analysis of interactions in *Drosophila* mRNA localization

Dissertation

der Mathematisch-Naturwissenschaftlichen Fakultät

der Eberhard Karls Universität Tübingen

zur Erlangung des Grades eines

Doktors der Naturwissenschaften

(Dr. rer. nat.)

vorgelegt von

Prashali Bansal

aus Meerut, Indien

Tübingen

2018

TABLE OF CONTENTS

List of Abbreviations

APS	Ammonium persulfate
BLRP	Biotin ligase recognition peptide
BSA	Bovine serum albumin
CCR4	C-C chemokine receptor type 4
cDNA	complementary DNA
co-IP	co-immunoprecipitation
CRISPR	Clustered regularly interspaced short palindromic repeats
C-terminus	carboxyl-terminus
dATP	2'-deoxy-adenosine triphosphate
dCTP	2'-deoxy-cytosine triphosphate
dd	double distilled
dGTP	2'-deoxy-guanosine triphosphate
DIG	Digoxigenin
DMSO	Dimethylsulfoxide
DNA	Deoxyribonucleic acid
DNase	Deoxyribonuclease
dNTP	2'-deoxy-nucleoside triphosphate
ds	double stranded
DTT	Dithiothreitol
dTTP	deoxythymidine triphosphate
EDTA	Ethylene diamine tetraacetic acid
EGFP	Enhanced green fluorescent protein
eIF	Eukaryotic translation initiation factor
FBS	Fetal bovine serum
FDR	False discovery rate
g	gravitational force
GFP	Green fluorescent protein
GST	Glutathione S-transferase
HEK	Human embryonic kidney
His	Hexahistidine
hnRNP	heterogeneous nuclear Ribonucleoprotein
HPLC	High performance liquid chromatography
IgG	Immunoglobulin G
IP	Immunoprecipitation
kb	kilobase
kDa	kiloDalton
LB	Luria-Bertani broth
LC	Liquid chromatography
M	Molar concentration
m/z	Mass-to-charge ratio
m^7G	7-methyl-guanosine
MBP	Maltose binding protein
MCP	MS2 coat protein

miRNA	microRNA
ml	millilitre
mm	micrometer
mM	millimolar
MOPS	3-(N-morpholino) propanesulfonic acid
mRNA	messenger RNA
mRNP	messenger ribonucleoprotein
MS	Mass spectrometry
MW	Molecular weight
NAD	Nicotinamide adenine dinucleotide
ncRNA	non-coding RNA
ng	nanogram
NMD	Nonsense-mediated decay
NOT	Negative regulator of transcription
NP-40	Nonidet P-40
N-terminus	amino-terminus
ºC	degree Celsius
ORF	Open reading frame
PAGE	Polyacrylamide gel electrophoresis
PAN	PolyA nuclease
PBS	Phosphate-buffered saline
PCR	Polymerase chain reaction
PEG	Polyethylene glycol
PFA	Paraformaldehyde
piRNA	PIWI-interacting RNA
PIWI	P element-induced wimpy testis
poly(A)	poly-adenylate
RBP	RNA-binding protein
RISC	RNA-induced silencing complex
RNA	Ribonucleic acid
RNAi	RNA interference
RNase	Ribonuclease
rpm	rotations per minute
RT	Room temperature
RT-PCR	Reverse transcription polymerase chain reaction reaction
S	Svedberg unit
SDS	Sodium dodecyl sulfate
sGFP	superfold green fluorescent protein
SILAC	Stable isotope labeling by amino acids in cell culture
SL	Stem-loops
snRNAs	small nuclear RNAs
snRNP	small nuclear ribonucleoprotein
ss	single stranded
TAE	Tris/acetic acid/EDTA
TAP	Tandem affinity purification
Taq	*Thermus acquaticus*
TB	Terrific broth

TBE	Tris/boric acid/EDTA
td	tandem
TEMED	N,N,N,N-tetramethyl-methane-1,2-diamine
TEV	Tobacco etch virus
Tm	annealing temperature
Tris	2-Amino-2-hydroxymethyl-propane-1,3-diol
tRNA	transfer RNA
U	enzyme activity unit
UTR	Untranslated region
UV	Ultraviolet
V	Volt
YFP	Yellow fluorescent protein
μg	microgram
μl	microlitre

Summary

mRNA localization is a common mechanism of gene regulation, studied across various cell types in numerous organisms. The subcellular targeting of mRNAs is involved in a broad range of biological processes including embryonic patterning, asymmetric cell division and cell migration. To study the underlying principles of mRNA localization, *Drosophila melanogaster* is an excellent model, as many RNAs display a localized pattern both in the oocyte and in the early embryo. In *Drosophila*, asymmetric deposition of maternal *oskar (osk), nanos* and *bicoid* mRNAs defines the antero-posterior polarity, while deposition of *gurken* mRNA plays an essential role in dorso-ventral axis specification. This differential targeting of mRNAs in a defined spatio-temporal manner requires several *trans*-acting factors which assemble with the mRNA into messenger ribonucleoprotein particles (mRNPs). Many *trans*-acting factors are RNA-binding proteins (RBPs) that recognize specific *cis*-acting elements in the RNA, and often function both in the localization and translational regulation of the transcript.

The heterogeneity of mRNPs poses a challenge to a comprehensive understanding of the underlying mechanism of mRNA regulation. Although individual RBPs have been identified and extensively studied for their role in mRNA localization, less is known about their interaction network. Often the same RBPs bind to differentially localized transcripts and it is unclear how transcript specificity and differential targeting is achieved. A possibility is that while these RBPs form the core of the mRNP, a higher level of transcript-specific regulation comes from the regulatory partners that interact directly with them.

To gain further insights into the functional components of an mRNP and possibly understand the regulation of RBPs, in my PhD project, I performed co-purification studies of both a localizing mRNP and the RBPs associated with localizing transcripts in *Drosophila*. In the first part of the project, using a TAP (Tandem Affinity Purification) tagging approach, I established a protocol to biochemically purify *osk* mRNP. In this method, both the RNA and a known *trans*-acting factor of *osk* mRNP were tagged in parallel. To capture a transcript-specific complex, I generated transgenic fly lines expressing *osk* mRNA tagged with binding sites for the MS2 phage coat protein. Insertion of *MS2* aptamers did not affect *osk* localization as the tagged transcript was able to localize in an endogenous *osk* null background. By adding recombinant MS2 coat protein, I could successfully purify tagged *osk in vitro*. However, *in vivo osk* mRNP purification from isolated egg *chambers* will require further optimization.

In the second part of the project, I immunoprecipitated six tagged RBPs (eIF4AIII, Glorund, Hrp48, Nanos, Staufen and Vasa) that are known to regulate localization of one or more

maternal mRNAs at different developmental stages. As the starting material, I used egg chambers expressing sGFP-tagged RBPs at their endogenous levels. This ensures that the stoichiometry and structure of protein complexes are maintained close to the physiological state. I used co-purification conditions designed to preserve direct protein-protein interactions. By employing mass spectrometry (both labeled and label-free methods) and subsequent statistical analysis, I identified proteins significantly enriched with each tagged RBP and constructed an interactome. All the six RBP-associated proteomes are mostly independent, consistent with the spatial and temporal distribution of the target transcripts, but also showed some overlap. Interestingly, components of both translational and decay machinery co-purified with baits that have known functions in translational regulation of maternal mRNAs. Functional analysis using bioinformatics annotation tools further showed that the selected RBPs are involved in a broad range of events, such as RNA processing, mRNA splicing and regulation of cell cycle, in addition to their role in mRNA localization and translation during *Drosophila* development. By using co-immunoprecipitation assay in cultured HEK cells, I was able to validate several interactions identified in the mass spectrometric data. By transiently expressing tagged proteins, I found 26 novel interactions of potential RBP regulators, including several uncharacterized factors.

This work presents the foundation for *in vivo* functional and co-localization studies, as well as *in vitro* structural characterization of the identified interactants, to fully understand the relevance of these interactions in the regulation of mRNA localization.

Zusammenfassung

mRNA-Lokalisation ist ein weit verbreiteter Mechanismus der Genregulation, welcher in verschiedenen Zelltypen in vielen Organismen untersucht wird. Die Lokalisierung der mRNAs innerhalb der Zelle ist an einer Reihe biologischer Prozesse beteiligt, unter anderem an der embryonalen Musterbildung, der asymmetrischen Zellteilung und der Zellmigration. *Drosophila melanogaster* ist ein hervorragender Modellorganismus, mit dessen Hilfe sich die grundlegenden Prinzipien der mRNA Lokalisation untersuchen lassen, da viele mRNAs sowohl in der Oozyte als auch im frühen Embryo ein Lokalisierungsmuster aufweisen. In *Drosophila* bestimmt die asymmetrische Verteilung der maternalen mRNAs *oskar (osk)*, *nanos* und *bicoid* die anterior-posteriore Polarität, wohingegen die *gurken* mRNA bei der Festlegung der dorso-ventralen Achse eine essentielle Rolle spielt. Diese differenzierte Lokalisation von mRNAs in einer räumlich und zeitlich definierten Weise benötigt verschiedene Faktoren, welche die mRNA in Messengerribonucleoprotein-Partikel (mRNPs) zusammenfügen. Viele dieser Faktoren sind RNA-bindende Proteine (RBPs), welche spezifische *cis*-wirkende Elemente in der RNA erkennen und häufig eine Funktion sowohl in der Lokalisation als auch in der translationalen Regulation des Transkripts haben.

Die Heterogenität der mRNPs stellt eine Herausforderung für ein umfassendes Verständnis der zugrundeliegenden Mechanismen der mRNA Regulation dar. Obwohl einzelne RBPs identifiziert wurden und deren Rolle innerhalb der mRNA Lokalisation ausführlich untersucht wurde, ist nur wenig über deren Interaktionsnetzwerk bekannt. Darüber hinaus ist unklar, wie eine Spezifität für ein Transkript und eine unterschiedliche Lokalisation erreicht wird, da von einigen RBPs bekannt ist, dass sie für die Lokalisation von mehr als einer mRNA notwendig sind. Eine mögliche Erklärung ist, dass während diese RBPs den Kern des mRNP bilden, Regulationspartner, die direkt mit den RBPs interagieren, eine höhere Ordnung an transkriptspezifischer Regulation ermöglichen.

Um weitere Einblicke in die funktionellen Komponenten der mRNPs zu erhalten und möglicherweise die Regulation von RBPs zu verstehen, habe ich während meiner Doktorarbeit Ko-Reinigungs-Experimente sowohl mit einem lokalisiertem mRNP, als auch den RBPs, welche mit der Lokalisation von Transkripten in *Drosophila* assoziiert sind, durchgeführt. Im ersten Teil des Projekts habe ich unter Nutzung eines TAP-tagging Ansatzes (engl.: Tandem Affinity Purification, gekoppelte Affinitätsreinigung) ein Protokoll zur biochemischen Reinigung eines lokalisierten mRNP etabliert. Bei dieser Methode wurden sowohl die RNA, als auch ein bekannter *trans*-wirkender Faktor eines mRNP parallel mit einem Tag versehen. Um einen transkriptspezifischen Komplex aufzureinigen habe ich transgene Fliegenlinien generiert, welche *osk* mRNA mit einem Tag , der die Bindestelle für

das MS2 Phagenhüllen-Protein enthält, exprimieren. Das Einfügen der *MS2*-Aptamere hatte keinen Einfluss auf die Lokalisation von *osk*, da das getaggte Transkript in Hintergrund eines endogenen *osk* Nullallels korrekt lokalisieren konnte. Durch Zugabe von rekombinantem MS2 Phagenhüllen-Protein konnte ich erfolgreich getaggtes *osk in vitro* reinigen, allerdings mit geringer Effizienz und Spezifität. Des Weiteren benötigt die Reinigung des mRNP *in vivo* aus isolierten Einährkammern weitere Optimierung.

Im zweiten Teil des Projekts habe ich sechs getaggte RBPs (eIF4AIII, Glorund, Hrp48, Nanos, Staufen und Vasa), die die Lokalisation von einer oder mehreren maternalen mRNAs in verschiedenen Entwicklungsstadien regulieren, immunopräzipitiert. Zu diesem Zweck habe ich Fliegenlinien verwendet, welche sGFP-getaggte RBPs exprimierten. Diese getaggten Proteine werden auf ihren endogenen Leveln exprimiert um eine nahezu physiologische Stöchiometrie und Struktur der Proteinkomplexe zu erhalten. Darüber hinaus wurden Aufreinigungsbedingungen verwendet, die direkte Protein-Protein-Interaktionen erhalten. Mit Hilfe von Massenspektrometrie (sowohl markiert als auch markierungsfrei) und darauffolgender statistischer Analyse identifizierte ich für jedes getaggte RBP Proteine welche signifikant angereichert wurden und konstruierte ein Interaktom. Alle sechs RBP-assoziierten Interaktome sind größtenteils unabhängig voneinander. Dies ist im Einklang mit der räumlichen und zeitlichen Verteilung ihrer Zieltranskripte. Interessanterweise konnte ich mehrere Proteine identifiziert, die mit mehreren Zielproteinen assoziiert waren. Komponenten der Translations- und der Abbaumaschinerie konnten mit RBPs mit bekannter Funktion in der translationalen Regulation mütterlicher mRNAs aufgereinigt werden. Eine funktionelle Analyse mit Hilfe bioinformatischer Annotationswerkzeuge konnte darüber hinaus zeigen, dass die untersuchten RBPs an vielen verschiedenen Prozessen wie der RNA-Prozessierung, mRNA-Splicing und der Regulation des Zellzyklus zusätzlich zu ihrem Beitrag in der mRNA-Lokalisation und -Translation während der *Drosophila*-Entwicklung beteiligt sind.

Um die Interaktionen, welche mit Hilfe der Daten aus der Massenspektrometrie identifiziert wurden, zu validieren, habe ich einen Coimmunopräzipitationsassay in kultivierten HEK Zellen genutzt. Indem ich die getaggten Proteine transient exprimiert habe, konnte ich sechsundzwanzig neue Interaktionen potentieller RBP-Regulatoren verifizieren, darunter einige bisher nicht charakterisierte Proteine.

Zusammengefasst stellt diese Arbeit die Grundlage für funktionelle *in vivo* und Kolokalisationsstudien und für die strukturelle *in vitro* Charakterisierung der identifizierten Interaktionspartner dar um die Relevanz dieser Interaktionen bei der Regulation der mRNA-Lokalisation vollkommen zu verstehen.

1. Introduction

1.1 Regulation of gene expression

The control of gene expression is a fundamental biological process in all organisms, as every aspect of cellular function is regulated by a set of genes and their products expressed in a given cell. As explained by the Central Dogma (Crick, 1958), the information for these gene products is carried in the DNA, which is copied to make a RNA molecule and the information in RNA is then decoded by the ribosomes to build proteins. Thus, when and how much a protein is to be made is regulated at multiple steps starting with transcription, RNA processing and transport, translation, RNA and protein modification and degradation (Fig. 1). All the steps are remarkably interconnected and interdependent, not only temporally but also spatially.

As the first step of information transfer, transcription is subjected to a tight control, which is mediated by Transcription Factors (TFs) that bind to *cis*-regulatory elements in the DNA, along with the proteins that modulate their activity. In cells, an additional level of complexity is added by the packaging of DNA into chromatin and epigenetic modifications, thereby regulating patterns of gene expression. Subcellular compartmentalization in eukaryotes separates transcription from translation, allowing regulation at multiple levels. In eukaryotes, a key control is exerted at the post-transcriptional level which ultimately regulates the expression of a considerable fraction of the transcriptome.
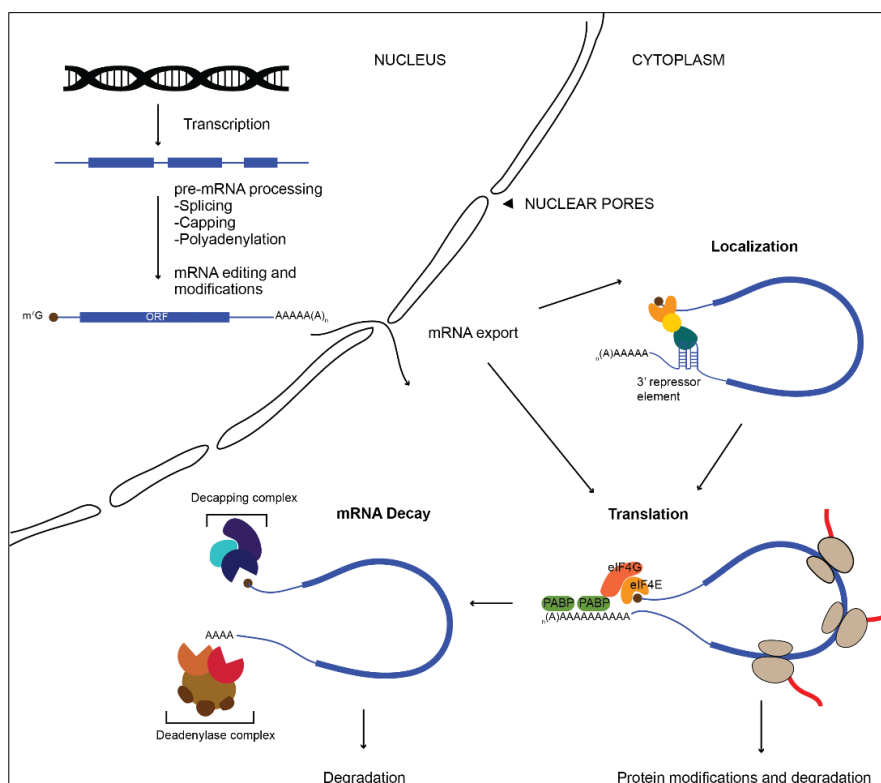
Fig. 1. Central steps of mRNA metabolism in eukaryotes

mRNAs are synthesized in the nucleus through transcription. Co-transcriptionally (shown as a second step for clarity), the mRNA is modified at both 5' and 3' ends, and the introns are removed by splicing. The processed mRNA is exported out of the nucleus through nuclear pores, and is translated in the cytoplasm. Translation involves initiation, elongation and termination, and at each step, the mRNA associates with a number of factors in addition to the ribosomes. Alternatively, the mRNA can be localized (in a translationally repressed state), prior to translation. At the end of its lifecycle, mRNA is degraded with the aid of decapping and deadenylase complexes.

1.2 Post-transcriptional control via pre-mRNA processing

Frequently, co-transcriptional capping, splicing and cleavage/polyadenylation are the key pre-mRNA processing events that regulate the fate of the mRNA (Maniatis and Reed 2002; Proudfoot 2003). While 5' m^7G cap and 3' poly(A) tail (mostly 150-250 nucleotides long; Darnell et al, 1971; Subtelny et al., 2014; Chang et al., 2014) additions remain the key modifications, several other internal modifications, most notably m^6A, have been identified (reviewed in Li and Mason, 2014; Roundtree et al., 2017). These modifications not only regulate mRNA metabolism but have also been found to be instrumental in regulating splicing, export, small RNA processing, translation and decay by various mechanisms (reviewed in Karijolich et al., 2010; Covelo-Molares et al., 2018).

1.2.1 Pre-mRNA splicing

A critical step in the processing of pre-mRNA is splicing, which involves precise removal of the interdispersed non-coding introns to make the correct message for translation. Through alternative splicing (AS), this mechanism also serves as a major contributor of proteome diversity by expanding the coding capacity of the genome and controlling tissue- and development-specific expression of splicing isoforms. Splicing is mediated by highly conserved large ribonucleoprotein complexes known as spliceosomes, which contain five major snRNAs (small nuclear RNAs) along with several associated proteins to form snRNPs (small nuclear ribonucleoproteins). While the Sm proteins interact with the snRNAs through specific site elements to form the snRNP core structure (Raker et al., 1996), several other proteins, mainly DExD/H-box RNA-dependent ATPases/helicases are required for distinct steps of spliceosome formation, activation, catalysis and disassembly (reviewed by Chen and Cheng, 2012). On the mRNA, *cis*-acting auxiliary sequences which act as a binding platform for non-snRNP regulatory proteins, mainly SR proteins (exonic splicing enhancers) and hnRNP family of proteins (exonic splicing silencers), facilitate molecular rearrangements during assembly and alter the splice site recognition leading to AS (reviewed by House and Lynch, 2008; Lee and Rio, 2015). Apart from their role in constitutive splicing, DExD/H

proteins have also been implicated in the regulation of AS (Hönig et al., 2002; Park et al., 2004).

Several processes that regulate AS have been well-studied, including epigenetic processes, promoter architecture, RNA secondary structures, non-coding RNAs (ncRNAs) and post-translational modifications (Buratti and Baralle, 2004; Susannah et al., 2010; Luco and Misteli, 2011; McManus and Graveley, 2011; Lev Maor et al., 2015; Ramanouskaya and Grinev, 2017; Romero-Barrios et al., 2018; Dvinge, 2018). Additionally, AS-coupled Nonsense-Mediated Decay (AS-NMD) has been shown to regulate expression levels of both core spliceosomal components and AS regulatory factors, establishing a link between mRNA processing and mRNA decay. (Sureau et al., 2001; Wollerton et al., 2004; Hase et al., 2006; Lareau et al., 2007a; Lareau et al., 2007b; Saltzman et al., 2008). Splicing has also been shown to be closely linked to transcription and post-transcriptional gene regulatory processes, including 5' capping and 3' cleavage/polyadenylation, mRNA transport; microRNA (miRNA) biogenesis and RNA degradation (Montes at al., 2012; Cordin and Beggs, 2013; Agranat-Tamir et al., 2014; Wang et al., 2015b), suggesting pre-mRNA splicing as a major regulator of gene expression.

Exon Junction Complex (EJC)

The EJC plays a central role in linking nuclear splicing to post-transcriptional events such as mRNA export, localization, quality control (NMD) and translation. The EJC is a multiprotein complex consisting of 4 core proteins-eIF4AIII (the main RNA-binding platform), the heterodimer Magoh-Y14, Barentz-and several other peripherally associated factors (reviewed in Woodward et al., 2017; Gerbracht and Gehring, 2018). During splicing, EJC proteins eIF4AIII and Mago-Y14 are recruited to the activated spliceosome through eIF4AIII interaction with CWC22 (Alexandrov et al., 2012; Barbosa et al., 2012; Steckelberg et al., 2012). Upon exon ligation and release, eIF4AIII dissociates from CWC22 by an unknown mechanism, enabling it to bind to the mRNA in the presence of ATP (Ballut et al., 2005; Andersen et al., 2006; Bono et al., 2006). Conformational changes caused by eIF4AIII binding to RNA and ATP leads to stable deposition of EJC proteins on the nascent transcripts, 20-24 nucleotides upstream of spliced exon-exon junctions, in a sequence-independent manner (Le Hir et al., 2000; Ballut et al., 2005; Bono et al., 2006; Andersen et al., 2006; Nielsen et al., 2009). Following splicing, Barentz associates with the complex (either in the nucleus or the cytoplasm) and the EJC-loaded mRNA is exported to the cytoplasm, where it serves as a binding platform to several other downstream effectors (Le Hir et al., 2001; Bono et al., 2004; Diem at al., 2007; Gehring et al., 2009; reviewed in Woodward et al., 2017).

In the cytoplasm, the EJC is believed to be removed by translocating ribosomes in the pioneer round of translation and the core proteins are reimported to the nucleus to re-enter the cycle (Dostie and Dreyfuss 2002; Lejeune et al., 2002). In *Drosophila,* deposition of EJC proteins eIF4AIII, Mago and Y14 on nascent transcripts of genes on polytene chromosomes could be independent from the presence of introns or splicing factor CWC22 (Choudhury et al., 2016). Moreover, in *Drosophila*, Mago-Y14 can associate with the transcripts independently of eIF4AIII and eIF4AIII persistently associates with actively translated mRNAs (Choudhury et al., 2016), thus indicating a new role of EJC proteins, independent of splicing and EJC assembly. In mammals, the EJC also plays a crucial role in NMD and has been discussed in detail, later in the chapter.

Contrary to a sequence-independent ubiquitous model of EJC distribution, it has been observed that EJC associates with only a subset of spliced junctions and is not solely present at canonical positions (Saulière et al., 2010, 2012; Mühlemann, 2012; Singh et al., 2012). EJC loading on exon junctions can also vary within the same transcript and the function of EJC can differ from one splice site to another, as observed for localization of *oskar* (*osk*) mRNA in *Drosophila* (Hachet and Ephrussi, 2004; Ghosh et al., 2012; Simon et al., 2015). The EJC was also found to be dispensable for NMD in *Drosophila* (Gatfield et al., 2003; Saulière et al., 2010). Furthermore, EJC loading can also serve as a splicing modulator of neighboring introns in *Drosophila*, though only for a subset of transcripts (Roignant and Treisman, 2010; Ashton-Beaucage et al., 2010; Malone et al., 2014; Hayashi et al., 2014). Together these observations suggest that EJC assembly is not an obligatory consequence of splicing, but is rather a differential and regulated process with widespread implications in gene regulation.

1.3 Post-transcriptional control by mRNA decay

mRNA synthesis and mRNA decay are the two fundamental post-transcriptional mechanisms which dictate mRNA turnover. mRNA decay can significantly influence mRNA metabolism by altering the mRNP (messenger ribonucleoprotein) composition, as well as the translational status of the mRNA and ensures that only functional proteins are produced. Accumulating evidences suggest coupling of transcription to mRNA decay (Braun and Young, 2014; Das et al., 2017), as well as co-translational decay (reviewed in Heck and Wilusz, 2018), further stressing the key role of mRNA degradation in the regulation of gene expression.

RNA degradation is facilitated by ribonucleases (endonucleases, 3'-5' and 5'-3' exonucleases), which are often multifunctional, and their co-factors (helicases, polymerases, chaperons and small RNAs) which confer the specificity (reviewed in Houseley and Tollervey, 2009). Although initially exonucleases were thought to be the key players in eukaryotic RNA

decay, several novel endonucleases involved in both cytoplasmic and nuclear RNA degradation and surveillance have been discovered (reviewed in Tomecki and Dziembowski, 2010).

Although most transcripts are targeted for decay in the cytoplasm, errors in nuclear pre-mRNA processing and formation of export-competent mRNP can lead to degradation or retention in the nucleus, by nuclear exosomes (Lemieux et al., 2011; Perez-Ortin et al., 2013). In the cytoplasm, exoribonucleolytic cleavage is mainly triggered by deadenylation (removal of poly(A) tail), often followed by decapping (removal of cap structure) (Fig. 2; Coutett et al., 1997; Yamashita et al., 2005). Deadenylation, which is a reversible process, and thought to be biphasic, is initiated by the PAN2-PAN3 complex. After initial trimming of poly(A) tail by PAN2-PAN3, the remaining bulk is deadenylated by the CCR4-NOT complex (Fig. 2A; Tucker et al., 2001; Yamashita et al., 2005; Bonisch et al., 2007). The CCR4-NOT deadenylase complex consists of NOT1, which acts as a scaffold protein for docking of conserved core subunits, CCR4, CAF1/POP2, CAF40, NOT2 and NOT3/5. Additional complex subunits include: NOT4; NOT10 and NOT11 in humans and flies; TAB182 in mammals and CAF130
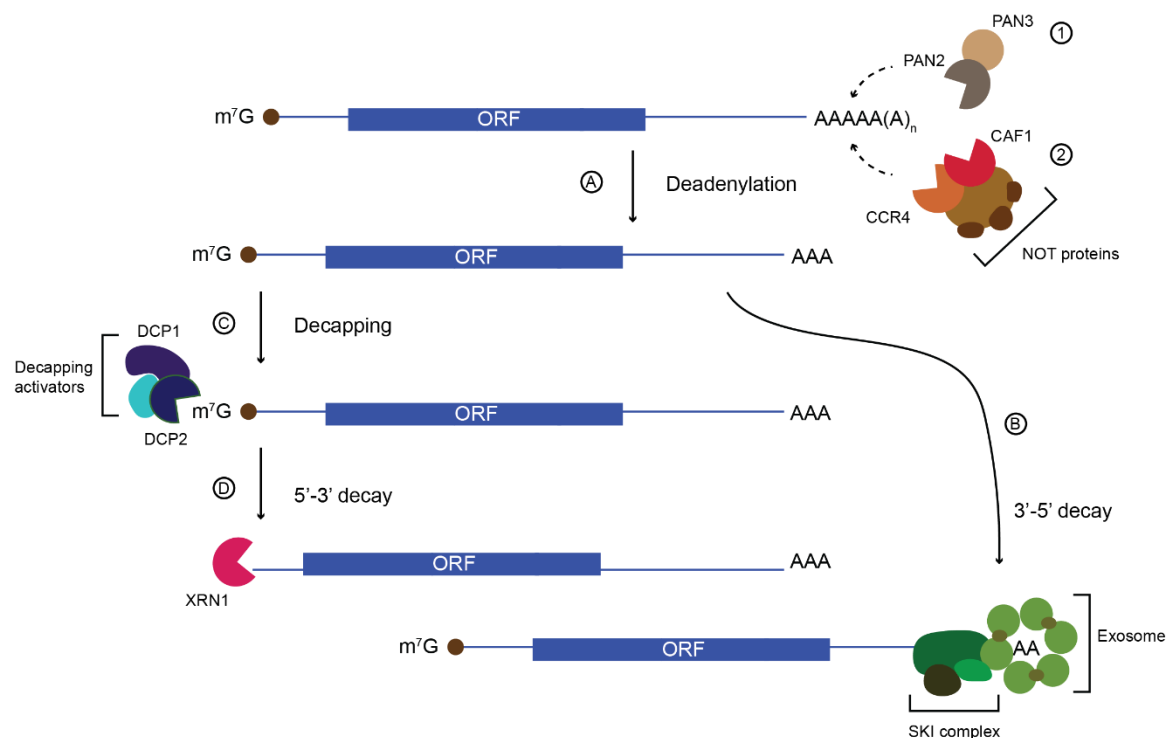
Fig. 2. General mRNA decay pathways

Bulk mRNA decay is initiated by deadenylation (A). Initial trimming of poly(A) tail by PAN2-PAN3 complex is followed by CCR4-NOT complex-mediated deadenylation. Following deadenylation, mRNAs can be degraded by 3'-5' exonucleolytic digestion catalyzed by exosome and the SKI complex

(B), or undergo decapping mediated by the DCP1-DCP2 complex (C) and subsequent degradation by 5' to 3' exonuclease XRN1 (D). Adapted from Eulalio et al. (2007a).

in yeast (reviewed in Collart and Panasenko, 2012; Collart, 2016). In addition to PAN2, CCR4 and CAF1, other deadenylases such as PARN, Nocturnin and ANGEL1/2 also regulate the poly(A) tail length in eukaryotes (reviewed in Labno et al., 2016). Several examples of translation termination-dependent deadenylation have been reported in both yeast and mammalian systems, linking mRNA translation to decay (Hosoda et al., 2003; Funakoshi et al, 2007; Jolles et al., 2018). It has been proposed that in mammals, dissociation of eukaryotic termination factor 3 (eRF3) from poly(A)-binding protein (PABP) triggers deadenylation, as the two deadenylase complexes can then bind to PABP, leading to their activation (Funakoshi et al., 2007).

After deadenylation, mRNAs can be degraded by 3'-5' exonucleolytic activity of cytoplasmic exosomes, followed by cap hydrolysis by the DcpS scavenger decapping enzyme (Fig. 2B; reviewed in Tucker and Parker, 2000; Wilusz et al., 2001). Often, deadenylation is followed by decapping by the DCP1-DCP2 complex of enzymes (along with associated factors) and subsequent degradation by 5'-3' exonucleolytic activity of XRN1 (Fig. 2C, 2D; Muhlrad et al., 1994; Tritschler et al., 2009; reviewed in Ling et al., 2011; Braun et al., 2012). A recent study in *S. cerevisiae* has shown that the NOT proteins (NOT2, NOT3, and NOT5) promote mRNA decapping by recruiting decapping factors. Moreover, NOT3 and NOT5 were shown to bind to decapping activator protein PAT1 (Alhusaini and Coller, 2016), further coupling deadenylation with decapping. Deadenylation-independent degradation via direct decapping (reported in *S. cerevisiae* by Muhlrad and Parker, 1994; Badis et al., 2004; Muhlrad and Parker, 2005) or endonucleolytic cleavage followed by degradation of the resulting fragments by XRN1 and/or exosomes has also been reported (reviewed in Garneau et al., 2007; Schoenberg, 2011).

Similar to deadenylation, uridylation, oligoadenylation and CUCU-addition at the mRNAs 3'end, have also been shown to activate degradation pathways (via the same downstream mechanisms as deadenylation) (reviewed in Labno et al., 2016).

1.3.1 Regulation of mRNA decay by *cis*-acting elements and their binding proteins

RNA-binding proteins (RBPs) and their binding to *cis*-acting elements present in the 3' untranslated region (UTR) have been widely known to influence mRNA stability and to regulate mRNA decay. Cytoplasmic polyadenylation elements (CPE), GU-rich sequences (GREs), AU- rich sequences (AREs) and miRNA target sites, are well-studied examples of such *cis*-acting elements (reviewed in Wu and Brewer, 2012; Schoenberg and Maquat,

2012). Among these, AREs represent the best-studied group of *cis*-acting elements located in the 3' UTRs of many short-lived RNAs, regulating the expression of proteins involved in cell growth regulation or response of an organism to external factors, in a ARE-dependent mechanism termed as AMD (ARE-Mediated Decay) (Barreau et al., 2005; Bakheet et al., 2006; Spasic et al., 2012). Besides 3'UTRs, elements in 5' UTRs, open reading frames (ORF) and even promoters (modulated by transcription factor binding) can also regulate mRNA decay (reviewed in Perez-Ortin et al., 2013).

Among the *trans*-acting factors that bind to mRNA motifs and structures, several ARE-binding proteins (ARE-BPs) have been identified, which recruit decay machinery via interaction with one or more factors, including exosomes, PARN or CCR4 deadenylases or decapping enzymes (reviewed in Schoenberg and Maquat, 2012; Perez-Ortin et al., 2013; Garcia-Mauriño et al. 2017). While binding of ARE-BPs to AU-rich elements is one of the best characterized mechanisms of transcript-specific mRNA decay, several other examples have been discovered and studied in various model organisms. These include: Puf proteins in budding yeast and Pumilio, a Puf-related protein in *Drosophila*, that recognize UG-rich sequences and recruit CCR4-NOT deadenylase to trigger decay (Wreden et al., 1997; Wickens et al., 2002; Goldstrohm et al., 2006); Staufen-Mediated Decay (SMD) of target RNAs containing 3'UTR Staufen Binding Sites (SBS), via interaction with NMD factor Up-frameshift 1 (Upf1; Kim et al., 2005); CCR4-NOT-mediated decay of *Hsp83* transcript by *Drosophila* protein Smaug (Smg; Semotok et al., 2005); binding of mammalian protein Roquin to Constitutive Decay Element (CDE) in the 3'UTR of *TNF-α* mRNA, to promote its degradation by recruiting CCR4-NOT complex in macrophages (Leppek et al., 2013) and histone mRNA decay by Stem-Loop-Binding Protein (SLBP) that binds 3' stem-loop structure and recruits Upf1 for subsequent degradation (Kaygun and Marzluff, 2005). Recently, two novel regulatory motifs, preferentially found in 3' UTRs of many transcripts encoding regulatory proteins, recognized by hnRNPs A2/B1 and A1 were shown to trigger CCR4-NOT-mediated deadenylation (Geissler et al., 2016).

1.3.2 Regulation of mRNA decay by miRNAs

Small RNA target sites are another example of *cis*-acting elements that regulate mRNA decay. miRNAs are evolutionary conserved small ncRNAs, encoded in nearly all eukaryotic genomes and participating in the regulation of almost every cellular function. They are known to be major regulators of post-transcriptional gene expression by affecting both the translational state and the stability of the mRNA (reviewed in Bartel, 2004; Bushati and Cohen, 2007; Jonas and Izaurralde, 2015). Processed by endonucleases Dicer and Drosha, along with other associate proteins, miRNAs function together with Argonaute proteins (AGO) as components of RNP complexes, referred to as miRNA-induced silencing complexes

Box 1: Mechanism of translation initiation in eukaryotes

As the first step of translation, translation initiation is subjected to a very tight control and is rate-limiting. Initiation of translation of bulk mRNAs in eukaryotes is facilitated by binding of the small ribosomal unit (40s) loaded with Met-tRNAi (methionyl tRNA specialized for initiation) in a pre-initiation complex (PIC), comprising of eIF2, eIF3, eIF1, eIF1A and eIF5, to the capped 5'end of the mRNA and identification of the start codon (AUG), commonly through scanning. Recruitment of the PIC to the mRNA is assisted by PABP and the eIF4 group of factors, mainly by the assembly of the eIF4F complex (eIF4E, eIF4G and eIF4A), eIF4B and eIF4H. Through a series of conformational changes, finally, the ribosomal attachment is achieved by a chain of m^7G-eIF4E-eIF4G-eIF3-40S interactions. The scanning is facilitated by DEAD-box helicases such as eIF4A and Dhx29, with contribution from eIF1, eIF1A, eIF2, eIF3 and eIF5, eIF4G and eIF4B. eIF1 also plays a key role in AUG recognition. Identification of the start codon triggers the arrest of scanning and leads to joining of the large ribosomal subunit (60s). This requires the activities of eIF5 and eIF5B to dissociate eIF1, eIF1A, eIF3 and eIF2 and form the elongation-competent 80s ribosome. eIF2B further recycles eIF2 for the next round of initiation (the detailed mechanism has been reviewed in Jackson et al., 2010; Hinnebusch, 2014). The subsequent steps in protein synthesis: elongation, translocation, termination and release of polypeptide further require elongation factors and release factors, and are also highly regulated (reviewed in Mathews et al., 2007).

A distinct mode of translation initiation, first discovered in viral systems (Pelletier and Sonenberg, 1998; Jang et al., 1988), is the 5' cap-independent initiation. In this mechanism, the direct recruitment of PIC to the start codon is mediated by special sequences called IRESs (Internal Ribosome Entry Sites; reviewed in Vagner et al., 2001; Hellen and Sarnow, 2001; Komar and Hatzoglou, 2005). In addition to viruses, several cellular IRESs have been reported in the human genome, residing not only in the 5'UTRs but also in the coding regions and 3'UTRs of the transcripts (Cornelis et al., 2000; Coldwell et al., 2001; Candeias et al., 2006; Wellensiek et al., 2013; Du et al., 2013; Weingarten-Gabbay et al., 2016). IRESs-mediated initiation has been shown to promote translation under various physiological conditions, including apoptosis, hypoxia, cellular stress, mitosis and viral infections, allowing expression of specific proteins when cap-dependent translation is limiting (reviewed in Hellen and Sarnow, 2001; Spriggs et al., 2008). Additionally, cap-independent translation can also be facilitated by m^6A methylation of mRNAs (Meyer at al., 2015; Wang et al., 2015a; Coots et al., 2017). A new idea of Cap-Independent Translation Enhancers (CITEs) elements in mammalian mRNAs, has been proposed by Shatsky and colleagues (2018). These elements can be located in both 5' and 3' UTR of mRNAs and bind components of the translation machinery that recruit ribosomes to the mRNA.

(miRISCs). They bind to complementary sequences in the 3' UTRs of the target genes, mostly imperfectly, leading to post-transcriptional silencing (Fig. 3; Filipowicz et al., 2008; Bartel, 2009; Carthew and Sontheimer, 2009; Fabian and Sonenberg, 2012).
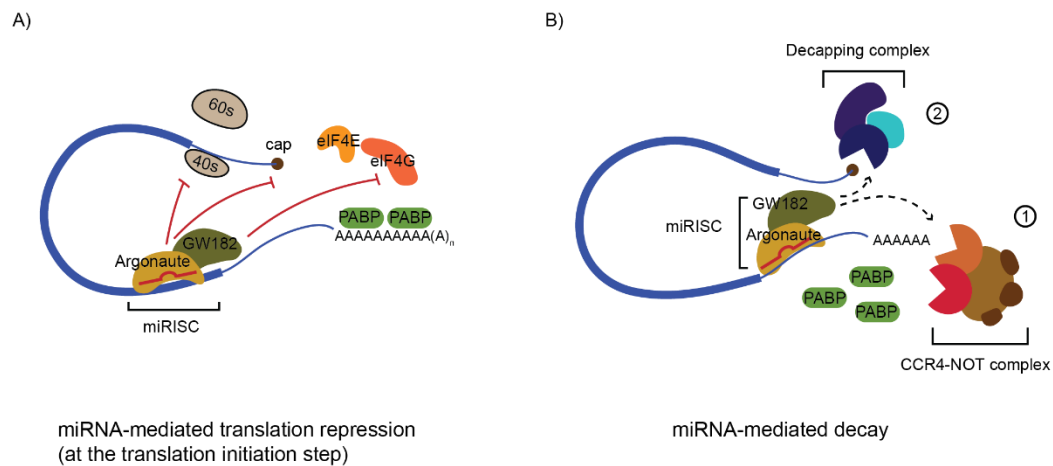
Fig. 3. Mechanisms of miRNA-mediated gene silencing

(A) Translational repression by inhibition of translation initiation. AGO proteins compete with the cap-binding protein eIF4E, for binding to the cap structure (brown dot) or prevent the joining of large ribosomal subunit with the small subunit, by recruiting eIF6. Alternatively, GW182 interferes with PABP-eIF4G interaction by binding with PABP, thus inhibiting the formation of mRNA closed-loop structure. Please note that miRNAs can also inhibit translation at post-initiation steps, not shown here (B) miRNA-mediated mRNA decay. GW182-mediated recruitment of deadenylases trigger deadenylation and subsequent decapping and degradation of the target mRNA. Adapted from Eulalio et al. (2008b).

In recent years, the GW182 protein has emerged as a central player in miRNA-mediated gene silencing. Besides directly interacting with AGO proteins, GW182 proteins facilitate silencing by recruiting deadenylases (PAN2-PAN3 and CCR4-NOT complex). In addition, they also interact with PABP to associate miRISCs to target RNAs or inhibit translation (reviewed in Fabian and Sonnenberg, 2012; Braun et al., 2012; Jonas and Izaurralde 2015). Association of AGO1 with GW182 has been shown to be essential and required in *Drosophila* for miRNA-mediated translational repression (Behm-Ansmant et al., 2006; Eulalio et al., 2008a). However, GW182 and CCR4-NOT-independent silencing mechanisms have also been reported, at least in *Drosophila* (Fukaya and Tomari 2011; 2012; Wu et al., 2013; Fukaya et al., 2014).

Studies have shown that miRNA-mediated translational repression precedes deadenylation and decapping (Fabian et al., 2009; Djuranovic et al., 2012; Bazzini et al., 2012; Béthune et al., 2012). However, contrasting studies have demonstrated that active translation or

translational repression is not a requirement for deadenylation (Mishima et al. 2006; Wu et al. 2006; Eulalio et al. 2009; Beilharz et al., 2009; Zekri et al., 2009) and at least in yeast, mRNAs can also be co-translationally deadenylated (Hu et al., 2009). Conversely, miRISCs can also repress translation in a deadenylation-independent manner (Wu et al., 2006; Eulalio et al., 2009; Braun et al., 2011; Chekulaeva et al., 2011; Fukaya and Tomari 2011, 2012; Mishima et al., 2012; Ricci et al., 2013; Zekri et al., 2013). Moreover, recruitment of CCR4-NOT complex has also been shown to trigger translational repression, independently from deadenylation (Cooke et al., 2010; Chekulaeva et al., 2011; Braun et al., 2011; Zekri et al., 2013). Together these observations suggest that translational repression and deadenylation are two independent mechanisms used by miRNAs to silence target mRNAs. However, they influence each other and can still be mechanistically linked, perhaps through the CCR4-NOT complex, which has been shown to interact with GW182, in both *Drosophila* and mammalian system (Braun et al., 2011; Chekulaeva et al., 2011; Fabian et al., 2011; Huntzinger et al., 2013; Chen et al., 2014). These observations also suggest a central role of CCR4-NOT complex as a conserved downstream effector of miRNA-mediated gene silencing, capable of eliciting both the effects of translational repression and deadenylation.

Other than recruiting deadenylases, miRISC can also promote decay by recruiting decapping factors directly (Nishihara et al., 2013; Makino et al., 2014; reviewed in Iwakawa and Tomari, 2015). Instead of immediate degradation, deadenylated and translationally repressed mRNAs may also be stored as such, depending on the cell type and/or target mRNA.

1.4 mRNA quality control

To further ensure that erroneous proteins are not produced, mRNA surveillance events occur on the ribosomes, modulating mRNA turnovers. Loss of these pathways leads to increased aggregation of proteins, further stressing their importance in modulating proteomes (Jamar et al., 2018). Three cytoplasmic surveillance pathways are best known to selectively target and degrade different classes of defective mRNAs: Nonsense-Mediated Decay or NMD (targets mRNAs with premature stop codon), Non-Stop Decay or NSD (targets mRNAs lacking a stop codon) and No-Go Decay or NGD (degradation of mRNAs with potential stall-inducing sequences). RNAs targeted via all three mechanisms are then subjected to endonucleolytic cleavage, followed by degradation by exosomes and/or XRN1, digestion of derived aberrant peptides by proteasomes and ribosome recycling (reviewed in Shoemaker and Green, 2012). However, in NMD, deadenylation-dependent and deadenylation-independent decapping pathways have also been reported in addition to endonucleolytic cleavage (Muhlrad and Parker, 1994; Mitchell and Tollervey, 2003; Lejeune et al., 2003; Cao and Parker, 2003; Chen and Shyu, 2003; Gatfield and Izaurralde, 2004; Couttet and Grange,

2004; Yamashita et al., 2005; Huntzinger et al., 2008; Eberle et al., 2009; Cho et al., 2013; Loh et al., 2013).

BOX 2: Regulation of mRNA decay in P-bodies

In eukaryotic cells, translationally repressed mRNAs can accumulate in cytoplasmic granules called Processing bodies (P-bodies) or GW bodies (reviewed in Parker and Sheth, 2007; Kulkarni et al., 2010; Decker and Parker, 2012). These are dynamic and reversible structures, containing pools of nontranslating mRNPs, formed as a consequence of deadenylation (Andrei et al., 2005; Kedersha et al., 2005; Zheng et al., 2008). Although the exact composition of P-bodies is unclear, they are enriched in factors involved in translational repression, deadenylation, decapping, 5'-3' decay machinery, NMD pathway (under certain conditions), AMD pathway, miRNA-mediated decay (in metazoans) and several other RBPs associated with mRNA translation/decay (Andersen and Kedersha, 2006; Parker and Sheth, 2007; Kulkarni et al., 2010; Standart and Weil, 2018). Translationally silenced mRNAs can be recruited to P-bodies either for storage, where they can re-enter translation or are destined for decay, thus allowing rapid adaptation of the transcriptome to the cell requirements (Cougot et al., 2004; Brengues et al., 2005; Bhattacharyya et al., 2006; Hubstenberger et al., 2017). However, recent studies in mammalian systems support their primary role in storage rather than decay (Stalder and Mühlemann, 2009; Hubstenberger et al., 2017; Standart and Weil, 2018). Interestingly, P-bodies are generally devoid of ribosomes, translation initiation factors (except eIF4E and eIF4E-T) and PABP, further supporting the fact that they are sites of repressed mRNPs (Brengues et al., 2005; Andrei et al., 2005; Teixeira et al., 2005; Ferraiuolo et al., 2005; Kedersha et al., 2005). Moreover, it has been shown that they are formed as a consequence, rather than the cause of translational repression, as disrupting P-bodies does not affect the pathways in which P-body components are involved, including mRNA decay, NMD and miRNA-mediated silencing (Pillai et al., 2005; Chu and Rana, 2006; Eulalio et al., 2007b).

In addition to P-bodies, several other functionally linked RNA granules: stress granules, germ cell granules and transport granules are known, that play important roles in post-transcriptional regulation (reviewed in Andersen and Kedersha, 2005; Eulalio et al., 2007a).

1.4.1 NMD

NMD is a conserved mRNA surveillance mechanism, which elicits rapid degradation of premature termination codon (PTC)-containing or abnormally 3'-extended transcripts (reviewed in Chang et al., 2007; Nicholson et al., 2010; Nicholson and Mühlemann, 2010). In addition, NMD also differentially targets unspliced pre-mRNAs, mRNAs resulting from an out-of-frame initiation codon, mRNAs with upstream open reading frames (uORFs), mRNAs subjected to frameshifting and products of alternative splicing, bicistronic mRNAs, transcripts of pseudogenes, transposable elements and unproductively rearranged genes (He et al., 1993, 2003; Morrison et al., 1997; Welch and Jacobson, 1999; Wang et al., 2002). NMD shares its regulators with translation, thereby coupling both processes.

First discovered in *S. cerevisiae*, Upf proteins (Upf1, Upf2, and Upf3) constitute the core NMD machinery (Culbertson et al., 1980; He et al., 1997; Lykke-Andersen et al,. 2000; Serin et al., 2001). In metazoans, additional NMD factors have been identified, which include the SMG group of proteins that determine the phosphorylation status of Upf1 (Page et al., 1999; Denning et al., 2001; Pal et al., 2001; Yamashita et al., 2001; Okada-Katsuhata et al., 2012). Although considerable information is available on the structure and interactions of NMD factors, the exact mechanism remains controversial and different models have been proposed for different organisms. According to the widely accepted "faux 3'UTR model" proposed in yeast and *C. elegans*, the key determinant of NMD activation is the competitive reaction between PABP and Upf1 for binding to release factor eRF3 on the terminating ribosomes, largely influenced by the length of 3'UTR (reviewed in Kervestin and Jacobson, 2012). In mammals, the proposed model involves splicing-dependent PTC recognition. In this case, EJC retained on an intron or an exon-exon junction and downstream of PTC serves as a signal for NMD (Fig. 4). In this model, ribosomal release factors recruit Upf1 and associated SMG1 complex (SMG1, SMG8, SMG9) to the terminating ribosomes to form the SURF complex. Upf1 and SMG1 complex subsequently form a complex with Upf2-Upf3 associated with EJC positioned downstream of the PTC. This induces the formation of the decay complex that activates ATPase and helicase activity of Upf1, via phosphorylation by SMG1. Phosphorylated Upf1 then interacts with SMG6 and/or SMG5-SMG7 triggering independent and redundant decay pathways (Fig. 4; reviewed in Kervestin and Jacobson, 2012). Although EJC-independent NMD has been reported not only in mammals, but also in other models (Zhang et al., 1998a; Rajavel and Neufeld, 2001; Gatfield et al., 2003; Delpy et al., 2004; LeBlanc and Beemon, 2004; Bühler et al., 2006; Matsuda et al., 2007; Longman et al., 2007; Eberle et al., 2008; Singh et al., 2008; Kerényi et al., 2008; Wen and Brogna, 2010), the presence of EJC has been shown to enhance NMD in human cells (Bühler et al., 2006; Singh et al., 2008; Metze et al., 2013). Therefore, degradation of NMD targets occurs

Nonsense-mediated decay via EJC
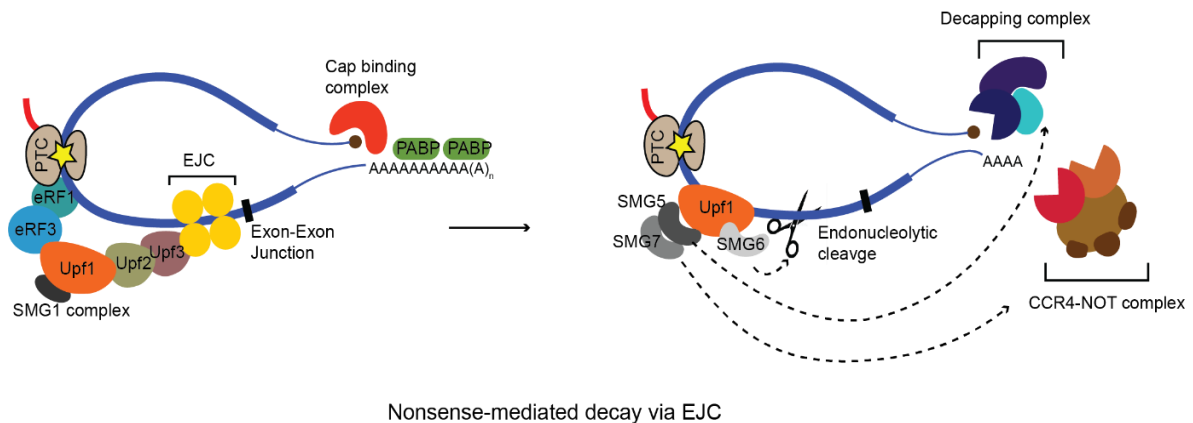
Fig. 4. Mechanism of EJC-mediated NMD

In case of a transcript carrying a premature termination codon (PTC), the EJC downstream of the PTC is not removed by the pioneer ribosomes. The eukaryotic release factors (eRF1 and eRF3) associated with the terminating ribosome are joined by additional factors to form the transient SURF complex, which includes Upf1 and the SMG1 complex. If the ribosome-SURF complex forms $\geq 50-55$ nucleotides upstream of an exon-exon junction that has a bound EJC, NMD is initiated. The Upf1-Upf2 interaction causes a conformational change leading to the activation of Upf1. Phosphorylation of Upf1 results in recruitment of the SMG6 endonuclease, while SMG5-SMG7 recruits the CCR4-NOT deadenylase complex, leading to decapping by the DCP1-DCP2 complex and subsequent degradation by general exoribonucleases. Adapted from Popp and Maquat (2016).

via different pathways in different organisms. In yeast, NMD involves targeting mRNAs to P-bodies for subsequent degradation. In contrast, in metazoans, P-bodies are dispensable for NMD, reflecting mechanistic differences in the degradation of NMD targets (Sheth and Parker, 2006; Eulalio et al., 2007b; Stalder and Mühlemann, 2009).

Besides decay of bulk mRNA, NMD factors have also been studied for their role in regulation of expression of splicing factor and ribosomal proteins (via AS-NMD), embryonic development, antiviral immunity, telomere maintenance, histone mRNA degradation and SMD. In addition, NMD factors also play an important role in proliferation and maintenance of stem cells, neuronal cell differentiation, cellular response to stress, and DNA replication and repair, thus indicating a global regulation of physiological processes by NMD (reviewed in Nicholson et al., 2010; Lykke-Andersen and Jensen, 2015; Ottens and Gehring, 2016; da Costa et al., 2017).

1.5 Translational control

After pre-mRNA processing, mature mRNA is exported out of the nucleus, often associated with a large number of proteins, and can then either localize in a repressed state or undergo translation (reviewed in Besse and Ephrussi, 2008; Palazzo and Akef, 2012; Buchan, 2014; Katahira, 2015).

Translation can be regulated by two main mechanisms: (i) by impacting the initiation factors or ribosomes (ii) impacting mRNA itself, either via RBPs or miRNAs.

(i) The modifications of both the RNA (2′-O methylation and pseudouridylation) and the protein (stoichiometry and post-translational modifications) components of the ribosomes have been shown to modulate the rate as well as the fidelity of translation (Guo, 2018). Additionally, ribosome-associated factors (for example: RACK1, Reaper, FMRP and several metabolic enzymes) have also been shown to influence the translation of specific mRNAs (Colon-Ramos et al., 2006; Darnell et al., 2011; Fuchs et al., 2011; Chen et al., 2014; Thompson et al., 2016; Simsek et al., 2017). Recent studies have also suggested a regulatory role of ribosomal proteins in the translation of certain mRNAs, by interacting with specific *cis*-regulatory elements, such as IRESs (Mauro and Edelman, 2007; Gilbert, 2011; Xue and Barna, 2012, 2015; Mauro and Matsuda, 2015; Guo, 2018).

Modification of initiation factors by phosphorylation is one of the key regulatory mechanism of translation. Several initiation factors are known to be phosphorylated including eIF1, eIF4B, eIF4H, eIF5, eIF5B, eIF2, eIF4F and several eIF3 subunits (Jackson et al., 2010; Andaya et al., 2014). In addition, eIF4E and the eIF4E-binding proteins (4E-BPs) are also regulated via phosphorylation (Pyronnet et al., 1999; Mader et al., 1995; Haghighat et al., 1995; Marcotrigiano et al., 1999; Shveygert et al., 2010). It has been proposed that eIF4E phosphorylation is facilitated by eIF4G that recruits the protein kinase Mnk1 (Pyronnet et al., 1999; Shveygert et al., 2010). However, the role of eIF4E phosphorylation in enhancing mRNA translation remains unclear (Scheper and Proud, 2002). 4E-BPs, in a reversible reaction, when hypophosphorylated, block translation initiation by preventing the eIF4F assembly, as they compete with eIF4G for eIF4E binding (Gingras et al, 1999; Marcotrigiano et al., 1999). Proteolytic cleavage of eIF4G and PABP are other mechanisms to modulate translation (Bushell et al., 2000; Marissen et al., 2004).

(ii) While the canonical eIFs/ribosomes regulate global mRNA translation, RBPs and miRNAs provide mRNA-specific control by selectively binding to distinct regions of specific transcripts. They often work in concert with the translation machinery, forming distinct regulatory complexes to direct gene expression.

Several RBPs have been identified and characterized to play a crucial role in the regulation of translation by binding to motifs in the coding sequence, 5'UTRs and more commonly in the 3'UTRs of the transcripts (reviewed in Babitzke et al., 2009; Jackson et al., 2010; Harvey et al., 2018). RBP interaction is mostly inhibitory, but exceptions are known such as stimulatory effect of the poly(A) tail binding of PABP (reviewed in Jackson et al., 2010). RBPs also play a crucial role during development across various organisms and are discussed in detail later in this chapter.

Among small ncRNAs, miRNAs are important regulators of gene expression via mRNA degradation and/or translational repression. Similar to RBPs, miRNAs have also been shown to regulate translation by interacting mostly with 3'UTRs of the target mRNA (in conjugation with sequence-specific RBPs), although targets in 5'UTRs and coding regions have also been reported (Kloosterman et al., 2004; Lewis et al, 2005; Lytle et al., 2007; Easow et al., 2007; Chi et al., 2009; Hafner et al., 2010; Fang and Rajewsky, 2011; Gu et al., 2014). Apart from their function as cytoplasmic regulators, via miRISC formation, recent evidence also suggest their function in the nucleus at the transcription level, where they may act both as gene activators or repressors (reviewed in Catalanotto et al., 2016).

miRNA-mediated translational repression may occur at the initiation (interfering with ribosomal recruitment, cap recognition, scanning, 80s assembly; recruitment of repressors; PABP displacement), post-initiation or elongation steps (recruitment of proteolytic enzymes; ribosomal drop-off; rate of association with polysomes) (reviewed in Fabian et al., 2010; Oliveto et al., 2017). Depending on the complementarity, miRNA-directed endonucleolytic cleavage of the target mRNAs is another mechanism by which miRNAs can inhibit translation (Hutvagner and Zamore, 2002; Yekta et al., 2004; Barth et al., 2008). Under certain conditions of stress or starvation, miRNA-mediated translational activation has also been reported via interaction with 3'UTR or 5'UTR sequences (reviewed in Fabian et al., 2010; Oliveto et al., 2017).

1.6 mRNA localization and regulated translation

mRNA targeting coupled with local translation is yet another critical posttranscriptional regulatory mechanism by which gene products are confined to specific regions of a cell. The best illustrated examples of spatial and temporal restriction of gene expression have been derived from transcripts whose protein products play specialized roles within highly polarized asymmetrical cells, most notably oocytes or embryos. This polarization is achieved through asymmetrical localization of maternally inherited mRNAs that are targeted to defined subcellular compartments. The best-studied examples include: *ASH1* mRNA in budding yeast, which is localized to the bud tip of a dividing cell, producing daughter cells with a

distinct mating type (Bobola et al., 1996; Long et al., 1997; Paquin and Chartrand, 2008); targeting of the maternal mRNAs *osk*, *bicoid (bcd)*, *nanos (nos)* and *gurken (grk)* to distinct regions of the *Drosophila* oocyte, which establishes the future embryonic axes (reviewed in Kugler and Lasko, 2009); localization of *VegT* mRNA to the vegetal pole of the *Xenopus* oocyte, to induce mesodermal and endodermal cell fates in the embryos (King et al., 2005) and asymmetric localization of *β-actin* and *macho-1* mRNAs in ascidian eggs and embryos (Jefferey et al., 1983; Nishida and Sawada, 2001). mRNAs are also asymmetrically localized in differentiated somatic cells such as fibroblasts (Liao et al., 2015); oligodendrocytes (Smith, 2004); astrocytes (Sakers et al., 2017) and axons (Jung et al., 2012). Moreover, mRNA localization is not just limited to animal cells, but cases have also been documented in bacteria (Buskila et al., 2014; Kannaiah and Choder, 2014); algae (Colon-Ramos et al., 2003) and plants (Okita and Choi, 2002; Muench et al., 2012), establishing intracellular transport of mRNAs as a mechanism with widespread implications, across diverse cell types and organisms.

Significant advancements in RNA detection methods have established mRNA localization as a global cellular feature regulating a large proportion of expressed transcripts. The most striking example is *Drosophila*, where 71% of 2314 detectable transcripts in early embryos (Lécuyer et al., 2007) and 35% of the 3475 detectable transcripts in oocytes (Jambor et al., 2015), were observed in spatially distinct patterns. Similar observations have been made in diverse cell types and cellular features such as mitotic apparatus (Blower et al., 2007; Sharp et al., 2011); migrating fibroblasts (Mili et al., 2008); dendrites (Moccia et al., 2003; Poon et al., 2006; Zhong et al., 2006; Suzuki et al., 2007; Cajigas et al., 2012); astrocytes (Thomsen et al., 2013) and axons (Andreassi et al., 2010; Zivraj et al., 2010; Gumy et al., 2011). Moreover, mRNAs are also found to be localized in cell organelles such as mitochondria, endoplasmic reticulum, endo/lysosomes, peroxisomes and centrosomes (reviewed in Weis et al., 2003; Blower, 2013; Ryder and Lerit, 2018), suggesting that mRNA localization is a prevalent mechanism and is a key contributor to cellular functions.

Localizing a transcript prior to translation has several advantages. Besides spatially restricting gene expression to a defined region, it is energetically beneficial to locally translate an mRNA, rather than transporting individual protein molecules from their site of synthesis. mRNA localization also enables efficient assembly of functional protein complexes, as co-targeting can generate high local protein concentrations, also allowing co-translation of different subunits (Batada et al., 2004; Mingle et al., 2005; Lécuyer et al., 2007). Besides enabling cells to differentially respond to extracellular stimuli or acquire different cell fates (Martin and Ephrussi, 2009; Jung et al., 2012), localized translation can also limit deleterious effects of toxic proteins to certain regions of the cell, as exemplified by the localization of

MBP mRNA in oligodendrocytes (Smith, 2004). Finally, targeted protein synthesis offers the possibility to alter the properties of locally translated proteins, as compared to pre-existing copies, via posttranslational modifications or folding pathways (Lin and Holt, 2007).

1.6.1 mRNA localization mechanisms

Targeting of mRNAs to distinct subcellular locations is a multistep process. The initial steps are determined by the information encoded in *cis*-acting elements called "zipcodes" or "localization elements", recognized by *trans*-acting RBPs, which associate with the mRNA to form mRNP complexes. Assembled mRNPs, in most cases, are then packed into RNA transport granules which associate with motor proteins to propel the RNA along the cytoskeletal structures. Once the mRNA reaches its final destination, it is anchored in place and the translational repression is lifted off, either directly upon arrival or until specific signals lead to its translational activation (reviewed in Besse and Ephrussi, 2008; Hilliker, 2014). Several studies have suggested that nuclear history of an mRNA is also critical to determine its eventual cytoplasmic targeting, as in the case of *osk,* for which pre-mRNA splicing is essential for its proper localization (Hachet and Ephrussi, 2004; Ghosh et al., 2012).

Studies in diverse systems have proposed three principal mechanisms of mRNA localization, mediated by RNA localization elements: random diffusion combined with local anchoring, general degradation coupled with localized stabilization and directed transport along the cytoskeleton, the most common mechanism (reviewed in Martin and Ephrussi, 2009). Another potential mechanism is the dimerization of transcripts for localization, facilitated by the *cis* stem-loop structures, which is best illustrated by *Drosophila* maternal transcripts *osk* and *bcd* (Ferrandon et al., 1997; Wagner et al., 2001; Jambor et al., 2011). However, oligomerization is not an obligatory mechanism for localization (Jambor et al., 2011; Amrute-Nayak and Bullock, 2012), except for one known case (Ferrandon et al., 1997). Although it has been reported for very few transcripts, the presence of multiple RNA molecules in localizing mRNPs (Lange et al., 2008; Mhlanga et al., 2009) suggest that RNA:RNA interactions might be a common mechanism for localization. However, as mRNA oligomers formed by heterologous mRNAs have not been reported so far, this possibility needs to be further investigated.

Emerging evidence of spatially controlled mRNA degradation and factors common to both localization and degradation pathways has led to the hypothesis of existence of quality control mechanisms for mRNA localization. This is also supported by the general coordination between localization, translation and degradation machineries. According to a model proposed by Walters and Parker (2014), upon transport to the cytosol, mRNPs become substrate for both localization and deadenylation processes. Mislocalized mRNAs fail to

outcompete the decay machinery with the translation machinery, resulting in their degradation through canonical pathways. Though the model remains to be validated, this hypothesis proposes an additional layer of control to ensure spatial restriction of mRNAs.

1.6.2 *Cis*-acting elements in mRNA localization

Cis-acting elements that direct localization can range from few to hundreds of nucleotides and reside primarily in the 3'UTR of the mRNAs. However, functional elements have also been reported in the 5'UTRs and coding sequences (reviewed in Martin and Ephrussi, 2009). Although several attempts have been made to characterize localization elements, very few localization signals have been mapped so far and no clear consensus has emerged at a sequence level. This is probably due to the fact that their molecular features are not solely defined by the primary sequence, but also by the secondary/tertiary structures or a combination of both (reviewed in Bergalet and Lécuyer, 2014). Furthermore, these elements may also function in a redundant or complementary manner, as indicated by the presence of multiple elements in a given mRNA, making it difficult to identify common signatures shared by localizing mRNAs (Gautreau et al., 1997; Macdonald and Kerr, 1997, 1998; Deshler et al., 1998; Bergsten and Gavis, 1999; Chan et al., 1999; Crucs et al., 2000). In some cases, different elements in an mRNA are required for distinct steps of localization, which may also involve events in different cellular compartments. This suggests that localization elements may work in a collaborative manner, both as general and specific elements to tightly regulate spatial restriction of mRNAs (Zhou and King, 1996; Ainger et al., 1997; Saunders and Cohen, 1999; Thio et al., 2000; Kloc et al., 2000; Hachet and Ephrussi, 2004; Ghosh et al., 2012). Additionally, there is evidence that the conformation of structured localization elements can be modulated by changes in the intracellular milieu, such as increased concentrations of divalent ions, thereby modulating protein interactions (Muslimov et al., 2006, 2011).

High-throughput *in vitro* approaches are being increasingly employed to identify localizing mRNAs (Zivraj et al., 2010; Gumy et al., 2011). However, for these techniques, a major challenge lies in successfully separating sub-cellular compartments with differentially localized transcripts. Following identification of such transcripts, motif analysis needs to be performed to identify sequence features. As regulatory elements tend to be evolutionary conserved in related species, several computational tools have been developed for secondary structure prediction, alignment and identification of elements involved in mRNA localization (Hamilton and Davis, 2011). However, our understanding of the localization of an mRNA to a particular region of a cell via specific recognition of RNA signals remains limited. Application of deep sequencing combined with development of more sophisticated structure-aware algorithms should help to gain new insights into localized RNA recognition.

1.6.3 RBPs and their diverse roles in mRNA localization

Association of RBPs with the mRNA regulates the localization, stability and translation of the transcript. RBPs are often highly modular in nature, containing RBDs (RNA-Binding Domains) and other protein-interaction motifs, allowing them to associate with specific RNAs and other co-factors to form functional mRNPs (Lunde et al., 2007). The same RBP can recognize multiple elements within an mRNA, which requires correct spatial positioning of these elements (Patel et al., 2012). Binding of all elements can significantly alter the binding affinity of the RBP for the target mRNA, due to the structural changes that the mRNA undergoes upon binding (Lunde et al., 2007; Chao et al., 2010). Conversely, RBPs also often contain multiple RBDs which act synergistically by inter/intra-molecular cooperativity (Lunde et al., 2007; Dienstbier et al., 2009; Doyle and Kiebler, 2012). High degree of conservation within the RBDs suggest that the functional properties and RNA-binding specificities of RBPs are also likely to be conserved (Perrone-Bizzozero and Bolognani, 2002; Yisraeli, 2005). The functional diversity within RBPs also suggests a large diversity at the structural level, imparted by the structural modularity, auxiliary functional domains and post-translational modifications. Often, alternative splicing also adds to the cell's ability to expand its repertoire of RBPs (reviewed in Glisovic et al., 2008). Over the years, a large compendium of RBPs involved in mRNA localization across organisms has been generated (King et al, 2005; Kugler and Lasko, 2009; Jansen and Niessing, 2012; Tolino et al., 2012; Lasko, 2012; Singer-Krüger and Jansen, 2014; Bergalet and Lécuyer, 2014; Di Liegro et al., 2014; Haag et al., 2015). Identified through genetic and biochemical means, several RBPs have been extensively studied in *Drosophila* development and are discussed in detail in the following section.

1.7 *Drosophila*: an excellent model to study mRNA localization

Some of the best characterized examples of mRNA localization and translational regulation come from studies in *Drosophila melanogaster*. *Drosophila* offers many technical advantages over other vertebrate models as it is easy to culture and has a short life cycle of 10-12 days. The small genome (released in March 2000 by Adams and co-workers) and low number of chromosomes are highly advantageous for genetic manipulations and have been successfully exploited to study a diverse range of biological processes (reviewed in Jennings, 2011). Moreover, about 75% of known human diseases have counterparts in *Drosophila* (Reiter et al., 2001), further stressing its importance as a model, also for medical research. Due to its ease of manipulation, an extensive range of genetic tool kits have been developed and a vast assortment of transgenic strains are available through stock centers. All the available literature about the estimated 14,000 protein-coding genes (annotated with a "CG number") has been collated in FlyBase (Gramates et al., 2017) and new genes are continuously being characterized by researchers all over the globe.

1.8 *Drosophila* oogenesis

Drosophila oogenesis has been extensively studied and has emerged as a powerful tool to investigate mechanisms of mRNA localization. The main events of *Drosophila* oogenesis have been characterized in detail and are summarized in Johnstone and Lasko (2001), Bastock and St Johnston (2008) and Kugler and Lasko (2009), among many others.

Drosophila females have a pair of ovaries, where oogenesis takes place in an assembly-like manner (Fig. 5). Each ovary consists of about 20 ovarioles and a single ovary contains all the stages of development, from stem cells to the mature egg, connected by somatic stalk cells (Spradling, 1993). The anterior end of the ovariole is formed by the germarium, where a stem cell divides asymmetrically to form another stem cell and a cystoblast, which differentiates to an oocyte. The cystoblast undergoes 4 rounds of mitotic divisions with incomplete cytokinesis to form 16 cells in a cyst, interconnected by cytoplasmic bridges called the ring canals. Determined by cell fate markers and markers of mitotic chromosome pairing, one of the 16 cells differentiates into an oocyte, while the remaining cells become the polyploid nurse cells. Nurse cells support the growth of the oocyte by providing nutrients and cytoplasmic components via the ring canals. As the cyst matures, it is enveloped by somatic follicle cells and moves along the germarium to finally pinch off as an egg chamber, led by a series of cell-signaling events. As the follicle cells migrate to surround the cyst, the oocyte comes to rest at the posterior of the cyst and becomes polarized, as the centrosomes and a set of RNA and proteins are differentially localized to the posterior of the oocyte.
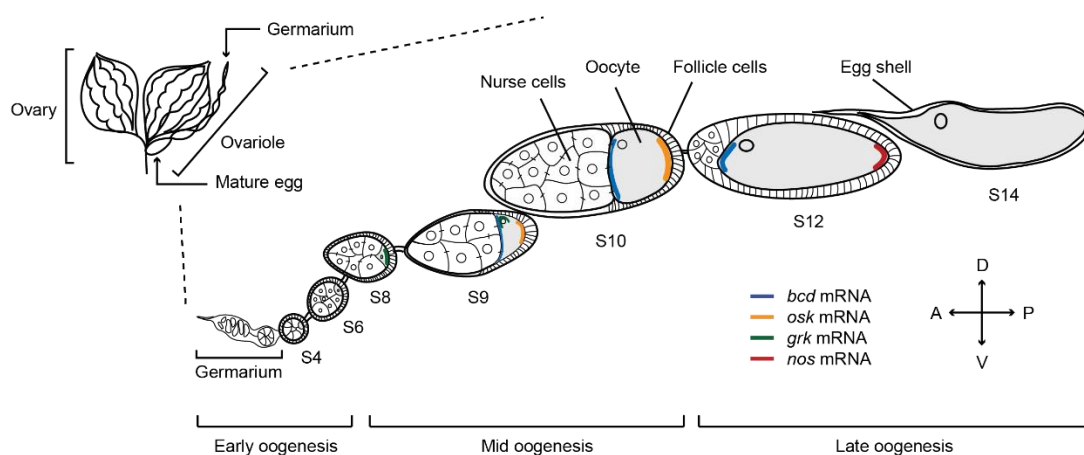

Fig. 5. Schematic representation of *Drosophila* ovaries and localization of maternal mRNAs during oogenesis. The oocyte is highlighted in grey. S: Stages of oogenesis; A: Anterior; P: Posterior; D: Dorsal; V: Ventral.

Oogenesis has been divided into 14 morphologically distinct stages, further divided into three broad categories: early oogenesis (until stage 6); mid oogenesis (stage 7-stage 10) and late oogenesis (stage 11 onwards); stage 1 is defined as the budding of the egg chamber from the germarium, while the mature egg marks stage 14 (Fig. 5). The first step in establishing anterior-posterior asymmetry is the posterior positioning of the oocyte during early oogenesis, which later translates into anterior-posterior axis of the oocyte. At this stage, microtubule minus-ends are concentrated at the posterior pole of the oocyte, along with the nucleus, *grk* mRNA and Grk protein. Posterior localization of Grk induces a posterior identity to a subset of overlying follicle cells that send back an unidentified signal triggering repolarization of the oocyte. In response, the microtubules reorganize during mid oogenesis, directing the localization of *grk*, *osk* and *bcd* mRNAs. Initially, plus ends accumulate in the middle of the oocyte, but later point towards the posterior, driving localization of *bcd* to the anterior and *osk* to the posterior of the oocyte, establishing the anterior-posterior axis. This reorganization of microtubules also allows for the migration of nucleus, *grk* mRNA and Grk protein to the dorsal-anterior corner, which determines the dorsal side of the egg chamber, thus establishing the dorsal-ventral axis (reviewed in Steinhauer and Kalderon, 2006). In late oogenesis, the polarized microtubule array disassembles and vigorous streaming of the ooplasm occurs, directed by short subcortical microtubules. This streaming coincides with nurse cells dumping their bulk cytoplasm into the oocyte, in an event called "nurse cell dumping". At the same time, the localization of some specific factors such as *nos* mRNA takes place. The posterior localization of *nos* is required for germ cell development and embryonic abdominal patterning (Gavis et al., 2007). Nurse cells eventually degenerate and are removed by apoptosis (Foley and Cooley, 1998; Jenkins et al., 2013) to form the mature egg.

1.8.1 Localization of maternal mRNAs during oogenesis

Maternal mRNAs are produced in the nurse cells and transported to the oocyte. All three localized mRNAs *osk*, *bcd* and *grk* utilize the same conserved pathway dependent on the complex of two interacting proteins Egalitarian (Egl) and Bicaudal-D (BicD). These proteins link the mRNA to the microtubules and minus-end directed motor dynein/dynactin (Mach and Lehmann, 1997; Bullock and Ish-Horowicz, 2001; Clark et al., 2007; Dienstbier et al., 2009; Sladewski et al., 2018). In the oocyte, *grk* first accumulates at the anterior and is then transported laterally towards the oocyte nucleus (MacDougall et al., 2003; Jaramillo et al., 2008). Though both steps are dynein- and microtubule-dependent, the second step is thought to be mediated by the oocyte nucleus, which nucleates a distinct population of microtubules to facilitate lateral movement of the mRNA (MacDougall et al., 2003; Januschke et al., 2006; Delanoue et al., 2007). During mid oogenesis, *osk* initially localizes to the anterior margins of the oocyte (at stage 8), before it localizes to the posterior by stage 9, (Ephrussi et

al., 1991; Kim-Ha et al., 1991) as shown in Fig. 5. This posterior localization is driven by the heavy chain of the plus-end directed motor kinesin (Khc; St Johnston, 2005). Visualization of *osk* mRNPs in living oocytes has shown that mRNP particles move actively in all directions, with a slight bias towards the posterior (Zimyanin et al., 2008). Two recent studies have reported that Khc is recruited to *osk* RNA molecules by atypical RNA-binding tropomyosin Tm1C (Veeranan-Karmegam et al., 2016; Gaspar et al., 2017). Khc is probably recruited already in the nurse cell cytoplasm, and is activated in the oocyte by a properly assembled EJC/SOLE (Spliced *oskar* Localization Element) to drive the posterior localization of *osk* mRNA (Clark et al., 1994; Brendza et al., 2000; Gaspar et al., 2017).

Although both *nos* and *osk* are targeted to the same region of the oocyte, the mechanism of posterior localization of *nos* is strikingly different from that of *osk*. Until mid-oogenesis, *nos* accumulates in dynamically changing asymmetric patterns and posterior enrichment begins only in late oogenesis, much later than *osk* (Forrest and Gavis, 2003). Contrary to *osk*, *bcd* and *grk* transcripts, *nos* enters the oocyte through nurse cell dumping and localizes mainly through diffusion (enhanced by cytoplasmic streaming) and local entrapment at the posterior pole. This process is facilitated by F-actin cytoskeleton (reviewed in Kugler and Lasko, 2009). In embryos, only ≤ 4% of *nos* mRNA is localized (Bergsten and Gavis, 1999). Non-localized, translationally silent *nos* is degraded by the CCR4-NOT complex, recruited by the protein Smg (Semotok et al., 2005; Zaessinger et al., 2006; Jeske et al., 2006) and components of germline-specific Piwi-interacting RNA (piRNA) machinery (Rouget et al., 2010).

Trans-acting factors involved in mRNA localization during oogenesis

Localized mRNPs assemble during transcription in the nucleus, where a core set of *trans*-acting factors bind to the maturing mRNAs. These *trans*-acting factors, many of which are RBPs, provide a platform for the formation of larger, dynamic assemblies in the cytoplasm, regulating mRNA transport, silencing and localized translation. As already mentioned, signals usually positioned in the 3' UTR are recognized during mRNP biogenesis/export by RBPs to ensure the correct cytoplasmic sorting of the transcript to be localized.

Targeting of transcripts to distinct regions of the oocyte requires a large number of *trans*-acting factors. Anterior accumulation of *bcd* is facilitated by Exuperantia (Exu) during mid-oogenesis (Berleth et al., 1988; St Johnston et al., 1989) and Staufen (Stau) in late oogenesis (St Johnston et al., 1989; Ferrandon et al., 1994), while its anchoring requires Swallow, the γ-tubulin ring complex components, the ESCRT II complex and microtubule-associated protein Mini Spindles (reviewed in Lasko, 2012). Interestingly, Exu and Stau are also components of *osk* RNPs and are required for proper *osk* localization (St Johnston et al., 1991; Ephrussi *et al.*, 1991; Kim-Ha *et al.,* 1991, 1995; Wilhelm et al., 2000). Stau is required

for kinesin-based transport of *osk* mRNA (Brendza et al., 2000) while it localizes *bcd* in a dynein-dependent manner (Ferrandon et al., 1994; Bullock and Ish-Horowicz, 2001). This indicates that Stau associates with different motor proteins for transport to different locations in the oocyte. Structural analysis of Stau suggests that distinct domains might allow its association with different factors that direct localization (Micklem et al., 2000; Ramos et al., 2000). Indeed, during oogenesis, ectopic expression of Miranda, a Stau-interacting protein, couples Stau-*osk* complexes to the anterior localization machinery (Irion et al., 2006). Moreover, Stau associates with *osk* during mid oogenesis but does not associate with *bcd* until late oogenesis (St Johnston et al., 1989, 1991), suggesting a temporal regulation of transport complexes. Initially *osk* colocalize with *bcd* at the anterior, along with proteins such as Exu. This has led to the suggestion of a model (Wilhelm et al., 2000) that these mRNAs use a same core complex, as they start their localization process in the nurse cells. Following their arrival in the oocyte, the mRNPs are sorted, presumably at the anterior. While *bcd* is anchored at the anterior, *osk* is transported further to the posterior of the oocyte (St Johnston et al., 1989; Kim-Ha et al., 1991; Wilhelm et al. 2000). This hypothesis is supported by the evidence that mutants of Stau and tropomyosin (TmII) block the release and transport of *osk* to the posterior, rather than affecting its early anterior localization (Ephrussi et al., 1991; Kim-Ha et al,. 1991; Erdelyi et al., 1995; Tetzlaff et al., 1996). The proposed anterior sorting may further involve recruitment of additional factors or modifications of the transport machinery, but the molecular mechanism remains unclear.

Posterior localization of *osk* also requires EJC components, nascent protein associated complex (NAC), decapping protein DCP1 and several hnRNP proteins (reviewed in Kugler and Lasko, 2009). Splicing of the first intron of the *osk* transcript assembles the SOLE, essential for the posterior targeting of *osk* mRNA (Hachet and Ephrussi, 2004; Ghosh et al., 2012; Simon et al., 2015). Additionally, splicing results in EJC deposition, raising the possibility that the SOLE regulates the association of EJC with *osk*, either via direct binding or mediated by an adaptor protein (Ghosh et al., 2012; Simon et al., 2015). Besides the SOLE, other regulatory elements in the *osk* 3' UTR are required for its posterior enrichment (Kim-Ha et al., 1993). Intriguingly, *osk* can also localize by "hitchhiking", via dimerization elements in its 3'UTR (Jambor et al., 2011). This "hitchhiking" can be exploited by localization-incompetent mRNA molecules, by their inclusion in transport-competent mRNPs.

Very few *trans*-acting factors involved in *nos* mRNA localization have been identified so far. Among those are the hnRNP M homolog Rumpelstiltskin (Rump; Jain and Gavis, 2008), Lost (Sinsimer et al., 2011) and Aubergine (Aub; Becalska et al., 2011). Interestingly, Rump and Lost are also required for posterior accumulation of *osk*, specifically during late oogenesis, and for subsequent amplification of the germ plasm (Sinsimer et al., 2011).

Role of hnRNPs in mRNA localization during oogenesis

hnRNP A/B family member Hrp48 colocalizes with *osk* throughout oogenesis and its mutants specifically abolish *osk* localization (Huynh et al., 2004; Yano et al, 2004). Mislocalization of both *osk* mRNA and Stau in Hrp48 mutants further suggests its involvement in the formation of Stau-*osk* particles (Huynh et al., 2004; Yano et al, 2004), ultimately affecting proper *osk* deployment. However, it is unclear if Hrp48 has a direct effect on *osk* localization, as some alleles of Hrp48 show microtubule polarity defects (Yano et al., 2004). In addition to its role in *osk* localization, Hrp48 also mediates translational repression of *osk* during transport, by binding to repressor elements in the 3'UTR, coupling *osk* localization with translational control (Gunkel et al., 1998; Yano et al., 2004).

Other hnRNPs involved in *osk* localization are Squid (Sqd; Norvell et al., 2005), Glorund (Glo; Kalifa et al., 2009) and Syncrip (Syp; McDermott et al., 2012). Notably, Hrp48 and Sqd, along with Ovarian tumor (Otu) act together to regulate localization and translation of *grk* mRNA. They also influence nurse cell chromosome dynamics during oogenesis (Goodrich et al., 2004; Norvell et al., 1999). Otu also participates in *osk* localization (Tirronen et al., 1995), and it is possible that, similar to *grk* regulation, the same complex of Sqd-Hrp48-Otu acts in *osk* localization as well. Furthermore, Syp is also required for localization and translational regulation of both *grk* and *osk* mRNAs and co-immunoprecipitates with Sqd and Hrp48 (McDermott et al., 2012). These observations suggest the existence of a core module of hnRNPs required for regulation of localizing transcripts.

Besides mRNA localization, hnRNP F/H family protein Glo has multiple functions during oogenesis, including development of dorsal appendages of the eggs, regulation of nurse cell dumping and chromatin organization in the nurse cells (Kalifa et al., 2009). Similar to Sqd and Hrp48, Glo mutant ovaries also exhibit mislocalization and ectopic translation of *grk* transcripts (Norvell et al., 1999; Goodrich et al., 2004; Kalifa et al., 2009). Glo has also been shown to be required for proper *osk* localization in both embryos and ovaries, possibly mediated by its direct association with Hrp48 (Kalifa et al., 2009). Glo interaction with the splicing factor Half pint (Hfp or pUF68) suggests that, together with Hrp48, it might also participate in nuclear splicing, independently of its function in mRNA localization/translation (Kalifa et al., 2009). Additionally, Glo also represses translation of non-localized *nos* in oocytes by specifically interacting with a Translational Control Element (TCE) in its 3'UTR (Fig. 6B; Kalifa et al., 2006). Discrete RNA-binding surfaces allow Glo to specifically recognize different targets, possibly facilitated by interacting proteins, which explains the functional diversity of Glo and perhaps also of other hnRNPs (Tamayo et al., 2017).

1.8.2 Translational regulation of maternal mRNAs during oogenesis

mRNA localization is often coupled to translational regulation, which allows maternally deposited mRNAs to direct embryonic development. This localized translation is often achieved by transporting the mRNAs in a translationally repressed state, which is released when the mRNA reaches its destination, together with selective distribution or regulation of factors required for its translational activation/repression.

osk undergoes extensive translational regulation as the mRNA needs to be translationally repressed prior to its localization and the localized fraction must be activated, while the unlocalized fraction must remain silent. In early oogenesis, translational repression of *osk* occurs through proteins associated with RNAi pathway including *A*rmitage (Armi), Aub, Krimper (Krimp), Cutoff (Cuff), Maelstrom (Mael), Spindle-E (Spn-E), Zucchini (Zuc)*, and S*quash (Squ) (reviewed in Kugler and Lasko, 2009). Repression during mid-oogenesis predominantly relies on pathways that target cap-dependent translation initiation. This is primarily mediated by Cup, a 4E-BP that interferes with the eIF4E-eIF4G interaction (Fig. 6A*;* Nakamura et al., 2004). Cup is recruited to *osk* by Bruno (or Aret), which directly binds to BRE (Bruno-Response Element) sequences in the *osk* 3'UTR (Kim-Ha et al., 1995; Webster et al., 1997; Snee et al., 2008). Cup-mediated repression can also occur by direct recruitment of the CCR4-NOT deadenylase complex to maintain its target mRNAs in a repressed state (Igreja and Izaurralde, 2011). Cup together with Bruno, Hrp48 and Sqd also act to mediate translational repression of *grk* prior to its localization (Fig. 6A; Norvell et al., 1999; Filardo and Ephrussi, 2003; Clouse et al., 2008). Additionally, Cup is required to repress *nos* in embryos, by binding to the protein Smg (Fig. 6B; reviewed in Lasko, 2011). Therefore, Cup is a central player in the translational regulation of several localizing maternal mRNAs.
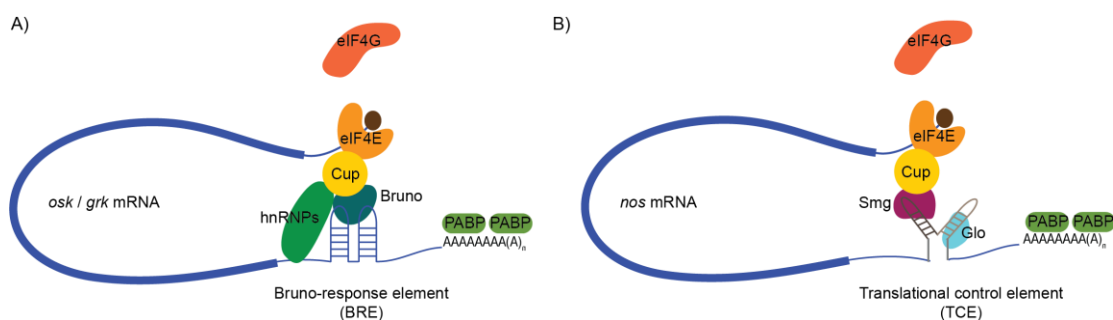

Fig. 6. General mechanisms of cap-dependent translational regulation of maternal mRNAs.

(A) *osk* and *grk* are regulated by binding of Bruno to the BREs in the 3'UTRs. Bruno-mediated recruitment of Cup prevents the eIF4E-eIF4G interaction, thereby repressing translation. Co-

purification of hnRNPs such as Hrp48 and Sqd with Cup, suggest that they are part of the repressor complex. (B) Recruitment of Cup to *nos* is mediated by binding of Smg to the loop of the stem-loop II of the Translational Control Element (TCE), which contains a Smaug Recognition Element (SRE). Additionally, Glo binds to the stem of the stem-loop III of the TCE in the *nos* 3'UTR, to repress *nos* translation, by an unknown mechanism.

Cap-independent translational repression mechanisms have also been reported, as in the case of Bruno, that facilitates *osk* oligomerization and forms large silencing particles, rendering *osk* inaccessible to the translation machinery (Chekulaeva et al., 2006). A similar mechanism of promoting *osk* oligomerization is mediated by direct binding of the hnRNP Polypyrimidine Tract Binding protein (Heph/PTB) to elements in the *osk* 3'UTR (Besse et al., 2009). Translational repression of localizing *osk* in early oogenesis by PTB (Besse et al., 2009) further suggests a functional link between assembly of high-order RNPs and translational repression.

Other translational repressors of *osk* include the conserved DEAD-box helicase Maternal expression at 31B (Me31B; that associates with Cup-Bruno-eIF4E complex), Y-box containing protein Ypsilon schachtel (Yps; by directly interacting with Exu) and *Drosophila* homolog of vertebrate Zipcode-binding protein-1, Imp (reviewed in Kugler and Lasko, 2009). Imp also contributes to localized expression of *grk*, by associating with Sqd and Hrp48, though it is believed to act redundantly (Geng and Macdonald, 2006). Embryonal *nos* repressor complex includes Me31B, Trailer Hitch (Tral) and RNA-dependent ATPase Belle (Bel), along with Cup, Smg, eIF4E and PABP (Götze et al., 2017). Additionally, miRNA-independent role of AGO1, recruited by Smg, is also involved in the translational repression of *nos* (Pinder and Smibert, 2013).

While *bcd* and *nos* are activated after fertilization, *osk* and *grk* are translated during mid oogenesis. Orb has been shown to be required for efficient polyadenylation of both *osk* and *grk* mRNAs (Chang et al., 1999, 2001; Castagnetti and Ephrussi, 2003), thus activating their translation. Orb also interacts with poly(A) polymerases such as PAP and Wispy (Benoit et al., 2008), suggesting that polyadenylation is one of the key factors involved in regulation of maternal mRNAs. This is further supported by the studies of RBP Bicaudal-C (BicC), a negative regulator of *osk* translation (Saffman et al., 1998). BicC directly recruits CCR4-NOT deadenylase complex to regulate the expression of target mRNAs, potentially including *osk* (Chicoine et al., 2007). Additionally, BicC also interacts with Orb, PAP and Wispy, possibly inhibiting their association with mRNAs (reviewed in Kugler and Lasko, 2009) to regulate translation.

Nos protein is expressed in two waves during oogenesis, firstly during the early stages of germarium, where it is thought to promote stem cell or cystoblast divisions, and then during

late oogenesis (Wang et al., 1994). At stage 10, Nos is highly expressed in the cytoplasm of nurse cells, and has been shown to be functional, as this cytoplasm is able to rescue abdominal defects when transplanted in posterior-group mutant embryos (Sander and Lehmann, 1988). However, no protein is detected after stage 12, possibly due to formation of chorion and vitelline membrane, which blocks antibody penetration and hence detection. Ectopic expression of *nos* at the posterior inhibits *bcd* translation, suggesting that the exclusion of Nos from the oocyte is essential to prevent it from interfering with *bcd* expression (Wharton and Struhl, 1989; Wang and Lehmann, 1991; Gavis and Lehmann, 1992), although the mechanism is not clear as *bcd* remains untranslated until embryogenesis.

1.8.3 Pole plasm assembly and abdominal patterning

Pole plasm/germ plasm is a specialized cytoplasm containing electron-dense particles called polar granules. Polar granules are enriched in RNA and ribosomes, and are incorporated into germline precursor pole cells during embryogenesis (reviewed in St Johnston and Nüsslein-Volhard, 1992). Components of pole plasm are synthesized in the nurse cells and transported to the oocyte, where they are localized to the posterior. Formation of pole plasm is dependent on the posterior localization and expression of *osk*. Upon localization, *osk* needs to be anchored in place. Anchoring requires the F-actin cytoskeleton along with F-actin associated proteins and endosomal proteins (reviewed in Kugler and Lasko, 2009). Localization of *osk* functions to restrict synthesis of Osk protein to the posterior, where it initiates the assembly of pole plasm. Translation of *osk* from different start sites produces two isoforms, short Osk and long Osk, with different localization patterns (Markussen et al., 1995; Rongo et al., 1997). While short Osk induces pole plasm assembly, the long isoform is required for anchoring of *osk* mRNA and of short Osk (Ephrussi et al., 1991; Markussen et al., 1995; Rongo et al., 1997; Vanzo and Ephrussi, 2002). Long Osk spatially restricts and maintains the integrity of pole plasm throughout oogenesis, ensuring proper germline formation and embryonic patterning (Vanzo and Ephrussi, 2002).

Pole plasm assembly is initiated by short Osk, which recruits components for both germline formation and embryonic patterning. A key function of pole plasm assembly is the posterior localization and translational activation of *nos* mRNA, which directs abdominal development during embryogenesis (Ephrussi et al., 1991; Gavis and Lehmann, 1992; Ephrussi and Lehmann, 1992; Forrest and Gavis, 2003). In embryos, translational repression and deadenylation of *nos* are relieved by Osk, by preventing Smg binding to *nos* 3'UTR (Dahanukar et al., 1999; Zaessinger et al, 2006; Jeske et al., 2011).

A number of genes (posterior class of maternal-effect genes), based on the loss-of-abdominal patterning phenotype, are implicated in the formation of abdominal segments: *cappuccino*

(capu), spire (spir), osk, stau, vasa (vas), valois (vls), tudor (Tud), mago, nos and *pumilio (pum)* (Boswell and Mahowald, 1985; Lehmann and Nusslein-Volhard, 1986, 1987, 1991; Schüpbach and Wieschaus, 1986; Manseau and Schüpbach, 1989; Boswell et al., 1991). Most of them, except *nos* and *pum*, also display a loss-of-pole cell phenotype (Lehmann and Nusslein-Volhard, 1987, 1991; Barker et al, 1992), suggesting that abdominal defects are a consequence of defective pole plasm assembly. Mutants of genes required for pole plasm assembly fail to efficiently localize *nos* mRNA to the posterior of the embryos and show weak abdominal segmentation phenotypes (Wang et al., 1994), further demonstrating that *nos* translation is required for abdominal development.

Genetic analysis has revealed that pole plasm assembles in a stepwise manner in which *capu, spir, stau* and *mago* act upstream of *osk*, which in turn acts upstream of *vas*, followed by *tud* and *vls* (Hay et al., 1990; Lasko and Ashburner, 1990; Kim-Ha et al., 1991; Ephrussi et al., 1991; St Johnston et al, 1991; Ephrussi and Lehmann, 1992). Additionally, it was shown that *osk, vas* and *tud* are essential for germ-cell determination and abdomen formation, while *capu, spir, stau* and *vls* are dispensable for both processes (Ephrussi and Lehmann, 1992). In line with these observations, posterior anchoring of Vas is mediated by Osk and the Osk-Vas interaction is a pre-requisite for polar granule formation (Breitwieser et al., 1996). Furthermore, *vas* and *tud* are also required for Osk accumulation (Markussen et al., 1995), revealing that they are essential components of pole plasm.

Vas is a highly conserved DEAD-box RNA helicase localized in the polar granules and is a germline-specific translation regulator (reviewed in Lasko, 2013). In addition to Osk protein, regulators of accumulation and stabilization of Vas at the posterior of the oocyte include the deubiquitinating enzyme Fat facets (Faf; Liu et al., 2003) and ubiquitin ligase specificity receptors, Gustavus (Gus) and F-box synaptic protein, Fsn (Styhler et al., 2002; Kugler et al., 2010; Gustafson et al., 2011).

Vas is required at several stages of development. During early oogenesis, Vas is involved in germline cyst maintenance, oocyte differentiation and maturation (Lasko and Ashburner, 1988; Styhler et al., 1998). *vas* null mutant ovaries also display inefficient accumulation of certain oocyte-localized RNAs (*BicD, orb, nos* and *osk*), and also of Grk protein (Styhler et al., 1998; Tomancak et al., 1998). This suggests a vital role of Vas in translational activation of *grk* mRNA and thus in the establishment of oocyte polarity. In embryogenesis, Vas is required for pole cells formation and embryonic patterning (Schüpbach and Wieschaus, 1986) and might be involved in translational activation of RNAs localized to the germ plasm, such as *nos* and *osk* (Markussen et al., 1995; Gavis et al., 1996; Dahanukar and Wharton, 1996).

Vas also has a translation-independent function in the *Drosophila* germline, as it is required to regulate mitotic chromosome condensation (Pek and Kai, 2011) and piRNA-mediated transposable element silencing (Vagin et al., 2004; Lim and Kai, 2007; Malone et al., 2009). Recent studies have revealed even a broader expression of Vas, including somatic gonadal precursor cells of *Drosophila* (Renault, 2012), and multipotent cells (Gustafson and Wessel, 2010), suggesting that Vas is not exclusively a germline marker and has wider implications in organismal development.

1.8.4 Cytoplasmic mRNP particles and their role in oogenesis

Germline granules are well conserved RNP complexes that play a critical role in the regulation of mRNA degradation, localization, translational regulation, and fertility. These are electron dense, membrane-free cytoplasmic structures, found across organisms with shared features, suggesting commonalities of functions in addition to potentially more specialized roles.

In *Drosophila* egg chambers, three classes of germline RNPs have been observed, based on morphology and subcellular localization. These are: polar granules, nuage particles and sponge bodies (reviewed in Schisa, 2012). As mentioned before, polar granules are found in pole plasm and contain the determinants for pole cell specification and posterior patterning (Mahowald, 2001). Several proteins, including Osk, Vas, Tud, Me31B, Aub, eIF4A, ER-associated protein TER94 and several mRNAs have been identified as *bona fide* components of polar granules (Thomson et al., 2008; Kugler and Lasko, 2009).

Nuage particles are perinuclear cytoplasmic structures found in the nurse cells, in close proximity to nuclear pores. Although evolutionary conserved, their role and mechanism of function in the germ cells is unclear. In *Drosophila*, nuage particles share components with polar granules such as Vas, Tud and Aub and are possibly involved in assembly or re-organization of mRNP complexes during oogenesis (Snee and Macdonald, 2004). Localization of piRNA pathway factors including, Tejas (Tej), Spn-E, Aub, AGO3, Krimp, Mael, Zuc, Cuff and Squ to nuage suggest an additional role of nuage particles as a site for processing germline piRNAs, thereby regulating germline gene expression (Findley et al., 2003; Vagin et al., 2004; Lim and Kai, 2007; Pane et al., 2007; Chen et al., 2007; Malone et al., 2009; Patil and Kai, 2010; Ryazansky et al., 2016).

Sponge bodies are dynamic structures found in the nurse cell cytoplasm and ooplasm and are often associated with nuage particles (Wilsch-Brauninger et al., 1997). These structures are compositionally and perhaps functionally similar to yeast and mammalian P-bodies and the two terms are often used interchangeably in *Drosophila*. A multitude of proteins such as Exu, Btz, Cup, eIF4E, Me31B, Yps, Gus, DCP1, DCP2, Hrp48, Sqd, BicC, Orb, Bruno, Tral

and Lost have been found associated with sponge bodies (Snee and Macdonald, 2009 and the references within; Weil et al., 2012). Consistent with the presence of these proteins, sponge bodies have been implicated in regulation of localization of *grk* mRNA (Delanoue et al., 2007). Intriguingly, ultrastructure analysis and super-resolution microscopy has revealed a stratified organization of sponge bodies, where the edge region of sponge bodies is translation-competent while the core is translationally silent (Weil et al., 2012). Localized transcripts like *grk* and *bcd*, are differentially translated by virtue of their association with distinct sponge body zones (Weil et al., 2012), highlighting a key role of sponge bodies in spatio-temporal regulation of developmental mRNAs.

1.9 mRNP purification: RNA-centric vs protein-centric approaches

As discussed above, a large number of RBPs involved in mRNA localization have been identified, by both genetic and biochemical means. Although information is available on the identification and nucleic acid recognition specificity of many RBPs, we have limited understanding of the structure, composition and dynamics of native mRNPs. We know little about the hierarchy of interactions, when and where mRNP components are acquired, their specific roles, and conformations during assembly, transport and disassembly of the localizing mRNPs. A major bottleneck has been the lack of a robust method to selectively enrich a given mRNP at a defined spatial location in the cell.

To explore the composition of an mRNP, both protein-based and RNA-based approached have been developed. Protein-based *in vivo* approaches essentially rely on the purification of a known RBP by immunoprecipitation (IP) together with the associated RNAs, which are then identified by cDNA cloning, coupled to microarray (RIP-Chip; Keene et al., 2006) or high-throughput RNA sequencing (RIP-Seq; Zhao et al., 2010). Recent techniques like CLIP (Cross-linking and Immunoprecipitation; Ule et al., 2005) and its variants PAR-CLIP (Hafner et al., 2010), iCLIP (König et al., 2011) and HITS-CLIP (Licatalosi et al., 2008), which combine IP, UV cross-linking and high-throughput sequencing, have emerged as efficient tools for transcriptome wide high-resolution identification of RBP binding sites. Circumventing the need of antibodies, RBPs also can be tagged directly and affinity purified. For affinity purifications, fusion of two affinity modules in tandem, separated by a protease cleavage site, is particularly advantageous. This method of Tandem Affinity Purification (TAP) allows purification in mild conditions in two consecutive steps with significantly reduced non-specific background (Rigaut et al., 1999; Puig et al., 2001). Purified complexes can be stabilized by UV irradiation and the recovered RNA fragments can be analyzed using high-throughput sequencing (Granneman et al., 2009). While UV cross-linking allows to detect previously undetected protein associations, this approach has the disadvantage of potentially producing

artefacts, including mutations caused by UV light and biases in cross-linking efficiency of specific residues, nucleotides and dsRNA-binding RBPs (reviewed in Wheeler et al., 2018).

Alternatively, RNA-centric approaches can be very promising since they involve co-purification of a single mRNA with its associated proteins. Bound proteins are then identified using mass spectrometry (MS) or protein arrays. For RNA tagging *in vivo*, use of naturally occurring RNA aptamers has emerged as a powerful tool. In this approach, the high affinity interaction between viral RBPs and cognate RNA sequences is utilized to tag specific mRNAs. Sequence-specific RNA-protein recognition systems for regulation of genes in bacteriophages have been characterized both biochemically and structurally. These include the RNA hairpin-binding proteins from bacteriophages GA (Gott et al., 1991), R17 (Carey et al., 1983), Lambda (Chattopadhyay et al., 1995), P22 (Hilliker and Botstein, 1976) and Qβ (Lim et al., 1996). A major breakthrough has been the characterization of the specific interaction between the MS2 bacteriophage coat protein (MCP) with its cognate genomic RNA (Uhlenbeck and his colleagues; reviewed in Johansson et al., 1997). A similar system from bacteriophage PP7, whose coat protein shows only 13% amino acid sequence identity to that of the MCP has also been well studied (Lim et al., 2001). In addition to viral genomic RNA sequences, other naturally occurring RNA aptamers include the stem loop domain from human U1snRNA (called U1hpII) which binds to U1A protein (Piekna-Przybylska et al., 2007) and the hairpin loop from a thermostable SRP RNA that forms a stable complex with *Thermotoga maritima* Ffh protein (Kieft and Batey, 2004).

In contrast to naturally occurring aptamers, *in vitro* synthesized RNA tags with high affinity for specific ligands such as streptavidin, streptomycin, or tobramycin have been produced and effectively used to analyze the protein components of an mRNP (Bachler et al. 1999; Srisawat and Engelke 2001; Hartmuth et al. 2002; Deckert et al., 2006; Vasudevan and Steitz, 2007; Ward et al., 2011; Leppek and Stoecklin, 2014; Dong et al., 2015). *In vitro* transcribed RNAs immobilized to a solid support via RNA aptamers (Dienstbier et al., 2009; Iioka et al., 2011; Dix et al., 2013) or chemically modified ribonucleotides (Rouault et al., 1989; Sharma, 2008) are other methods to assemble and purify mRNPs *in vitro*. Use of affinity-tagged anti-sense oligonucleotides presents another powerful tool to isolate RNA baits and associated proteins (Lingner and Cech, 1996; Blencowe and Lamond, 1999). In addition, a recently developed RNA affinity tag, utilizing *Pseudomonas aeruginosa* CRISPR/Csy4 system, has been shown to be highly efficient for *in vitro* purification of RBPs associated with specific RNAs (Lee et al., 2013).

Coupled with cross-linking, RNA-affinity purification methods with aptamers have been shown to effectively capture weak and transient interactions with high specificity. However, there are some limitations. Incorporation of foreign sequences or chemical modifications may

alter the target RNA structure and prevent the formation and correct assembly of the mRNP *in vivo*. Moreover, structural information about the target RNA is required to predict the best insertion site. Additionally, degradation of artificial aptamers by cellular nucleases might decrease the lifetime of the tagged RNA, decreasing the efficiency of purification.

1.9.1 *MS2*-MCP system in mRNP purification

The *MS2*-MCP system, pioneered in yeast by Singer and co-workers (Bertrand et al., 1998) has been well characterized to visualize mRNA trafficking in live cells (reviewed in Urbanek et al., 2014; Buxbaum et al., 2015) or to tether protein of interest to reporter mRNAs to follow their cell fates (Keryer-Bibens et al., 2008). Due to the high affinity (dissociation constant, K_d of 5nM) and specificity of the MCP to the cognate RNA, this system has the potential to be used for biochemical purifications. Moreover, many mutant variants of *MS2* RNA motif (Lowary and Uhlenbeck, 1987) and MCP (Peabody, 1993; Lim and Peabody, 1994; LeCuyer et al., 1995) have been designed to further improve the binding affinity, making it a useful tool for transcript-specific mRNP purifications. By fusing MCP with affinity tags such as Glutathione S-transferase (GST) or Maltose Binding Protein (MBP), the *MS2* system has been used to capture complexes in various cellular contexts, including human spliceosomal complexes (Das et al., 2000; Jurica et al., 2002; Zhou et al., 2002; Deckert et al., 2006), RNPs associated with ncRNAs (Said et al., 2009; Yoon et al., 2012; Gong et al., 2012) and ribosomal complexes (Youngman et al., 2004; Youngman and Green, 2005; Barrett and Chin, 2010). By incorporating fluorescent tags, for example GFP, this system can be used for simultaneous visualization and affinity purification (Slobodin and Gerst, 2010). Furthermore, by fusing MCP with multiple tags (separated by TEV protease cleavage sites) or by combining *MS2* system with other systems such as *PP7*, effective approaches for RNA purification and visualization have been developed (Tsai et al., 2011; Hocine et al., 2013; Halstead et al., 2015).

Although *MS2* system has been widely used to label RNAs, inefficient dimerization of MCP leads to high background fluorescence due to unbound MCP in the imaging experiments (Wu et al., 2012, 2014). As not all the stem-loops are occupied by MCPs, RNAs are often not uniformly labeled, complicating the quantitative analysis (Fusco et al., 2003; Wu et al., 2012). These factors also contribute to the inefficient recovery of the target mRNAs in biochemical purifications. Previous studies using the *MS2* system to capture RNA-protein complexes assembled *in vivo*, have reported an efficiency ranging from 1 to 9% (Said et al., 2009; Tsai et al., 2011; Leppek and Stoecklin, 2014). Due to the high binding affinity between MCP and *MS2* stem-loops, elution of the purified complexes under native conditions is problematic. In addition to these difficulties, necessity of making transgenics, unclear rules on positioning the

stem-loops, acceptable limits on loop numbers and formation of aggregates on overexpression of coat proteins are the other limitations of this approach.

1.9.2 Proteomic analysis of RBPs: an alternative approach

Purification of protein complexes in an RNA-independent manner, is yet another approach for the identification of the core set and other associated *trans*-acting factors which possibly govern RNA-specific mRNP formation. Taking the advantage of its robustness, this method can be used to construct an inventory of proteins involved in cellular processes such as mRNA localization, to reconstitute higher order assemblies from recombinant proteins for functional and structural studies.

Due to the lack of comprehensive antibody collections or availability of efficient and/or specific antibodies, a more generic purification strategy is to fuse the protein of interest with a sequence readily recognizable by an antibody specific to the tag. *In vivo* purification of protein complexes essentially involves tagging a protein (bait), which will be incorporated into complexes with endogenous partner proteins. The bait can then be immunoprecipitated via the tag with high specificity in a single step, or in a two-step manner, as in the case of TAP tagging (Rigaut et al., 1999; Puig et al., 2001) and interactants can then be identified using MS. Together with chemical cross-linking, transient and weak interactions can also be captured, allowing detection of unstable protein complexes. Recently developed methods of BioID (Roux et al., 2013) and its variant Split-BioID (Munter et al., 2017; Schopp et al., 2017), which utilize a promiscuous biotin ligase to label proteins based on proximity, are other powerful tools to selectively isolate physiological protein complexes. Finally, isolated complexes can be integrated into interactome networks to gain functional insights into poorly characterized proteins while enhancing network-based analysis of sub-complex formation.

Several *Drosophila* systems that recapitulate *in vivo* conditions have been generated using homologous recombination (Dunst et al., 2015) or transposon-mediated cassette insertion (Protein-trap: Morin et al., 2001; Clyne et al., 2003; Quinones-Coello et al., 2006; Buszczak et al., 2007; Lowe et al, 2014; and Gene-trap: Venken et al, 2011; Nagarkar-Jaiswal et al., 2015), to study protein distribution at endogenous expression levels. More recently, BAC (Bacterial Artificial Chromosome) or fosmid transgeneomics have been utilized to tag genomic sequences and express the reporter gene as a third copy allele (Zhang et al., 1998b, 2008; Dolphin and Hope, 2006; Sarov et al., 2006, 2012, 2016; Poser et al., 2008; Hubner et al., 2010; Hein et al., 2015). These engineered transgenes maintain the endogenous promoters, intron-exon structure and other regulatory elements, thus providing a tagged functional copy of the gene, expressed at physiological levels. These resources together with

the rapidly emerging CRISPR/Cas9 technology (reviewed in Xu et al., 2015; Ren et al., 2017), present a valuable tool for genome-wide analysis of cellular processes in *Drosophila*.

IP coupled to mass spectrometry (IP-MS)

With the availability of gene/genome sequence databases and technical advances especially in instrumentation, IP-MS-based proteomics is becoming increasingly popular to analyze protein complexes and identify novel protein interactions. A typical IP-MS workflow is depicted in Fig. 7. Shotgun proteomics which does not focus on specific sites or proteins of interest, is the most commonly used method. Purified proteins are digested with a protease, commonly trypsin, and the resulting collection of peptides are separated by Liquid Chromatography (LC). The sequentially eluting peptides are ionized and analyzed by MS. By performing another MS measurement (tandem MS or MS/MS), additional information specific for the amino acid sequence of the peptide is recorded, making it possible to identify every
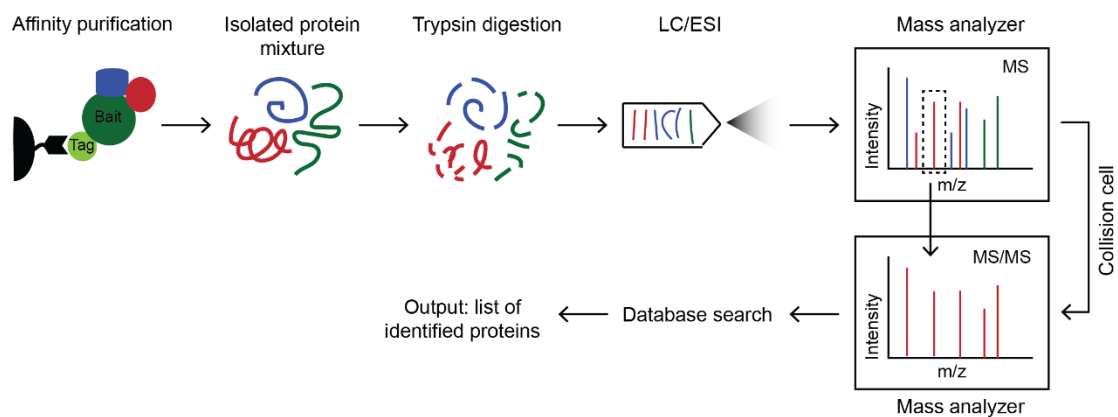
Fig. 7. Schematic representation of the IP-MS workflow

The workflow of IP-MS-based shotgun proteomics consists of multiple steps. Protein complexes isolated by affinity purification are digested proteolytically and the resulting peptides are separated by LC and ionized by electrospray (electrospray ionization, ESI). The ionized peptides are then transferred into the mass spectrometer for analysis. The instrument first records the peptide masses and ion intensities, referred to as MS1 (or MS) spectra. The individual peptides are then isolated and fragmented by the mass spectrometer. Fragments are recorded in the second spectral scan, referred to as MS2 or MS/MS. The peptide and fragment masses are used to identify the peptide, while the ion intensity is used for the quantification. Adopted from Meissner and Mann, 2014.

peptide unambiguously. For peptide identification, the raw MS/MS data is analyzed by matching the mass measurements to theoretical sequences, digested *in silico*, derived from a protein sequence database for the respective organism (reviewed in Angel et al., 2012).

To identify true interactants in an IP-MS experiment, it is desirable to know the exact amount of proteins in a given sample, or to be able to compare relative protein abundances among different samples. Methods have been developed for both absolute and relative quantification of proteins in MS experiments (reviewed in Elliott et al., 2009; Li et al., 2017). Absolute quantification, which provides the copy number of a protein in a cell or its concentration, can be obtained by spiking standard known amounts of the targeted protein or peptide into the samples. Quantification is done by comparison of the spiked compound to the target analyte. Relative quantification determines changes in the protein amounts relative to a control sample. The two main approaches for relative quantification are stable isotope-based labeling (quantitative) and label-free (semi-quantitative) methods. Labeled versions of specific molecules can be incorporated into the proteins or peptides, either by metabolic labeling (at the protein level; Ong et al., 2002; Shenoy and Geiger, 2015), enzymatic labeling (peptide level; Yao et al., 2001) or by chemical labeling (both protein and peptide levels; Gygi et al., 1999; Zhou et al., 2002; Li et al., 2003). Relative abundances are then calculated by comparing the intensities of isotopic isoforms derived from the same peptide in different samples (reviewed in Elliott et al., 2009; Li et al., 2017).

Metabolic labeling is accomplished by the addition of isotopically-labeled amino acids as a part of the normal protein synthesis, most commonly in cell culture (SILAC; Ong et al., 2002) and recently expanded to tissue samples and model organisms, including *Drosophila* (reviewed in Shenoy and Geiger, 2015). However, approaches used to label tissue samples and complete organisms are both costly and time-consuming, limiting the use of metabolic labeling to certain sample types. An alternative to metabolic labeling is *in vitro* chemical labeling, where the proteins/ peptides of a protein sample are labeled with stable-isotope containing reagents. Various approaches for chemical labeling have been developed, such as Isotope-Coded Affinity Tag (ICAT; Gygi et al, 1999), Dimethyl labeling (Hsu et al., 2003) and incorporation of isobaric mass tags (Thompson et al., 2003; Ross et al., 2004). In ICAT, cysteine residues in proteins are labeled using a thiol-specific reagent while in Dimethyl labeling, primary amines (N-terminus and side chain of Lysine residues) are converted to dimethyl amines to label the peptides (reviewed in Elliott et al., 2009; Hsu and Chen, 2016). Isobaric tagging techniques use a family of tags (up to 12-plex; Frost et al., 2015) which have overall identical mass, but differ structurally in the distribution of the heavy isotopes. These tags are mostly amine-reactive but tags that label cysteine residues and carbonyl groups are also available as commercial kits (reviewed in Rauniyar and Yates, 2014). The most commonly used isobaric tags are Tandem Mass Tags (TMT; Thompson et al., 2003), isobaric Tag for Relative and Absolute Quantification (iTRAQ; Ross et al., 2004) and the recently developed N,N-Dimethyl Leucine tags (DiLeu; Xiang et al., 2010). However, ICAT is limited in the exclusive tagging of cysteine residues and the isobaric labeling techniques show

variability in labeling efficiencies and require expensive reagents. In contrast, Dimethyl labeling techniques use relatively cheap reagents and have high reaction yields, accuracy and reproducibility (reviewed in Hsu and Chen, 2016).

While labeling-based MS methods are more accurate and reproducible, label-free methods are powerful alternatives to labeled MS as they are simpler, cost-effective and provide a deeper proteome coverage (Li et al., 2012). Label-free quantification relies on the observation that protein amounts correlate well with the peptide ion intensity (extracted ion currents, XIC), given sufficient mass resolution of the peptides. Alternatively, the counts of peptides selected for MS/MS sequencing (spectral counts) can also be used to calculate protein abundances. However, XIC-based approaches are superior as compared to spectral counting algorithms, especially for low-intensity peptide species and are more accurate and reliable (reviewed in Wong and Cagney, 2009). With technical advances in the LC-MS instruments and development of sophisticated algorithms such as MaxLFQ (Cox et al., 2014) for protein quantification, label-free MS is being effectively and routinely used, especially in experiments where relatively large fold changes (greater than fourfold) are expected (Cox and Mann, 2011; Nahnsen et al., 2013). For MS data acquisition and analysis, a wide range of proteomics softwares are freely available. The MaxQuant software (Cox and Mann, 2008), developed by Jürgen Cox and others at MPI of Biochemistry (Martinsried, Germany) can be used for analysis of both labeled and label-free data. MaxQuant output can be further analyzed by statistical tools for analysis of high-dimensional omics data, for example by the comprehensive Perseus framework (Tyanova et al., 2016).

2. Results

2.1 Biochemical characterization of a localized mRNP in *Drosophila*

2.1.1 Aims and significance

To date, our ability to systematically purify native mRNPs, to identify all associated components has been limited. Purifying a selected mRNP is particularly challenging as it requires a robust protocol which can efficiently enrich for a specific transcript from the pool of mRNAs, which represents a small percentage (3-5%) of the total RNAs in a cell (Jankowsky and Harris, 2015).

The aim of this project is to biochemically purify a localized mRNP from *Drosophila* egg chambers by combining Tandem Affinity Purification (TAP) tagging with RNA-based approaches of mRNP isolation. By generating novel transgenic flies where both the mRNA and the protein components of the mRNP are fused with affinity tags, I aim to purify an mRNP expressed at physiological levels, with high specificity. By isolating an mRNP in close to native purification conditions, the stoichiometry and structure of the complex can be preserved. Mass Spectrometric (MS) analysis will further help to identify associated *trans*-acting factors, including possibly novel components. As a starting point, *oskar* (*osk*) mRNA makes an excellent choice for this study, as it is abundant and has been very well characterized over the years (Lehmann and Nusslein-Volhard, 1986; Kim-Ha et al., 1991; Vanzo and Ephrussi, 2002; Jenny et al., 2006; Yang et al., 2015; Jeske et al., 2015; Hurd et al., 2016; Kistler et al., 2018; reviewed in Kugler and Lasko, 2009).

By specifically purifying an *osk* localizing complex in close to native conditions, the mRNP components can be identified and characterized. This information can then be used to reconstitute higher order assemblies *in vitro* for functional and structural studies. By extending this study further to other differentially localized mRNAs (such as *bicoid; bcd*), this two-step purification strategy may prove to be a powerful tool to identify core and transcript-specific components of localized mRNPs. Given the high degree of evolutionary conservation of several known components of the *osk* localizing complex such as the Exon Junction Complex (EJC; Tange et al., 2004) and Bruno (Webster et al., 1997), such a study can prove to be a valuable framework to transfer information to other systems, potentially providing a general understanding of the formation and regulation of localized mRNPs.

2.1.2 mRNP purification strategy

The experimental strategy I developed in this study to purify a transcript-specific mRNP includes several steps (Fig. 8). The key steps are:

1) Generation of transgenic fly lines where both mRNA and a known protein component of the *osk* mRNP are tagged in parallel.
2-4) Establishment of a hybrid TAP protocol using both a protein tag and an RNA tag to purify mRNPs. This includes optimizing material preparation and RNA tag-binding protein purification.
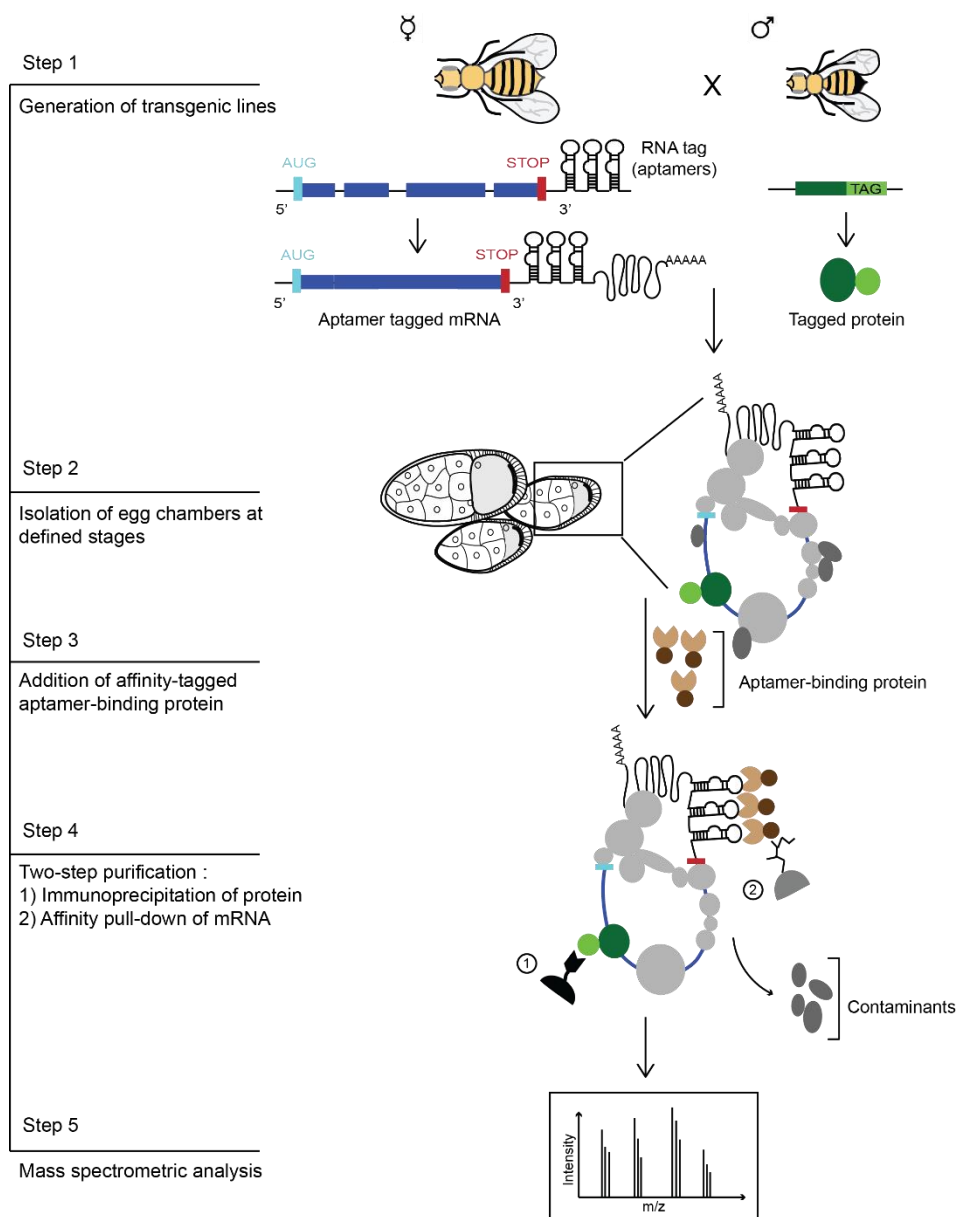5) MS analysis of native mRNPs isolated from egg chambers.

Fig. 8. Schematic representation of the experimental strategy

Step 1: Generation and characterization of fly lines expressing tagged osk mRNA

In order to generate flies expressing tagged RNA and protein, I first generated transgenic fly lines expressing tagged *osk* mRNA. Using naturally occurring bacteriophage derived aptamers, *MS2* and *PP7* (Bernardi and Spahr, 1972; Lim et al., 2001), I tagged *osk* genomic fragments with all the regulatory elements, to maintain endogenous levels of expression. *MS2* and *PP7* are well characterized RNA motifs and have been extensively used for *in vivo* RNA imaging (Bertrand et al., 1998; Forrest and Gavis, 2003; Zimyanin et al., 2008; Halstead et al., 2015; reviewed in Urbanek et al., 2014; Pena et al., 2015). These aptamers form hairpin loop structures, which are recognized by the corresponding coat protein with high specificity and affinity (Bernardi and Spahr, 1972; Lim and Peabody, 1994; Lim et al., 2001). To insert the aptamers, I used recombineering as it allows rapid and efficient modification of large fragments, independent of the restriction sites (Ejsmont et al., 2009, 2011). Using homologous recombination in *E. coli*, I first recombined the RNA aptamers into *osk* genomic fragments, and the clones were then introduced into the *Drosophila* genome as a third copy allele, at a specific site. I performed these experiments in collaboration with Dr. Pavel Tomancak, at MPI-CBG, Dresden.

To minimize the chances of a tag interfering with the localization or function of *osk*, I inserted the tags at a characterized site after the stop codon (Zimyanin et al., 2008). This region is predicted to be unstructured and is not conserved in insects. This region is also upstream of the BRE-AB (Bruno responsive elements; Kim-Ha et al., 1995; Webster et al., 1997) that ensures that Osk protein translation remains switched off during *osk* transport. In order to identify a tag with minimal effects on *osk* function but with maximal binding capacity, I created a series of tags with different number of aptamer repeats and in different combinations: *MS2-6X*, *MS2-12X*, *PP7-24X* and *MS2-12X+PP7-24X*. To select for the optimal tag to use in the mRNP purification, I assessed various parameters such as expression, localization, and the ability to rescue *osk* defects.

osk mRNAs tagged with *MS2-12X* and *MS2-6X* were observed to be localized as expected (in the endogenous background), as the otherwise uniformly expressed Venus-tagged MS2 coat protein (MCP) was then observed at the posterior of the oocyte (Fig. 9A). Moreover, both the constructs were found to be expressed well at near endogenous levels, which is critical to preserve the complex stoichiometry in subsequent purifications (Fig. 9B). The other two constructs either failed to localize correctly (*MS2-12X+PP7-24X*) or were not detectable by Northern blot (*PP7-24X*), and hence were not examined further.

osk 3'UTRs, independent of the coding sequence, are capable of localizing by forming dimers with the endogenous transcripts (Jambor et al., 2011). This "hitchhiking" can be exploited by

localization-incompetent transcripts, by associating with mRNAs in transport-competent mRNPs, for their efficient localization (Hachet and Ephrussi, 2004; Jambor et al., 2011). Therefore, it was important to check if the tagged constructs can localize correctly in an *osk* RNA null background. For this, I recombined the transgenes with an *osk* deficiency [Df(3R)p-XT103] and then crossed them with an *osk* RNA null mutation [*oskA87*]. By staining the RNA in the ovaries of the trans-heterozygotes, via *in situ* hybridization assay, I could show that both *MS2-6X* and *MS2-12X* constructs can localize correctly to the posterior of the oocyte, also in the absence of endogenous *osk* (Fig. 9C). Genetic crosses further revealed that these constructs can also rescue early oogenesis defects of *osk* mRNA null mutation, as eggs were successfully laid. However, only some of the eggs could hatch into adults and these flies exhibited grandchild-less phenotype, suggesting that the tagged mRNAs are not fully functional (Fig. 9D). While full rescue of *osk* null phenotypes would be ideal, posterior enrichment of *MS2*-tagged RNAs suggests that the complex required for *osk* localization was preserved in these transgenics.

Characterization of fly lines expressing known osk mRNA-binding proteins

Through genetic and biochemical studies, several *osk* mRNA-binding proteins have been identified and characterized (reviewed in Kugler and Lasko, 2009). For this study, I selected transgenic fly lines expressing tagged versions of five such proteins, namely eIF4AIII, Staufen (Stau), Hrp48, Glorund (Glo) and Vasa (Vas). These fly lines are a part of the fly-TransgeneOme (fTRG) library (Sarov et al., 2016) and express C-terminal superfold-GFP (sGFP)-tagged proteins. I assessed all the selected fly lines for localization of the tagged protein and the ability to rescue mutant phenotype. Details are provided in second part of this chapter.
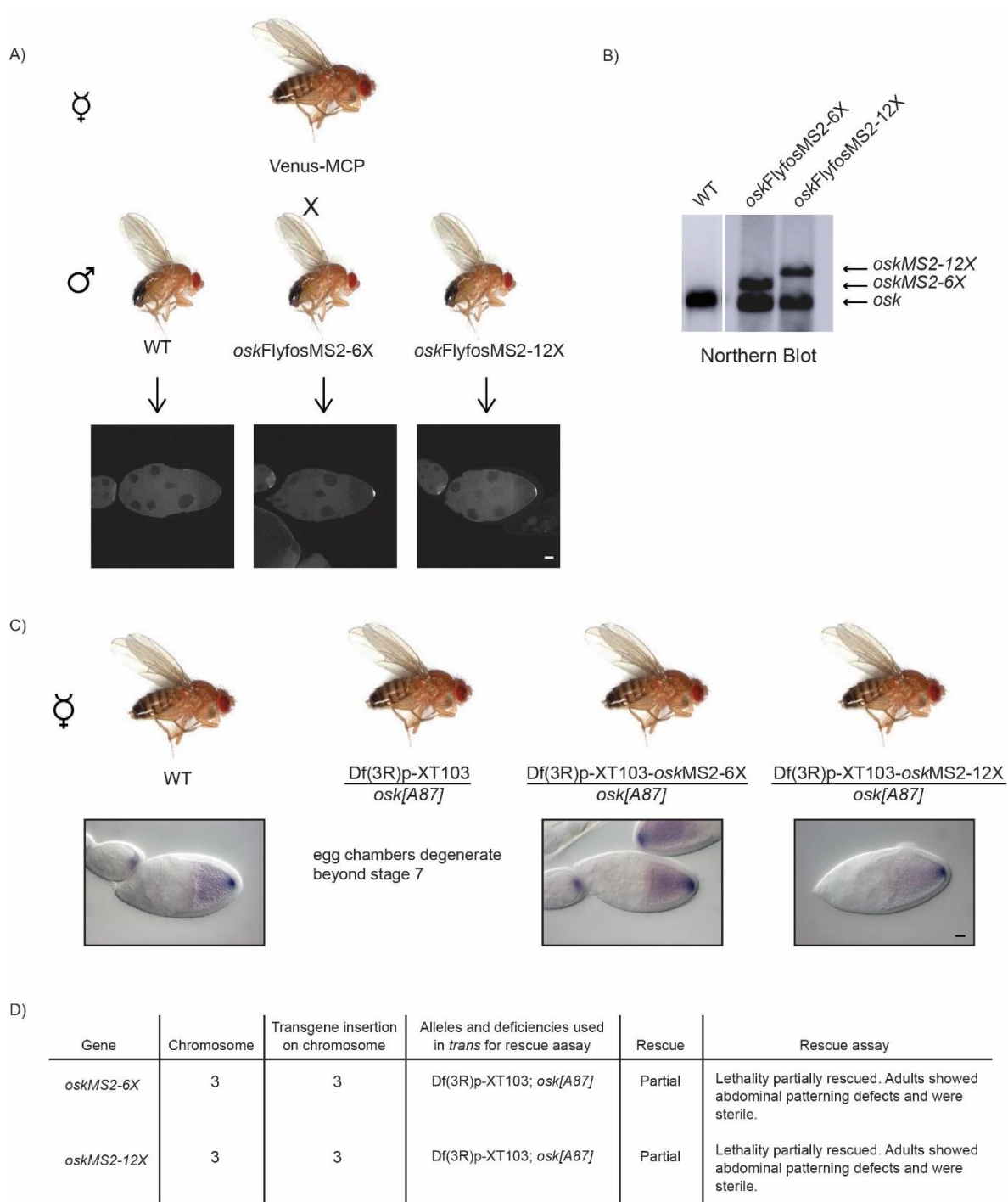
Fig. 9. Characterization of transgenic flies expressing *MS2*-tagged *osk* mRNA

(A) Flies expressing tagged *osk* were crossed to flies expressing the fluorescently labeled MCP and stage 9 egg chambers of the offsprings were examined. Flies expressing MCP alone were used as a negative control (left most). Shown below the crosses are the confocal images of the egg chambers analyzed. In all the images, Venus signal is shown. (B) Expression levels of tagged *osk* mRNAs were analyzed using Northern blot. Wild-type flies were used as a positive control. (C) A DIG-labeled anti-sense *osk* RNA probe was used to analyze the localization of tagged mRNA in an *osk* null background. Shown are the microscopy images of the *in situ* hybridization assay. Anterior is to the right and posterior is to the left. Scale bar 20 *µ*m. (D) Rescue assay results: females expressing tagged *osk*, in an *osk* null background, were crossed to wild-type males and offsprings were scored for viability and fertility.

Step 2: Optimized protocol for large-scale isolation of stage-specific egg chambers
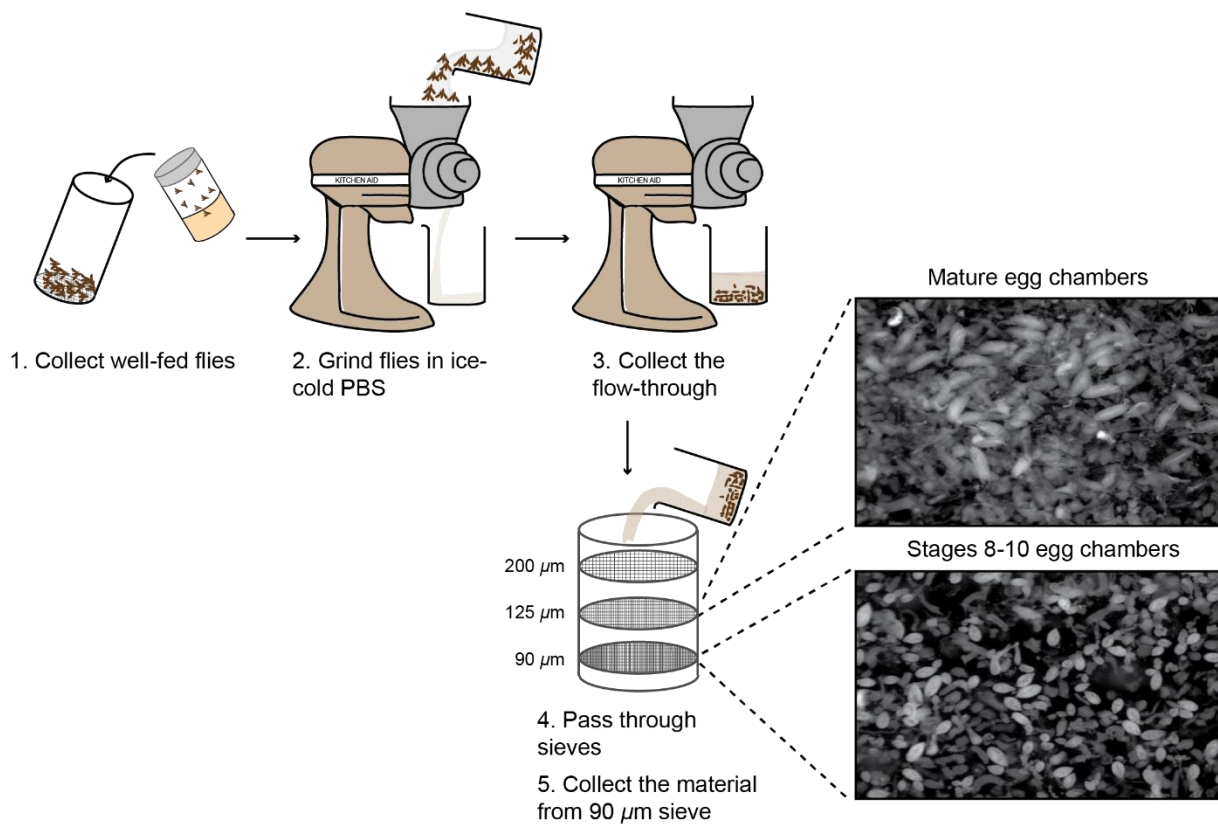
Fig. 10. Schematic representation of the method used to isolate egg chambers, at defined stages, on a mass scale. In the images on the right, the material collected from 125 *μ*m and 90 *μ*m sieves is shown.

Purifying mRNPs is a challenging task as mRNAs are often expressed at low levels and various *trans*-acting factors bind transiently to the mRNAs, making it difficult to obtain quantities sufficient for subsequent analysis. During *Drosophila* oogenesis, mRNAs are transported from the nurse cells to the oocyte in a translationally repressed state and are activated upon localization. This tight regulation is achieved by association of several proteins at different stages of localization, changing the composition of the mRNP both spatially and temporally. Therefore, in order to purify a homogenous population of a specific mRNP, it is important to isolate egg chambers at defined stages. For this, I optimized an established protocol from the Tomancak lab to isolate egg chambers on a mass scale (Jambor et al., 2015). In this method, I mechanically disrupted the ovaries and using size-selection steps, isolated stages 8-10 egg chambers in large amounts (Fig. 10). These stages of egg chambers are ideal for purifying a localized *osk* mRNP, as *osk* mRNA begins to accumulate at the

posterior of the oocyte at late stage 8 (Markussen et al., 1995). On inspecting the isolated material under the microscope, I observed that egg chambers collected with a sieve of mesh size 90 μm best represented the desired developmental stages, as shown in Fig. 10.

Step 3: Protein purification of recombinant MCP

MCP binds to *MS2* hairpin as a dimer, with high specificity and affinity (Bernardi and Spahr, 1972; Lim and Peabody, 1994; Ni et al., 1995; Chao et al., 2008). In order to co-precipitate *MS2*-tagged *osk* mRNA, MCP fused with an affinity tag was expressed in *E. coli*. To select an optimal tag, I expressed MCP with a series of different N-terminal tags: His, GST and His-MBP (hereafter referred to as MBP). A recent study by Wu et al. (2012) showed that tagged single-chain dimers of MCP are more efficient for *in vivo* imaging, as these constructs are able to dimerize more efficiently and hence can effectively label the RNA at lower concentration, resulting in a lower signal-to-noise ratio. Therefore, I also expressed a tandem version of the MCP, as N-terminal MBP-tagged (MBP-tdMCP), in *E.coli* cells. I optimized a protocol to purify all the MCP variants in large scale, along with MBP, to serve as a control. GST control was purified by Jonas Mühle in the lab. I could successfully purify all the tagged MCPs, as shown by Size Exclusion Chromatography (SEC) profiles in Fig. 11. Chromatograms of the intermediate steps are shown in supplementary Fig. 1.

To ensure that the purified proteins can bind to their target RNA with high specificity *in vitro*, I incubated purified GST-MCP with the *MS2* hairpin. An unstructured ssRNA (U_{20}) and an unrelated structured RNA (UA-rich sequence) were used as controls. Upon analyzing the resulting RNA-protein complexes by SEC, I could demonstrate that recombinant MCP binds specifically to its cognate hairpin, but not to ssRNA or to an unrelated RNA hairpin (Fig. 12). This shows that the *MS2*-specific binding activity of the MCP has been preserved during the purification process. The same approach was used to verify other MCP fusion proteins, such as MBP-MCP (supplementary Fig. 2), indicating that the tags did not interfere with the binding activity of the coat protein.
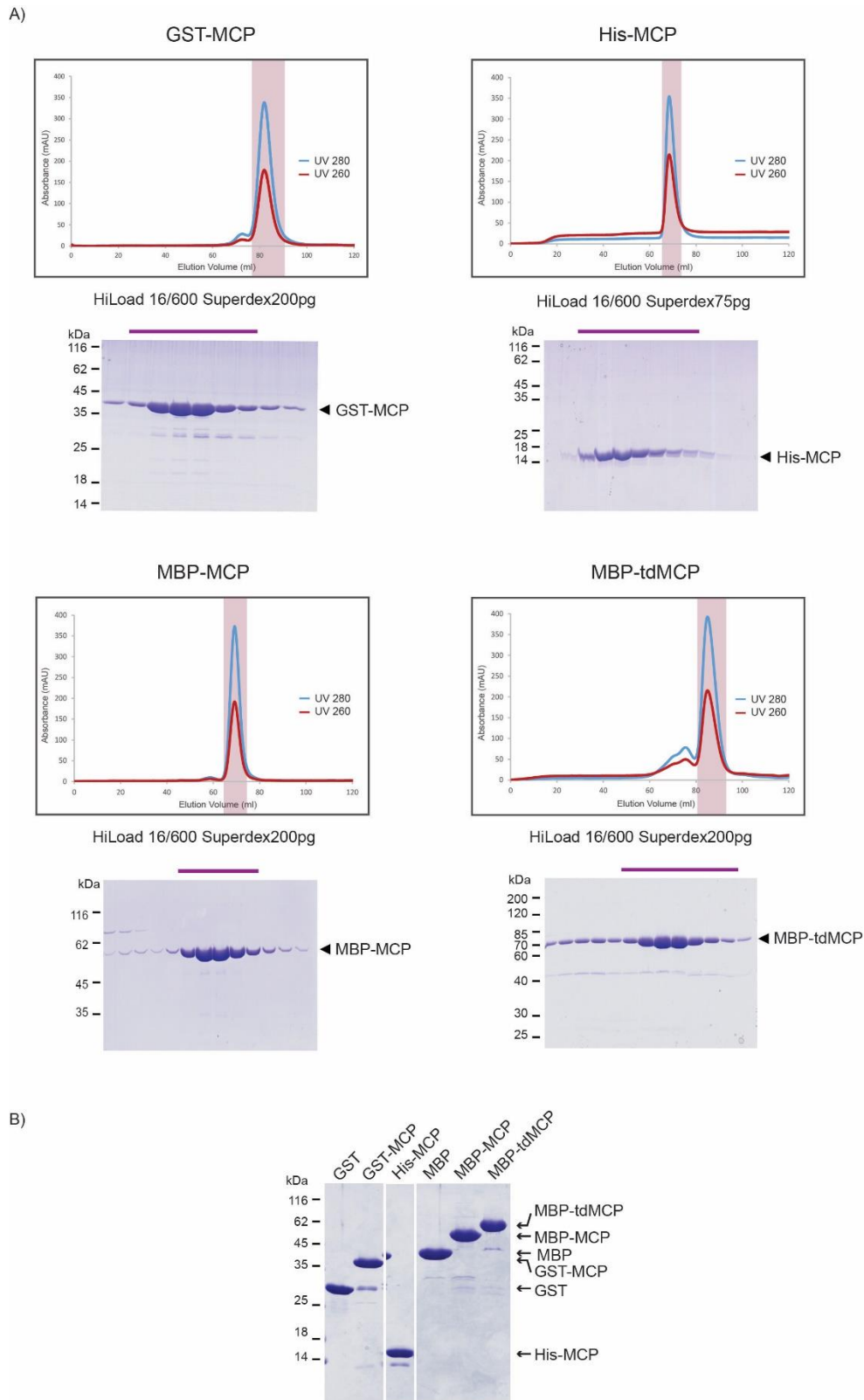
Fig. 11. All recombinant MCP fusions could be purified successfully.

(A) Representative SEC profiles of the differently tagged MCP. Highlighted are the peak fractions collected and the corresponding protein bands as observed on SDS-PAGE gels (below). Elution profiles show UV absorption at 280nm (blue) and 260nm (red). (B) A representative SDS-PAGE gel showing all the purified proteins.
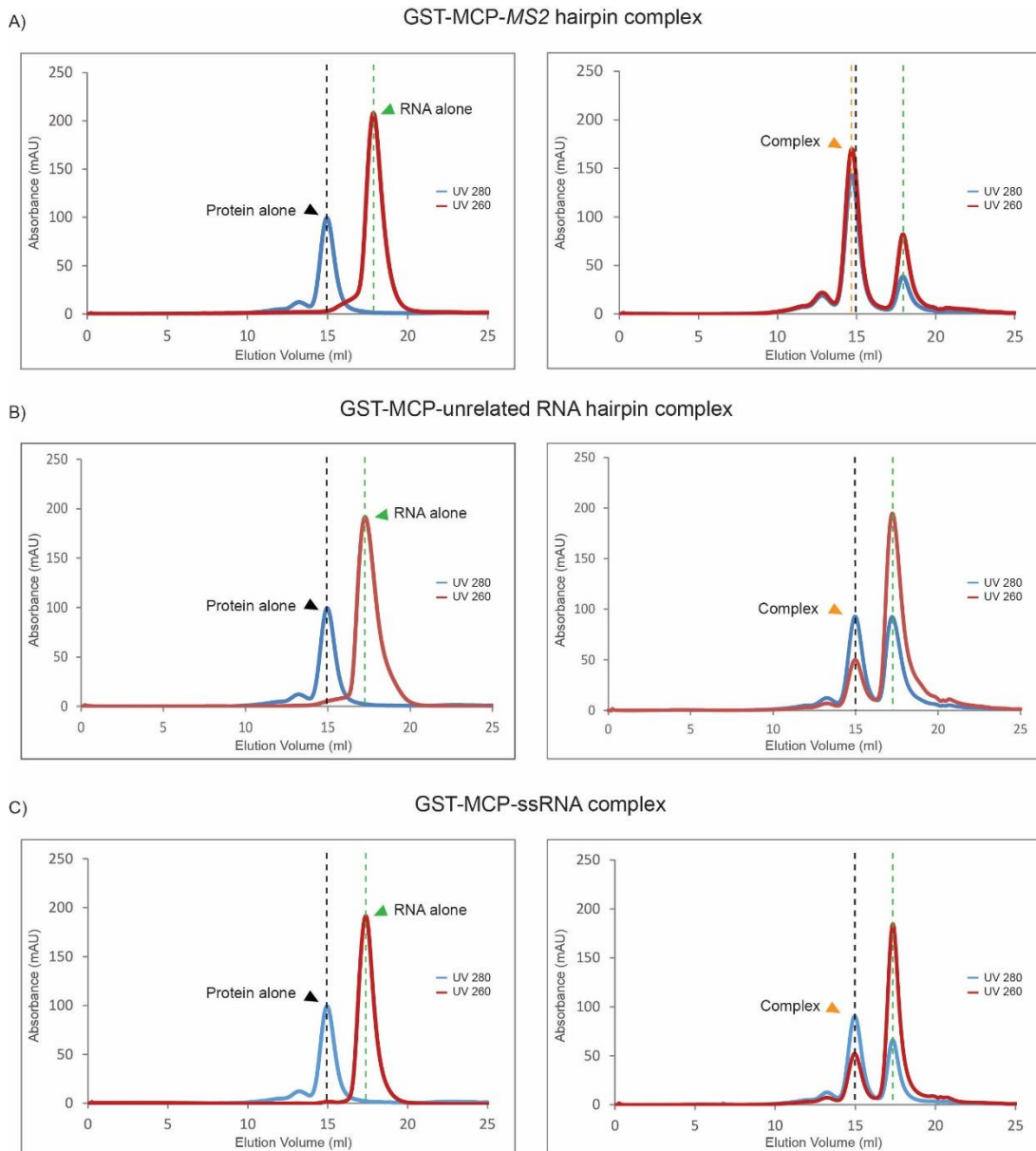
Fig. 12. MCP binds to *MS2* hairpin with high specificity

SEC profiles of the GST-tagged MCP in complex with *MS2* hairpin (A), an unrelated RNA hairpin (B) and ssRNA (C). Profiles for RNA and protein are shown on the left, while the RNA-protein complex is shown on the right. Elution profiles show UV absorption at 280nm (blue) and 260nm (red). Elution volume of the reference protein is marked by a dotted black line; the reference RNA in a dotted green line and the complex in a dotted orange line.

Step 4.1: Protein pull-down by immunoprecipitation (IP)

For the first step of mRNP purification, I established an optimized protocol to pull-down a tagged *osk*-binding protein from isolated egg chambers. By selecting different proteins, temporally and spatially separated *osk* mRNPs can be isolated. IPs were done using the

GFP-TRAP system (Chromotek). All the proteins could be successfully purified. Details are provided in second part of this chapter.

Step 4.2: mRNA purification using affinity-tagged MCP

For the second step of mRNP purification, I developed a protocol to purify and detect the tagged mRNAs. This is a key step for the isolation of a transcript-specific mRNP. In order to set up optimal conditions for the purification, I used total RNA extracted from the isolated stage-specific egg chambers of flies expressing *MS2-12X*-tagged *osk* mRNA. I then tested different tags and tandem/non-tandem versions of MCP for their ability to capture the aptamer-tagged *osk* and analyzed the results using Northern blotting. I further optimized the buffer conditions (see methods and materials) to maximize the recovery and purity of the tagged mRNA. I also used a constitutively and abundantly expressed *ribosomal protein 49 (rp49)* mRNA as an internal control, to assess the specificity of MCP (Fig. 13).

Even though I could successfully purify the tagged mRNA, only up to a maximum of 29% of the input tagged RNA could be retained on beads (quantified by comparing the band intensities of the input and pull-down samples on the Northern blot; Fig. 13). MBP-tdMCP showed the highest efficiency (29.3%) as compared to GST-MCP (24.5%) or MBP-MCP (7.7%). Endogenous *osk* was also enriched with the tagged *osk*, which can be explained by the dimerization of the osk 3'UTRs (Jambor et al., 2011). However, in the absence of tagged *osk* (in the wild-type samples), MCP still enriched the endogenous transcript, irrespective of the tag used. This suggests a general binding of the MCP to unspecific RNAs present in the lysate, as the tags in the absence of MCP showed no binding. This is further demonstrated by the detection of *rp49* in the MCP pull-downs.

In order to obtain a transcript-specific mRNP, the issue of specificity and homogeneity needs to be solved. The recovery of the tagged transcript also needs to be improved to obtain amounts sufficient for subsequent analysis.
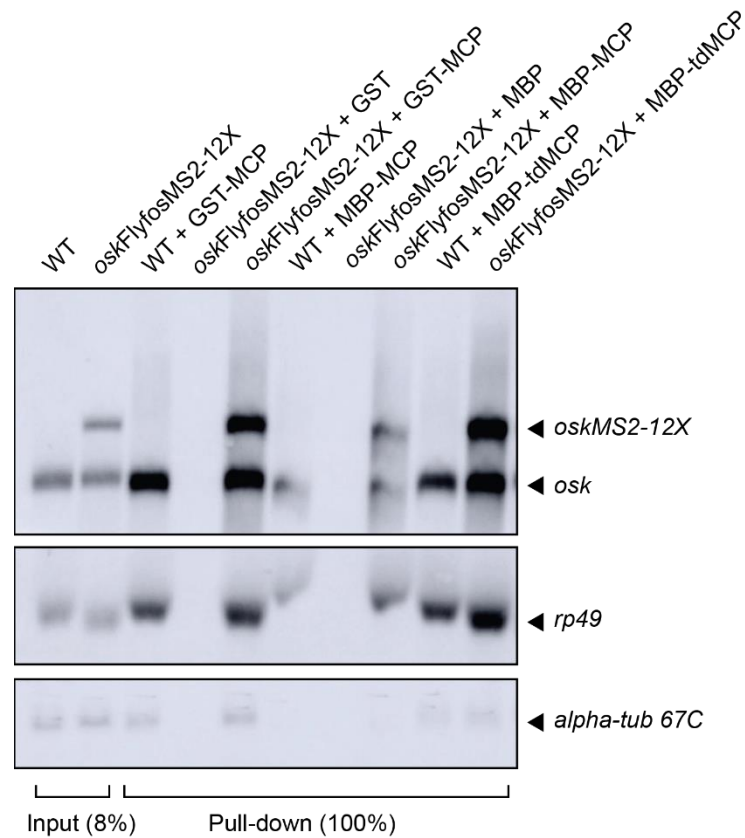
Fig. 13. Recombinant MCPs can successfully precipitate aptamer-tagged *osk* mRNA *in vitro*.

Shown above is a representative Northern blot. *MS2*-12X-tagged *osk* mRNA was affinity-purified using GST-MCP, MBP-MCP and MBP-tdMCP, from total RNA extracted from isolated egg chambers. Wild-type *osk* mRNA and tag alone (GST and MBP) were used as negative controls. The membrane was hybridized with *osk* and *rp49* probes to check for efficiency and specificity, respectively. *Alpha-tubulin (at 67C)* was used as a loading control in the input and as a purity check of the precipitate in the pull-down.

2.2 Proteomic analysis of RNA-binding proteins (RBPs) in mRNA localization in *Drosophila*

2.2.1 Aims and significance

Genetic and biochemical studies in *Drosophila* have identified several proteins involved in the localization of four key maternal transcripts which define the future embryonic axes: *bcd*, *osk, gurken (grk)* and *nanos (nos)*. For efficient localization, RBPs must bind to specific elements in these transcripts and couple them to the appropriate localization machinery. Interestingly, several of these RBPs are required for localization of more than one mRNAs, suggesting that common RNA localization factors might be coupled with additional interactors to regulate localization of mRNAs to distinct regions of the oocyte.

While several global proteomic datasets from different developmental stages (including oocytes, embryos, larvae, pupae, adults) as well as cell lines (S2 and Kc) are available (Brunner et al., 2007; Kronja et al., 2014; Valentzas et al, 2015), few attempts have been made to construct an inventory of proteins involved in mRNA localization in *Drosophila* oocytes. The aim of this project is to purify several RBPs that are known to regulate the localization of maternal mRNAs at different developmental stages and identify their interactants. This constitutes the first step to construct an inventory of proteins for future functional studies. By comparing the RBP-associated proteomes, this approach can prove to be a useful tool to identify components of the localization machinery and also possibly to decipher how the differential targeting of these mRNAs is achieved. Constructing an interaction network of proteins will further help to gain mechanistic insights into the functional components of a localized mRNP and will help to provide a general understanding of the regulation of developmental mRNAs.

2.2.2 Characterization of fly lines expressing RBPs involved in mRNA localization

To perform IPs, I selected six RBPs, eIF4AIII, Glo, Hrp48, Nos, Stau and Vas, that are known to regulate localization of one or more maternal mRNAs at different developmental stages in *Drosophila*. The fly lines expressing these tagged RBPs are a part of recently published fTRG library (Sarov et al., 2016). These transgenic lines express C-terminally-tagged proteins, close to endogenous levels. The 40kDa tagging cassette consists of "2XTY1-sGFP-V5-preTEV-BLRP-3XFLAG" (Sarov et al., 2016) that can be used for affinity purification. To serve as a control, I generated a transgenic line expressing the tag alone (hereafter referred to as GFP for simplicity). To avoid overexpression of GFP, I placed the the tag under a promoter of a moderately expressing gene (*exu*) and the construct was inserted in the genome at a specific site. The embryo injections to generate the transgenics were performed by Kristina Ile in the lab.

In order to ensure that the RBP fusions are functional *in vivo*, various approaches were used. First, I checked their localization patterns *in vivo*, using confocal microscopy. For this, I examined egg chambers at different stages of oogenesis (Fig. 14A, B) and could show that all the proteins localize as expected (Hay et al., 1988a, 1988b; St Johnston et al., 1991; Wang et al., 1994; Liang et al., 1994; Yano et al., 2004; Palacios et al., 2004; Kalifa et al., 2006). Egg chambers from flies expressing GFP showed a uniform expression in the nurse cells and the oocyte nucleus, while the wild-type egg chambers (control for autofluorescence) showed no signal, demonstrating that these flies serve well as controls (Fig. 14A). In agreement with the previous reports, eIF4AIII-GFP signal was observed in the nucleus of the nurse cells and localized to the posterior of the oocyte at stage 5. (Fig. 14A; Palacios et al., 2004). eIF4AIII enriches weakly at the posterior at stage 9 (Palacios et al., 2004), which however, could not be detected in my samples (Fig. 14A). Glo-GFP was detected in the nucleus of the nurse cells, oocyte and in the surrounding follicle cells (Fig. 14A; Kalifa et al., 2006). Hrp48-GFP was present in the cytoplasm of the nurse cells and was observed to be localized to posterior of the oocytes at stage 9, similar to Vas-GFP (Fig. 14A; Yano et al., 2004). The nuage localization of GFP-tagged Vas at early stages was also observed, consistent with the previous studies (Fig. 14A; Hay et al., 1988a, 1988b; Liang et al., 1994). At stage 8, Stau-GFP was concentrated at the anterior of the oocyte, while stage 9 egg chambers showed a strong posterior enrichment (Fig. 14A; St Johnston et al., 1991). Nos-GFP could be detected only via antibody staining (Fig. 14B). In embryos, Nos primarily localizes to the posterior (Wang and Lehmann, 1991). In the nurse cells of stage 10 egg chambers, it showed a strong uniform GFP expression, as also observed by Wang and colleagues (1994). Nos function at this stage is not known, making it an interesting protein to investigate further.

Since all the transgenes were introduced in a wild-type background, I next checked their ability to rescue the effects of mutations that cause either lethality or sterility. For this, I set up the crosses and assessed the trans-heterozygotes for embryonic lethality or female sterility. For *nos, stau* and *vas,* the phenotype of the individual is dependent on the genotype of the mother (maternal gene effects). Therefore, the trans-heterozygous females of these genes were further crossed to wild-type males to test for phenotypic rescue. The crosses and the results are summarized in Fig. 14C. Only half of the transgenes assayed were found to be fully functional (Fig. 14C), probably due to the instability of the fusion protein. However, the ability to recapitulate endogenous protein localization pattern (Fig. 14A, B) suggests partial functionality, which is adequate for my experiments since I am interested in the localization events during oogenesis.
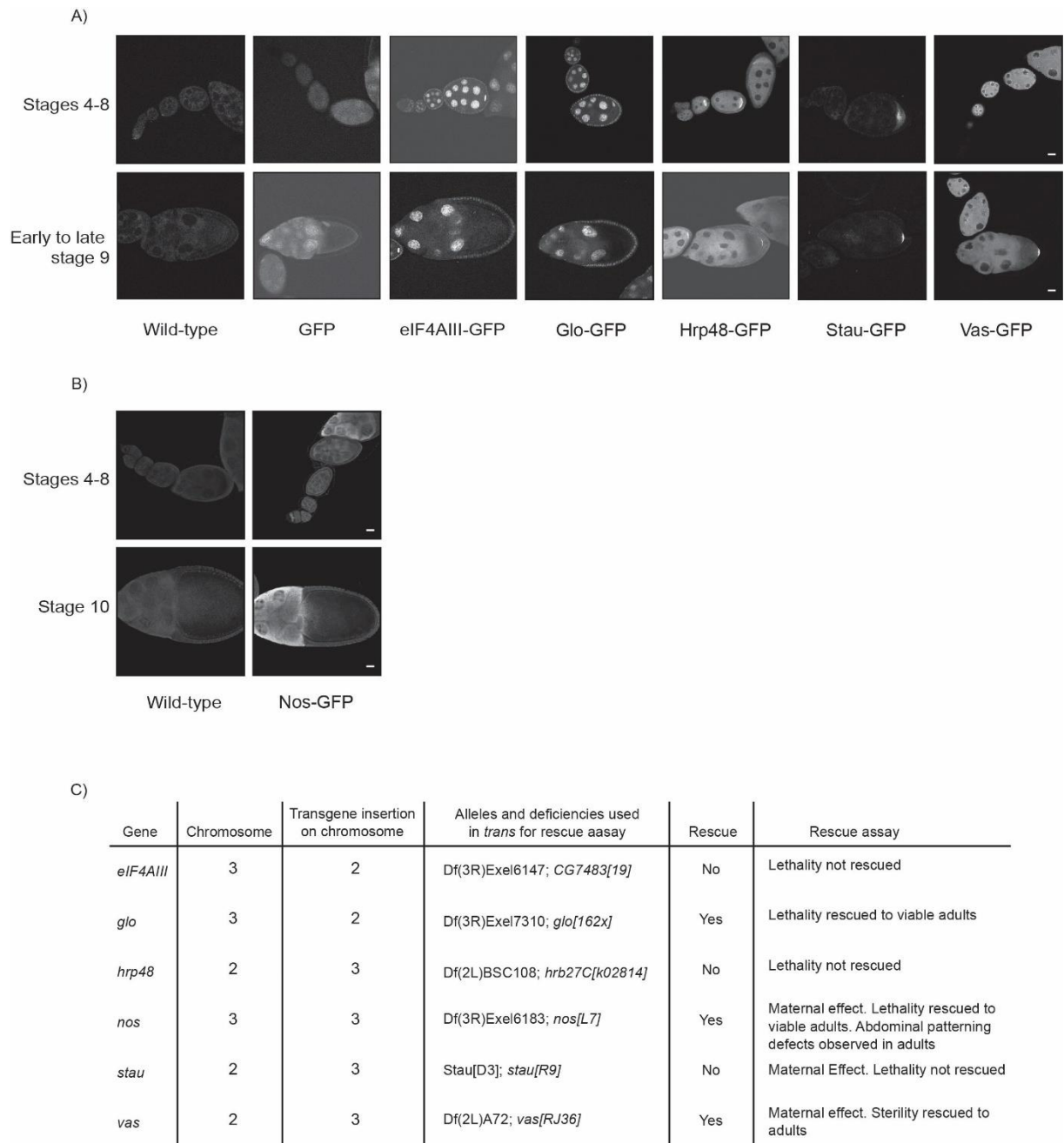
Fig. 14. Localization patterns in the egg chambers and genetic rescue of the RBP fusions

(A) Images showing localization of the GFP-tagged proteins, in stages 4-9 egg chambers. Wild-type flies and flies expressing GFP serve as negative and positive controls, respectively. (B) *nos* ovaries immunostained for GFP show a uniform expression in the nurse cells of stage 10 egg chambers. Wild-type flies serve as a negative control. In panels A and B, GFP signal is shown. Anterior is to the left and posterior is to the right. Scale bar, 20 *µ*m. (C) Table summarizing the genetic rescue of the mutant phenotypes with the transgenes. Respective mutations used for the rescue assay to assess the functionality of the transgenes *in vivo*, are indicated.

The table in panel C:

Gene	Chromosome	Transgene insertion on chromosome	Alleles and deficiencies used in *trans* for rescue aasay	Rescue	Rescue assay
eIF4AIII	3	2	Df(3R)Exel6147; *CG7483[19]*	No	Lethality not rescued
glo	3	2	Df(3R)Exel7310; *glo[162x]*	Yes	Lethality rescued to viable adults
hrp48	2	3	Df(2L)BSC108; *hrb27C[k02814]*	No	Lethality not rescued
nos	3	3	Df(3R)Exel6183; *nos[L7]*	Yes	Maternal effect. Lethality rescued to viable adults. Abdominal patterning defects observed in adults
stau	2	3	Stau[D3]; *stau[R9]*	No	Maternal Effect. Lethality not rescued
vas	2	3	Df(2L)A72; *vas[RJ36]*	Yes	Maternal effect. Sterility rescued to adults

2.2.3 Isolation and identification of protein complexes by IP-MS

To co-purify factors associated with each of the RBPs involved in mRNA localization in the oocytes, I performed IPs from lysates of ovaries isolated from flies expressing GFP-tagged proteins (Fig. 15). IP from flies expressing GFP alone was used as a negative control to identify proteins binding unspecifically to the tag.
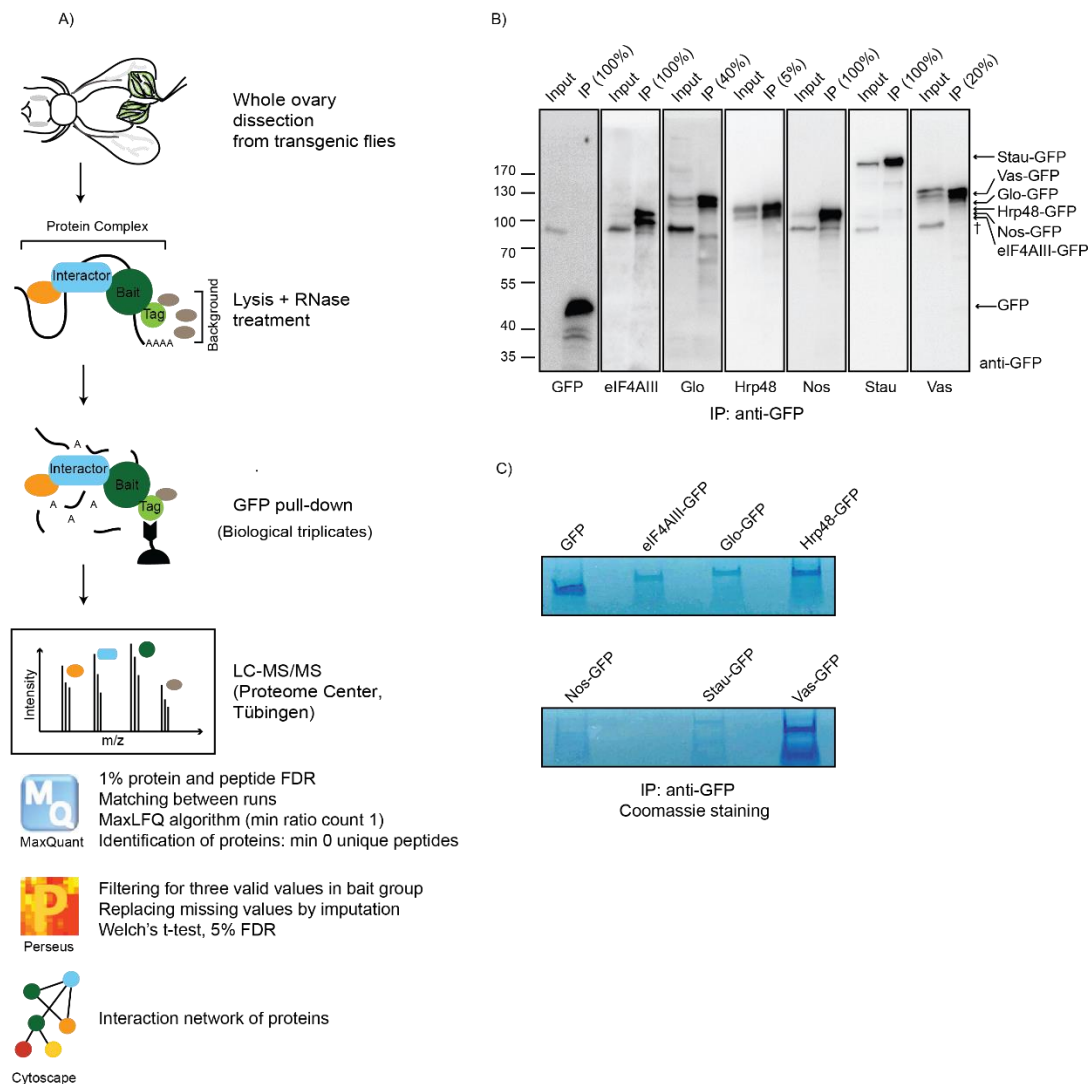
Fig. 15. Overview of the IP-MS workflow

(A) Schematic representation of the workflow (FDR: False Discovery Rate). (B) IPs were performed and analyzed by Western blot using anti-GFP. Inputs and eluates were loaded in different amounts for efficient visualization. Input of the total lysate: 2.1% for GFP, eIF4AIII, Nos; 4.2% for Glo, Vas, Stau and 1.2% for Hrp48. Loading of the respective eluates is highlighted on the top of each lane.† is an unspecific detection by the antibody (C) Shows a representative SDS-PAGE gel used for MS analysis. IPs were performed and bands were visualized by Coomassie staining. IP from transgenic line expressing GFP served as a negative control (B, C).

For IPs, whole ovaries were hand-dissected and maintained on ice to minimize protein degradation. They were collected in batches and flash-frozen for subsequent use. To be able to purify complexes close to their native composition, I performed lysis in mild salt and detergent conditions and developed an efficient protocol to purify complexes using the GFP-TRAP system (Chromotek). As I am interested in identifying RNA-independent protein-protein interactions, I performed the experiments in the presence of RNases and could successfully purify all the proteins (Fig. 15B). Since the transgenes are regulated by their endogenous promoters, their expression levels were highly different. This can be observed by comparing the intensity of input signals on the Western blots (Fig. 15B). Please note that for effective visualization, different amounts of inputs and eluates were loaded on the blots, as indicated in Fig. 15B.

To identify protein-protein interactions, label-free MS analysis was employed. Label-free quantification, which is a semi-quantitative approach, offers high processivity in terms of samples that can be compared at the same time, making it a suitable approach for multiple IP experiments. For analysis, experiments were performed in triplicates. To compensate for the variability in the expression levels, the number of flies for each transgene were up scaled accordingly (see methods and materials), to achieve a visible band on the gel (Fig. 15C). Given the sensitivity of the assay, weak bands such as those of Nos-GFP and Stau-GFP, were sufficient for the analysis.

Identification of significantly enriched proteins associated with selected RBPs by semi-quantitative label-free MS analysis

MS was done in collaboration with Prof. Dr. Boris Macek's group at the Proteome Center, University of Tübingen. LC-MS/MS reads were collected on a Proxeon Easy-nLC 1200 (Thermo Fisher Scientific) coupled to a QExactive HF mass spectrometer (Thermo Fisher Scientific). All the measurements were performed by Johannes Madlung in the lab of Prof. Dr. Boris Macek, at the Proteome Center. For confident identification of proteins and accurate intensity-based Label-Free Quantification (LFQ; Cox et al., 2014), I processed the raw data using the MaxLFQ module of the MaxQuant software (Cox and Mann, 2008). For generic statistical testing, I further used Perseus software (Tyanova et al., 2016) to identify specific interactors of the selected RBPs (hereafter referred to as baits for simplicity).

To effectively distinguish true interactors from contaminants, I designed an optimal MaxQuant workflow. For this, I tested different combinations of two MaxQuant parameters, namely the minimum ratio count (minimum number of peptide ratios required to consider protein ratios valid, for relative quantification; Cox et al., 2014) and the number of unique peptides (minimum number to unique peptides required for the identification of a protein). On using a minimum ratio count of 2, information on small proteins (for example the EJC component

Mago, which is a known interactant of eIF4AIII; Palacios et al., 2004) and the low-intensity background was lost, thus creating an enrichment bias. Relaxing the stringency of unique peptides to 0 resulted in the identification of Tral (including various isoforms), which is a known translational repressor of *nos* mRNA (Götze et al., 2017) and is a part of mRNP that includes other localization/translation factors such as Cup, Me31B and PABP (Wilhelm et al., 2005; Igreja and Izaurralde, 2011; Götze et al., 2017; Wang et al., 2017). This suggested that the combination of "minimum ratio count of 1" and "minimum unique peptides 0" are optimal parameters, as they retained positive controls without increasing the background noise and were used for the analysis. Additionally, I activated "matching between runs" algorithm to quantify unidentified or unsequenced peptides in the samples, by transferring peptide identifications among replicates.

Global analysis of the proteomes resulted in the identification of 14,978 peptides mapping to 1885 protein groups, at the FDR of 1% at the peptide and protein level. 1870 proteins were quantified in at least one of the 21 samples. Of these, 1850 proteins were unique, which account for 88% of the total ovary proteome of *Drosophila*, as previously reported (Velentzas et al., 2015).

Since normally distributed data is advantageous for statistical testing, I log transformed the LFQ intensity values and plotted the histograms for each sample separately, to verify that the data followed a normal distribution (Fig. 16). I then calculated Pearson correlation coefficients for all the samples (depicted as a heat map in Fig. 17A) and could show that all the replicates correlate well. Overall, the coefficient values ranged from 0.49 to 0.97, while the average correlation within replicates ranged from 0.72 (Glo) to 0.91 (Hrp48). To further assess the quality of the data, I generated a heat map (with hierarchical row clustering) of the LFQ intensities of all the samples (Fig. 17B) and demonstrated that all the baits were consistently enriched and the replicates profiles looked largely similar, with only minor differences due to technical variability. However, the number of proteins identified with each bait varied highly, as can be observed in the heat map, marked by the absence of quantitative information (Fig. 17B).

To enable statistical analysis, the missing values needed to be replaced by imputation. To prevent introducing artefacts, the random values generated should represent a normal distribution around the detection limit of the mass spectrometer. Since there was a considerable difference between the numbers of identifications for each bait (Fig. 17B), I grouped the replicates (of a given bait) together, to preserve the normality of the data for subsequent analysis. Imputation was performed on a bait-control pair, after discarding the proteins that were not reproducibly detected in one of the two replicate groups. This filtering

and imputation was repeated for each pair. Since it is important that these simulated low-intensity values fit well into the profiles of low abundant proteins, I plotted the histograms again and could show that the substitution of missing values did not disturb the overall distribution (Fig. 18). An overlay of histograms pre- and post-imputation is presented in supplementary Fig. 3.

To identify significantly enriched proteins associated with each bait, I performed the Welch's t-test (with the 5% FDR cutoff), post-imputation, on each bait-control matrix. Results are presented as volcano plots in Fig. 19. All the baits were highly enriched and I observed a minimal background, indicating the high specificity of the purifications. For some baits, such as eIF4AIII-GFP and Glo-GFP, few interactors were found to be significantly enriched, as compared to others. This difference in the number of detections is not likely due to differences in sample amounts used for MS analysis (as eIF4AIII-GFP was enriched in higher amounts as compared to Nos-GFP; Fig. 15C) but possibly due to loss of interactions upon RNase treatment. The partial functionality of some of the tagged proteins, suggested by the lack of rescue (Fig. 14C), might also be an explanation for the loss of associations.

For most baits, I found several known interactants (which served as positive controls) to be significantly enriched. This indicates that both the experimental conditions, as well as the parameters used for data analysis were optimal to preserve and identify true interactions. For example, all the other three core components of the EJC were co-purified with eIF4AIII-GFP (Palacios et al., 2004; Tange et al., 2005; Bono et al., 2006). Known partners of Vas, involved in the pole plasm assembly in the oocyte or piRNA-mediated gene silencing in the *Drosophila* germline, were also significantly enriched (Fig.19). In addition, other known components of both of these functionally distinct cellular pathways were also found to be associated with Vas-GFP, suggesting that not only direct interactants, but whole complexes were efficiently purified (supplementary Fig. 4).
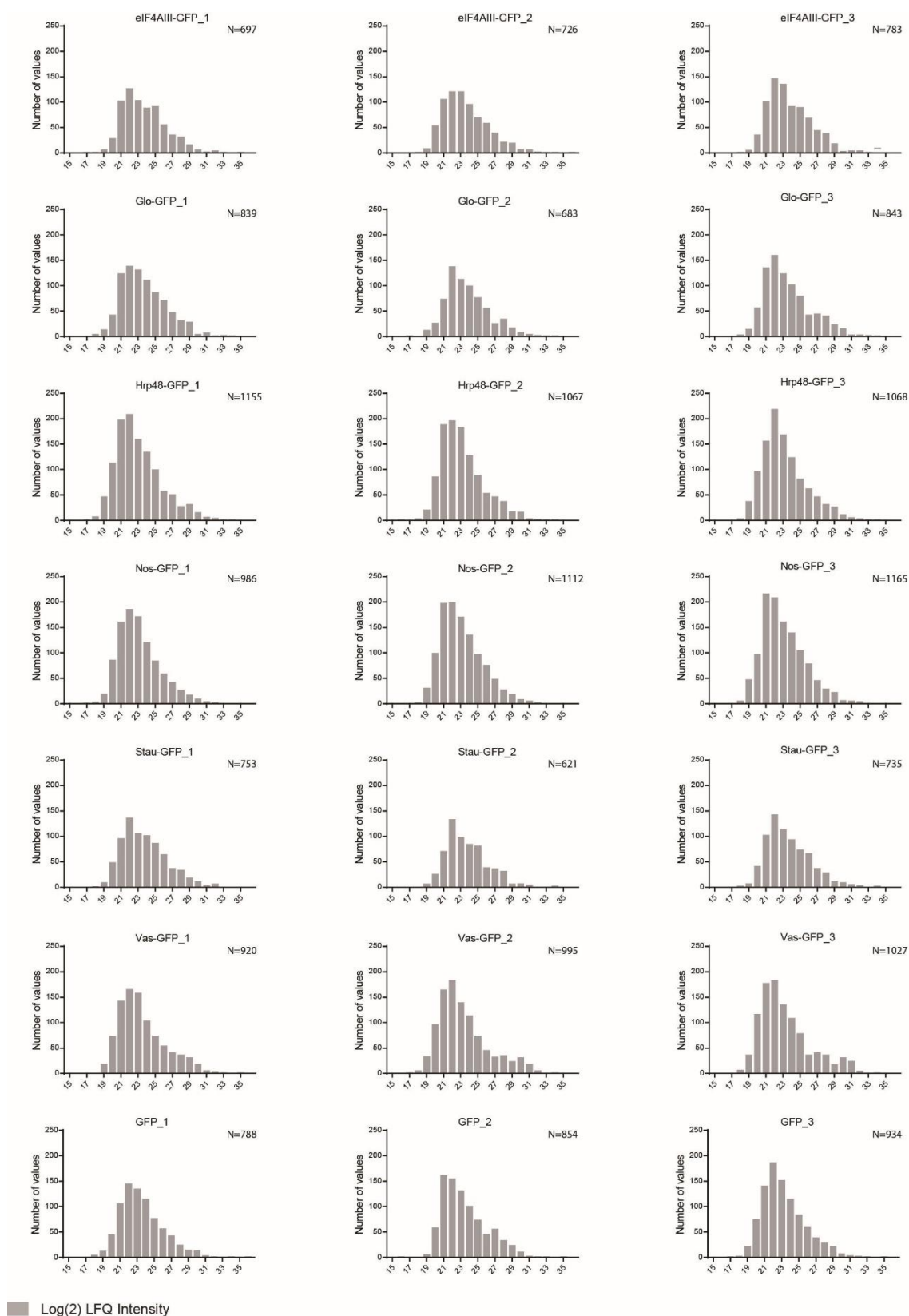
Fig. 16. The IP-MS data follows a normal distribution.

Frequency distribution of the logarithmized (Log2) LFQ intensities of all the proteins quantified in each IP, without data imputation. N is the total number of values. X axis represents the range of values; Y axis represents the number of values.

Fig. 17. Baits are consistently enriched in all the IPs

(A) Heat map representation of the matrix of Pearson correlation coefficients calculated for all the IP samples. The zoomed plots show the highest and lowest coefficient values (r) among the replicates. (B) Heat map of the logarithmized (Log2) LFQ intensities of all proteins quantified in each sample. Hierarchical row clustering was performed on data without imputation. The zoomed area shows the high enrichment of eIF4AIII-GFP and Hrp48-GFP in the three replicates. Missing quantitative information is highlighted in grey.

Fig. 18. The normality of the data is preserved post-imputation

Frequency distribution of the logarithmized (Log2) LFQ intensities of all the proteins quantified in each IP, after filtering and data imputation. The missing values were replaced with the substituted values from the normal distribution, for each bait-control matrix. For simplicity, control (GFP) plots are not shown. X axis represents the range of values; Y axis represents the number of values.
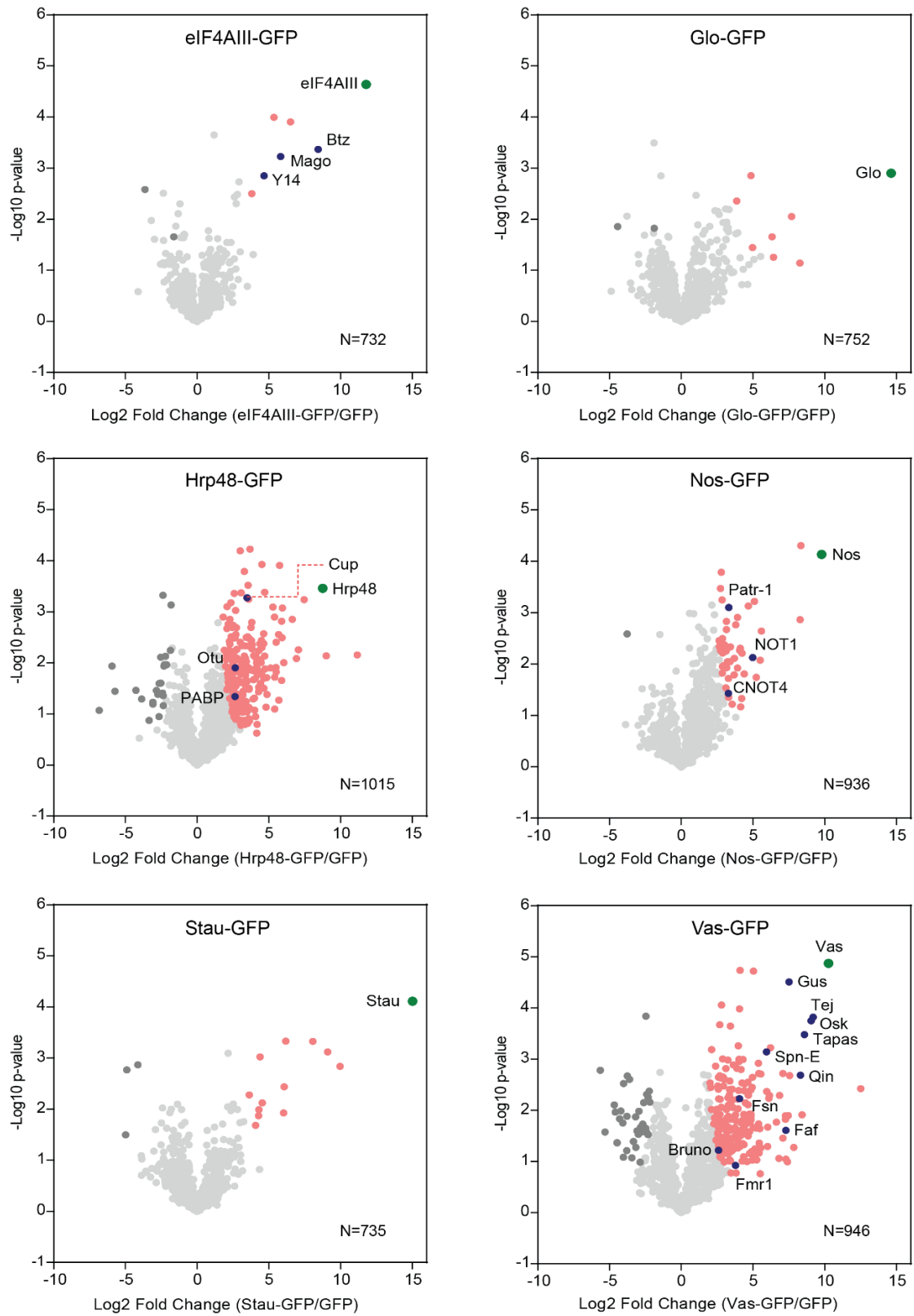
Fig. 19. Bait-associated proteomes differ in amount and composition

Volcano plots of proteins identified associated with each bait in the label-free MS analysis, after filtering and data imputation. The significance of enrichment was calculated using the two-tailed Welch's t-test with a 5% FDR cutoff. IP from GFP expressing sample served as a negative control. For each bait-

control pair, the resulting differences between the logarithmized means of the two groups "Log2(bait/control)" and the negative logarithmized p values were plotted against each other. N indicates the number of protein groups plotted. All the IPs were measured in triplicates. Each identified protein is represented as a dot in light grey; each bait is highlighted in green; significantly enriched proteins are highlighted in pink; known interactants are highlighted in blue; background binders are highlighted in dark grey.

Interestingly, I observed ribosomal proteins (components of both large and small subunits), which due to their abundance are typical background binders (Mellacheruvu et al., 2013), to be significantly enriched with Vas-GFP and Hrp48-GFP, but not with other RBPs analyzed (Fig. 20). Previous studies have shown the requirement of Vas in translational activation of *osk, nos* and *grk* mRNAs (Styhler et al., 1998; Tomancak et al., 1998; Gavis et al., 1996; Dahanukar and Wharton, 1996; Markussen et al., 1995). However, the molecular mechanism by which Vas activates translation is unclear. Studies in *Drosophila* have shown that Vas directly binds translation initiation factor eIF5B to regulate *grk* translation and possibly other germline-specific transcripts (Carrera et al., 2000; Johnstone and Lasko, 2004). In addition, Vas also interacts genetically with the translation initiation factor eIF4A for efficient germ cell formation (Thomson et al., 2008). However, in contrast to these reports, both eIF5B and eIF4A were either not detected or enriched in this dataset. Instead, I observed a high enrichment of other translation initiation factors such as eIF4G, eIF4E, eIF2, eIF3 subunits and eIF2B subunits (Fig. 20). These results suggest that Vas might be directly involved in the early steps of translation initiation. It is possible that Vas assists in recruiting factors required for mRNA activation and pre-initiation complex formation, and as a consequence binds to eIF5B. As eIF5B is released upon ribosome assembly, this binding to Vas can be transient and thus could not be detected (general translation initiation mechanism reviewed in Jackson et al., 2010; Hinnebusch, 2014).

Similar to Vas, Hrp48 is also involved in translational regulation of maternal mRNAs. However, in contrast to the translational activation function of Vas, Hrp48 is required for translational repression of *osk* and *grk* mRNAs (Gunkel et al., 1998; Goodrich et al., 2004; Yano et al., 2004). Interestingly, several lines of evidence, such as its binding to a derepressor element in *osk* 5'UTR (Gunkel et al., 1998) and co-immunoprecipitation with PABP (Clouse et al., 2008), suggest a yet uncovered role of Hrp48 in translational activation. Similar to Vas-GFP, ribosomal proteins along with translation initiation factors, especially eIF4E and eIF4G, were also observed to be significantly enriched with Hrp48-GFP (Fig. 20). However, further experimentation is required to exclude the possibility that the enrichment of translation initiation factors and ribosomal proteins in isolated Vas-GFP and Hrp48-GFP complexes are biochemical impurities.
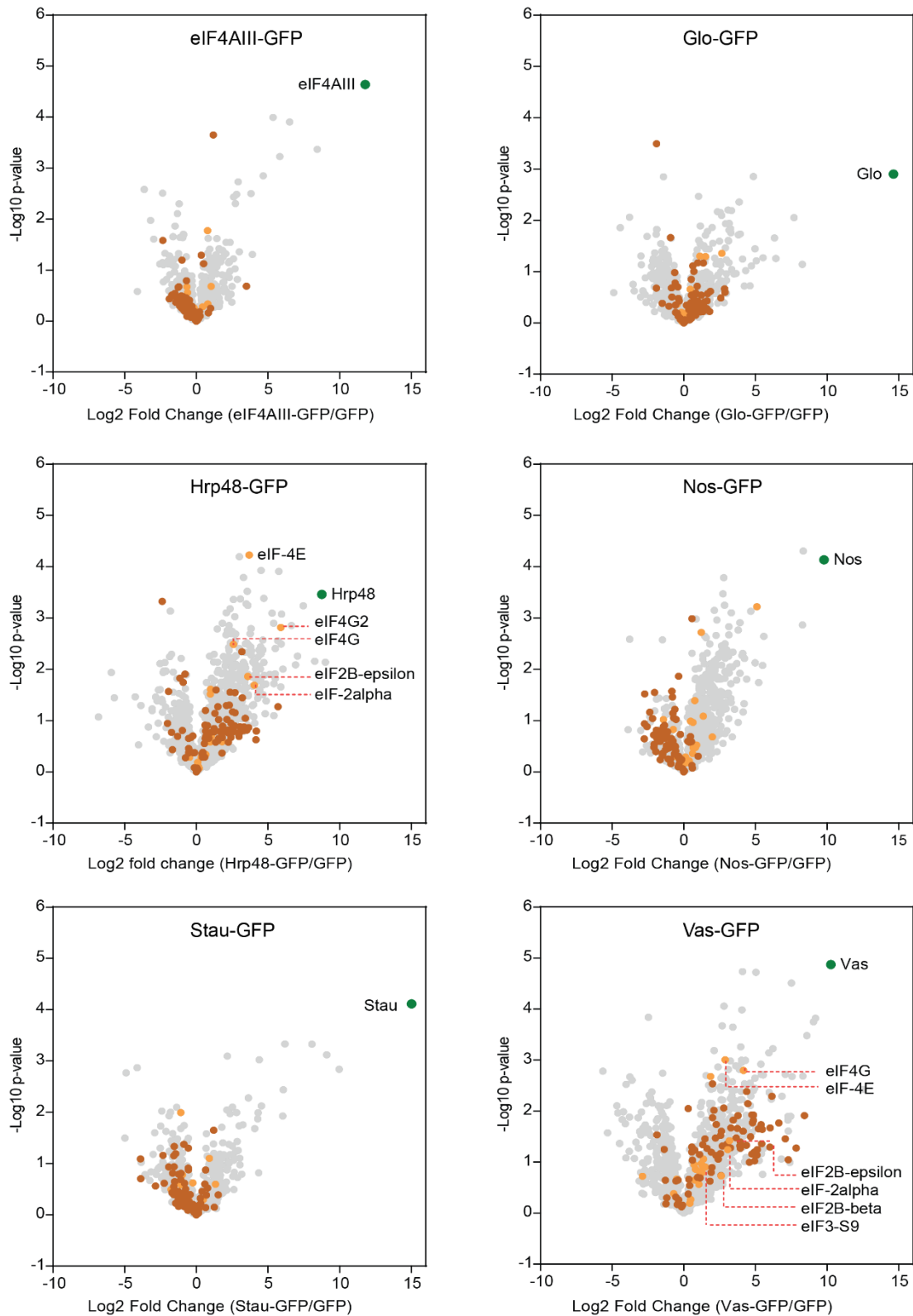
Fig. 20. Vas-GFP and Hrp48-GFP show higher enrichment of ribosomal proteins and translation initiation factors, differentially from the other RBPs but overlapping with each other.

Volcano plots showing the distribution of ribosomal proteins and translation initiation factors found associated with each bait in the label-free MS analysis, after filtering and data imputation. Significance of enrichment was calculated using the two-tailed Welch's t-test with a 5% FDR cutoff. IP from GFP sample served as a negative control. For each pair, the resulting differences between the logarithmized

means of the two groups "Log2(bait/control)" and the negative logarithmized *p* values were plotted against each other. N indicates the number of protein groups plotted. All the IPs were measured in triplicates. Each identified protein is represented as a dot in light grey; baits are highlighted in green; ribosomal proteins are highlighted in brown; translation initiation factors are highlighted in orange.

Quantitative analysis of proteins associated with Hrp48- and Vas-GFP, using Dimethyl labeling MS

Label-free MS techniques have several advantages. However, they are more sensitive to technical variability and do not provide accurate quantitative information. Conversely, labeling MS approaches can prove to be a helpful tool to detect small fold changes in protein abundances, due to the robustness and precise quantification. Therefore, the combination of labeled and label-free MS data can provide a comprehensive view of proteomes. Since its introduction in 2003 (Hsu et al., 2003), *in vitro* Dimethyl labeling of peptides has emerged to be one of the fastest and reliable chemical-labeling strategies for quantitative proteomics, especially for organisms such as *Drosophila*, where metabolic isotopic labeling is still challenging. However, the method is limited by its requirement of sufficient background to be able to calculate protein abundance ratios and the absence of background binding often leads to loss of information.

In Dimethyl labeling approach, peptides are labeled with isotopomeric dimethyl labels (light, medium and heavy), differing in mass by at least 4 Da. The labeled samples are mixed together and analyzed by LC-MS/MS, whereby proteins/peptides from different samples are distinguished based on the mass difference of the labels. Protein intensity is calculated by statistical evaluation of the peptide ratio counts while the abundance ratios are calculated by comparing the intensity of the differently labeled peptides (Boersema et al., 2009; reviewed in Hsu and Chen, 2016).

The experimental strategy for Dimethyl labeling MS is depicted in Fig. 21. Since only three conditions can be compared at a time, I selected Hrp48- and Vas-GFP, along with the GFP control, as these proteins express very well and have known interactions data available to serve as positive controls. I performed the experiments in duplicates and prepared the samples the same way as for label-free MS (Step 1, Fig. 21). All the subsequent steps were performed by Johannes Madlung in the lab of Prof. Dr. Boris Macek, at the Proteome Center. After in-gel digestion, peptides were labeled with heavy, medium or light isotopes and the labels were inverted in the replicate, to minimize the variability due to labeling procedures (Step 2, Fig. 21). LC-MS/MS reads were collected on a Proxeon Easy-nLC 1200 (Thermo Fisher Scientific) coupled to a QExactive HF mass spectrometer (Thermo Fisher Scientific)

(Step 3-5, Fig. 21). The raw data were processed (also by Johannes Madlung) using MaxQuant software (Cox et al., 2014), providing confident identification of proteins (1% FDR) and normalized protein abundance ratios (Step 6, Fig. 21).

Analysis of Vas- and Hrp48-associated proteomes resulted in the identification of a total of 4027 peptides, mapping to 615 protein groups. Out of these, protein intensities were calculated for 594 protein groups, in at least one of the samples. For Hrp48-GFP IP samples, protein intensities were calculated for 450 proteins in both the replicates and protein abundance ratios (over control) for 268 proteins were calculated reproducibly (Fig. 22A). Similar observations were made for Vas-GFP IP samples, where protein intensities were calculated for 435 proteins in both the replicates and 268 protein abundance ratios were calculated reproducibly (Fig. 22B). Abundance ratios calculated within the replicates showed more than 80% overlap. Furthermore, replicates showed high correlation, suggesting an overall good quality of the data (Fig. 22A, 22B).

Proteins identified with an abundance ratio of more than 2 in both replicates, were considered to be significantly enriched. Consistently with the semi-quantitative analysis, several known interactors were found, most of them reproducibly enriched (Fig. 22). Proteins with high fold change were dominated by ribosomal proteins and many translational initiation factors were also identified to be enriched, in agreement with the label-free MS data (Fig. 20, 23).
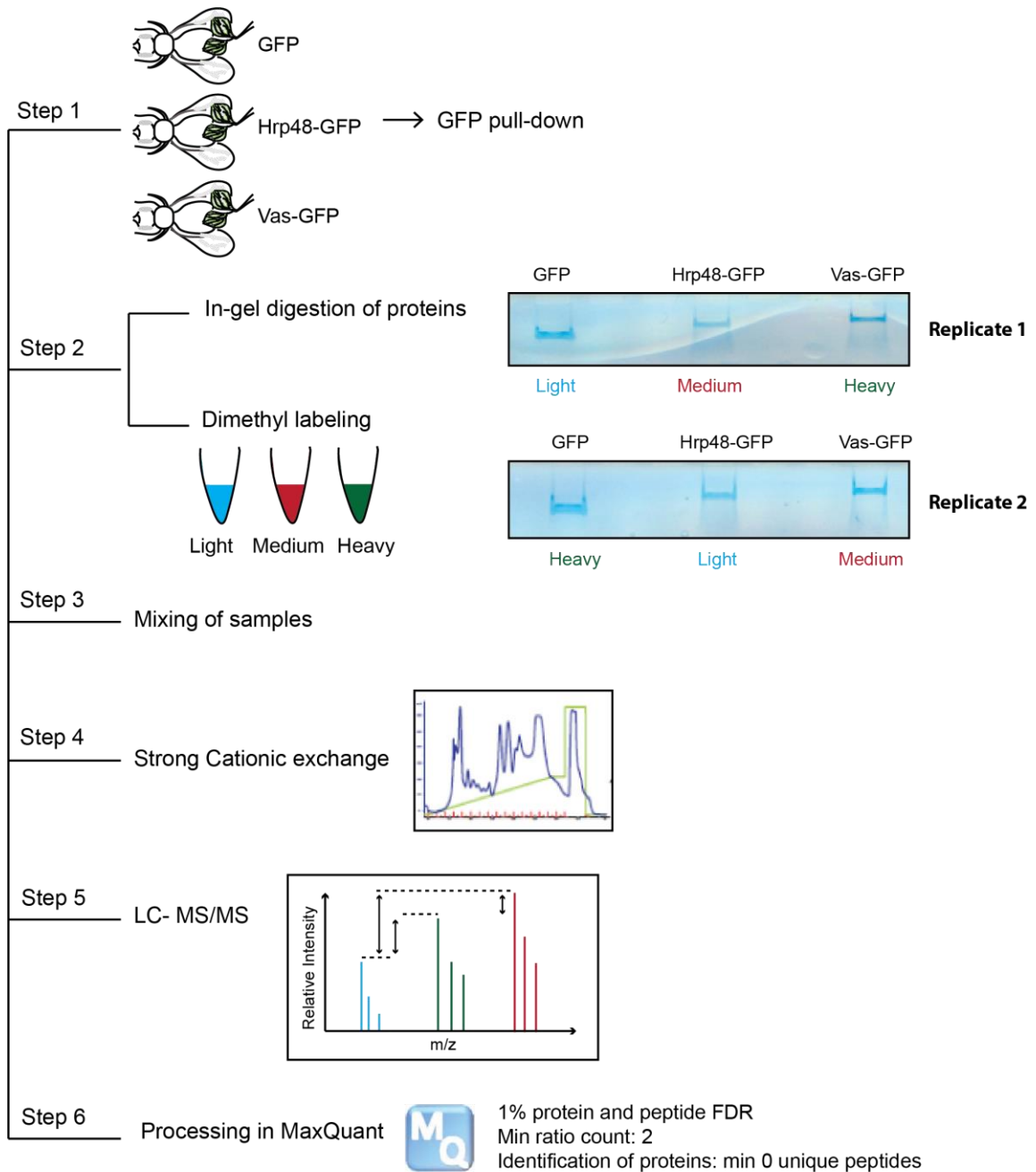
Fig. 21. Dimethyl labeling strategy for quantitative proteomics

Schematic representation of the experimental strategy. IPs were performed and bands were visualized by Coomassie staining. Representative Coomassie stained SDS-PAGE gels used for quantitative MS are shown on the right. IP from GFP sample served as a negative control.
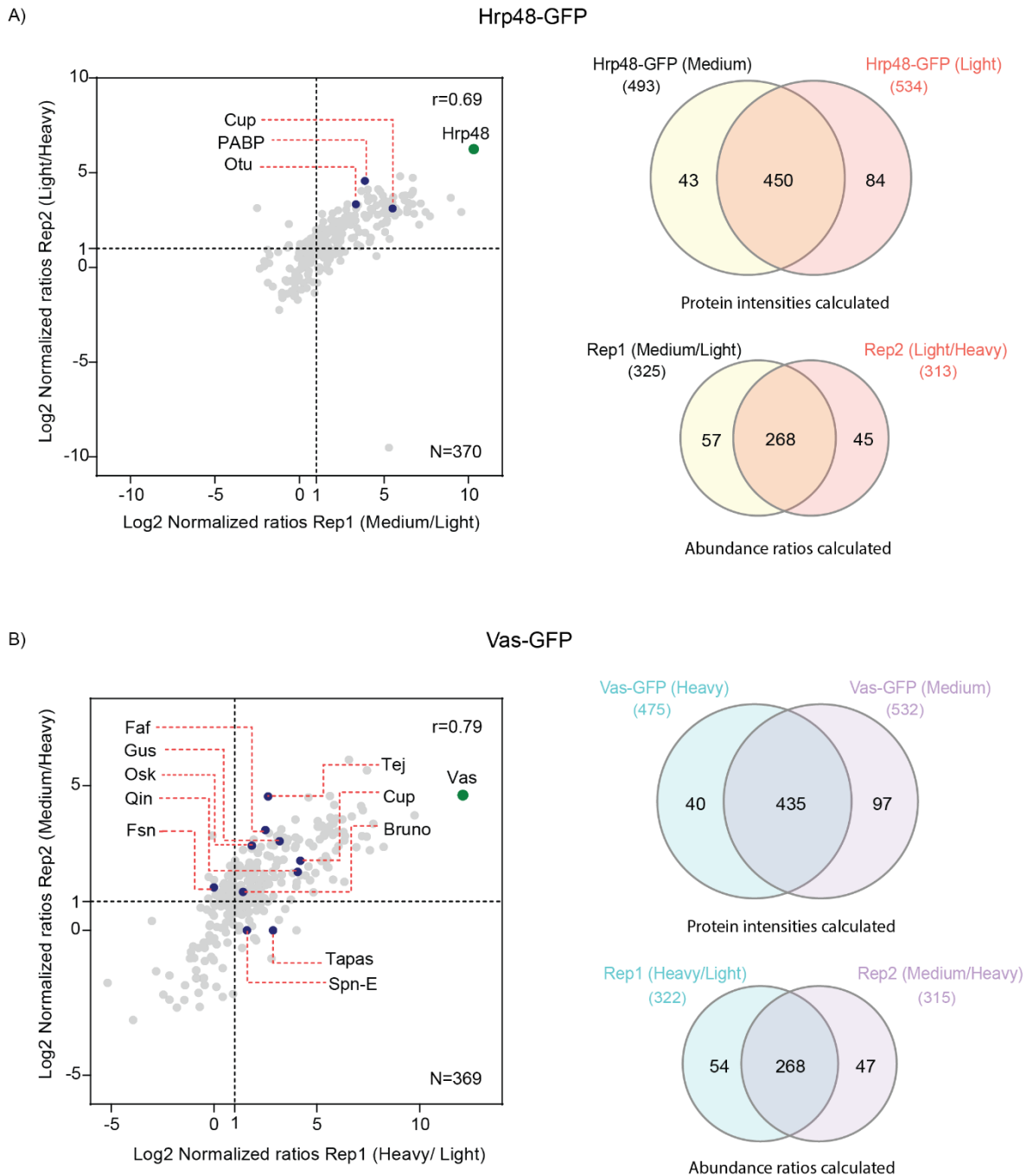
Fig. 22. Quantitative MS analysis reveals several interactors that associate with Hrp48-GFP and Vas-GFP with a high fold change.

Scatter plots of the proteins identified to be associated with Hrp48-GFP (A) and Vas-GFP (B) in the Dimethyl labeling MS analysis. Normalized ratios (Log2) of both the replicates are plotted against each other. IP from GFP sample served as a negative control. N denotes the number of protein groups plotted and "r" denotes the Pearson correlation coefficient. Dotted lines mark the proteins with more than 2 fold change over control, in each replicate. Venn diagrams on the right show the overlap of protein intensities calculated and abundance ratios calculated in the two replicates. Each identified protein is represented as a dot in light grey; baits are highlighted in green; known interactants are highlighted in blue; background binders are highlighted in dark grey.
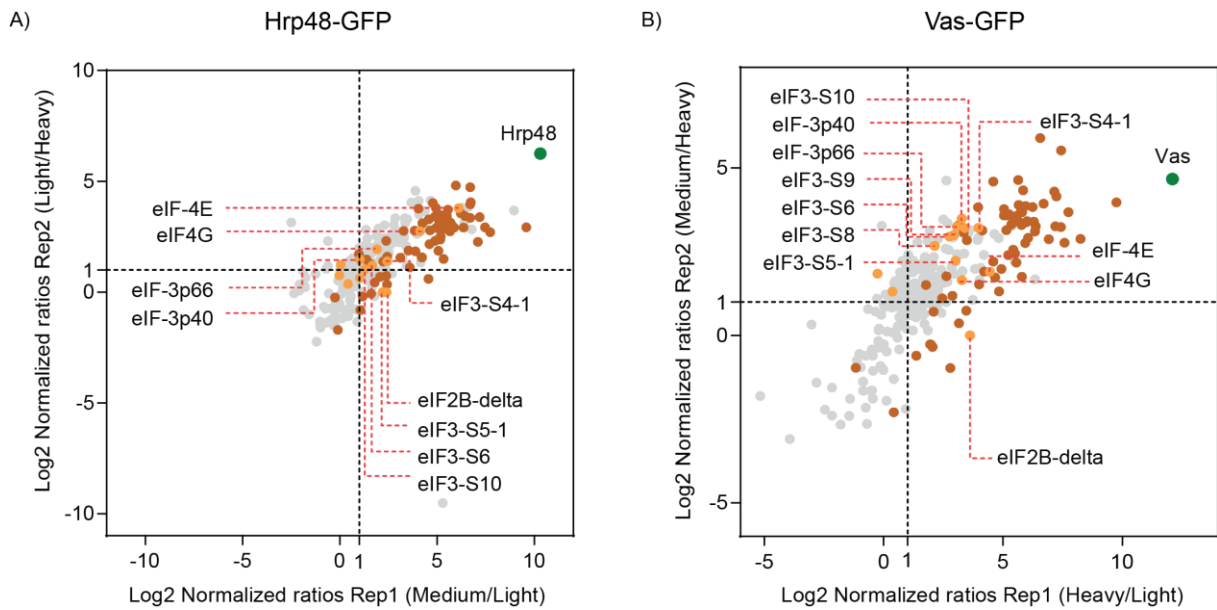
Fig. 23. Ribosomal proteins and translation initiation factors are significantly enriched and overlap in Hrp48-GFP and Vas-GFP IP samples, as analyzed by quantitative MS.

Scatter plots highlighting the distribution of ribosomal proteins and translation initiation factors found associated with Hrp48-GFP (A) and Vas-GFP (B) in the Dimethyl labeling MS analysis. Normalized ratios (Log2) of both the replicates are plotted against each other. IP from GFP sample served as a negative control. Dotted lines mark the proteins with more than 2 fold change over control, in each replicate. Each identified protein is represented as a dot in light grey; baits are highlighted in green; ribosomal proteins are highlighted in brown; translation initiation factors are highlighted in orange.

To check how semi-quantitative and quantitative analyses relate with each other and whether both methods yielded similar associated proteomes, I mapped the proteins identified in labeled MS analysis onto the label-free MS data. As shown in Fig. 24, significantly enriched proteins (more than 2 fold in both replicates) and background proteins (less than 2 fold in both replicates) identified in the labeled MS followed the same profile as in the label-free MS analysis and showed a good overlap in Venn diagrams (Fig. 24).
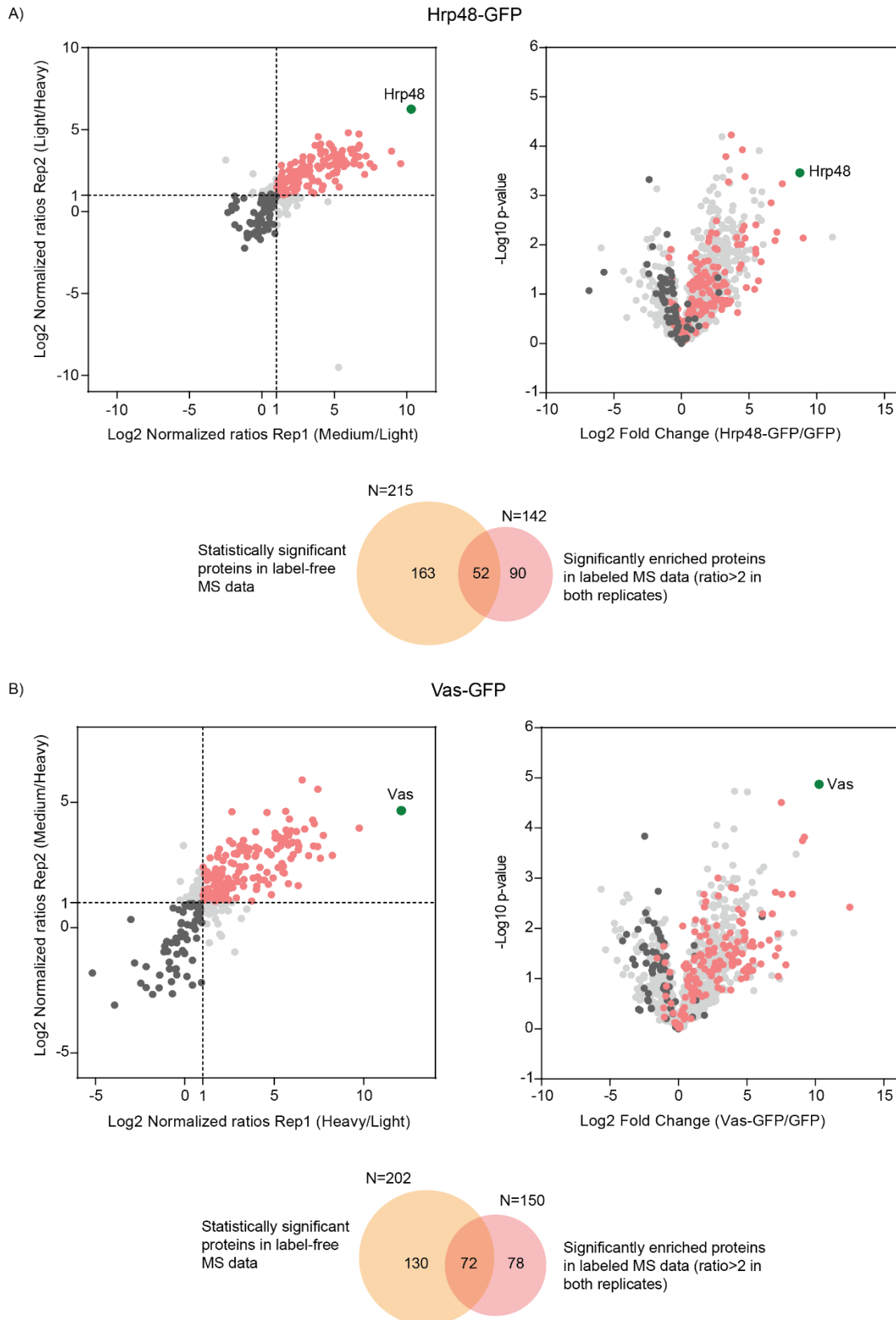
Fig. 24. Quantitative MS data supports the semi-quantitative MS data

Volcano plots (on the right) with an overlay of the labeled MS data (on the left) analyzed for Hrp48-GFP (A) and Vas-GFP (B) IPs. At the bottom of each panel, Venn diagrams represent the overlap between the significantly enriched interactants found in the two datasets. In the scatter/volcano plots,

each identified protein is represented as a dot in light grey; baits are highlighted in green; significantly enriched proteins are highlighted in pink; background binders are highlighted in black.

2.2.4 Global analysis of proteomes associated with the tagged RBPs

To understand how the proteomes identified with each bait interact with each other, I built a composite network of all the statistically significant interactants identified in the label-free MS data analysis (Fig. 25). While each bait has its distinct proteome, the network is also highly connected. In particular, a considerable overlap can be observed between functionally related proteins. To gain a systemic understanding of the network, I mapped the known protein-protein associations from curated databases, such as String (Szklarczyk et al., 2017) and FlyBase (Gramates et al., 2017) onto the network, resulting in a complex and dense interactome, as shown in Fig. 26.
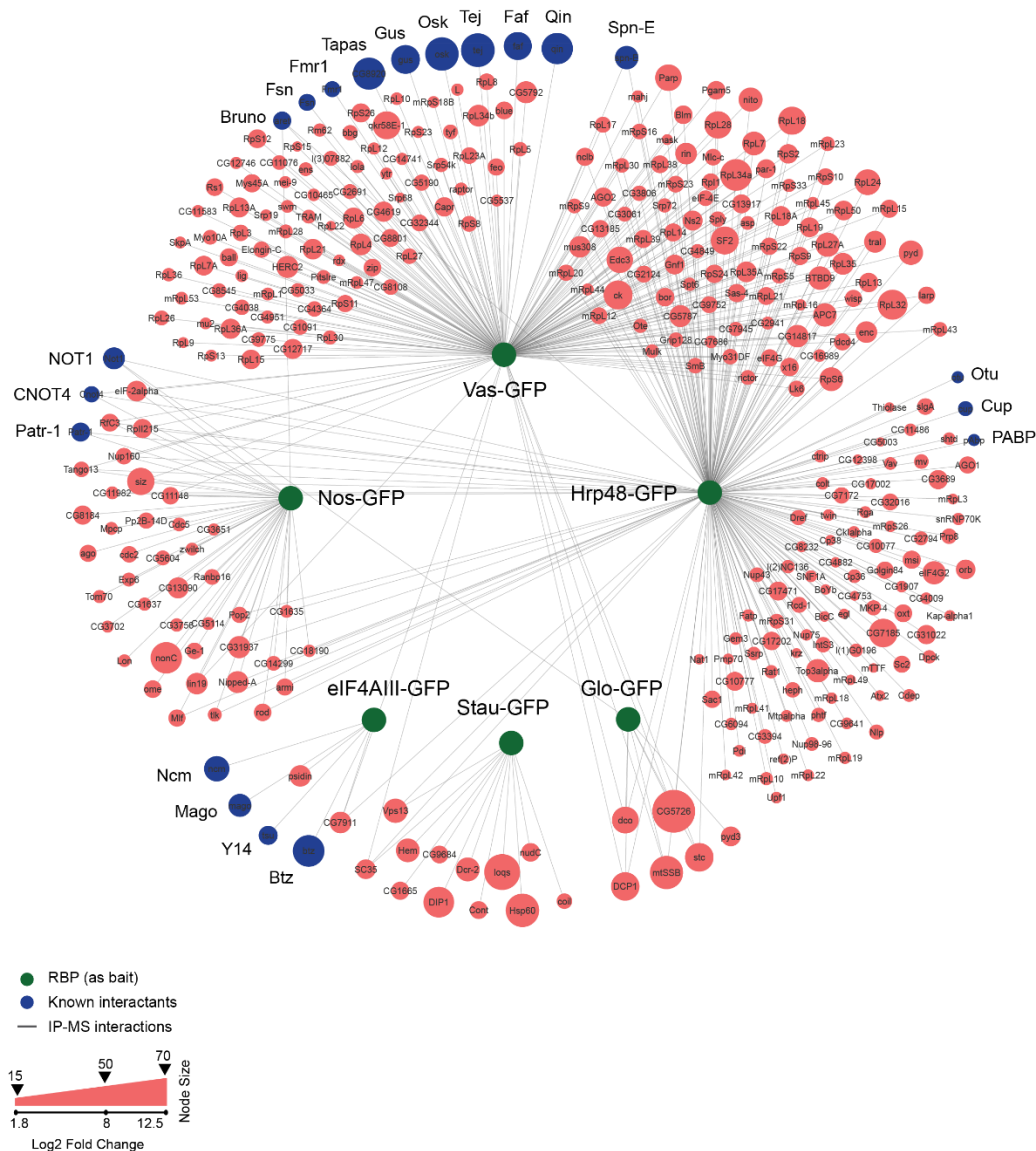
Fig. 25 The global interactome reveals novel protein interactions

Shown is the interaction network of significantly enriched proteins, identified to be associated with each bait in the label-free MS analysis. Nodes are presented as circles: green nodes represent the baits; pink nodes represent the interactants; blue nodes represent the known interactants identified in the respective IPs; connecting edges represent the interactions. The size of the node (except the green nodes that represent the baits) indicate the fold change (Log2) over control; highest fold change values were considered for the interactants found associated with multiple baits.
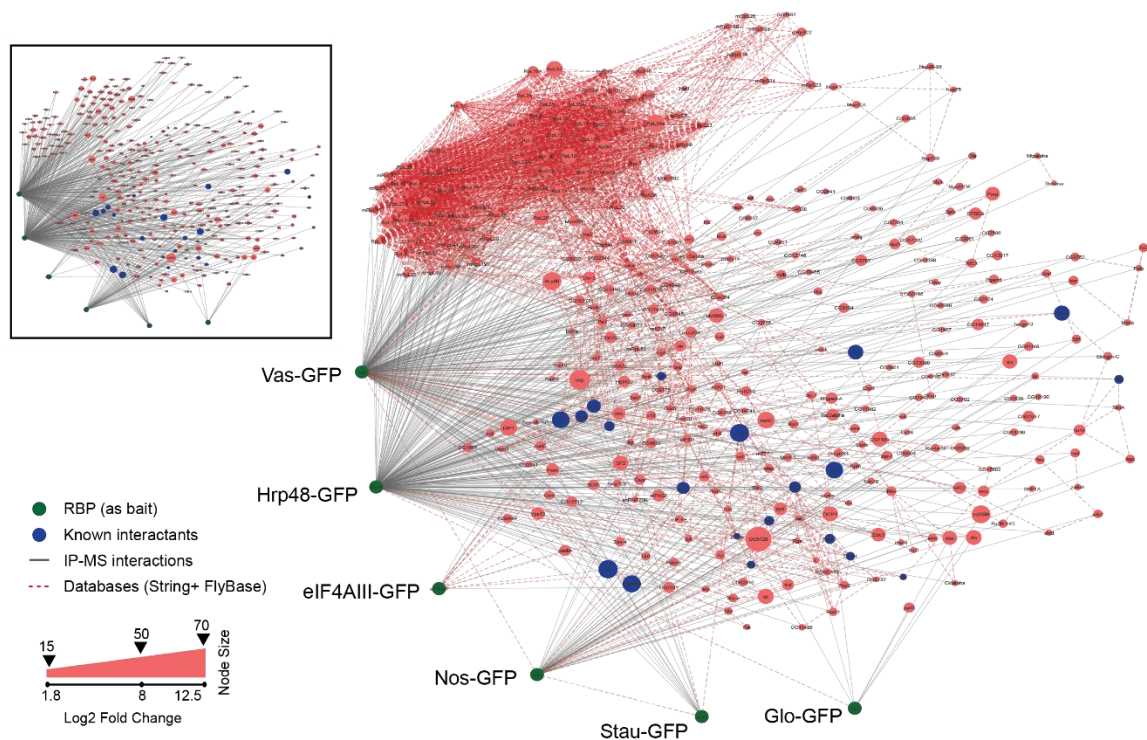
Fig. 26 Network complexity increases upon addition of protein-protein interaction data retrieved from database sources.

The interactome built from label-free MS analysis (inset) was integrated with the existing interaction data extracted from String (Szklarczyk et al., 2017) and FlyBase (Gramates et al., 2017). Nodes are presented as circles: green nodes represent the baits; pink nodes represent the interactants; blue nodes represent the known interactants identified in the respective IPs; connecting edges represent the interactions. IP-MS data is highlighted by solid grey edges while the database information is highlighted by dotted pink edges. The size of the node indicates the fold change (Log2) over control.

To further characterize the interactome functionally, I performed an enrichment analysis to identify which Gene Ontology (GO) terms are overrepresented in my gene set (as compared to the *Drosophila* genome). For this, I used the functional annotation tool from DAVID (**D**atabase for **A**nnotation, **V**isualization and **I**ntegrated **D**iscovery; Huang et al., 2009a,b) and

clustered the results in the representative subset of terms using REVIGO (**Re**duce + **Vi**sualize **G**ene **O**ntology; Supek at al., 2011). As expected, I found several terms related to RNA processes and translation. GO Biological Process analysis showed a very high enrichment of proteins involved in the regulation of *osk* mRNA translation and localization, cytoplasmic mRNA processing, cytoplasmic and mitochondrial translation, ribosome assembly, and mRNA splicing and polyadenylation. Similarly, for molecular functions, terms for dsRNA binding, RNA helicase activity, translation initiation and regulator activity were enriched. The analysis of cellular compartments/complexes revealed high enrichment of proteins as part of ribosomes, pole plasm, P-bodies, RISC complex and the EJC (Fig. 27).
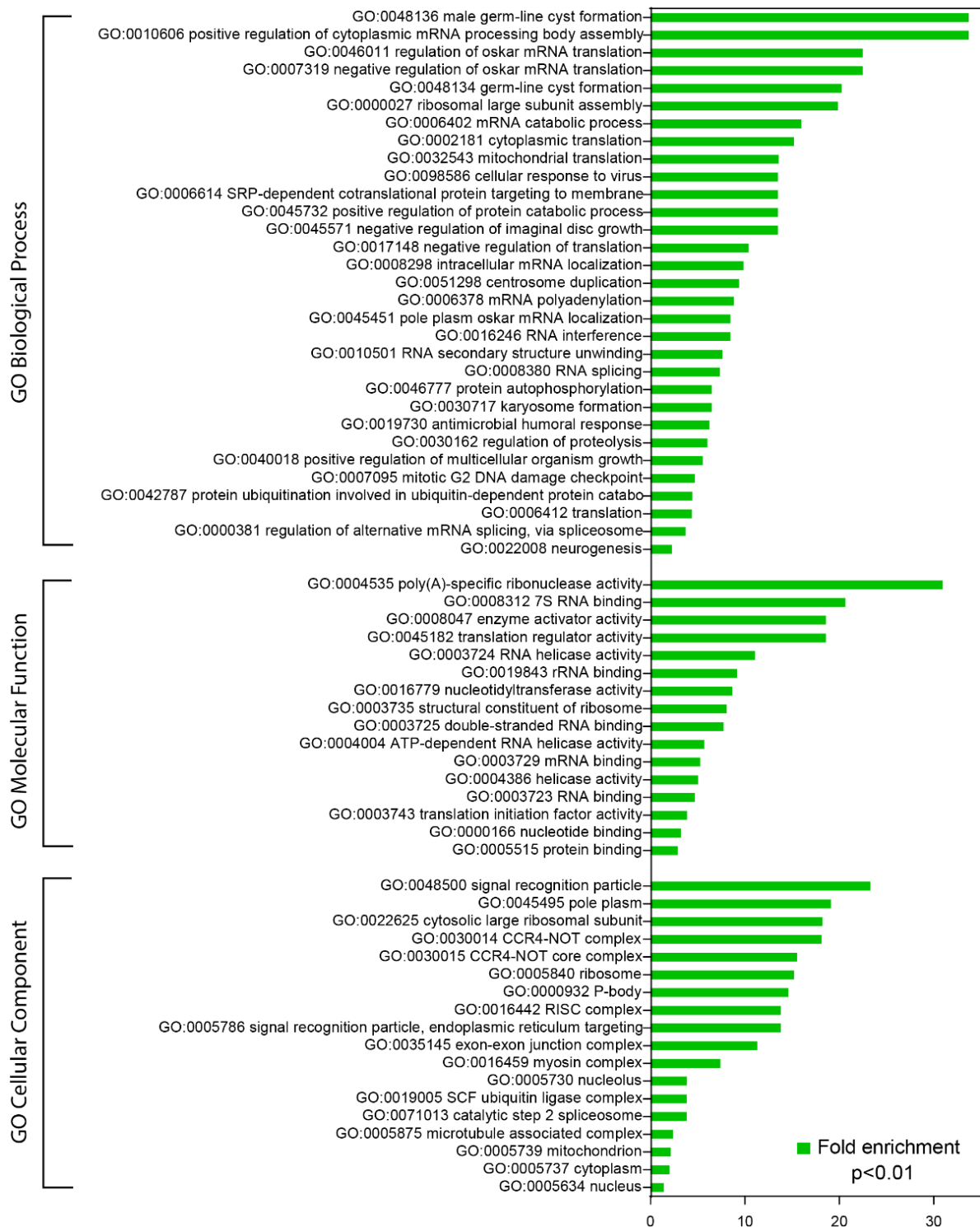
Fig. 27 Enrichment analysis of the proteins identified to be significantly enriched with each bait

All the proteins identified to be significantly associated with each bait in the label-free MS analysis were functionally annotated for their roles in biological processes, molecular functions and cellular components using GO terms. Analysis was done using functional annotation tool from DAVID (Huang et al., 2009a,b). Fisher Exact test with a p-value cutoff of 0.01 was employed to find enriched categories (as compared to the *Drosophila* genome). Results were summarized using REVIGO (Supek et al., 2011).

2.2.5 *In vitro* validation of interactants using co-immunoprecipitation (co-IP) assay

The inherent complex and dynamic nature of protein interactions render the interpretation of large-scale proteomic datasets particularly challenging, despite the technological advances in instruments, algorithms and analysis tools. One of the major concerns in MS-related studies is the identification of false positives due to artefacts caused by protein destabilization or aggregation and by bringing together unrelated proteins that might not interact with each other in native conditions. Therefore, follow up biological studies are imperative to validate functionally relevant protein associations.

One of the ways to validate interactions *in vitro*, is by co-IP of overexpressed candidate pairs in a heterologous cell system. This method relies on the stable interaction between bait and prey proteins in the sample solution, which can be precipitated together by a bait-specific antibody. Due to their ease of culture and high transfection efficiency, human HEK cells have been extensively used to transiently express recombinant proteins. Since I am working with *Drosophila* proteins, this system can be effectively used to study direct protein-protein interactions, with reduced possibility of involvement of additional endogenous proteins mediating these associations.

For validation by co-IP, I selected candidates from the list of protein partners that were determined to be statistically significant in the label-free MS data analysis (i.e. based on the combination of fold change and 5% FDR cut-off). Additionally, I also considered functionally relevant partners, enriched with at least a 2 times fold change in the label-free MS data, otherwise excluded by statistical filtering. For Hrp48 and Vas, where quantitative information was also available, I selected the candidates from the combined list of interacting proteins identified in both the datasets, based on high enrichment and/or functional relevance.
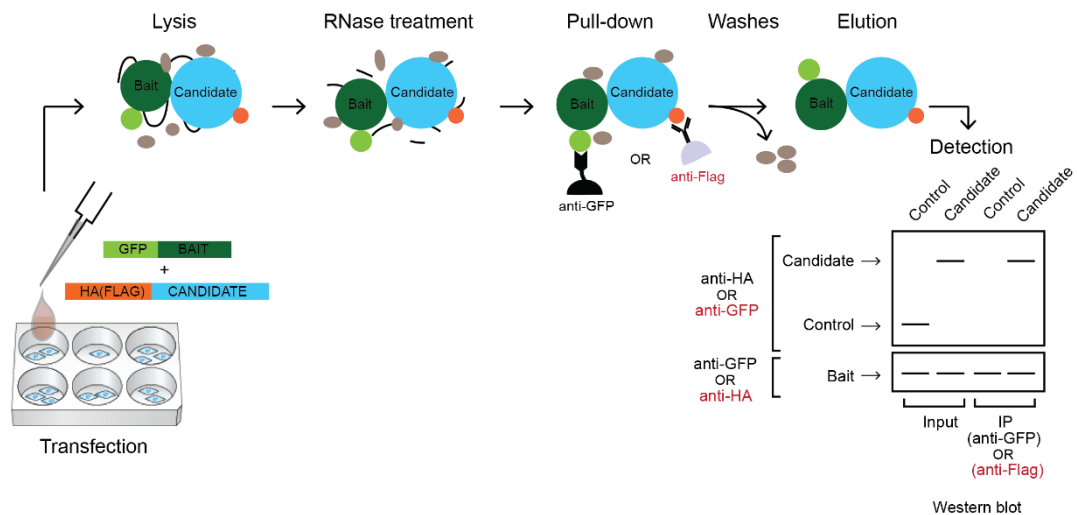
Fig. 28 Schematic representation of co-IP validation strategy in HEK cells

The experimental strategy is depicted in Fig. 28. Typically, I co-expressed an EGFP (referred to as GFP for simplicity) -tagged bait with an HA-tagged candidate protein, and performed the IP using the GFP-TRAP system (Chromotek). I observed that small proteins (<25kDa) express poorly as fusions with HA/HA-Flag and substitution with the GFP tag improved the expression significantly in all the cases tested. To be able to validate the interactions of such small proteins, I co-expressed an HA-Flag-tagged candidate with a GFP-tagged bait and performed the IP using anti-Flag (Fig. 29.2D, 29.5C). Since Vas does not express well as an HA/HA-Flag fusion, the small proteins could not be assayed efficiently for interaction with Vas. To serve as negative controls, I used MBP or GFP, as these tags are presumed inert, with minimal effects on the activity or distribution of the tagged protein. I also included known interactions as positive controls, wherever possible.

I analyzed the co-IP results by Western blotting using anti-GFP and anti-HA antibodies (Fig. 28). To confirm the IP, baits were detected with anti-GFP (or anti-HA in the case of anti-Flag IPs) and to confirm the co-IP, partner candidates were detected with anti-HA (or anti-GFP in case of anti-Flag IPs). Since the proteins are expressed at different levels, I frequently observed that the stronger signals overshadowed the nearby weaker signals or saturated the blot. In such cases, increased exposure did not cause a linear increase in the density of the image, leading to the loss of information. To overcome this, I split the samples for effective visualization (via chemiluminescence) on the blots. For the same reasons, the amount of starting material, the concentration of lysate and the amount of input to be loaded were also balanced accordingly.

Out of 94 protein-protein interactions assayed, I could confirm 32 interactions (34%), of which 26 were found to be novel (summarized in Fig. 30). All positive interactions were confirmed at least 3 times, in independent experiments. In addition, I was also able to validate some of the interactions by reciprocal IP, as shown in Fig. 29.2C. In both the labeled and label-free MS data, Sqd was identified as an unspecifically binding protein with all the baits. I could confirm these interactions to be negative *in vitro* (Fig. 31), which shows that the pipeline constructed to analyze the MS data could effectively separate the background binders from the true interactants. Furthermore, interaction of Sqd with Hrp48 is RNA-dependent (Goodrich et al., 2004). This confirms that the RNases added during the purification could effectively disrupt RNA-mediated associations and only protein-protein interactions were identified. However, many interactions that were determined to be significant in the MS data analysis could not be validated, possibly due to the following reasons: lack of biochemical machinery required for post-translational modifications, misfolding of proteins, low affinity, transient interactions or interactions mediated by other proteins.

To gain a better perspective of the co-IP results, I integrated the validated interactions with the IP-MS data (both labeled and label-free), together with information from databases such as String (Szklarczyk et al., 2017) and FlyBase (Gramates et al., 2017) to create a subnetwork (Fig. 32). As the majority of the validated interactants are known regulators of maternal mRNAs, this subnetwork highlights a general machinery involved in oocyte development in *Drosophila*.

Fig. 29.1 Validation of selected eIF4AIII candidate partners

(A) Volcano plot highlighting all the candidate proteins that were assayed for interaction with eIF4AIII, through a co-IP screen in HEK cells. (B) GFP-tagged eIF4AIII was co-expressed with HA-tagged candidates, as indicated. IPs were performed using GFP-coated beads. Inputs and eluates were analyzed by Western blotting. For detection, eluates were split into 10% for IP (with anti-GFP) and 90% for co-IP (with anti-HA); indicated amounts of inputs were loaded equally for both IP and co-IP. HA-MBP served as a negative control. Molecular weight makers are shown on the left.
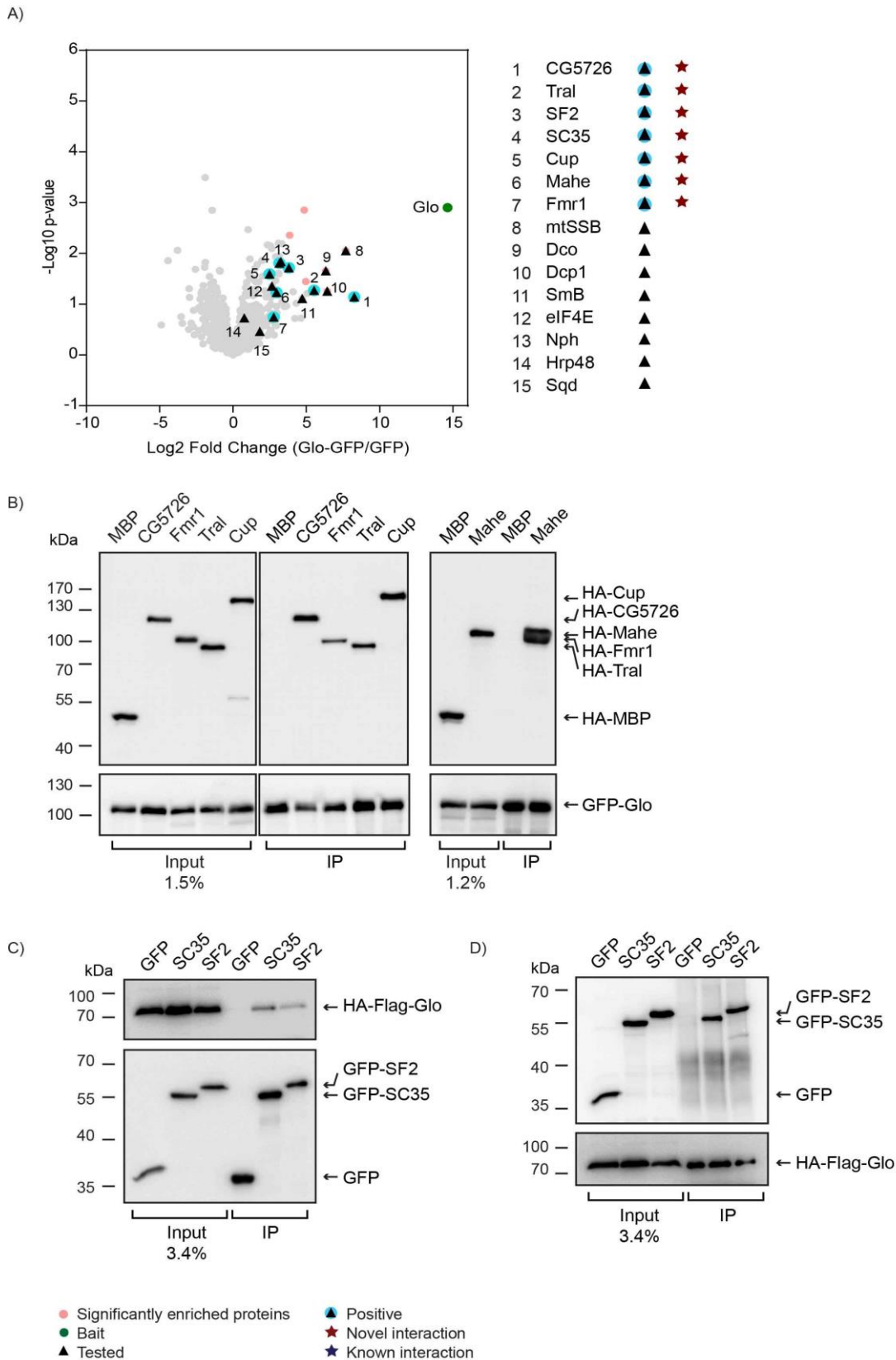
Fig. 29.2 Validation of selected Glo candidate partners

(A) Volcano plot highlighting all the candidate proteins that were assayed for interaction with Glo through a co-IP screen in HEK cells. (B) GFP-tagged Glo was co-expressed with HA-tagged candidates, as indicated. Co-IPs were performed using GFP-coated beads. HA-MBP served as a

negative control. (C) HA-Flag-tagged Glo was co-expressed with GFP-tagged candidates, as indicated and cell lysates were split for IP with anti-GFP and (D) anti-Flag. GFP served as a negative control. Inputs and eluates were analyzed by Western blotting. For detection, eluates were split into 10% for IP: with anti-GFP (B,C) or with anti-HA (D); 90% for co-IP: with anti-HA (B,C) or with anti-GFP (D); indicated amounts of inputs were loaded equally for both IP and co-IP. Molecular weight markers are shown on the left.

Fig. 29.3 Validation of selected Hrp48 candidate partners

(A) Volcano plot highlighting all the candidate proteins that were assayed for interaction with Hrp48 through a co-IP screen in HEK cells. (B) GFP-tagged Hrp48 was co-expressed with HA-tagged candidates, as indicated. IPs were performed using GFP-coated beads. Inputs and eluates were analyzed by Western blotting. For detection, eluates were split into 10% for IP (with anti-GFP) and 90% for co-IP (with anti-HA); indicated amounts of inputs were loaded equally for both IP and co-IP. HA-MBP served as a negative control. Molecular weight markers are shown on the left.
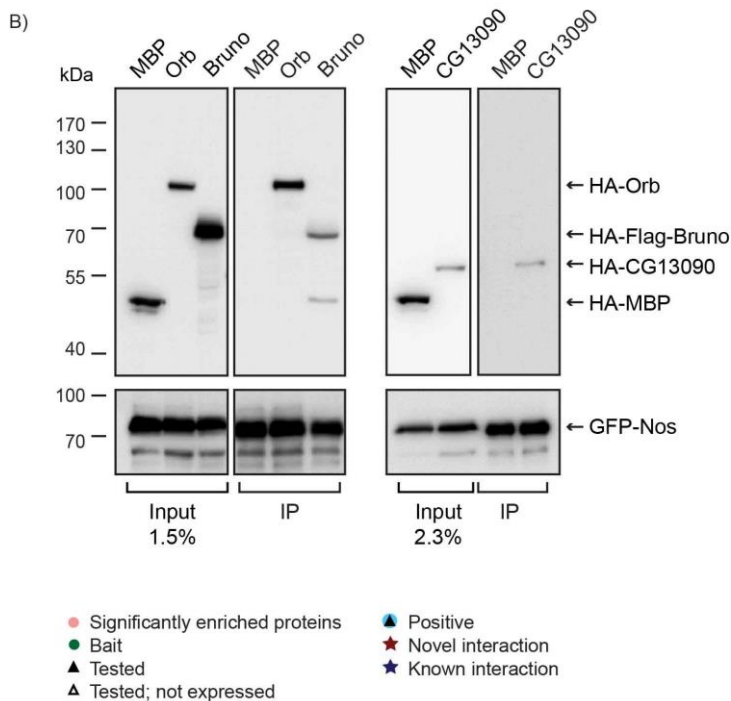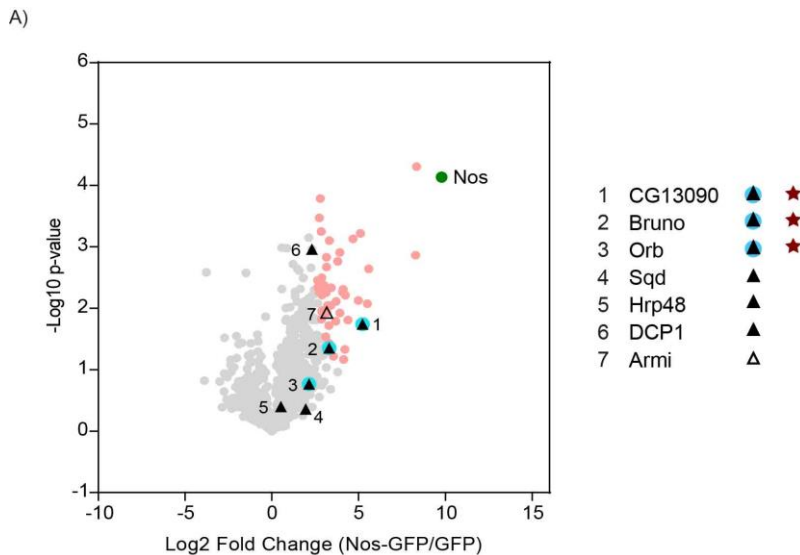
Fig. 29.4 Validation of selected Nos candidate partners

(A) Volcano plot highlighting all the candidate proteins that were assayed for interaction with Nos through a co-IP screen in HEK cells. (B) GFP-tagged Nos was co-expressed with HA-tagged

candidates, as indicated. IPs were performed using GFP-coated beads. Inputs and eluates were analyzed by Western blotting. For detection, eluates were split into 10% for IP (with anti-GFP) and 90% for co-IP (with anti-HA); indicated amounts of inputs were loaded equally for both IP and co-IP. HA-MBP served as a negative control. Molecular weight markers are shown on the left.
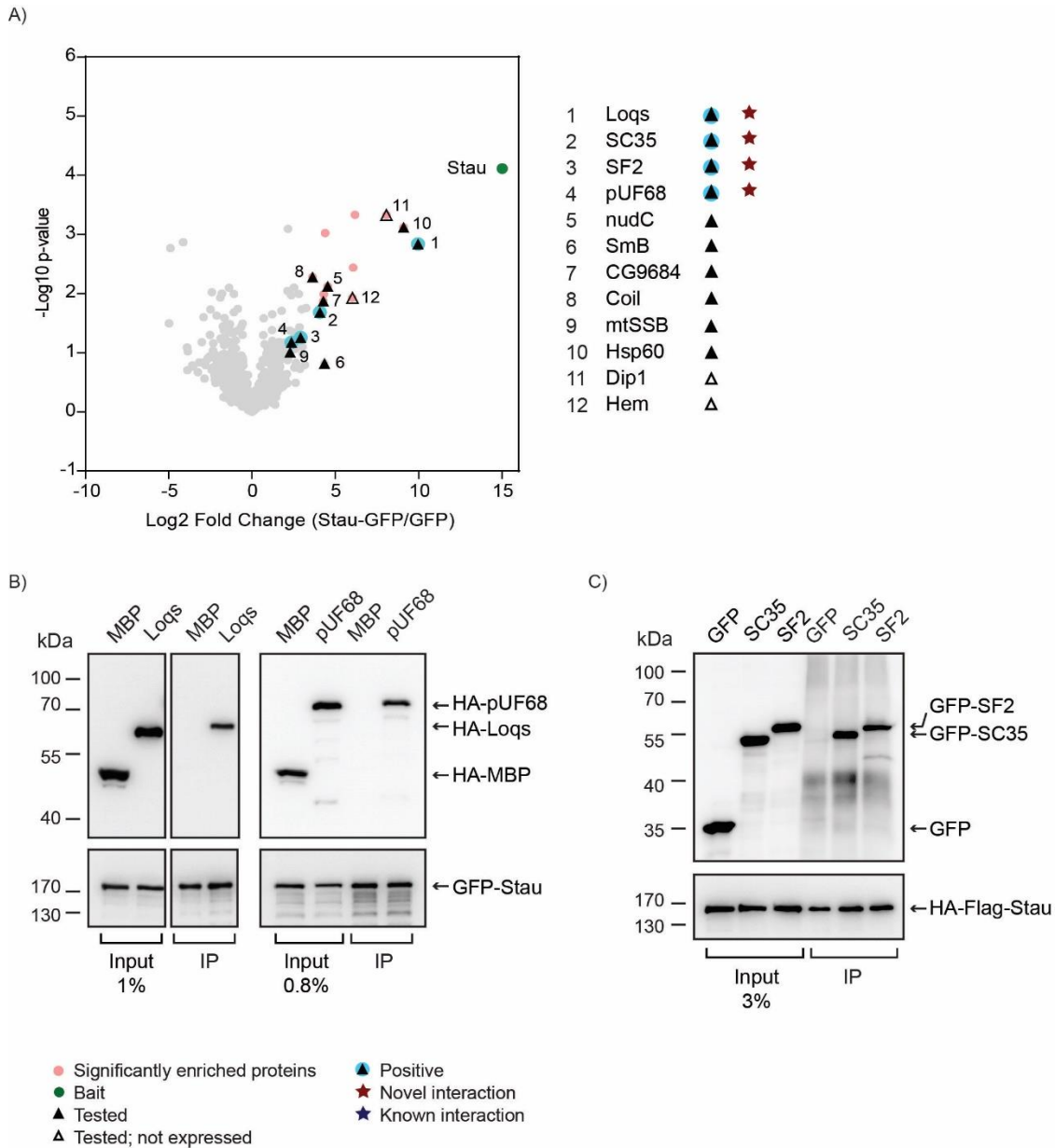
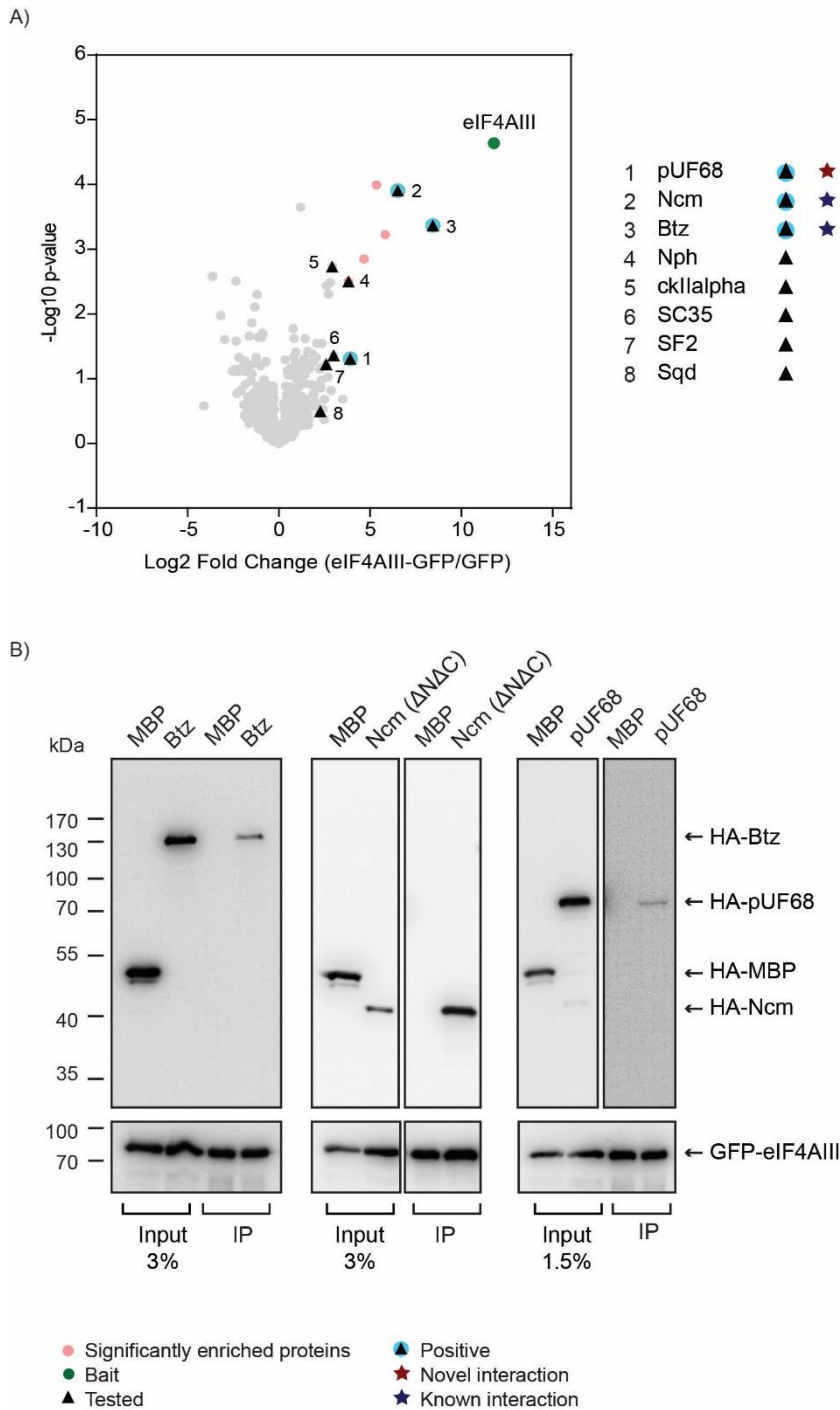
Fig. 29.5 Validation of selected Stau candidate partners

(A) Volcano plot highlighting all the candidate proteins that were assayed for interaction with Stau through a co-IP screen in HEK cells. (B) GFP-tagged Stau was co-expressed with HA-tagged candidates, as indicated. IPs were performed using GFP-coated beads. HA-MBP served as a negative control. (C) HA-Flag-tagged Stau was co-expressed with GFP-tagged candidates, as indicated and co-IPs were performed using anti-Flag. GFP served as a negative control. Inputs and eluates were analyzed by Western blotting. For detection, eluates were split into 10% for IP: with anti-GFP (B) or with anti-HA (C); 90% for co-IP: with anti-HA (B) or with anti-GFP (C); indicated amounts of inputs were loaded equally for both IP and co-IP. Molecular weight markers are shown on the left.
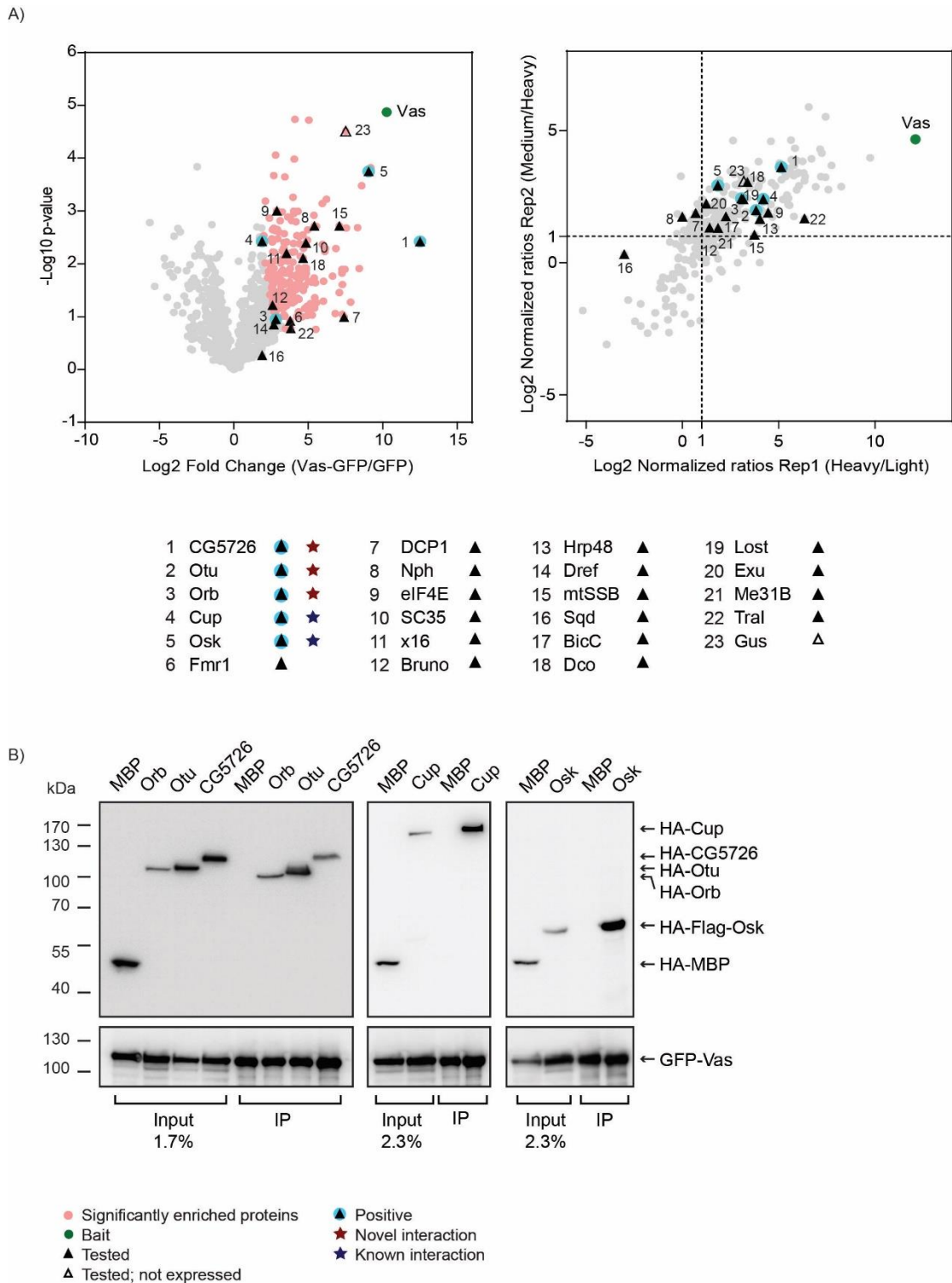
Fig. 29.6 Validation of selected Vas candidate partners

(A) Volcano plot highlighting all the candidate proteins that were assayed for interaction with Vas through a co-IP screen in HEK cells. (B) GFP-tagged Vas was co-expressed with HA-tagged candidates, as indicated. IPs were performed using GFP-coated beads. Inputs and eluates were analyzed by Western blotting. For detection, eluates were split into 10% for IP (with anti-GFP) and

90% for co-IP (with anti-HA); indicated amounts of inputs were loaded equally for both IP and co-IP. HA-MBP served as a negative control. Molecular weight markers are shown on the left.
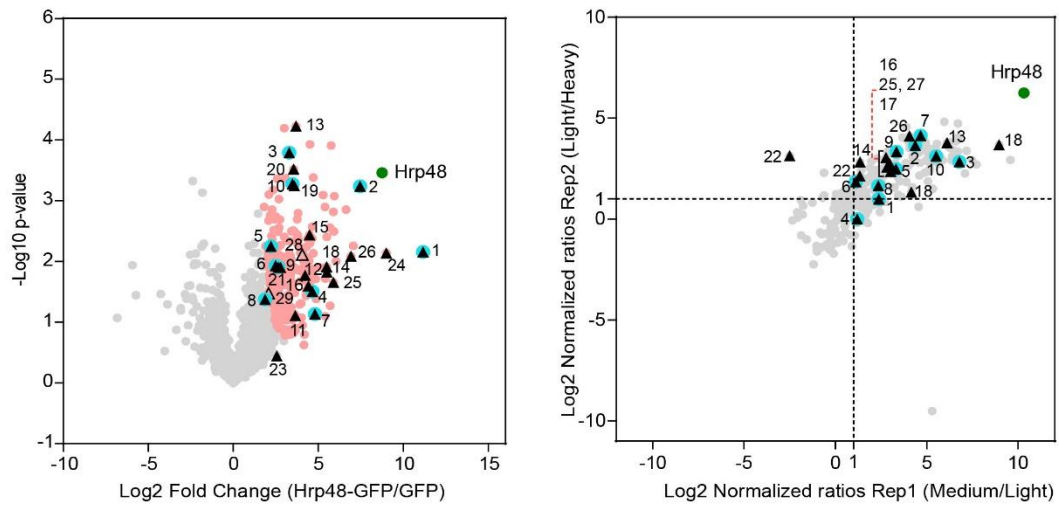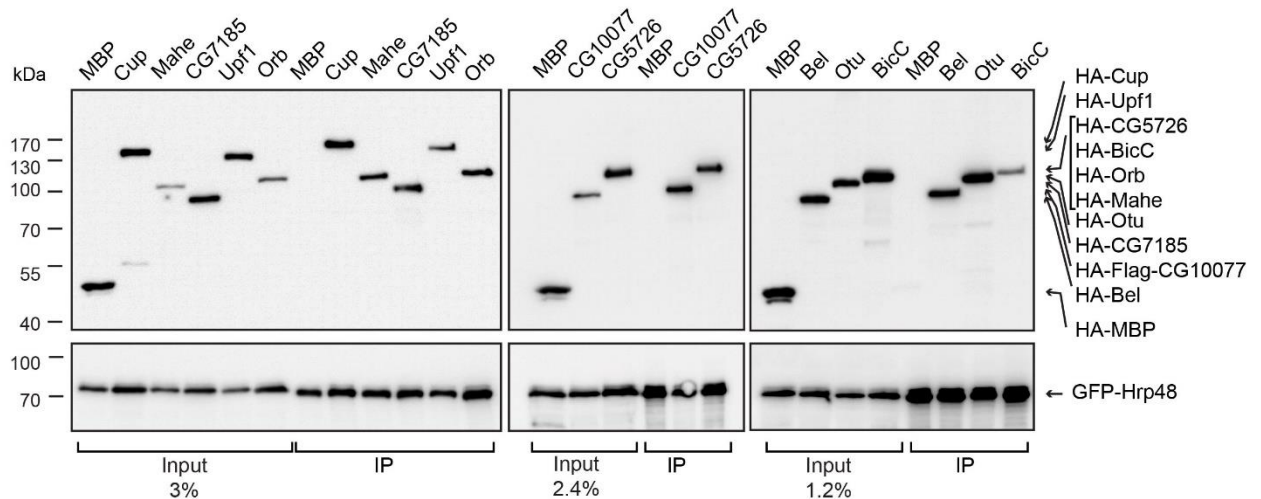
	Validated	Positive	Novel
eIF4AIII	8	3	1
Glo	15	7	7
Hrp48	29	10	8
Nos	7	3	3
Stau	12	4	4
Vas	23	5	3

Fig. 30. Summary of interactions assayed by co-IPs in HEK cells
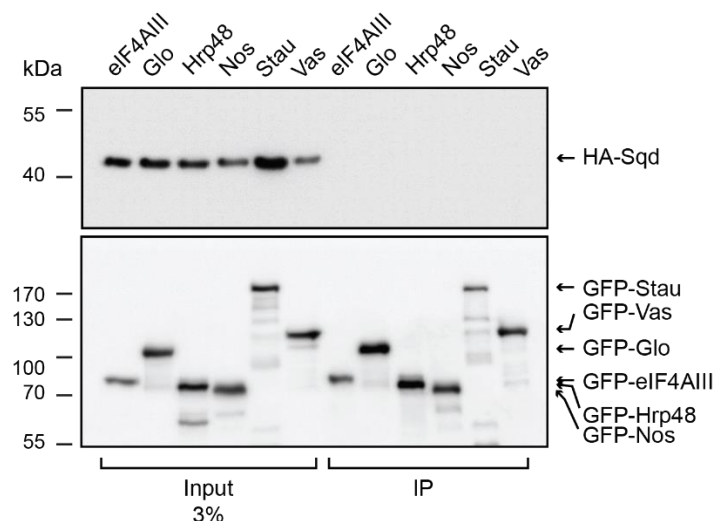
Fig. 31. Sqd shows negative interaction with the selected RBPs, consistent with the MS data analysis.

Shown above is the assay performed to analyze the interaction of Sqd with different baits in HEK cells. GFP-tagged baits were co-expressed with HA-tagged Sqd, as indicated. IPs were performed using GFP-coated beads. Inputs and eluates were analyzed by Western blotting. For detection, eluates were split into 10% for IP (with anti-GFP) and 90% for co-IP (with anti-HA); indicated amounts of inputs were loaded equally for both IP and co-IP. HA-MBP served as a negative control. Molecular weight markers are shown on the left.
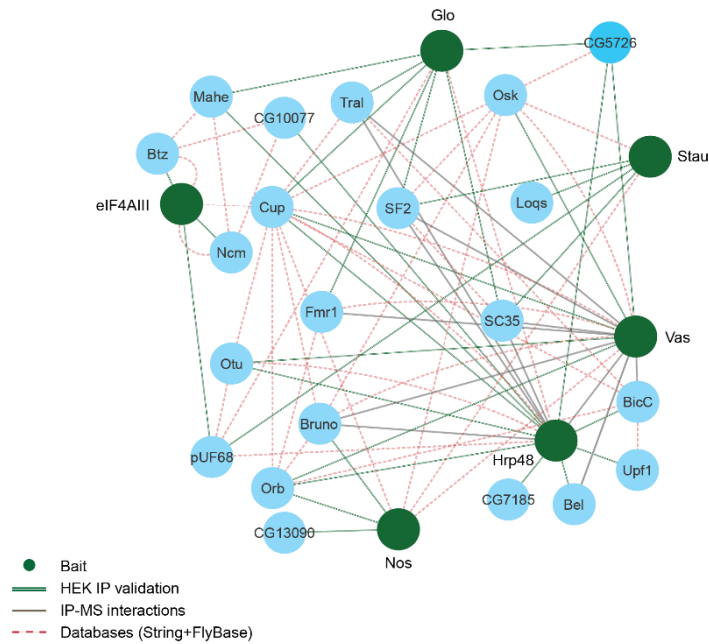
Fig. 32. Subnetwork of the protein interactions validated *in vitro*, integrated with the IP-MS data and information from String (Szklarczyk et al., 2017) and FlyBase (Gramates et al., 2017).

Analysis of co-IP validation results revealed that while the statistical analysis efficiently filtered out most of the non-specific interactors, some of the proteins that were excluded (due to the 5% FDR cutoff, despite high fold change) showed positive interactions upon validation *in vitro*. This suggested that the initial statistical filtering I used was very stringent, potentially leading to the loss of valuable information. Therefore, I altered the cut off used to determine significantly enriched proteins in the label-free MS analysis and set the new cut off based on the HEK IP validations. For this, I sorted all the proteins identified with each bait in the label-free MS data in decreasing order of fold change and included all the candidates until the last validated interaction, irrespective of the %FDR value of the interaction. This was done for all the baits, except Hrp48-GFP and Vas-GFP. Since quantitative MS data was available for both Hrp48 and Vas, I unified the significantly enriched interactants previously determined in both datasets independently, in a single list. These new lists of bait-associated proteins, identified with revised parameters were analyzed again.

To gain insights into which processes are differentially associated with each bait, I performed GO analysis for proteins identified with each bait (with revised parameters) separately. Proteins were functionally annotated for their roles in biological processes, molecular functions and cellular components, and were further mapped onto KEGG pathways (Fig. 33A-C), using DAVID (Huang et al., 2009a,b). Consistent with the initial analysis, functionally related baits (Vas and Hrp48) shared many processes. Interestingly, all baits, except Nos,

showed enrichment of proteins involved in pre-mRNA splicing. Proteins involved in negative regulation of cell cycle were identified with Nos, suggesting its yet unidentified role in cell cycle regulation during oogenesis.

B)
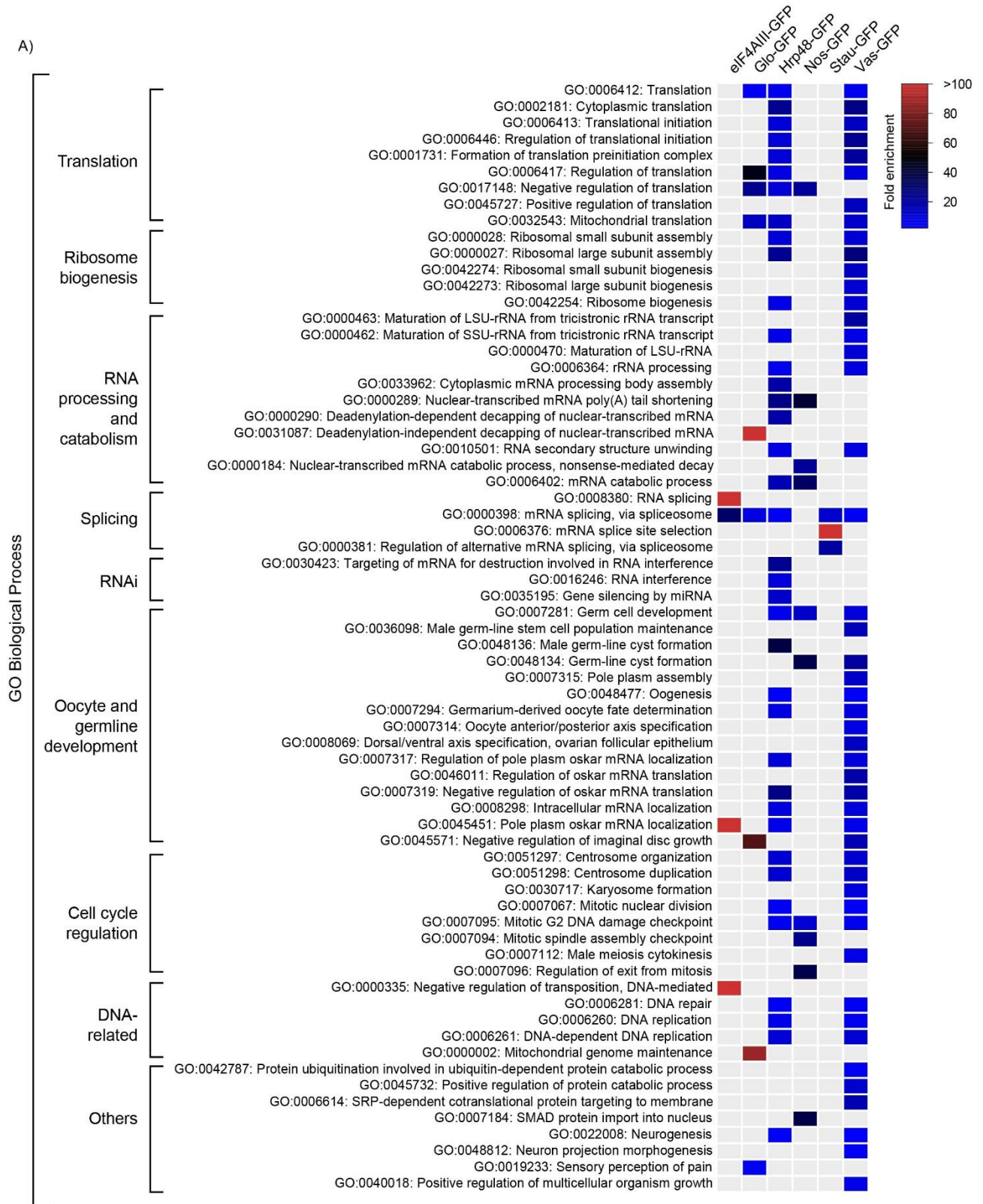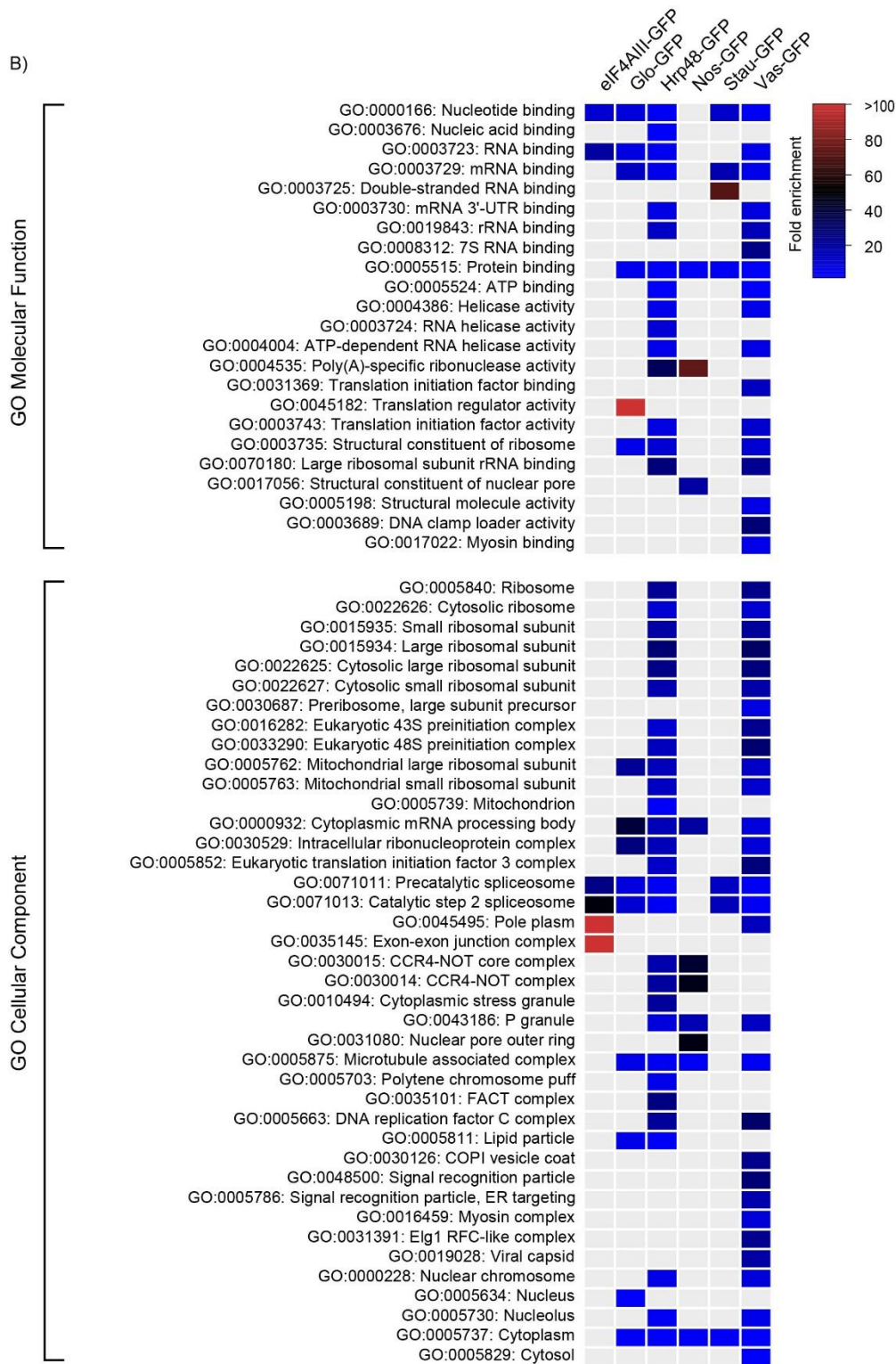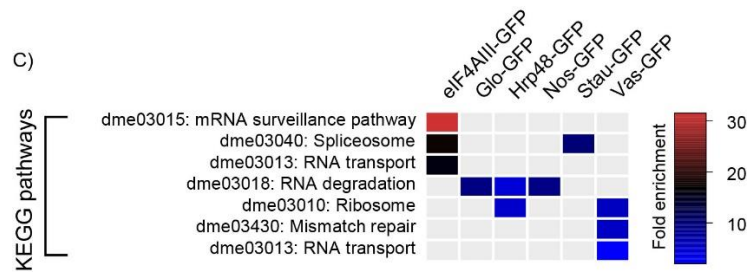
Fig. 33. GO term analysis of proteins associated with each bait

Shown above are the results of GO term analysis, depicted as heat maps. Bait-associated proteins included in the complement of *bona fide* interactants after revision of parameters were analyzed separately, using the functional annotation tool from DAVID (Huang et al., 2009a,b). Fisher Exact test with a p-value cutoff of 0.01 was employed to find categories enriched for (A) GO Biological Process (B) GO Molecular Function and GO Cellular Compartment (C) KEGG pathways, as compared to the *Drosophila* genome.

3. Discussion

The main objective of my PhD project was to gain a better understanding of the interactions underlying localization of maternal mRNAs involved in *Drosophila* oogenesis. For this, I combined RNA-based and protein-based approaches.

3.1 *MS2*-based methods are limited in their efficiency for purification of mRNPs assembled *in vivo*

3.1.1 *MS2* tagging can affect the functionality of transcripts

To purify a localizing mRNP assembled *in vivo*, I used an approach similar to the TAP tagging, in which both the RNA and a known protein component of the *osk* mRNP were tagged. As higher number of repeats result in stronger affinity during the capture step of the purification, I inserted tandem repeats of *MS2* stem-loop sequences upstream of the 3'UTR of a full-length *osk* genomic construct to tag the mRNA. Similar to the results previously reported by Zimyanin et al. (2008), insertion of either *MS2-6X* or *MS2-12X* tags did not interfere with *osk* mRNA localization suggesting that the complex required for localization was able to successfully assemble on these transcripts. However, both constructs could only rescue the early defects of oogenesis in an *osk* mRNA null mutant and failed to produce viable and/or fertile offsprings. Since posterior expression of *osk* is required for pole cell formation and abdominal patterning (Ephrussi and Lehmann, 1992; Markussen et al., 1995; Vanzo and Ephrussi, 2002), these observations suggest that the tag interfered with the translation of *osk* at the posterior pole of the oocyte. In addition to its role in pole plasm assembly, Osk protein levels also correlate with the number of pole cells formed (Ephrussi and Lehmann, 1992; Smith et al., 1992; Vanzo and Ephrussi, 2002). It is possible that when expressed in an endogenous *osk* null background, only a subset of the tagged transcript was able to localize and undergo translation. In some cases, a low level of the protein was sufficient to allow survival but gave rise to sterile adult flies. Therefore, to fully understand the effects of the insertion of exogenous aptamer tag in the *osk* mRNA, further visualization of both the *osk* mRNA and protein at late stages of oogenesis and embryogenesis, at a single molecule resolution, is required.

Recent studies in yeast have shown that insertion of *MS2* tags can affect the stability of some overexpressed transcripts, leading to the accumulation of 3' decay fragments (Garcia and Parker, 2015, 2016; Haimovich et al., 2016). This can potentially yield erroneous mRNA localization results. Here, I expressed the *osk* transgenes under their endogenous promoters to ensure that they are not overexpressed, which I could also confirm by Northern blotting

(Fig. 9B). To verify that the localized mRNAs are intact, I further characterized the *osk* transgenes by expressing them in the absence of endogenous *osk*. The posterior enrichment of tagged *osk* mRNA and its ability to rescue early oogenesis defects show that these transgenic transcripts are intact and not degraded transcripts acting as pseudo-full-length mRNAs. While the quantitative comparison of the localization of tagged *osk* with untagged endogenously expressed *osk* would be ideal, these qualitative measures support the stability of the *MS2*-tagged *osk* mRNAs.

3.1.2 mRNP purification using the *MS2* system: challenges and alternative strategies

To establish a protocol for the purification of a specific transcript from the native material, I co-purified *MS2*-tagged *osk* from a pool of total RNA (purified from egg chambers of transgenic flies), using MCP fused to affinity tags (purified from *E.coli* cells). I observed binding of MCP to the tagged *osk* to be inefficient and non-specific, irrespective of the affinity tag used (since only one-third of the input RNA could be recovered; Fig. 13). However, the low recovery of the tagged transcript is consistent with the yields obtained in previous studies using aptamer-based systems to capture RNA-protein complexes assembled *in vivo*. (Srisawat and Engelke 2001; Vasudevan and Steitz, 2007; Said et al., 2009; Tsai et al., 2011; Leppek and Stoecklin, 2014). This suggests a general difficulty in purifying mRNPs assembled on endogenously expressed tagged mRNAs from cellular samples. To note that most of the previous works have been carried out in either cell lines, yeast or bacterial cells, which have simpler transcriptome and proteome architecture than the *Drosophila* oocytes (Vasudevan and Steitz, 2007; Tsai et al., 2011; Said et al., 2009; Slobodin and Gerst, 2010; Leppek and Stoecklin, 2014). In addition, cultured cells can be easily upscaled to obtain sufficient amounts of purified mRNPs for subsequent analysis, which is particularly challenging when working with the *Drosophila* ovaries. This suggests that the aptamer-based systems are not very suitable for large-scale studies, where the starting material is a limiting factor.

In *MS2*-based imaging techniques *in vivo*, not all the *MS2*-binding sites are fully occupied by MCP, leading to a high background noise (Fusco et al., 2003; Wu et al., 2012, 2014). Therefore, the unspecific binding observed in this study can be attributed to the excess MCP, capturing unspecific mRNAs. Therefore, finding the optimal MCP concentration without compromising on the pull-down efficiency remains critical. One possibility would be to quantify the expressed tagged transcript and calculate the amount of MCP required. While such calculations are possible for purification of mRNPs assembled on *in vitro* transcribed mRNAs, this can be difficult for *in vivo* purifications. When working with *Drosophila* ovaries, the copy number of the tagged transcript needs to be determined both in a cell-specific and

stage-specific manner to obtain a homogeneous population of purified mRNPs, making it a challenge.

Similar to *in vivo* imaging, where incorporation of multiple *MS2*-binding sites has been shown to improve the signal of target-bound MCP over background MCP (Wu et al., 2012), increasing the number of aptamers on the mRNA can prove to be an effective strategy to increase both the specificity and efficiency of mRNP purification. However, large repetitive sequences are highly prone to recombinant deletion (Gebow et al., 2000; Bzymek and Lovett, 2001; Lovett, 2004; Wu et al., 2015). To circumvent this issue, an improved *MS2* system includes use of synonymous modifications in aptamer sequences as well as in tdMCP to remove the repetitiveness (Wu et al., 2015). Adapting the same model of stabilized repeats for effective mRNP purification presents a potential approach for improved specificity and efficiency. However, additional repeats are not always productive, as shown in the case of streptavidin aptamers, where higher than 4X aptamers were found to be less efficient for mRNP purification (Leppek and Stoecklin, 2014), suggesting that the number of repeats need to be empirically determined on a case-to-case basis.

For successful purification of a transcript-specific mRNP, the current strategy can be modified in several ways. This include co-expression of MCP in the ovaries, under the control of a moderately expressing promoter, for specific binding of MCP *in vivo*, thereby reducing the background binding. Use of cross-linking reagents is another alternative, which allows capturing of complexes under stringent conditions to retain true *trans*-acting components while removing non-specific binders (Slobodin and Gerst, 2010; Tsai et al., 2011). Pre-assembled *MS2* stem-loop-MCP complexes can be incubated with cell lysates, a strategy frequently used to purify spliceosomal complexes (Das et al., 2000; Jurica et al., 2002; Zhou et al., 2002; Deckert et al., 2006). Finally, replacing the *MS2* aptamers with tobramycin/streptavidin-binding aptamers, which do not require stem-loop binding proteins for their capture (Srisawat and Engelke 2001; Hartmuth et al. 2002; Deckert et al., 2006; Vasudevan and Steitz, 2007; Ward et al., 2011; Leppek and Stoecklin, 2014; Dong et al., 2015). However, a major consideration in screening different kinds of aptamers is the requirement of the generation and characterization of new transgenics, which is often a rate-limiting and a time consuming step.

Due to the various caveats of the *MS2* system in mRNP purification in general, I changed the strategy and opted for a protein-based approach. To gain a global overview of the factors and the interactions involved in mRNA localization, I co-purified protein complexes associated with six different RBPs that bind localized transcripts during *Drosophila* oogenesis.

3.2 IP-MS data provides new insights into the regulation of RBPs in localization and translation of maternal mRNAs

3.2.1 Label-free MS in combination with statistical analysis is an effective approach to distinguish true interactants from background binders

Label-free quantification is particularly advantageous for IP samples as large number of samples can be compared at the same time. Although label-free methods provide a wider proteome coverage, they lack the robustness of labeling methods. The low reproducibility of label-free MS techniques inevitably leads to the identification of a large number of unspecific binders, and requires a statistical pipeline to identify interactors with high confidence. This becomes especially important when comparing interactors of a diverse set of bait proteins for interactome studies.

In this study, I used the MaxLFQ algorithm (Cox et al., 2014) integrated in the MaxQuant software, (Cox and Mann, 2008; Cox et al., 2011) for label-free relative protein quantification. This approach has been shown to produce quantitative accuracies comparable to labeled MS techniques such as SILAC (Eberl et al., 2013). By implementing statistical filtering, I could effectively separate background and specific binders associated with each bait. Several well characterized interactions, acting as positive controls, were significantly enriched with most baits, indicating the efficacy of the workflow. Additionally, the MS data obtained from Dimethyl labeling of some of the samples was comparable to the corresponding label-free data (Fig. 24). Many interactions identified were novel and could be validated in cultured cells. Therefore, label-free MS, when combined with appropriate statistical methods, is a reliable and efficient method to map protein complexes, without resorting to exhaustive technical procedures.

3.2.2 Differential and common proteomes associated with each tagged RBP

While discrete proteomes were associated with each RBP, some baits shared components of common cellular machineries (supplementary Fig. 5). In addition to known regulators of mRNA localization, distinct nuclear and cytoplasmic complexes involved in different aspects of RNA metabolism were co-purified with baits, highlighting their diverse roles in post-transcriptional regulation of developmental mRNAs.

Consistent with the roles of Hrp48 and Vas in translational regulation of *osk*, *nos* and *grk* mRNAs (Markussen et al., 1995; Gavis et al., 1996; Dahanukar and Wharton, 1996; Styhler et al., 1998; Tomancak et al., 1998; Gunkel et al., 1998; Goodrich et al., 2004; Yano et al., 2004), ribosomal proteins and translation initiation factors were consistently enriched with both the RBPs (Fig. 20, 23). Furthermore, a considerable overlap was observed between the proteomes associated with both the baits (Fig 25; supplementary Fig. 5), in agreement with

the common mRNAs they regulate. Although no direct association is known, Hrp48 has been identified to be associated with Vas-containing complexes isolated from early embryos (Thomson et al., 2008). Consistent with this report, Hrp48 was enriched with Vas in the labeling MS data. Reciprocally, Vas was also enriched in one of the two replicates of Hrp48-GFP IP. However, these results could not be reproduced in label-free MS and the interaction could not be validated *in vitro* (data not shown). A possible explanation could be indirect association of Vas with Hrp48 mediated by other *trans*-acting factors. One such example could be protein Cup, which is a known translational regulator of *osk, grk* and *nos* mRNAs (Nelson et al., 2004; Nakamura et al., 2004; Clouse et al., 2008) and associates with both Hrp48 (Clouse et al., 2008) and Vas (Ottone et al., 2012). Cup was highly enriched in both Hrp48-GFP and Vas-GFP IPs and this interaction could also be validated *in vitro* (Fig. 29.3, 29.6).

3.2.3 Potential role of Hrp48 in regulating degradation of specific transcripts by recruiting additional partners

An interesting observation was the co-purification of Hrp48-GFP with components of decay machinery, most notably the CCR4-NOT deadenylase complex, in both label-free and labeled MS data (Fig. 35). This is consistent with the function of Hrp48 in translational repression of *osk* and *grk* mRNAs (Gunkel et al., 1998; Goodrich et al., 2004; Yano et al., 2004). However, the direct interaction of Hrp48 with components of the CCR4-NOT complex could not be tested. It is possible that this interaction is mediated by BicC, which negatively regulates target mRNAs in early oogenesis by recruiting the CCR4-NOT complex (Chicoine et al., 2007) and is also involved in translational regulation of *osk* mRNA (Saffman et al., 1998). BicC was enriched in Hrp48 IP and the interaction could be validated *in vitro* (Fig 29.3). Additionally, Hrp48 also interacts with Bel (Fig. 29.3), which is a part of *nos* repressor complex, together with components of the CCR4-NOT complex (Götze et al., 2017). These results suggest that by recruiting specific proteins such as Bel and BicC, Hrp48 might be able to differentially regulate expression of *nos* and *osk* mRNAs respectively (Saffman et al., 1998; Götze et al., 2017), possibly via CCR4-mediated deadenylation (Fig. 34). However, the role of Hrp48 in *nos* regulation remains unidentified and needs to be further investigated.
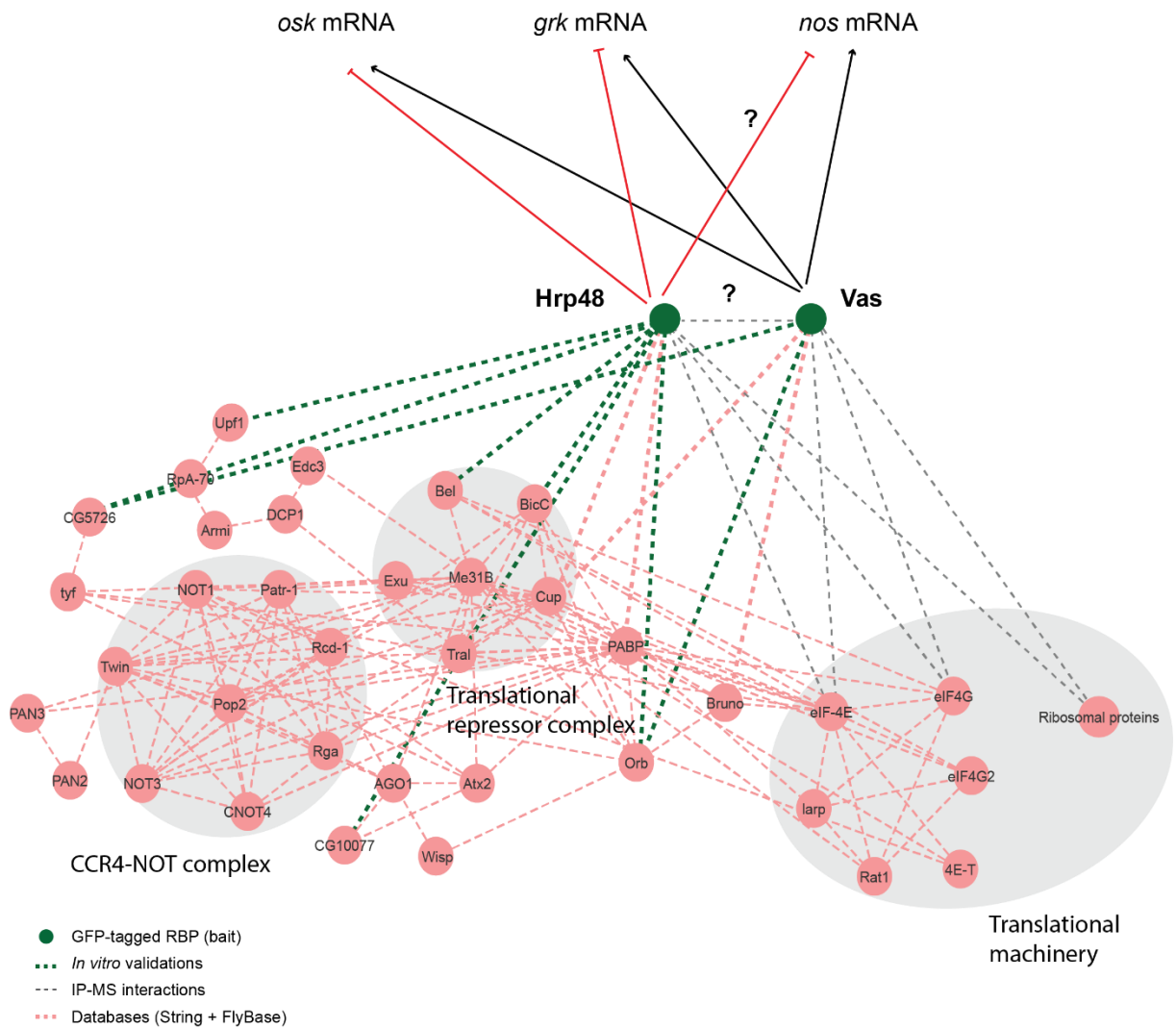
Fig 34. Model for the role of Hrp48-mediated protein associations in the regulation of maternal mRNAs

Shown above is a subset of protein complexes identified to be significantly enriched with Hrp48 (combining both label-free and labeled MS datasets), possibly involved in regulation of maternal mRNAs. Many of these proteins were also found to be enriched in Vas-associated complexes. Note that only *in vitro* validated or known interactions of Hrp48 and Vas are shown here, except for their association with the translation machinery which was identified in the IP-MS data. Proteins are represented as circles and the interactions are represented as dotted lines. Dotted pink lines represent the known interactions from databases; dotted grey lines represent the interaction identified in the IP-MS data; dotted green lines represent the *in vitro* validated novel interactions. Black arrows represent positive regulation while the red arrows represent negative regulation of mRNAs.
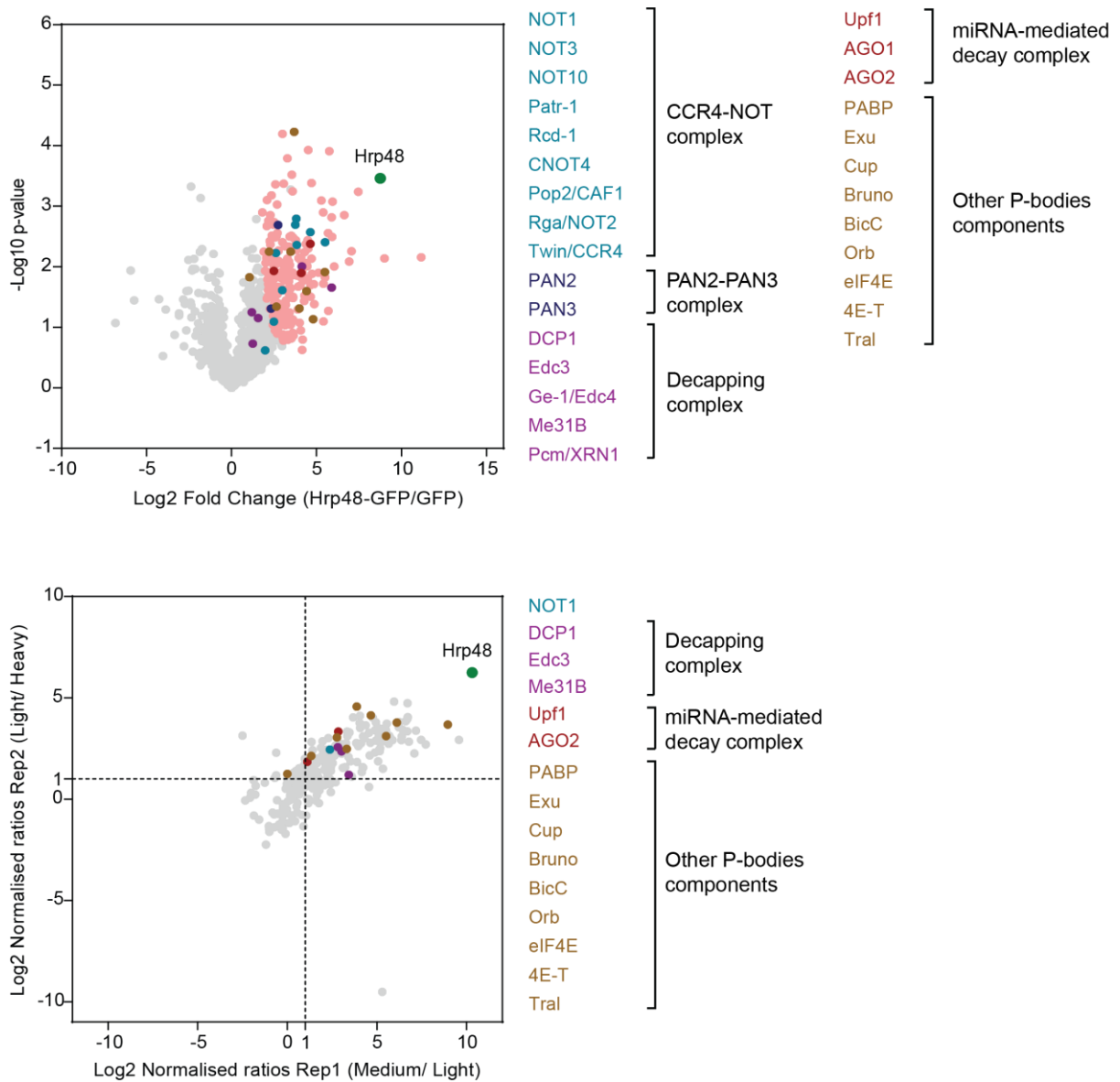
Fig 35. Co-purification of decay machineries and P-bodies components with Hrp48-GFP

Scatter plots highlighting the distribution of decay machineries and P-bodies components, found associated with Hrp48-GFP in the label-free MS (top) and the labeling MS analysis (bottom). IP from GFP sample served as a negative control. Each identified protein is represented as a dot in light grey; the bait is highlighted in green; significantly enriched proteins are highlighted in pink; components of different complexes are highlighted in different colors as indicated.

Co-precipitation of Hrp48 with components of the mRNA degradation pathways and translational repressors (Fig. 35), which are characteristic of P-bodies, is in agreement with previous findings of co-localization of Hrp48 with P-bodies (Weil et al., 2012). However, the high enrichment of ribosomal proteins observed in Hrp48 complexes is puzzling, as ribosomes are excluded from the core of P-bodies (Wilsch-Brüäuninger et al., 1997; Teixeira et al., 2005; Weil et al., 2012). Association of a small fraction of ribosomes with the P-bodies edges, as demonstrated by labeling of endogenous ribosomes by Immuno-Electron Microscopy (IEM), raises the possibility that Hrp48, via its association with ribosomal proteins, might be responsible for the dynamic patterning of silenced mRNPs in the P-bodies core to the translationally active P-bodies edges, as seen in the case of *grk* mRNA (Weil et al., 2012).

3.2.4 Nuclear processing is required for function of RBPs

In addition to their crucial role in pre-mRNA processing, splicing factors play an important role in affecting the cytoplasmic fates of mRNAs. For example, SmB, a Sm protein (which form the core of the functional unit of spliceosomes), is a known *osk* mRNP component and functions in germ cell specification by facilitating *osk* mRNA localization (Gonsalvez et al., 2010). Indeed, several splicing factors were enriched in the IPs of multiple baits. SmB was co-purified with Stau, a known interactant (Gonsalvez et al., 2010), and also with Glo, Hrp48 and Vas, suggesting it to be a *bona fide* component of the localization machinery. However, none of the interactions could be validated *in vitro*, possibly due to the lack of methylation in cultured cells, which has been proposed to be essential for the proper functioning of Sm proteins in *Drosophila* germ cell formation (Anne et al., 2007; Gonsalvez et al., 2006, 2010).

Additionally, two SR family proteins, SC35 and SF2, which function both in the early steps of splicing as well as in alternative splicing (Krainer et al., 1990; Ge and Manley, 1990), were found to be associated with most baits (though not significantly in all cases). Both SC35 and SF2 could also be validated for their interaction with Glo and Stau *in vitro* (Fig 29.2C, 29.2D, 29.5C), suggesting that they might be involved in *osk* regulation, together with other splicing factors. Co-purification of SF2 with the EJC in mammalian cells (Singh et al., 2012) and with the short isoform of Osk in *Drosophila* embryos (Hurd et al., 2016), support its potential role in *osk* mRNA localization and remain to be investigated.

3.2.5 Validation of several previously uncharacterized interactions

Numerous novel gene interactions were identified in the MS data. Out of 94 interactions tested, 26 novel interactions could be confirmed as direct protein-protein interactions in cell culture. Of these, most interesting are the ones of previously uncharacterized genes, with yet unknown functions. One such example is CG5726, which contains a MIF4G-like domain. This domain is found in many proteins involved in RNA metabolism including translation initiation

factors, NMD factors and nuclear cap-binding proteins. With no identifiable orthologs in humans, CG5726 protein shows up to 50% sequence identity among Drosophilids. In early embryos of *Drosophila melanogaster*, CG5726 interacts with short Osk (Hurd et al., 2016). In this study, CG5726 was found to be interacting with Glo, Hrp48 and Vas, both *in vivo* (by IP-MS) and *in vitro* (by co-IP; Fig 29.2, 29.3, 29.6), suggesting its potential role in mRNA localization.

Another example of novel interaction was the binding of Stau to Loquacious (Loqs). Loqs is a cytoplasmic double stranded RNA-binding protein (dsRBP), which is conserved in mammals and participates in RNAi pathways by binding to Dicer (Dcr; reviewed in Fukunaga and Zamore, 2012). RNAi plays an important role in *Drosophila* germline development and early phase of *osk* repression (Kugler and Lasko, 2009). Furthermore, *Drosophila* Loqs mutant females are sterile and their ovaries fail to sustain germ-line stem cells (Förstemann et al., 2005), indicating a critical role of Loqs in oogenesis. In this study, both Dcr and Loqs were found to be highly enriched in the Stau IP and Stau-Loqs interaction could be validated *in vitro* (Fig. 29.5). This suggests a potential role of Stau in translational repression of *osk*, by associating with the RNAi machinery. Although no such evidence have been presented in *Drosophila*, recent reports in *C.elegans* (LeGendre et al., 2013) and other insects (*Diaphorina citri* and *L. decemlineata;* Taning et al., 2016; Yoon et al., 2018) have shown a requirement of Stau in RNAi responses, suggesting a conserved role of Stau in RNAi-mediated gene silencing.

Several conserved RNA helicases, including Vas and Bel, have been shown to be required for oogenesis and female fertility (Raz, 2000; Johnstone et al., 2005; Lasko, 2013; Dehghani and Lasko, 2015; Wang et al., 2015c). Consistent with the crucial role of RNA helicases in embryonic development, two such genes were identified to be enriched in this study: the putative RNA helicase CG10077 and the DEAD-box RNA helicase Mahe (Maheshvara). While CG10077 is an ortholog of human DDX5, Mahe is an evolutionary conserved regulator of Notch signaling pathway and displays a wide range of phenotypes upon ectopic expression in *Drosophila* (Surabhi et al., 2015). Mahe is maternally expressed and displays strong neuronal expression during both embryogenesis and larval development (Surabhi et al., 2015). Both *in vivo* and *in vitro*, CG10077 binds Hrp48 (Fig. 29.3), while Mahe binds both Glo and Hrp48 (Fig. 29.2, 29.3). Whether these proteins also play a role in mRNA localization in *Drosophila*, needs to be further investigated.

Further *in vivo* characterization of the protein interactions uncovered in this study is imperative in order to delineate their functional relationships and discern their role in mRNA localization. Since the experiments were done in a transcript-independent manner, the current analysis relies on existing information to separate complexes that contain shared components into different entities. Isolating transcript-specific complexes, together with this dataset, would be highly informative in identifying functional units driving localization of different mRNAs. With the optimized IP conditions and the pipeline I developed for the filtering of MS data, up scaling the current dataset by including more bait proteins, separated by time and space during oogenesis, presents a potential tool to map the complete ovary interactome underlying mRNA localization in *Drosophila*.

4. Methods and Materials

4.1 Cloning

4.1.1 DNA amplification by PCR

For cloning purposes, cDNA was amplified from wild-type fly ovaries. Total RNA was extracted using TRI-Reagent® (Sigma #T9424), according to the manufacturer's instructions and reverse transcribed using Moloney Murine Leukemia Virus (M-MuLV) reverse transcriptase (Thermo Fisher Scientific # EP0352), in the presence of oligo (dT)$_{15}$ primers.

4.1.2 Reverse Transcription

4 μg of total RNA was mixed with 0.5 g of oligo (dT)$_{15}$ primers in a total volume of 11 μl; the RNA was denatured for 5 min at 70 °C and chilled on ice. The following components were then added, in the indicated order: 4 μl of 5X reaction buffer (250 mM Tris-HCl pH 8.3, 250 mM KCl, 20 mM MgCl$_2$, 50 mM DTT), 2 μl of dNTP mix (dATP, dCTP, dGTP and dTTP, 10 mM each; all from Fermentas), 0.5 μl *RiboLock™ RNase Inhibitor* (Thermo Fisher Scientific # EO0381) and ddH$_2$O to a final volume of 30 μl. The mixture was incubated for 5 min at 37 °C before the addition of 1 μl of M-MuLV reverse transcriptase (Thermo Fisher Scientific # EP0352). The mixture was then incubated for 2 hours at 42 °C and the enzyme was inactivated by heating the reaction mix for 10 min at 70 °C.

4.1.3 PCR amplification

Genes of interest were amplified using the *Phusion® High fidelity DNA polymerase* (NEB #M0530L). The reaction mixes were prepared according to the manufacturer's instructions. If a plasmid served as a template, 150–250 ng of DNA were used; if the template consisted of cDNA, 0.5-1 μl of the reverse transcription reaction were used. PCR conditions (annealing temperature and extension times) were adjusted each time according to the oligonucleotides and template used (Green and Sambrook, 2012). Oligonucleotides used in this study have been summarized in Table 13.

5 μl of the generated amplicons were analyzed by agarose gel electrophoresis (1% Agarose prepared in TAE buffer), visualized with Midori Green staining (*Midori green advance DNA stain*, Nippon genetics Europe GmbH #MG04) and the rest of the reaction was purified using the *QIAquick Gel Extraction Kit* (QIAGEN), according to the manufacturer's instructions; the purified DNA was eluted with 25 μl of ddH$_2$O and used for subsequent cloning either by standard restriction digestion-ligation approach (Green and Sambrook, 2012) or Gibson cloning (Gibson et al., 2009).

4.1.4 Digestion with restriction endonucleases

Cloning vectors (summarized in Table 14) and purified DNA amplicons were digested with appropriate restriction enzymes (supplied by NEB). Reactions were carried out using the optimal reaction buffers and conditions recommended by the supplier. Usually, 4-5 μg of vector or the entire PCR product (after purification) were digested each time. Restricted DNA fragments were further purified, to get rid of buffers and ions that may interfere with downstream steps, using the *QIAquick PCR Purification Kit* (QIAGEN), according to the manufacturer's instructions. Digested vectors were first analyzed by agarose gel electrophoresis and the desired fragments were purified from gel using the *QIAquick Gel Extraction Kit* (QIAGEN), according to the manufacturer's instructions. In both cases, the purified DNA was eluted with 30 μl of ddH$_2$O.

4.1.5 Ligation

After purification, the linearized vector and a gene (or gene fragment) with compatible ends were ligated using *T4 DNA ligase* (NEB #M0202L). Typically, 100 ng of the purified digested vector and 6X molar excess of the purified digested insert were ligated; the ligation reaction was performed in 20 μl, according to the manufacturer's instructions, at 16 °C overnight.

4.1.6 Gibson Assembly

As an alternative to standard restriction digestion-ligation based cloning, Gibson Assembly was used (Gibson et al., 2009). This method utilizes three enzymatic activities to assemble multiple DNA sequences in a single reaction, without the need for compatible restriction sites. The enzyme cocktail typically includes a 5' exonuclease which generates the long overhangs, allowing annealing of terminal homologous overlapping sequences. This is followed by extension by a polymerase and sealing by a ligase, to yield an assembled product.

Primers with ends overlapping (20-24 base pairs) with a linearized vector were used to amplify the insert (either from a plasmid or cDNA), using a standard PCR reaction with *Phusion® High fidelity DNA polymerase* (NEB #M0530L). 70 ng of the linearized vector and equimolar amount of the purified insert were mixed with 15 μl Gibson assembly mix (Table 1) in a total volume of 20 μl. The reaction was incubated at 50 °C for 60 min. Assembly reaction was either transformed in electrocompetent *E. coli* cells (strain XL1-Blue*;* Agilent Technologies) directly or stored at -20 °C for future use.

Table 1: Buffers for Gibson cloning

5X ISO Buffer (6 ml)		Gibson Assembly mix (for 120 μl)	
1 M Tris-HCl pH 8 at 4 ºC	3 ml	5X ISO buffer	32 μl
2 M MgCl$_2$	150 μl	10 U/ μl T5 exonuclease * (NEB #M0363S)	6.4 μl
100 mM dNTP mix (25mM each of dGTP, dCTP, dATP, dTTP)	240 μl	2 U/ μl Phusion polymerase (NEB # M0530L)	2 μl
1 M DTT	300 μl	40 U/ μl Taq ligase (NEB #M0208L)	16 μl
PEG-800	1.5 g		
50 mM NAD	600 μl	ddH$_2$O	to 120 μl
ddH$_2$O	to 6 ml		
Stored at -20 ºC in 32 μl aliquots		Stored at -20 ºC in 15 μl aliquots	

* 1 μl of T5 exonuclease was diluted in 100 μl of 50 mM Tris-HCl (pH 8 at 4 ºC), 100 mM NaCl.

4.1.7 Preparation of electro competent *E. coli* and transformation

For the transformation and propagation of the plasmids for DNA preparations, except for the tagging vector pTagNG (Ejsmont et al., 2011; provided by Mihail Sarov, MPI-CBG Dresden), *E. coli* strain XL1-Blue (Agilent Technologies) was used. For propagation of pTagNG, strain pir-116 (EPICENTRE) was used, as its R6K origin of replication requires the *pir* gene product to initiate the DNA amplification. For expressing recombinant proteins, *E. coli* strains BL21 (DE3) Star (Life technologies) and BL21 (DE3) Gold (Agilent technologies) were used. All the strains with their respective genotypes have been listed in Table 2.

Table 2: List of *E. coli* strains used in the study

E. coli strain	Genotype	Source
XL1-Blue	(*recA1 endA1 gyrA96 thi-1 hsdR17 supE44 relA1 lac* [F' *proAB lacIqZΔM15* Tn*10* (Tet^R)])	Agilent Technologies
EC100D™ *pir-116*	F- mcrA Δ(mrr-hsdRMS-mcrBC) Φ80dlacZ ΔM15 ΔlacX74 recA1 endA1 araD139 Δ(ara, leu)7697 galU galK λ- rpsL (Str^R) nupG pir-116(DHFR)	EPICENTRE
BL21 (DE3) Star	(F-ompT hsdS$_B$ (r$_B$-, m$_B$-) galdcmrne131 (DE3))	Life technologies
BL21 (DE3) Gold	(F⁻ ompT hsdS (rB⁻ mB⁻) dcm+ Tet^r gal λ(DE3) endA Hte)	Agilent Technologies

Electrocompetent cells preparation

Since electroporation is a rapid and efficient method of introducing foreign DNA into a wide range of cells, electrocompetent cells were preferred over chemically-competent cells.

Bacteria from a frozen glycerol stock were streaked out on Luria-Bertani (LB)-agar (10 g/l tryptone, 5 g/l yeast extract, 10 g/l NaCl, 15 g/l Agar), and incubated overnight at 37 ºC. A single colony was used to inoculate 50 ml of LB medium (10 g/l tryptone, 5 g/l yeast extract, 10 g/l NaCl), and bacteria were allowed to grow overnight at 37 ºC with vigorous shaking. 500 μl of the bacterial suspension was used to inoculate 500 ml of LB. The bacteria were grown at 37 ºC shaking at 180 rpm until they reached an optical density (measured at wavelength 600mn; OD_{600}) of 0.6-0.8 units. The culture was cooled on ice and bacteria were then pelleted by centrifugation at 5000 rpm in a pre-cooled rotor (4 ºC). The subsequent steps were performed at 4 ºC in a cold room, using pre-cooled reagents to increase the survival rate of the cells and therefore, their transformation efficiency. The cell pellet was resuspended twice in 200 ml of ice-cold double distilled water to remove any traces of salts from the media and pelleted again as described above. Finally, the pellet was resuspended in 10 ml of 10% glycerol. The cells were quickly dispensed in 50 μl aliquots, immediately transferred to liquid nitrogen and stored at −80 ºC.

Bacterial electroporation

For the transformation, 50 μl aliquots of competent bacteria were thawed on ice and DNA (1 μl of plasmid DNA, or 5 μl of a ligation/gibson reaction) was added before transferring the cells to electroporation cuvettes (2 mm gap cuvettes; Peqlab #PEQL71-2020). The cells were then electroporated via Micropulser (Biorad) with a pulse of 1.8kV for 5.80ms. To allow the cells to recover and express antibiotic resistance genes, 200 μl of LB was added to the cells. This suspension was transferred to a microcentrifuge tube and incubated for 30-40 min on a thermomixer at 37 ºC, shaking at 800 rpm. The cells were then plated onto LB-agar plates containing the appropriate antibiotic for selection (25 g/ml kanamycin or 100 g/ml ampicillin) and incubated overnight at 37 ºC.

To check the efficiency of the cloning, single colonies were picked and used to inoculate 2 ml LB cultures. After overnight incubation at 37 ºC, the cells were pelleted by centrifugation (6000*g* at RT for 3 min) and the plasmid was extracted using *Nucleospin® Plasmid EasyPure* kit (MACHEREY-NAGEL), following the manufacturer's instructions. The identity of the insert was verified first by restriction with appropriate endonucleases or by Colony PCR, and then by full sequencing of the insert (Genome facility, MPI Tübingen).

For Colony PCR, 20 μl reactions (complete with the enzyme; *Taq DNA polymerase*, NEB # M0267X) were assembled according to the manufacturer's instructions using appropriate primers. Picked colonies were briefly suspended directly into the PCR mixture to serve as the template. PCR program was run as described before.

For the propagation of the plasmid of interest, single colonies were used to inoculate 100 ml of LB medium, additioned with the appropriate antibiotic for selection, and incubated overnight at 37 ⁰C with vigorous shaking. The cells were then pelleted by centrifugation (5000*g* at RT) and the plasmid was extracted using *QIAGEN Plasmid Midi Kit* (QIAGEN), following the manufacturer's instructions.

4.1.8 Vectors and plasmid constructs

Constructs for MS2 coat protein (MCP) bacterial expression

Construct for MCP was purchased from Addgene (27122: pMS2-YFP) and subcloned into pET-MCN vectors (provided by Christophe Romier, IGBMC Strasbourg) bearing N-terminal Glutathione S-transferase (GST), Hexahistidine (His) and Hexahistidine- Maltose Binding Protein (His-MBP) tags. This version of MCP is optimized to prevent oligomerization (mutation: dlFG and A81G) and also binds more tightly to the stem-loops (SL) (mutation V29I) (Lim and Peabody, 1994; LeCuyer et al., 1995).

GST-MCP was obtained by inserting MCP sequence into the *Nde*I and *Hind*III sites of the pET-MCN-GST vector. Similarly, His-MCP and His-MBP-MCP were obtained by cloning the sequence in *Nde*I and *Bam*HI sites of pET-MCN-His and pET-MCN-His-MBP vectors respectively. A codon-optimized construct designed to express two copies of MCP in tandem, tandem-MCP (tdMCP), was synthesized by GenScript USA Inc. (https://www.genscript.com/). The sequence was subcloned into pET-MCN-His-MBP using *Nde*I and *Xba*I sites.

Constructs for recombineering

The constructs for cloning of *MS2* and *PP7*SL were purchased from Addgene: pCR4-24XMS2SL-stable (Addgene 31865); pCR4-24XPP7SL (Addgene 31864) and pCR4-12XMS2SL (Addgene 27119). These constructs, with several copies of the SL, are designed to prevent recombination among repeats and to achieve higher coat protein binding efficiency. For *MS2SL*, a variant of the wild-type sequence optimized for higher binding affinity, where U-5 has been substituted by C, was used (Lowary and Uhlenbeck, 1987). The SL fragments were subcloned into 5' *Eco*RI and 3' *Bam*HI sites of the tagging vector pTagNG (Ejsmont et al., 2011; provided by Mihail Sarov, MPI-CBG Dresden), using standard cloning

procedures. For preparing a construct expressing both *MS2* and *PP7SL*, MS2-12XSL fragment bearing 5' *Eco*RI and 3' *Bgl*II sticky ends and PP7-24XSL fragment bearing 5' *Bam*HI and 3' *Bgl*II sticky ends were ligated into pTagNG, digested with 5' *Eco*RI and 3' *Bam*HI.

Constructs for HEK cell expression

For expressing proteins in human HEK cells, all cDNAs, amplified as described before, were cloned in overexpression vectors bearing N-terminal HA, HA-Flag or EGFP tags (provided by Elisa Izaurralde, MPI Tübingen). Full-length cDNAs were cloned, except for protein "Ncm" where a sequence encoding amino acids 359-664 was amplified and used. The boundaries were designed based on the MIF4G domain of the human ortholog CWC22, which has been shown to bind eIF4AIII (Buchwald et al., 2013)**.** To serve as a control, either MBP or EGFP alone was used. Some of the clones prepared by Kristina Ile and Desiree Zerbst in the lab were also used in the study.

For a list and details of the plasmids used in this study, refer to Table 14.

4.1.9 Liquid culture recombineering

Liquid culture recombineering was done in collaboration with Helena Jambor, Tomancak lab (MPI-CBG Dresden). Tagging vector pTagNG was used for all cloning purposes (Ejsmont et al., 2011; provided by Mihail Sarov, MPI-CBG Dresden). The protocol was adapted from Ejsmont et al. (2009, 2011).

Using the constructs: pTagNG-MS2-12XSL; pTagNG-MS2-24XSL; pTagNG-PP7-24XSL; pTagNG-MS2-12X-PP7-24XSL as templates, the recombineering cassettes (2XTY1-(SL)-FRT-rpSL-KanR-FRT-3XFlag) were amplified. Primers binding to epitope tags TY1 (forward) and Flag (reverse) were used, which simultaneously introduced flanking sequences homologous to the *osk* 3'UTR region, downstream of stop the codon, for recombination.

Recombineering cassettes were amplified using Phusion Flash Mix (Phusion Flash High-Fidelity PCR master mix, Thermo Fisher Scientific # F-548S). Since the quality of the PCR product is a bottleneck for efficient recombineering, HPLC purified primers were used and only 18 cycles were programmed to avoid PCR induced mutations. To further increase the PCR efficiency, DMSO was added to disrupt secondary structure formation in the template and facilitate primer annealing. A reaction was prepared as follows:

25 ng	plasmid template
25 μl	10x Phusion Flash mix
2.5 μl	sense oligonucleotide (10 μM)
2.5 μl	antisense oligonucleotide (10 μM)
2.5 μl	DMSO
to 50 μl	ddH$_2$O

Amplification program: two-step protocol
1. 98 ºC   2 min
2. 98 ºC   15-20 sec
3. 72º C   30 sec/kb *
4. go to 2   x 18 X
5. 72 ºC   7 min

----
50 μl final volume

* 60 sec used for MS2-12X + PP7-24X construct

The PCR amplicons with different SLs were recombineered into a fosmid containing the *osk* genomic fragment (Ejsmont et al., 2009). Constructs were sequence-verified for successful recombination and purified using *QIAGEN Plasmid Midi Kit* (QIAGEN), following the manufacturer's instructions, for subsequent integration into the *Drosophila* genome. Upon sequencing *osk* fosmid tagged with *MS2-24XSL*, it was observed that a major part of the tag was lost, most likely due to recombinant deletion. As only six SL were remaining, the construct was renamed as *MS2-6XSL* and used for fly transformation.

4.2 *Drosophila* stocks and genetic rescue experiments

Fly stocks were maintained using standard conditions and all crosses were set up at room temperature.

To produce transgenic lines expressing aptamer-tagged *osk* mRNA (listed in Table 3), constructs were injected in embryos collected from flies expressing landing site on the 3rd chromosome, in a wild-type background. *osk*FlyfosPP7-24XSL and MS2-6XSL were injected at MPI-CBG in Dresden. Other constructs (*osk*FlyfosMS2-12XSL and MS2-12X+PP7-24XSL) were sent for injection to Bestgene Inc. (USA). Eye promoter-driven dominant selectable marker (dsRED) was used as an indicator of successful transgenesis and stable fly lines were established.

Fosmid lines (listed in Table 4) expressing GFP-tagged proteins were purchased from the Vienna *Drosophila* Resource Center (VDRC), except for Stau-GFP and eIF4AIII-GFP which were provided by the Tomancak lab (MPI-CBG, Dresden). The control fly line (expressing tag only, referred to as GFP) was injected in the lab by Kristina Ile. Fly lines used for rescue experiments were purchased from Bloomington *Drosophila* Stock Center (BDSC; listed in Table 3); *stau* mutant lines were provided by Uwe Irion (MPI Tübingen).

4.2.1 Construction of transgenic line expressing tag alone

To amplify the tag sequence (to serve as a control for IP-MS experiments), genomic DNA was prepared from flies expressing Stau-GFP. For this, 5 flies were frozen at -80 ºC before grinding them in 60 μl of lysis buffer (100 mM Tris-HCl pH 7.5, 100 mM EDTA, 100 mM NaCl, 0.5% SDS). The lysate was incubated at 65 ºC for 30 min. 120 μl of LiCl/KAc solution (1 part 5M KAc stock: 2.5 parts 6M LiCl stock) was added to remove RNA by selective precipitation, followed by incubation on ice for an additional 10 min. The lysate was cleared by centrifugation at 16000g at RT and the supernatant was transferred to a fresh tube. 90 μl of isopropanol was added for precipitation and DNA was pelleted by centrifugation at 16000g for 15 min at RT. The pellet was washed with 70% ethanol, air dried and resuspended in 30 μl of ddH$_2$O. 0.5 μl of the genomic DNA was used to set up a standard 2-step PCR reaction.

The amplified fragment was placed downstream of a moderately expressing *exu* promoter in pUI-Venus (an existing vector in the lab) using *Age*I and *Nhe*I sites, replacing the existing Venus sequence. The entire construct was then subcloned in a modified pUAST-attB vector (without UAS sites or SV40 poly(A) signal; original vector provided by Uwe Irion, MPI Tübingen) using *Kpn*I and *Bam*HI sites. The sequence verified vector was then purified using *QIAGEN Plasmid Midi Kit* (QIAGEN), following the manufacturer's instructions. The purified vector was injected into embryos expressing ΦC31 integrase (Groth et al., 2004) that recognizes a landing site on the 3rd chromosome, for site-specific integration. Transgenic flies were identified in the F1 generation by the presence of red eyes and a stable fly line was established.

4.2.2 Genetic rescue assay

To check if the tagged *osk* genes can rescue the null phenotype, the transgenes were recombined with an *osk* deficiency and then crossed with an *osk* RNA null mutation (*osk[A87]*; provided by Anne Ephrussi, EMBL Heidelberg). The resulting *osk* null females were crossed to wild-type males and the ability to lay eggs, viability and fertility of the offsprings were checked. dsRed was used as a selection marker for the presence of the transgene in every generation.

To check if the tagged proteins are fully functional, transgenes were tested against a deficiency in *trans* to a mutant allele, or two mutant alleles as in the case of *stau*, for the rescue of the respective phenotypes. For *nos*, the transgene was recombined with a *nos* deficiency, since the gene is located on the same chromosome as the insertion. The resulting trans-heterozygotes were checked for embryonic lethality or female sterility, to assess the functionality of the transgenes. For the maternal effect genes (phenotype of the individual is

dependent on the genotype of the mother), trans-heterozygotes were further crossed with wild-type males and the progenies were examined for their ability to rescue the phenotype. dsRed was used as a selection marker for all the transgenes in every generation.

Table 3: List of fly stocks

Gene/strain	Genotype	Origin	Chromosome
Wild-type	-	Lab stock	-
Balancer	w⁻ ; PrDr/ TM6C	Lab stock	3
Balancer	w⁻ ; If/CyO; MKRS/TM6B	Lab stock	1;2;3
Control line (tag)	w⁻ ; PBac(y+ w[+]-*exu*-promoter:: 2XTY1-sGFP-V5-preTEV-BLRP-3XFLAG-3B)	Lab stock (Kristina Ile)	3
stau	*stau[D3]*/CyO	Uwe Irion (MPI, Tübingen)	2
stau	w⁻ ; *stau[R9]*/SM6a	Uwe Irion (MPI, Tübingen)	1;2
*osk*FlyfosMS2-6XSL	y w⁻ ; PBac(y+ *osk*-2X TY1-*MS2*-6X-3X Flag-dsRED-3B)	Helena Jambor (MPI-CBG, Dresden)	1; 3
*osk*FlyfosMS2-12XSL	y w⁻ ; PBac(y+ *osk*-2X TY1-*MS2*-12X-3X Flag-dsRED-3B)	Addgene Inc.	1; 3
*osk*FlyfosPP7-24XSL	y w⁻ ; PBac(y+ *osk*-2X TY1-*PP7*-24X-3X Flag-dsRED-3B)	Helena Jambor (MPI-CBG, Dresden)	1; 3
*osk*FlyfosMS2-12X+PP7-24XSL	y w⁻ ; PBac(y+ *osk*-2X TY1-*MS2*-12X-*PP7*-24X- 3X Flag-dsRED-3B)	Addgene Inc.	1; 3
osk	w; *osk[A87]*/TM6C	Anne Ephrussi (EMBL, Heidelberg)	1; 3
Deficiency for *osk*	w; Df(3R)p-XT103 ru st e ca/TM6C	Uwe Irion (MPI, Tübingen)	1; 3
MS2 coat protein	w⁻ ; tandem-MS2Venus ST	Uwe Irion (MPI, Tübingen)	1; 3
osk	w; Df(3R)p-XT103 ru st e ca PBac(y+ *osk*-2X TY1-*MS2*-6X-3X Flag-dsRED-3B)/ TM6C	*Prashali Bansal*	1; 3
osk	w; Df(3R)p-XT103 ru st e ca PBac(y+ *osk*-2X TY1-*MS2*-12X-3X Flag-dsRED-3B)/ TM6C	*Prashali Bansal*	1; 3
nos	Df(3R)Exel6183- PBac(y[+]-Nos-2XTY1-sGFP-V5-preTEV-BLRP-3XFLAG-dsREd-3B) /TM6B	*Prashali Bansal*	3
eIF4AIII	*CG7483[19]* red[1] e[4]/TM3, Sb[1]	BDSC 2781	3
Deficiency for *eIF4AIII*	w[1118]; Df(3R)Exel6147, P{w[+mC]=XP-U}Exel6147/TM6B, Tb[1]	BDSC 7626	1;3
nos	st[1] *nos[L7]* e[1]/TM3, Sb[1] Ser[1]	BDSC 3285	3
Deficiency for *nos*	w[1118]; Df(3R)Exel6183, repo[*] P{w[+mC]=XP-U}Exel6183/TM6B, Tb[1]	BDSC 7662	1;3
vas	*vas[RJ36]* cn[1] bw[1]/CyO, *µl*(2)DTS513[1]	BDSC 5011	2
Deficiency for *vas*	Df(2L)A72, b[1] cn[1] bw[1]/CyO, Adh[nB]	BDSC 6058	2
glo	y[1] w[*]; P{ry[+t7.2]=neoFRT}82B *glo[162x]*/TM3, Sb[1]	BDSC 57693	1;3
Deficiency for *glo*	w[1118]; Df(3R)Exel7310/TM6B, Tb[1]	BDSC 7965	1;3
Deficiency for *hrp48*	w[1118]; Df(2L)BSC108/CyO	BDSC 8847	1;2
hrp48	y[1] w[67c23]; P{w[+mC]=lacW}*hrb27C[k02814]*/CyO	BDSC 10375	1;2
For transgenesis (tag control)	y[1] M{vas-int.Dm} ZH-2A w[*]; PBac{y[+]-attP-3B}VK00033	BDSC 24871	1; 3

	y[1] w[1118]; PBac{y[+]-attP-3B}VK00033	BDSC 9750	1; 3
For transgenesis (*osk*Flyfos lines)			

Table 4: List of fosmid fly lines

Fly line	Fosmid clone	Origin	Chromosome
fTRG 930 (Hrp48-GFP)	FlyFos024565(pRedFlp-Hgr)(*Hrb27C*28387::2XTY1-sGFP-V5-preTEV-BLRP-3XFLAG)dFRT	VDRC 318283	3
fTRG 1009 (Glo-GFP)	FlyFos018316(pRedFlp-Hgr)(*glo*19733::2XTY1-sGFP-V5-preTEV-BLRP-3XFLAG)dFRT	VDRC 318719	2
fTRG 700 (Nos-GFP)	FlyFos017035(pRedFlp-Hgr)(*nos*18565::2XTY1-sGFP-V5-preTEV-BLRP-3XFLAG)dFRT	VDRC 318195	3
fTRG 577 (Vas-GFP)	FlyFos031335(pRedFlp-Hgr)(*vas*41728::2XTY1-sGFP-V5-preTEV-BLRP-3XFLAG)dFRT	VDRC 318157	3
fTRG 1134 (eIF4AIII-GFP)	FlyFos022832(pRedFlp-Hgr)(*eIF4AIII*25582::2XTY1-sGFP-V5-preTEV-BLRP-3XFLAG)dFRT	Tomancak lab (MPI-CBG, Dresden)	2
fTRG 1404 (Stau-GFP)	FlyFos028195(pRedFlp-Hgr)(*stau*[29658]::S000169_fly_pretag)::2XTY1-sGFP-V5-preTEV-BLRP-3XFLAGdFRT	Tomancak lab (MPI-CBG, Dresden)	3

4.3 *In situ* hybridization

The protocol was adapted from Lécuyer et al. (2008).

For *in situ* hybridizations, digoxigenin (DIG)-UTP labeled *osk* (full length), *rp49* (CDS only) and *alpha-tubulin 67C* (full length) antisense RNA probes were prepared. Typically, 2 μg of the linearized template was transcribed using *T7 RNA polymerase* (Roche #10881767001) and DIG labeling mix (Roche #11277073910) according to the manufacturer's instructions. The reaction was purified using *Ambion MEGAclear™ Kit* (Invitrogen™ #AM1908) according to the manufacturer's instructions and probes were eluted in 30 μl of ddH$_2$O. An equal amount of formamide was added before storage at -20 ºC.

To check the localization of aptamer-tagged *osk* RNA, well-fed flies were dissected in PBT (PBS with 0.1% Tween-20) at RT and fixed in 4% PFA solution (in PBT) for 25 min. Extracted ovaries were then washed 4x in PBT, to remove any traces of fixing solution, followed by addition of 100% MeOH for dehydration and stored at -20 ºC overnight. The following day, they were rehydrated by washing 3x in PBT and fixed again, in 4% PFA solution, for 20 min. Post-fixation, ovaries were washed with PBT 3x for 2 min and samples were incubated with protein kinase (3 μg/ml in PBT) for 10 min at RT, followed by an hour incubation on ice. The digestion was stopped by washing twice with glycine solution (2 mg/ml in PBT), followed by washing 2x in PBT. Ovaries were fixed again as before and after washing with PBT 5x for 2

min, samples were pre-hybridized in hybridization buffer (50% de-ionized formamide, 5X SSC pH 6.8, yeast tRNA 36 μg/ml, heparin 100 μg/ml, salmon sperm DNA 100 μg/ml and 0.1% Tween-20) for at least 90 min at 70 ºC. The DIG-labeled probe was added in fresh buffer and samples were incubated at 70 ºC overnight. The following day, after washing with hybridization buffer for 20 min at 70 ºC, samples were washed in PBT and blocking buffer was added (1% milk in PBT). Samples were blocked for 1 hour at RT and alkaline phosphate-conjugated anti-DIG antibody (diluted 1:2.000 in blocking buffer) was added. Following incubation for 2 hours at RT, ovaries were washed several times in PBT and transferred to staining buffer (100 mM Tris-HCl, pH 8.0, 150 mM NaCl, 50 mM $MgCl_2$, 0.2% Tween-20). For colorimetric detection of alkaline phosphatase activity, the substrate, a mixture of NBT (nitro blue tetrazolium; Promega #S380C) and BCIP (5-bromo-4-chloro-3-indolyl-phosphate; Promega #S381C) was added to the staining buffer, according to the manufacturer's instructions and development of the chromogen was monitored. Staining was stopped by washing in PBT several times and finally in PBS to remove the detergent. All the washing steps were carried out on a nutator mixer.

Ovaries were mounted in *Fluoromount-G™* (Southern Biotech #0100-01c) and slides were stored at 4 ºC overnight. Images were acquired on a Zeiss AxioImager Z1 microscope, with a Plan-Apochromat 40X objective (NA 0.95) and a differential interference contrast (DIC) condenser. Image processing was done using FIJI (Schindelin et al., 2012).

4.4 Large-scale material preparation for mRNP purification

For mass isolation of the egg chambers, an optimized protocol adapted from Jambor et al. (2005) was employed. A kitchen aid grinder (KitchenAid, model: 5K45SS EWH #105759) fitted with a corn mill (KitchenAid, model: 5KGM # 100748) was used to process the flies. Flies fed on fresh yeast paste for 2 days were collected in PBS and passed through the mill twice. The flow-through was collected and sieved through a series of meshes: 200 μm, 125 μm and 90 μm; top to bottom (VWR International GmbH; # 510-4914; 510-4909; 510-4905). Material from 90 μm sieve was collected in a falcon. After a quick spin, the supernatant was removed and the material was transferred to a microcentrifuge tube. Another brief spin (1000g at 4 ºC) was employed to remove the remaining PBS. After weighing, samples were transferred to liquid nitrogen and stored at -80 ºC. All steps were performed in the cold room (at 4 ºC) with pre-cooled equipments and reagents.

4.5 Purification of affinity-tagged MS2 coat protein (MCP)

The recombinant MS2 coat proteins (MCP) were expressed in *E.coli* using either BL21 (DE3) gold or BL21 (DE3) star cells, grown in either TB or ZY medium (Table 5), supplemented with

respective antibiotics. Cells were cultivated initially at 37 ºC until the required OD_{600} was reached (0.6-0.8 units for TB media and 1.8-2.0 units for ZY media) and then grown overnight at 20 ºC. In case of TB media, protein expression was induced by addition of isopropyl β-D-1-thiogalactopyranoside (IPTG) to a final concentration of 1mM, at required OD_{600}. Cells were pelleted by centrifugation at 4000 rpm for 20 min at 4 ºC and stored at -80 ºC.

Table 5: Composition of TB and ZY media

TB media (per litre)		10X Phosphate buffer (per litre)	
Bacto tryptone	12 g	0.17 M Potassium dihydrogen phosphate	23.1 g
Bacto yeast extract	24 g	0.72 M di-Potassium hydrogen phosphate	125.4 g
87% Glycerol	5 ml		
10X Phosphate buffer	100 ml		

ZY media (per litre)		20X NPS composition (per litre)	
Bacto tryptone	10 g	Ammonium sulphate	66.07 g
Yeast extract	5 g	Potassium hydrogen phosphate	136.09 g
20X NPS	50 ml	Di-sodium hydrogen phosphate dihydrate	177.99 g
50X 5052	20 ml		
1 M $MgSO_4$	1 ml		

50X 5052 composition (per litre)	
Glucose	25 g
Lactose	100 g
Glycerol (87%)	287 ml

Typically, cells were lysed in a high salt buffer (500 mM - 1.2 M) and affinity purified on cobalt resin (His-MCP, His-MBP-MCP, His-MBP-tdMCP) or glutathione resin (GST-MCP). Proteins were further applied to Heparin Sepharose 6 Fast Flow columns and finally to Size Exclusion columns to obtain pure proteins (HiLoad 16/600 Superdex75pg or HiLoad 16/600 Superdex200pg). All the purified proteins were aliquoted and stored at -80 ºC.

His-MCP was purified by cobalt affinity chromatography in lysis buffer (20 mM Tris-HCl pH 7.5 at 4 ºC, 1.2 M NaCl, 20 mM imidazole, 1 mM 2-mercaptoethanol) supplemented with protease inhibitors (cOmplete™, EDTA-free Protease inhibitor cocktail, Roche # 04693132001). After washing in buffer A (20 mM Tris-HCl pH 7.5 at 4 ºC, 300 mM NaCl, 20 mM imidazole, 1 mM 2-mercaptoethanol), the recombinant protein was eluted from the resin with a gradient to 500 mM imidazole. The imidazole was subsequently removed by dialysis overnight at 4 ºC, in dialysis buffer (20 mM Tris-HCl pH 7.5 at 4 ºC, 100 mM NaCl, 1 mM DTT). 10% glycerol was added to prevent precipitation and His-MCP was further purified on a Heparin Sepharose 6 Fast Flow column in the buffer: 20 mM Tris-HCl pH 7.5 at 4 ºC, 100 mM NaCl, 10% glycerol, 1 mM DTT; eluted with a gradient to 1 M NaCl, and finally applied

on a HiLoad 16/600 Superdex75pg column, 120 ml (GE Healthcare) and eluted in the buffer: 20 mM Tris-HCl pH 7.5 at 4 ⁰C, 100 mM NaCl, 10% glycerol, 1 mM DTT.

GST-MCP was affinity-purified on glutathione resin in lysis buffer (20 mM Tris-HCl pH 7.5 at 4 ⁰C, 500 mM NaCl, 1 mM DTT) supplemented with protease inhibitors (cOmplete™, EDTA-free Protease inhibitor cocktail, Roche # 04693132001). After washing in lysis buffer, the recombinant protein was eluted from the resin with a gradient to buffer B (lysis buffer plus 20 mM reduced glutathione). GST-MCP was dialyzed overnight at 4 ⁰C in dialysis buffer (20 mM Tris-HCl pH 7.5 at 4 ⁰C, 35 mM NaCl, 10% glycerol, 1 mM DTT) and further purified on Heparin Sepharose 6 Fast Flow columns (GE Healthcare), eluted with a gradient to 1 M NaCl. The unbound fraction was then applied on a HiLoad 16/600 Superdex200pg column (GE Healthcare) and eluted in the buffer: 20 mM Hepes pH 7.5, 100 mM NaCl, 10% glycerol, 1 mM DTT.

His-MBP-MCP and His-MBP-tdMCP were purified by cobalt affinity chromatography in lysis buffer (20 mM Tris-HCl pH 7.5 at 4 ⁰C, 1.2 M NaCl, 0.5 mM DTT) supplemented with protease inhibitors (cOmplete™, EDTA-free Protease inhibitor cocktail, Roche # 04693132001). After washing in buffer A (20 mM Tris-HCl pH 7.5 at 4 ⁰C, 300 mM NaCl, 0.5 mM DTT), the recombinant proteins were eluted from the resin with a gradient to 500 mM imidazole. The imidazole was subsequently removed by dialysis overnight at 4 °C, in dialysis buffer (20 mM Tris-HCl pH 7.5 at 4 ⁰C, 50 mM NaCl, 10% glycerol, 1 mM DTT). His-MBP-MCP and His-MBP-tdMCP were further purified on a Heparin Sepharose 6 Fast Flow column and eluted with a gradient to 1 M NaCl, and finally applied on a HiLoad 16/600 Superdex200pg column, 120 ml (GE Healthcare) and eluted in the buffer: 20 mM Hepes pH 7.5, 100 mM KCl, 10% glycerol, 1 mM DTT.

4.6 RNA binding assay

For RNA-binding assays, 500 μg of gel filtrated recombinant proteins (GST-MCP and His-MBP-MCP) were incubated with 1.1 molar excess (or 1.4 molar excess in the case of GST-MCP) of different RNAs (*MS2* hairpin, UA-rich hairpin, polyU$_{20}$; Integrated DNA Technologies) in 2:1 ratio, for 1.5 hours at 4 ⁰C. Complexes were then loaded on a Size Exclusion column (Superdex200 10/300GL; GE Healthcare) in 25 mM Hepes pH 7.5, 150 mM KCl and 1 mM DTT. For comparison, protein alone and RNA alone samples were incubated and loaded the same way.

4.7 RNA pull-down

To pull-down *MS2-12X* tagged *osk* mRNA, total RNA was extracted from the material collected by mass isolation, using Tri-Reagent® (Sigma #T9424) according to the manufacturer's instructions. To facilitate proper secondary structure formation, 75 μg of RNA was incubated in buffer (25 mM Hepes, pH 7.5, 150 mM KCl, 250 mM Sucrose, 1 mM MgCl$_2$, 0.1% NP-40, 1 mM DTT) for 30 min at RT. 25 μl of bead slurry: Glutathione resin (Protino® Glutathione Agarose 4B, MACHEREY-NAGEL # 745500.100) in case of GST and Amylose resin (NEB #E8021S) in case of MBP pull-down, was incubated with 50 μg of purified MCP for 2 hours at 4 ºC. Unbound protein was removed by washing the beads with buffer 3x and RNA was added to the MCP-coated beads and incubated for 2 hours at 4 ºC. After washing 4x with buffer, RNA was extracted from beads by addition of Tri-Reagent® (Sigma #T9424) according to the manufacturer's instructions. RNA was precipitated using Isopropanol and the pellet was resuspended in Glyoxal reaction mixture directly (Table 7) to denature RNA. After incubation at 74 ºC for 10 min, samples were immediately chilled on ice and RNA loading dye (95% deionized formamide, 0.05% SDS, 0.05% Xylene cyanol FF, 0.05% Bromophenol blue) was added.

4.7.1 Northern Blot

Samples were separated on 1.2% agarose gels, supplemented with SYBR™ Gold nucleic acid gel stain (Thermo Fisher Scientific # S11494), under denaturing conditions. MOPS was used as a running buffer (Table 6).

Table 6: Buffers for Northern blot: gel electrophoresis and transfer

10X MOPS (pH 7.0)		Glyoxal reaction mixture (2ml)		20X SSC (pH 7.0)	
MOPS	200 mM	DMSO	1.2 ml	NaCl	3M
NaOAc	80 mM	Deionized glyoxal	0.4 ml	NaCitrate	300 mM
EDTA	10 mM	10X MOPS running buffer	0.24 ml		
		Glycerol	0.12 ml		
		ddH$_2$O	40 μl		

Gel electrophoresis was performed over 5–6 hours at 5 V/cm, at RT. The gel was then blotted onto a positively charged nylon membrane (*GeneScreen Plus® Hybridization Transfer Membrane*, Perkin Elmer® #NEF1017001PK) by upward capillary transfer driven by saline-sodium citrate (SSC) buffer (Table 7). After transfer, the RNA was cross-linked to the membrane by UV light using a UV crosslinker (CL-1000 Ultraviolet Crosslinker, UVP).

Membranes were pre-hybridized at 65 ºC in Church hybridization buffer (500 mM sodium phosphate pH 7.0, 7% SDS, 1 mM EDTA) containing denatured salmon sperm DNA (50

µg/ml; Thermo Fisher Scientific # 15632011). After an hour incubation, the purified DIG-labeled probe (prepared as described before) was added and hybridizations were carried out overnight at 65 ℃.

After washing 4x for 20 min with Church wash buffer (40 mM sodium phosphate pH 7.0, 1% SDS, 1 mM EDTA), the membrane was equilibrated in Maleic acid wash buffer (Maleic acid buffer with 0.3% Tween-20) for 5 min at RT. After blocking the membrane (1% milk solution in Maleic Acid buffer) for 30 min at RT, freshly prepared antibody solution was added: alkaline phosphate-conjugated anti-DIG fragments (Roche #11093274910) diluted 1:10,000 in blocking buffer. After 30 min incubation, the membrane was washed again 2x for 15 min with Maleic acid wash buffer (Table 7).

Table 7: Buffers for Northern blot: detection

Maleic Acid Buffer (pH 7.5)		Detection Buffer (pH 9.5)	
Maleic Acid	0.1 M	Tris-HCl	0.1 M
NaCl	0.15 M	NaCl	0.1 M
		$MgCl_2$	50 mM

For detection, the membrane was equilibrated in detection buffer (Table 8) before adding substrate (Tropix CSPD, Applied Biosystems #T2142) to the membrane. After 5 min incubation, chemiluminescence was detected by exposing the membrane to *Amersham Imager 600* (GE Healthcare).

4.8 Cell culture and transfection

Human HEK293 cells were grown in Dulbecco's Modified Eagle Medium (DMEM, produced in-house; Gibco™ DMEM powder # 52100039, 20 g Sodiumhydrogen carbonate, enriched with CO_2 for 10 min), at 37 ℃ in the presence of 5% CO2. The medium was supplemented with 10% heat-inactivated Fetal Bovine Serum (Gibco #10500064), 2 mM L-Glutamine (Sigma Aldrich #G7513) and 1X Penicillin-Streptomycin solution (Sigma #P4333).

One day before transfection, cells were washed with PBS (produced in-house; Gibco™ DPBS powder # 21600044, pH 7.1) and trypsinized (0.25% Trypsin-EDTA solution from Sigma #T4049). After resuspension, cells were counted in a cell counter (*Cellometer Auto 2000* from Nexcelom Bioscience) and diluted to 0.325 x10^6 /ml. 6-well plates were seeded with 0.65 x10^6 cells/well (i.e. 2 ml of diluted cells/ well).

Cells were transfected at ~90% confluency using Lipofectamine™ 3000 (Invitrogen # L3000-008) according to the manufacturer's recommendations. 5 µg of DNA was transfected in each

well with 4 μl of Lipofectamine reagent and 5 μl of p3000 reagent. Typically, two plasmids were co-transfected; the ratio was adjusted based on their expression levels. If required, a third empty plasmid with HA tag was supplemented, to reach a total amount of 5 μg. The cells were incubated at 37 °C for 48 hours before harvesting.

4.9 Immunoprecipitations and Western blots

4.9.1 Immunoprecipitation from *Drosophila* ovaries:

Flies were fed on fresh yeast paste for 2 days at RT. Ovaries were dissected in PBS and immediately transferred to a microcentrifuge tube (filled with PBS) maintained on ice. Flies were dissected in batches of 40, immediately transferred to liquid nitrogen and stored at -80 °C.

For immunoprecipitation, frozen ovaries were thawed on ice in lysis buffer (50 mM Tris-HCl pH 7.5 at 4 °C, 100 mM NaCl, 250 mM Sucrose, 0.1% NP-40 and 1 mM DTT) and pooled together to reach the required amounts (Table 8,9). The extra buffer was removed and ovaries were resuspended in the appropriate amount of lysis buffer (320 μl/ 40 dissected flies) supplemented with 2.5X protease inhibitors (cOmplete™, EDTA-free Protease inhibitor cocktail, Roche # 04693132001). Ovaries were teased apart by gently pipetting up and down and then mechanically homogenized with 30 strokes in a tissue homogenizer with a glass pestle (2 or 5 ml round bottom from Hartenstein GmbH). The lysate was cleared by centrifugation at 21000g for 20 min at 4 °C and supernatant was transferred to a fresh tube avoiding the thick fat layer on the top. 2 μl of *RNase A/T1* (Thermo Fisher Scientific #EN0551) per 400 μl of lysis buffer was added to the lysate and incubated at 4 °C for 30 min on a rotating wheel. The lysate was cleared again at 21000g at 4 °C for 15 min and transferred to a fresh tube; 30 μl of lysate was taken aside as input. *GFP-TRAP® MA* beads (Chromotek #gtma-100), prewashed 3x with lysis buffer, were added to the supernatant and incubated for 1 hour at 4 °C in rotation. Beads were then washed 4x in lysis buffer and collected by magnetic separation using *DynaMag™-2 magnet* (Invitrogen #12321D). All the washing steps were done in the cold room. Proteins were eluted with 2X protein sample buffer (100 mM Tris-HCl pH 6.8, 4% SDS, 20% Glycerol, 200 mM DTT, 0.05% Bromophenol blue) by boiling at 95 °C for 10 min.

For mass spectrometric (MS) analysis, immunoprecipitations were performed as described above. Proteins were eluted with 30 μl of 2X protein sample buffer and separated by PAGE, using *NuPAGE ™* Bis-Tris precast 4-12% gradient gels (Invitrogen # NP0321) with MES-SDS running buffer (50 mM Tris base, 50 mM MES, 0.1% SDS, 1 mM EDTA pH 7.3).

Samples were run approximately 2 cm into the gel and bands were visualized with a 0.1% *Colloidal Coomassie Blue* stain (Coomassie® Brilliant Blue G 250 from Serva #17524).

Table 8: Summary for Label-free MS
(replicates were prepared on different days)

	No. of dissected flies			Lysate (µl)			Amount of beads (µl)		
	Rep.1	Rep.2	Rep.3	Rep.1	Rep.2	Rep.3	Rep.1	Rep.2	Rep.3
GFP	320*	320*	320*	2560	2560	2560	50	50	50
eIF4AIII-GFP	200	400*	400*	1600	320	320	50	60	60
Glo-GFP	200	200	200	1600	1600	1600	50	30	30
Hrp48-GFP	80	80	80	640	640	640	30	30	30
Nos-GFP	200	400*	400*	1600	320	320	50	60	60
Stau-GFP	200	400*	400*	1600	320	320	50	60	60
Vas-GFP	80	80	80	640	640	640	30	30	30

Table 9: Summary for Quantitative MS
(both replicates were prepared on the same day)

	No. of dissected flies		Lysate (µl)		Amount of beads (µl)	
	Rep.1	Rep.2	Rep.1	Rep.2	Rep.1	Rep.2
GFP	400*	400*	320	320	60	60
Hrp48-GFP	80	80	640	640	30	30
Vas-GFP	80	80	640	640	30	30

* For processing samples with more than 200 dissected flies, the lysate was split into half after homogenization. IPs were treated separately and half the amount of indicated beads were added in each tube. After washing, beads were pooled together and proteins were eluted.

4.9.2 Co-immunoprecipitations from HEK293 cells:

Cells were grown and transfected as described before. Two days after transfection, for co-immunoprecipitations (co-IP), cells were washed with ice-cold PBS and scraped off the wells in lysis buffer (50 mM Tris-HCl pH 7.5 at 4 ºC, 100 mM NaCl, 250 mM Sucrose, 0.1% NP-40, 1 mM DTT) supplemented with protease inhibitors (cOmplete™, EDTA-free Protease inhibitor cocktail, Roche # 04693132001). 400 µl of lysis buffer per well was used. For efficient lysis, cells were incubated on ice for 15 min and were mechanically sheared by passing them through a needle (Sterican® 21G 7/8" Ø 0.8X22mm) several times (6-7x). After lysis, cell lysates were spun at 16000*g* for 15 min at 4 ºC and supernatants were transferred to a fresh tube. 2 µl (per well) of *RNase A/T1* (Thermo Fisher Scientific #EN0551) was added to the lysate and incubated at 4 ºC for 30 min on a rotating wheel. The lysate was cleared again at 16000*g* for 15 min and transferred to a fresh tube; 30 µl of lysate was taken aside as input. For GFP pull-downs, 12-20 µl of pre-washed *GFP-TRAP® MA* beads (Chromotek #gtma-

100) were added to the supernatant and incubated for an hour at 4 ºC. Washing and elution steps were done as described above.

For Flag pull-downs, 1.8 μl (per 400 μl of lysate) of anti-Flag (mouse monoclonal Anti-Flag® M2 from Sigma # F1804-1MG) was added to the supernatant. Samples were incubated for 1 hour at 4 ºC in rotation; after incubation 20 μl of pre-washed *GammaBind Plus Sepharose®* beads (GE Healthcare #17-0886-01) were added, and the mixtures were rotated for an additional hour at 4 ºC. Beads were then washed 4x with lysis buffer and collected by centrifugation at 2000*g* at 4 ºC. Proteins were eluted as described before.

The amount of material for each co-IP was adjusted based on the expression level of the proteins (visualized by western blot; see below). Typically, one or two wells per IP were used and the lysate was prepared as described above. However, for some proteins with low expression, cells from 2 wells were pooled together in a total of 600 μl of buffer, thus concentrating the lysate 1.5X. The corresponding lysates for control IP were prepared accordingly. Following steps were performed the same way as described above.

Eluates were separated by SDS-polyacrylamide gel electrophoresis (SDS-PAGE), as described in Sambrook et al. (2001); Laemmli running buffer (25 mM Tris base, 192 mM glycine, 0.1% SDS) was used. Home-made 10% polyacrylamide gels were used for efficient protein separation.

After electrophoresis, the proteins were transferred to a nitrocellulose membrane (Sartorius # 11306-41BL) in a wet transfer system (BioRad), for 1.5 hours at 50V. The transfer buffer contained 20 mM Tris base, 150 mM glycine, 20% MeOH, 0.1% SDS.

Membranes were blocked in 5% milk solution in PBT (PBS + 0.1% Tween-20) for an hour and incubated with primary antibodies (diluted in 5% milk in PBT; Table 11) overnight at 4 ºC. The blots were then washed with PBT 3x, for 15 min each and incubated with Horseradish Peroxidase (HRP)-conjugated secondary antibody (Table 11) solutions for at least an hour at RT. Blots were washed again 3x with PBT, 15 min each. Detection was done with enhanced chemiluminescence (ECL) reagents, produced in-house (Table 10). After incubation with the substrate, chemiluminescence was detected by exposing the membrane in an *Amersham Imager 600* (GE Healthcare).

Table 10: ECL reagents for western blot detection

ECL SOLUTION A (200 ml)		ECL SOLUTION B (10ml)		DETECTION MIX (FRESH)	
0.1 M Tris-HCl pH 8.6	200ml	DMSO	10 ml	5 ml	Solution A
Luminol	50 mg	p-Coumaric acid	11 mg	0.5 ml	Solution B
				1.8 μl	H_2O_2 35%

Table 11: List of antibodies used for Western blot

Antigen	Organism and description	Company (catalog nº)	Dilution
HA	Mouse (monoclonal)	BioLegend® (901501)	1:5000
GFP	Rabbit (polyclonal)	Thermo Fisher Scientific (A11122)	1:2500
Mouse IgG	Goat (polyclonal), HRP-conjugated	Dianova (115-035-003)	1:8000
Rabbit IgG	Goat (polyclonal), HRP-conjugated	Dianova (111-035-003)	1:8000

4.10 Mass spectrometry and Data analysis

4.10.1 Sample preparation and data processing

Immunoprecipitation samples from ovaries were sent for MS analysis at the Proteome Center Tübingen (PCT), University of Tübingen. Gel slices were processed by Johannes Madlung, in the lab of Prof. Dr. Boris Macek's lab at PCT. For label-free MS, proteins were digested in-gel using trypsin. LC-MS/ MS reads were collected on a Proxeon Easy-nLC 1200 (Thermo Fisher Scientific) coupled to a QExactive HF mass spectrometer (Thermo Fisher Scientific); method: 60 min, Top12 HCD. For Dimethyl labeling, after tryptic in-gel digestion derived peptides were loaded on C18-stage tips and dimethylated (Boersema et al., 2009). Measurements were done the same way as for the unlabeled.

Raw data of Dimethyl labeling MS was processed by Johannes Madlung. All 6 samples were processed together using MaxQuant version 1.5.2.8. False discovery rate (FDR) setting was 1% on peptide as well as protein level.

For label-free MS, raw data files for all the 21 samples (biological triplicates for six baits+ controls) were processed together using MaxQuant software suite v. 1.6.0.1 (Cox and Mann, 2008). Using Andromeda search engine (Cox et al., 2011), the spectra were searched against UniProt *D. melanogaster* proteome database (canonical and isoform entries; downloaded in July 2017; http://www.uniprot.org/proteomes/UP000000803) and a database comprising a sequence of the tag alone.

Briefly, MaxLFQ algorithm was activated and the minimum number of peptide ratio count was set to 1, to quantify proteins across the samples (Cox et al., 2014). To transfer peptide identifications to unidentified or unsequenced peptides between samples, for quantification, matching between runs option was selected, with a match time window of 0.7 min and an alignment time window of 20 min. Matching was performed only between replicates by controlling the fraction numbers. Determined by a target-decoy approach, 1% FDR filter was set for PSM (peptide spectrum match) and protein identification. For a protein group to be considered for identification, the parameters were set to a requirement of minimum 1 peptides; minimum 1 razor+ unique peptides and 0 unique peptides. Protein reversal method was used to generate the decoy database.

4.10.2 Data analysis for Label-free MS

Bioinformatics analysis was done using Perseus v. 1.6.0.7 (Tyanova et al., 2016). MaxQuant output file was loaded into the program. Proteins identified were arranged in rows and the LFQ intensity values for each experiment were arranged in columns. The data was filtered for proteins identified as potential contaminants, identified only by a modification site and identified by peptides derived from the reversed sequence of the decoy database. All the intensity values were then Log2 transformed and histograms were plotted for all the samples (Frequency distribution analysis using GraphPad Prism v.7.0.0 for windows; www.graphpad.com). After removing the empty rows (by filtering for at least one valid value in total) heat maps with hierarchical clustering on rows (Euclidean distance) and Pearson correlations for columns were generated. This was done in Perseus software (Tyanova et al., 2016).

Significantly enriched proteins were identified using a pipeline constructed in Perseus software (Tyanova et al., 2016). For this, replicates for each bait were grouped together and the data was analyzed in a pairwise fashion i.e. each individual bait group against the control group. After log transformation, proteins were filtered based on the identification of min 3 valid values in at least one replicate group. The missing values were imputed using normal distribution (0.3 width reduction and 1.8 standard deviations downshift) on the whole matrix, enabling statistical analysis. Histograms were checked again to ensure sustained normal distribution. Both-sided Welch's t-test was used with S0 parameter of 2 (this controls the artificial within-group variance). For each test, to filter the rows a requirement of at least 2 valid values in the bait group was set, further controlling the effects of imputation. A 5% FDR cut-off (permutation-based; number of randomizations: 250 without preserving groupings) was set to determine significantly enriched proteins. The same pipeline was employed for all the pairwise analyses.

All the scatter plots and the volcano plots were generated using GraphPad Prism v.7.0.0 for windows (www.graphpad.com). For creating networks, Cytoscape v. 3.5.1 (Shannon et al., 2003) was used. To integrate IP data with literature, databases like String (Szklarczyk et al., 2017) and FlyBase (Gramates et al., 2017) were used. For String, only experimental data with medium confidence range was considered. Physical interaction data from FlyBase was extracted for each protein individually.

For GO term analysis, DAVID (**D**atabase for **A**nnotation, **V**isualization and **I**ntegrated **D**iscovery) v.6.8 functional annotation tool was used (Huang et al., 2009a,b), which adopts Fisher Exact test to measure the gene-enrichment in annotation terms. Following parameters were used: background: *Drosophila* genome; count threshold (minimum number of genes for that term) of 2; maximum ease score (modified Fisher Exact P-value) of 0.01. To reduce redundancy in the GO terms, DAVID output was fed into REVIGO (**Re**duce + **Vi**sualize **G**ene **O**ntology; Supek at al., 2011) and p-values were used to select and cluster GO terms with a similarity score of 0.7 (medium). In advanced options, whole UniProt (default) was used for GO term sizes.

For comparing GO terms across baits, the analysis was done using DAVID v.6.8 functional annotation tool (Huang et al., 2009a,b), for each bait separately, as described above. Data was compiled manually and heat maps were generated using GraphPad Prism v.7.0.0 for windows (www.graphpad.com)

4.11 Immunofluorescence and Microscopy

To visualize the localization of *MS2*-tagged *osk* mRNA, flies were fed on fresh yeast paste for 2 days and ovaries were dissected in PBS at RT. Ovarioles were teased apart using forceps, breaking the anterior fibrous tissue and leaving them attached at the posterior end. This allows the ovary to be moved through the steps as a single unit while allowing fixative and the antibody to access all the cells. Ovaries were then fixed in 4% PFA (in PBS) for 30 min, washed in PBS 3x, 10 min each and dehydrated in 100% MeOH overnight. After rehydration the following day, ovaries were washed again in PBS 4x and mounted on slides in *Fluoromount-G™* (Southern Biotech #0100-01).

To visualize the GFP tagged proteins, sample slides were prepared the same way as above, except a short fixing step (in 4% PFA) of 4 min was done and samples were mounted directly after washing in PBS. All steps were carried out on a nutator mixer. Slides were stored at 4 ºC overnight before imaging.

For immunofluorescence, ovaries were dissected in PBT (0.1% Tween-20 in PBS) and ovarioles were separated. All the following steps were carried out on a nutator mixer.

Ovaries were fixed in 4% PFA (in PBT) for 20 min and washed 4x in PBT to remove any traces of fixing solution. They were then dehydrated by addition of 100% MeOH and stored at -20 ºC overnight. The following day, they were rehydrated by washing 4x in PBT and blocked for 60 min (in PBT, 10 % BSA). They were equilibrated in PBT containing 1% BSA and stained with anti-GFP (diluted in PBT, 1% BSA; Table 12) for 3 days at RT. Primary antibody was removed by washing 4x in PBT containing 1% BSA, before incubation with secondary antibody (in PBT, 1% BSA; Table 12) for at least one hour at RT. Secondary staining was stopped by washing 3x in PBT, 15 mins each. After washing twice with PBS, slides were prepared and stored at 4 ºC.

Images were acquired on a FluoView1200 laser scanning confocal microscope (Olympus), with an UPlanSApo 40.0X air objective (NA 0.95) and processed using FIJI (Schindelin et al., 2012).

Table 12: List of antibodies used for Immunofluorescence

Antigen	Organism and description	Company (catalog nº)	Dilution
GFP	Rabbit (polyclonal)	Thermo Fisher Scientific (A11122)	1:1000
Rabbit IgG	Donkey (polyclonal), Alexa Flour 488 coupled	Invitrogen (A21206)	1:1000

Table 13: List of oligonucleotide sequences used for cloning

Code	Primer Name	Sequence	Cloning Type
PBA01	Dm_CG5726_fwd	GCTCAAGCTTCGAATTCTGATCATATGGAAATGGCCAACAACATG	Gibson
PBA02	Dm_CG5726_rev	AATAAACAAGTTAACAACAACAATTGTCATTTCTGGGCCGACAAATAG	Gibson
PBA03	Dm_Loqs-PB_fwd	CAAGCTTCGAATTCTGATCATATGGACCAGGAGAATTTCCACG	Gibson
PBA04	Dm_Loqs-PB_rev	ATAAACAAGTTAACAACAACAATTGCTACTTCTTGGTCATGATCTTC	Gibson
PBA05	Dm_Nph_fwd	TCAAGCTTCGAATTCTGATCATATGGAGTCCGAGTCGTTTTATG	Gibson
PBA06	Dm_Nph_rev	ATAAACAAGTTAACAACAACAATTGCTACTTCTTCTTATTACTCTTG	Gibson
PBA07	Dm_SC35_fwd	AAGCTTCGAATTCTGATCATATGAGCAACGGTGGTGGTGCCG	Gibson
PBA08	Dm_SC35_rev	AATAAACAAGTTAACAACAACAATTGCTAGGAGCGACTGCGACTAC	Gibson
PBA09	Dm_Vasa_2_fwd	ATCTCGAGCTCAAGCTTCAGAATTCATGTCTGACGACTGGGATGATG	Gibson
PBA10	Dm_Vasa_2_rev	TTATCTAGATCCGGTGGATCCCGGGTCAATCCCATTGCTCTTCTTC	Gibson

PBA11	Dm_X16_fwd	GCTTCGAATTCTGATCATATGTCGCGCCATCCGAGCGATAGAAAG	Gibson
PBA12	Dm_X16_rev	ACAAGTTAACAACAACAATTGCTAGTCCCTTGAAACGGATCGTG	Gibson
PBA13	Dm_Armi_fwd	GCTTCGAATTCTGATCATATGTTCACATACGTTAGCAAGTTTTTC	Gibson
PBA14	Dm_Armi_rev	ACAAGTTAACAACAACAATTGTTAGTTCAAATCATCTGTAGTATTC	Gibson
PBA15	Dm_Dref_fwd	GCTTCGAATTCTGATCATATGATGAGCGAAGGGGTACCAGCG	Gibson
PBA16	Dm_Dref_rev	ACAAGTTAACAACAACAATTGCTAATTGTTGTGATGATGAAGAAAG	Gibson
PBA17	Dm_Gus_fwd	GCTTCGAATTCTGATCATATGATGGGTCAAAAAATTAGTGGCG	Gibson
PBA18	Dm_Gus_rev	ACAAGTTAACAACAACAATTGTTATCTACGGTTTTTATACAATAAAT	Gibson
PBA19	Dm_Dco_fwd	ATCTCGAGCTCAAGCTTCGAATTCTATGGAGCTGCGCGTGGG	Gibson
PBA20	Dm_Dco_rev	TTATCTAGATCCGGTGGATCCCGGGTTATTTGGCGTTCCCCAC	Gibson
PBA21	Dm_SF2_fwd	ATCTCGAGCTCAAGCTTCGAATTCTATGGGATCACGCAACGAG	Gibson
PBA22	Dm_SF2_rev	TTATCTAGATCCGGTGGATCCCGGGTTAATAGTTAGAACGTGAG	Gibson
PBA23	Dm_CG7185_fwd	ATCTCGAGCTCAAGCTTCGAATTCTATGGCCGACGTGGTCTTGG	Gibson
PBA24	Dm_CG7185_rev	TTATCTAGATCCGGTGGATCCCGGGTCAATGCCGGGAACGGTG	Gibson
PBA25	Dm_mtSSB_fwd	ATCTCGAGCTCAAGCTTCGAATTCTATGCAACACACAAGGCGC	Gibson
PBA26	Dm_mtSSB_rev	TTATCTAGATCCGGTGGATCCCGGGTTAGTTGTTGGCATCACG	Gibson
PBA27	Dm_Glo_fwd	ATCTCGAGCTCAAGCTTCAGAATTCATGTCCAACGCAGACGTG	Gibson
PBA28	Dm_Glo_rev	TTATCTAGATCCGGTGGATCCCGGGTTAGATGCGCCGCGAAAAG	Gibson
PBA29	Dm_CG13090_fwd	ATCTCGAGCTCAAGCTTCAGAATTCATGATGGAATCCGAGGTAG	Gibson
PBA30	Dm_CG13090_rev	TTATCTAGATCCGGTGGATCCCGGGTTAGTATATGGGAAAACTG	Gibson
PBA31	Dm_CG9684_fwd	ATCTCGAGCTCAAGCTTCAGAATTCATGCTAGCACAAAAGTCAG	Gibson
PBA32	Dm_CG9684_rev	TTATCTAGATCCGGTGGATCCCGGGTTACAAGCTCAACAGCTTC	Gibson
PBA33	Dm_ckIIalpha_fwd	ATCTCGAGCTCAAGCTTCAGAATTCATGACACTTCCTAGTGCGG	Gibson
PBA34	Dm_ckIIalpha_rev	TTATCTAGATCCGGTGGATCCCGGGTTATTGCTGATTATGGG	Gibson
PBA35	Dm_Coil-D_fwd	ATCTCGAGCTCAAGCTTCAGAATTCATGCAACACTCCAGCATG	Gibson
PBA36	Dm_Coil-D_rev	TTATCTAGATCCGGTGGATCCCGGGTCAGTCAATTGTGGCTAC	Gibson
PBA37	Dm_Dip1-D_fwd	ATCTCGAGCTCAAGCTTCAGAATTCATGAAGCGAAATCGTCGTG	Gibson
PBA38	Dm_Dip1-D_rev	TTATCTAGATCCGGTGGATCCCGGGTTAAGTGGTGTCGCTGTAG	Gibson
PBA39	Dm_Hsp60_fwd	ATCTCGAGCTCAAGCTTCAGAATTCATGTTCCGTTTGCCAGTTTC	Gibson
PBA40	Dm_Hsp60_rev	TTATCTAGATCCGGTGGATCCCGGGTTACATCATGCCACCCATG	Gibson
PBA41	Dm_nudC_fwd	ATCTCGAGCTCAAGCTTCAGAATTCATGGCTGCTGAGGAGGGAAAG	Gibson
PBA42	Dm_nudC_rev	TTATCTAGATCCGGTGGATCCCGGGTTAATTGAATTTACACTTGGAG	Gibson
PBA43	Dm_puf68_fwd	ATCTCGAGCTCAAGCTTCAGAATTCATGGGAAGCAACGACAGAG	Gibson

PBA44	Dm_puf68_rev	TTATCTAGATCCGGTGGATCCCGGGCTAACCGGACAGATCTCCC	Gibson
PBA45	Dm_SmB_fwd	ATCTCGAGCTCAAGCTTCAGAATTCATGACGATCGGCAAGAAC	Gibson
PBA46	Dm_SmB_rev	TTATCTAGATCCGGTGGATCCCGGGTTAATAGCCACCCCTGCC	Gibson
PBA47	Dm_ncm359 - 664_fwd	ATCTCGAGCTCAAGCTTCAGAATTCATGGCAGACAATGAAACCG	Gibson
PBA48	Dm_ncm359-664_rev	TCTAGATCCGGTGGATCCCGGGTCATCCCAGGATCTCACGACTTAG	Gibson
PBA49	Dm_Vasa_fwd	CAAGCTTCGAATTCTGATCATATGTCTGACGACTGGGATGATG	Gibson
PBA50	Dm_Vasa_rev	ATAAACAAGTTAACAACAACAATTGTCAATCCCATTGCTCTTCTTC	Gibson
PBA51	Dm_Lost_NdeI_fwd	ATACATATGGAGGACCAAAGCAACGCAGCC	Standard
PBA52	Dm_Lost_MfeI_rev	ATACAATTGCTATACTGTGGTGGTGTCGACAGC	Standard
PBA53	Dm_Hem_HindIII_fwd	TTAAAAGCTTTGATGGCACGCCCAATTTTTC	Standard
PBA54	Dm_Hem_BamHI_rev	TTAAGGATCCTTAGAGTGCCAGCCCTAAG	Standard
PBA55	Dm_BicC_NdeI_fwd	AAACATATGTTGTCCTGTGCCTCTTTCAATAAAC	Standard
PBA56	Dm_BicC_XbaI _rev	AAATCTAGATCACCACTGGTTGGAGGGACGGC	Standard
PBA57	fTRGtag_AgeI_fwd	ATAACCGGTATGGAAGTGCATACCAATCAGGACC	Standard
PBA58	fTRGtag_NheI_rev	ATAGCTAGCTTACTTGTCGTCGTCATCCTTG	Standard
PBA59	Osk_recomb_fwd	CGCGTACTGCAAGTTATTGAAACGAGTCTGGAGTATTAAGTTGGGTTCTTGAAGTGCATACCAATCAGGACCCGC	Recombineering
PBA60	Osk_recomb_rev	GTCGGTTCCGGTGCCAGCCCAGTCAAAATTTGCATATATGTATCTTGATTCTTGTCGTCGTCATCCTTGTAGTCA	Recombineering
PBA61	Dm_alphatub67C_fwd	AATCAGCGAACCAACTAACCTGAG	Standard
PBA62	Dm_alphatub67C_rev	TTGTAATGACTGAAGTCTGGCTGG	Standard
PBA63	Dm_rp49_fwd	ACCAGTCGGATCGATATG	Standard
PBA64	Dm_rp49_rev	GTTCTCTTGAGAACGCAG	Standard
PBA65	MS2cp_NdeI_fwd	ATACATATG GCCGTTAAAATGGCTTC	Standard
PBA66	MS2cp_HindIII_rev	ATAAAGCTTTTAAGCGTAGATGCCGGAG	Standard
PBA67	MS2cp_BamHI_rev	ATAGGATCCTTAAGCGTAGATGCCGGAG	Standard

Table 14: List of plasmids

Code	Plasmid name	Insert	Source	Oligos used	Parent plasmid
M105	pHA-C1-MCSNdeI	HA (Hemagglutinin)	Elisa Izaurralde (MPI, Tübingen)	-	-
M216	pHA-ckIIalpha	Casein kinase II alpha	*Prashali Bansal*	PBA33, PBA34	M105
M178	pHA-Armi	Armitage	*Prashali Bansal*	PBA13, PBA14	M105
M180	pHA-BicC	Bicaudal C	*Prashali Bansal*	PBA55, PBA56	M105
M214	pHA-CG13090	CG13090	*Prashali Bansal*	PBA29, PBA30	M105
M179	pHA-CG5726	CG5726	*Prashali Bansal*	PBA01, PBA02	M105
M159	pHA-CG7185	CG7185	*Prashali Bansal*	PBA23, PBA24	M105
M222	pHA-CG9684	CG9684	*Prashali Bansal*	PBA31, PBA32	M105
M217	pHA-Coil	Coilin (isoform D)	*Prashali Bansal*	PBA35, PBA36	M105
M167	pHA-Dco	Discs overgrown	*Prashali Bansal*	PBA19, PBA20	M105

M223	pHA-Dip1	Disco interacting protein 1 (isoform D)	*Prashali Bansal*	PBA37, PBA38	M105
M168	pHA-Dref	DNA replication-related element factor	*Prashali Bansal*	PBA15, PBA16	M105
M169	pHA-Gus	Gustavus	*Prashali Bansal*	PBA17, PBA18	M105
M181	pHA-Hem	HEM-protein	*Prashali Bansal*	PBA53, PBA54	M105
M218	pHA-Hsp60	Heat shock protein 60A	*Prashali Bansal*	PBA39, PBA40	M105
M160	pHA-Loqs	Loquacious (isoform PB)	*Prashali Bansal*	PBA03, PBA04	M105
M224	pHA-Ncm (ΔNΔC)	Nucampholin (359-664)	*Prashali Bansal*	PBA47, PBA48	M105
M219	pHA-nudC	NudC	*Prashali Bansal*	PBA41, PBA42	M105
M221	pHA-pUF68	pUF68	*Prashali Bansal*	PBA43, PBA44	M105
M162	pHA-Nph	Nucleophosmin	*Prashali Bansal*	PBA05, PBA06	M105
M166	pHA-X16	X16 splicing factor	*Prashali Bansal*	PBA11, PBA12	M105
M163	pHA-SC35	SR family splicing factor 35	*Prashali Bansal*	PBA07, PBA08	M105
E66	pHA-eIF4AIII	eIF4AIII	Kristna Ile	-	M105
C645	pHA-Hrp48	Heterogeneous nuclear ribonucleoprotein at 27C	Kristna Ile	-	M105
C586	pHA-Nos	Nanos (isoform B)	Kristna Ile	-	M105
C597	pHA-Stau	Staufen	Kristna Ile	-	M105
M134	pHA-Mahe	Maheshvara	Kristna Ile	-	M105
C633	pHA-Fmr1	Fragile X mental retardation protein 1	Kristna Ile	-	M105
C604	pHA-Cup	Cup	Kristna Ile	-	M105
C608	pHA-DCP1	Decapping protein 1	Kristna Ile	-	M105
C581	pHA-eIF4E	eIF4E (isoform C)	Kristna Ile	-	M105
C590	pHA-Orb	oo18 RNA-binding protein	Kristna Ile	-	M105
B96	pHA-Egl	Egalitarian	Kristna Ile	-	M105
M130	pHA-Heph	Hephaestus	Kristna Ile	-	M105
C606	pHA-Otu	Ovarian tumor	Kristna Ile	-	M105
C641	pHA-Sqd	Squid (isoform B)	Kristna Ile	-	M105
C700	pHA-Upf1	Up-frameshift 1	Kristna Ile	-	M105
M137	pHA-Bel	Belle	Kristna Ile	-	M105
C578	pHA-Exu	Exuperantia	Kristna Ile	-	M105
C611	pHA-Tral	Trailer hitch	Kristna Ile	-	M105
E64	pHA-Btz	Barentz	Kristna Ile	-	M105
M63	pEGFP-EGFP-C1	Enhanced green fluorescent protein	Elisa Izaurralde (MPI, Tübingen)	-	-
M173	pEGFP-eIF4AIII	eIF4AIII	*Prashali Bansal*	-	E66
M187	pEGFP-Glo	Glorund	*Prashali Bansal*	PBA27, PBA28	M02
M175	pEGFP-Hrp48	Heterogeneous nuclear ribonucleoprotein at 27C	*Prashali Bansal*	-	C645
M174	pEGFP-Nos	Nanos (isoform B)	*Prashali Bansal*	-	C586

M182	pEGFP-Stau	Staufen	*Prashali Bansal*	-	C597
M177	pEGFP-Vas	Vasa	*Prashali Bansal*	PBA09, PBA10	M63
M176	pEGFP-Nph	Nucleophosmin	*Prashali Bansal*	-	M162
M186	pEGFP-SC35	SR family splicing factor 35	*Prashali Bansal*	-	M163
M184	pEGFP-SF2	Splicing factor 2	*Prashali Bansal*	PBA21, PBA22	M171
M220	pEGFP-SmB	Small ribonucleoprotein particle protein SmB	*Prashali Bansal*	PBA45, PBA46	M63
M183	pEGFP-mtSSB	mitochondrial single stranded DNA-binding protein	*Prashali Bansal*	PBA25, PBA26	M170
M185	pEGFP-X16	X16 splicing factor	*Prashali Bansal*	-	M166
M104	pHA-Flag-C1-MCSNdeI	HA-FLAG	Elisa Izaurralde (MPI, Tübingen)	-	-
M154	pHA-Flag-Lost	Lost	*Prashali Bansal*	PBA51, PBA52	M104
C583	pHA-Flag-Me31B	Maternal expression at 31B	Kristna Ile	-	M104
C574	pHA-Flag-Osk (short)	Oskar (isoform short)	Kristina Ile	-	M104
C646	pHA-Flag-Hrp48	Heterogeneous nuclear ribonucleoprotein at 27C	Kristina Ile	-	M104
M133	pHA-Flag-CG10077	CG10077	Kristina Ile	-	M104
C610	pHA-Flag-Bruno	Bruno (isoform A)	Kristina Ile	-	M104
C638	pHA-Flag-Glo	Glorund	Kristina Ile	-	M104
C596	pHA-Flag-Stau	Staufen	Kristina Ile	-	M104
E65	pHA-Flag-eIF4AIII	eIF4AIII	Kristina Ile		M104
M165	pHA-Flag-Vas	Vasa	-	PBA49, PBA50	M104
M101	pUAST-attB	for transgenesis	Uwe Irion (MPI, Tübingen)	-	-
C665	pUI-Venus	Venus	Daniela Lazzaretti	-	-
M125	pUI-fTRG	2XTY1; sGFP; V5; Pre-scission; TEV; BLRP; 3XFLAG	*Prashali Bansal*	PBA57, PBA58	C665
C685	pUAST-fTRG	2XTY1; sGFP; V5; Pre-scission; TEV; BLRP; 3XFLAG	*Prashali Bansal*	-	M101, M125
M81	pCR4-24XMS2SL-stable	24X- *MS2SL*	Addgene 31865	-	-
M82	pCR4-24XPP7SL	24X- *PP7SL*	Addgene 31864	-	-
M80	pCR4-12XMS2SL	12X- *MS2SL*	Addgene 27119	-	-
M85	pTagNG	Recombineering cassette	Helena Jambor, Tomancak lab (MPI-CBG Dresden)	-	
M71	pTagNG-MS2-12XSL	12X- *MS2SL*	*Prashali Bansal*	-	M85, M80
M72	pTagNG-MS2-24XSL	24X- *MS2SL*	*Prashali Bansal*	-	M85, M81
M73	pTagNG-PP7-24XSL	24X- *PP7SL*	*Prashali Bansal*	-	M85, M82
M74	pTagNG-MS2-12X-PP7-24XSL	12X- *MS2 SL*; 24X- *PP7SL*	*Prashali Bansal*	-	M85, M80, M82

HJ1	*osk*Flyfos	*oskar* gene	Helena Jambor, Tomancak lab (MPI-CBG Dresden)	-	-
-	*osk*FlyfosMS2-6X	*osk* gene tagged with 6X- *MS2SL*	*Prashali Bansal*	PBA59, PBA60	HJ1, M72
-	*osk*FlyfosMS2-12X	*osk* gene tagged with 12X- *MS2SL*	*Prashali Bansal*	PBA59, PBA60	HJ1, M71
-	oskFlyfosPP7-24X	*osk* gene tagged with 24X- *PP7SL*	*Prashali Bansal*	PBA59, PBA60	HJ1, M73
-	*osk*FlyfosMS2-12X+ PP7-24X	*osk* gene tagged with 12X- *MS2 SL* + 24X- *PP7SL*	*Prashali Bansal*	PBA59, PBA60	HJ1, M74
-	pJET2.1	-	CloneJET PCR cloning kit (Thermo Fisher Scientific #K1231)	-	-
M95	pJET2.1-rp49	Antisense *rp49*	*Prashali Bansal*	PBA63, PBA64	-
M96	pJET2.1-alpha-tub67C	Antisense *alpha-tub 67C*	*Prashali Bansal*	PBA61, PBA62	-
C505	pBS-osk	Antisense *osk*	Uwe Irion (MPI, Tübingen)	-	-
M84	pMS2-YFP	MS2 coat protein	Addgene 27122	-	-
M3	pET-MCN-GST (pnEA-vG)	Glutathione S-transferase (GST)	Christophe Romier (IGBMC, Strasbourg)	-	-
M9	pET-MCN-His (pnEK-vH)	Hexahistidine (His)	Christophe Romier (IGBMC, Strasbourg)	-	-
M31	pET-MCN-His-MBP (pnEA-vHM)	Hexahistidine-Maltose-binding protein (His-MBP)	Christophe Romier (IGBMC, Strasbourg)	-	-
C542	pUC57-tdMCP	2X MS2 coat protein (tandem)	GenScript	-	-
C437	pET-MCN-GST-MCP (pnEA-vG-MCP)	GST-MS2 coat protein	*Prashali Bansal*	PBA65, PBA66	M3, M84
C446	pET-MCN-His-MCP (pnEK-vH-MCP)	His-MS2 coat protein	*Prashali Bansal*	PBA65, PBA67	M9, M84
C540	pET-MCN-His-MBP-MCP (pnEA-vHM-MCP)	His-MBP-MS2 coat protein	*Prashali Bansal*	PBA65, PBA67	M31, M84
C545	pET-MCN-His-MBP-tdMCP (pnEA-vHM-tdMCP)	His-MBP-2X MS2 coat protein (tandem)	*Prashali Bansal*	-	M31, C542

5. Contributions

The research work described in this thesis has been carried out under the supervision of Dr. Fulvia Bono during the period of January 2014 to March 2018 at the Max Planck Institute for Developmental Biology, Tübingen. I hereby declare that all experiments have been independently performed by me, with the exception of those listed below:

a) To tag the *osk* mRNA, recombineering was performed in the laboratory of Dr. Pavel Tomancak, MPI-CBG, Dresden, under the supervision of Dr. Helena Jambor.

b) Fly embryo injections to generate the transgenic lines expressing *MS2-12X-* and *MS2-12X+PP7-24X-* tagged *osk* mRNA were outsourced to BestGene Inc. (USA). Transgenic lines expressing *PP7-24X-* and *MS2-6X-* tagged *osk* mRNA were generated in the laboratory of Dr. Pavel Tomancak, MPI-CBG, Dresden.

c) Fly embryo injections to generate the transgenic line expressing GFP tag only, to serve as a control for IP-MS experiments, were performed by Kristina Ile in the lab.

d) All the fly lines expressing tagged RBPs and those used for genetic rescue assays were obtained from fly stock centers or colleagues.

e) GST tag, to serve as a control for affinity purification of *MS2*-tagged *osk* mRNA using GST-MCP, was purified by Jonas Mühle in the lab.

f) LC-MS/MS measurements for both label-free and Dimethyl labeling MS were performed by Johannes Madlung, in the laboratory of Prof. Dr. Boris Macek, Proteome Center Tübingen, University of Tübingen.

g) Raw data for Dimethyl labeling MS were processed by Johannes Madlung, in the laboratory of Prof. Dr. Boris Macek, Proteome Center Tübingen, University of Tübingen.

h) About half of the plasmid constructs used for co-immunoprecipitation assays in HEK cells were prepared by Kristina Ile and Desiree Zerbst in the lab.

Prashali Bansal
10 October 2018

6. References

Adams, M. D., Celniker, S. E., Holt, R. A., Evans, C. A., Gocayne, J. D., Amanatides, P. G., … Venter, J. C. (2000). The genome sequence of Drosophila melanogaster. *Science (New York, N.Y.)*, *287*(5461), 2185–2195.

Agranat-Tamir, L., Shomron, N., Sperling, J., & Sperling, R. (2014). Interplay between pre-mRNA splicing and microRNA biogenesis within the supraspliceosome. *Nucleic Acids Research*, *42*(7), 4640–4651.

Ainger, K., Avossa, D., Diana, A. S., Barry, C., Barbarese, E., & Carson, J. H. (1997). Transport and localization elements in myelin basic protein mRNA. *The Journal of Cell Biology*, *138*(5), 1077–1087.

Alexandrov, A., Colognori, D., Shu, M.-D., & Steitz, J. A. (2012). Human spliceosomal protein CWC22 plays a role in coupling splicing to exon junction complex deposition and nonsense-mediated decay. *Proceedings of the National Academy of Sciences*, *109*(52), 21313–21318.

Alhusaini, N., & Coller, J. (2016). The deadenylase components Not2p, Not3p, and Not5p promote mRNA decapping. *RNA (New York, N.Y.)*, *22*(5), 709–721.

Amrute-Nayak, M., & Bullock, S. L. (2012). Single-molecule assays reveal that RNA localization signals regulate dynein-dynactin copy number on individual transcript cargoes. *Nature Cell Biology*, *14*(4), 416–423.

Andaya, A., Villa, N., Jia, W., Fraser, C. S., & Leary, J. A. (2014). Phosphorylation stoichiometries of human eukaryotic initiation factors. *International Journal of Molecular Sciences*, *15*(7), 11523–11538.

Andersen, C. B. F., Ballut, L., Johansen, J. S., Chamieh, H., Nielsen, K. H., Oliveira, C. L. P., … Andersen, G. R. (2006). Structure of the exon junction core complex with a trapped DEAD-box ATPase bound to RNA. *Science (New York, N.Y.)*, *313*(5795), 1968–1972.

Anderson, P., & Kedersha, N. (2006). RNA granules. *The Journal of Cell Biology*, *172*(6), 803–808.

Andreassi, C., Zimmermann, C., Mitter, R., Fusco, S., De Vita, S., Saiardi, A., … Riccio, A. (2010). An NGF-responsive element targets myo-inositol monophosphatase-1 mRNA to sympathetic neuron axons. *Nature Neuroscience*, *13*(3), 291–301.

Andrei, M. A., Ingelfinger, D., Heintzmann, R., Achsel, T., Rivera-Pomar, R., & Lührmann, R. (2005). A role for eIF4E and eIF4E-transporter in targeting mRNPs to mammalian processing bodies. *RNA (New York, N.Y.)*, *11*(5), 717–727.

Angel, T. E., Aryal, U. K., Hengel, S. M., Baker, E. S., Kelly, R. T., Robinson, E. W., & Smith, R. D. (2012). Mass spectrometry-based proteomics: existing capabilities and future directions. *Chemical Society Reviews*, *41*(10), 3912–3928.

Anne, J., Ollo, R., Ephrussi, A., & Mechler, B. M. (2007). Arginine methyltransferase Capsuleen is essential for methylation of spliceosomal Sm proteins and germ cell formation in Drosophila. *Development*, *134*(1), 137–146.

Ashton-Beaucage, D., Udell, C. M., Lavoie, H., Baril, C., Lefrançois, M., Chagnon, P., … Therrien, M. (2010). The Exon Junction Complex Controls the Splicing of mapk and Other Long Intron-Containing Transcripts in Drosophila. *Cell*, *143*(2), 251–262.

Babitzke, P., Baker, C. S., & Romeo, T. (2009). Regulation of translation initiation by RNA binding proteins. *Annual Review of Microbiology*, *63*, 27–44.

Bachler, M., Schroeder, R., & von Ahsen, U. (1999). StreptoTag: a novel method for the isolation of RNA-binding proteins. *RNA (New York, N.Y.)*, *5*(11), 1509–1516.

Badis, G., Saveanu, C., Fromont-Racine, M., & Jacquier, A. (2004). Targeted mRNA Degradation by Deadenylation-Independent Decapping. *Molecular Cell*, *15*(1), 5–15.

Bakheet, T., Williams, B. R. G., & Khabar, K. S. A. (2006). ARED 3.0: the large and diverse AU-rich transcriptome. *Nucleic Acids Research*, *34*(Database issue), D111-4.

Ballut, L., Marchadier, B., Baguet, A., Tomasetto, C., Séraphin, B., & Le Hir, H. (2005). The exon junction core complex is locked onto RNA by inhibition of eIF4AIII ATPase activity. *Nature Structural & Molecular Biology*, *12*(10), 861–869.

Barbosa, I., Haque, N., Fiorini, F., Barrandon, C., Tomasetto, C., Blanchette, M., & Le Hir, H. (2012). Human CWC22 escorts the helicase eIF4AIII to spliceosomes and promotes exon junction complex assembly. *Nature Structural & Molecular Biology*, *19*(10), 983–990.

Barker, D. D., Wang, C., Moore, J., Dickinson, L. K., & Lehmann, R. (1992). Pumilio is essential for function but not for distribution of the Drosophila abdominal determinant Nanos. *Genes & Development*, *6*(12A), 2312–2326.

Barreau, C., Paillard, L., & Osborne, H. B. (2005). AU-rich elements and associated factors: are there unifying principles? *Nucleic Acids Research*, *33*(22), 7138–7150.

Barrett, O. P. T., & Chin, J. W. (2010). Evolved orthogonal ribosome purification for in vitro characterization. *Nucleic Acids Research*, *38*(8), 2682–2691.

Bartel, D. P. (2004). MicroRNAs: genomics, biogenesis, mechanism, and function. *Cell*, *116*(2), 281–297.

Bartel, D. P. (2009). MicroRNAs: Target Recognition and Regulatory Functions. *Cell*, *136*(2), 215–233.

Barth, S., Pfuhl, T., Mamiani, A., Ehses, C., Roemer, K., Kremmer, E., … Grasser, F. A. (2007). Epstein-Barr virus-encoded microRNA miR-BART2 down-regulates the viral DNA polymerase BALF5. *Nucleic Acids Research*, *36*(2), 666–675.

Bastock, R., & St Johnston, D. (2008). Drosophila oogenesis. *Current Biology*, *18*(23), R1082-7.

Batada, N. N., Shepp, L. A., & Siegmund, D. O. (2004). Stochastic model of protein-protein interaction: why signaling proteins need to be colocalized. *Proceedings of the National Academy of Sciences of the United States of America*, *101*(17), 6445–6449.

Bazzini, A. A., Lee, M. T., & Giraldez, A. J. (2012). Ribosome profiling shows that miR-430 reduces translation before causing mRNA decay in zebrafish. *Science (New York, N.Y.)*, *336*(6078), 233–237.

Becalska, A. N., Kim, Y. R., Belletier, N. G., Lerit, D. A., Sinsimer, K. S., & Gavis, E. R. (2011). Aubergine is a component of a nanos mRNA localization complex. *Developmental Biology*, *349*(1), 46–52.

Behm-Ansmant, I., Rehwinkel, J., & Izaurralde, E. (2006). MicroRNAs Silence Gene Expression by Repressing Protein Expression and/or by Promoting mRNA Decay. *Cold Spring Harbor Symposia on Quantitative Biology*, *71*(0), 523–530.

Beilharz, T. H., Humphreys, D. T., Clancy, J. L., Thermann, R., Martin, D. I. K., Hentze, M. W., & Preiss, T. (2009). microRNA- Mediated Messenger RNA Deadenylation Contributes to Translational Repression in Mammalian Cells. *PLoS ONE*, *4*(8), e6783.

Benoit, P., Papin, C., Kwak, J. E., Wickens, M., & Simonelig, M. (2008). PAP- and GLD-2-type poly(A) polymerases are required sequentially in cytoplasmic polyadenylation and oogenesis in Drosophila. *Development*, *135*(11), 1969–1979.

Bergalet, J., & Lécuyer, E. (2014). The Functions and Regulatory Principles of mRNA Intracellular Trafficking. In *Advances in experimental medicine and biology*, Vol. 825, 57–96.

Bergsten, S. E., & Gavis, E. R. (1999). Role for mRNA localization in translational activation but not spatial restriction of nanos RNA. *Development (Cambridge, England)*, *126*(4), 659–669.

Berleth, T., Burri1, M., Thoma, G., Bopp1, D., Richstein, S., Frigerio1, G., … Nusslein-Volhard, C. (1988). The role of localization of bicoid RNA in organizing the anterior pattern of the Drosophila embryo. *The EMBO Journal* Vol. 7.

Bernardi, A., & Spahr, P. F. (1972). Nucleotide sequence at the binding site for coat protein on RNA of bacteriophage R17. *Proceedings of the National Academy of Sciences of the United States of America*, *69*(10), 3033–3037.

Bertrand, E., Chartrand, P., Schaefer, M., Shenoy, S. M., Singer, R. H., & Long, R. M. (1998). Localization of ASH1 mRNA particles in living yeast. *Molecular Cell*, *2*(4), 437–445.

Besse, F., & Ephrussi, A. (2008). Translational control of localized mRNAs: restricting protein synthesis in space and time. *Nature Reviews Molecular Cell Biology*, *9*(12), 971–980.

Besse, F., Lopez de Quinto, S., Marchand, V., Trucco, A., & Ephrussi, A. (2009). Drosophila PTB promotes formation of high-order RNP particles and represses oskar translation. *Genes & Development*, *23*(2), 195–207.

Béthune, J., Artus-Revel, C. G., & Filipowicz, W. (2012). Kinetic analysis reveals successive steps leading to miRNA-mediated silencing in mammalian cells. *EMBO Reports*, *13*(8), 716–723.

Bhattacharyya, S. N., Habermacher, R., Martine, U., Closs, E. I., & Filipowicz, W. (2006). Relief of microRNA-Mediated Translational Repression in Human Cells Subjected to Stress. *Cell*, *125*(6), 1111–1124.

Blencowe, B. J., & Lamond, A. I. (1999). Purification and Depletion of RNP Particles by Antisense Affinity Chromatography. *RNA-Protein Interaction Protocols*, Vol. 118, 275–287. New Jersey: Humana Press.

Blower, M. D. (2013). Molecular insights into intracellular RNA localization. *International Review of Cell and Molecular Biology*, *302*, 1–39.

Blower, M. D., Feric, E., Weis, K., & Heald, R. (2007). Genome-wide analysis demonstrates conserved localization of messenger RNAs to mitotic microtubules. *The Journal of Cell Biology*, *179*(7), 1365–1373.

Bobola, N., Jansen, R. P., Shin, T. H., & Nasmyth, K. (1996). Asymmetric accumulation of Ash1p in postanaphase nuclei depends on a myosin and restricts yeast mating-type switching to mother cells. *Cell*, *84*(5), 699–709.

Boersema, P. J., Raijmakers, R., Lemeer, S., Mohammed, S., & Heck, A. J. R. (2009). Multiplex peptide stable isotope dimethyl labeling for quantitative proteomics. *Nature Protocols*, *4*(4), 484–494.

Bönisch, C., Temme, C., Moritz, B., & Wahle, E. (2007). Degradation of hsp70 and other mRNAs in Drosophila via the 5' 3' pathway and its regulation by heat shock. *The Journal of Biological Chemistry*, *282*(30), 21818–21828.

Bono, F., Ebert, J., Lorentzen, E., & Conti, E. (2006). The Crystal Structure of the Exon Junction Complex Reveals How It Maintains a Stable Grip on mRNA. *Cell*, *126*(4), 713–725.

Bono, F., Ebert, J., Unterholzner, L., Güttler, T., Izaurralde, E., & Conti, E. (2004). Molecular insights into the interaction of PYM with the Mago-Y14 core of the exon junction complex. *EMBO Reports*, *5*(3), 304–310.

Boswell, R. E., & Mahowald, A. P. (1985). Tudor, a gene required for assembly of the germ plasm in Drosophila melanogaster. *Cell*, *43*(1), 97–104.

Boswell, R. E., Prout, M. E., & Steichen, J. C. (1991). Mutations in a newly identified Drosophila melanogaster gene, mago nashi, disrupt germ cell formation and result in the formation of mirror-image symmetrical double abdomen embryos. *Development (Cambridge, England)*, *113*(1), 373–384.

Braun, J. E., Huntzinger, E., Fauser, M., & Izaurralde, E. (2011). GW182 Proteins Directly Recruit Cytoplasmic Deadenylase Complexes to miRNA Targets. *Molecular Cell*, *44*(1), 120–133.

Braun, J. E., Truffault, V., Boland, A., Huntzinger, E., Chang, C.-T., Haas, G., … Izaurralde, E. (2012). A direct interaction between DCP1 and XRN1 couples mRNA decapping to 5' exonucleolytic degradation. *Nature Structural & Molecular Biology*, *19*(12), 1324–1331.

Braun, K. A., & Young, E. T. (2014). Coupling mRNA synthesis and decay. *Molecular and Cellular Biology*, *34*(22), 4078–4087.

Breitwieser, W., Markussen, F. H., Horstmann, H., & Ephrussi, A. (1996). Oskar protein interaction with Vasa represents an essential step in polar granule assembly. *Genes & Development*, *10*(17), 2179–2188.

Brendza, R. P., Serbus, L. R., Duffy, J. B., & Saxton, W. M. (2000). A function for kinesin I in the posterior transport of oskar mRNA and Staufen protein. *Science (New York, N.Y.)*, *289*(5487), 2120–2122.

Brengues, M., Teixeira, D., & Parker, R. (2005). Movement of Eukaryotic mRNAs Between Polysomes and Cytoplasmic Processing Bodies. *Science*, *310*(5747), 486–489.

Buchan, J. R. (2014). mRNP granules. Assembly, function, and connections with disease. *RNA Biology*, *11*(8), 1019–1030.

Buchwald, G., Schüssler, S., Basquin, C., Le Hir, H., & Conti, E. (2013). Crystal structure of the human eIF4AIII–CWC22 complex shows how a DEAD-box protein is inhibited by a MIF4G domain. *Proceedings of the National Academy of Sciences*, *110*(48), 4611-4618.

Bühler, M., Steiner, S., Mohn, F., Paillusson, A., & Mühlemann, O. (2006). EJC-independent degradation of nonsense immunoglobulin-μ mRNA depends on 3′ UTR length. *Nature Structural & Molecular Biology*, *13*(5), 462–464.

Bullock, S. L., & Ish-Horowicz, D. (2001). Conserved signals and machinery for RNA transport in Drosophila oogenesis and embryogenesis. *Nature*, *414*(6864), 611–616.

Buratti, E., & Baralle, F. E. (2004). Influence of RNA Secondary Structure on the Pre-mRNA Splicing Process. *Molecular and Cellular Biology*, *24*(24), 10505–10514.

Bushati, N., & Cohen, S. M. (2007). microRNA Functions. *Annual Review of Cell and Developmental Biology*, *23*(1), 175–205.

Bushell, M., Poncet, D., Marissen, W. E., Flotow, H., Lloyd, R. E., Clemens, M. J., & Morley, S. J. (2000). Cleavage of polypeptide chain initiation factor eIF4GI during apoptosis in lymphoma cells: characterisation of an internal fragment generated by caspase-3-mediated cleavage. *Cell Death & Differentiation*, *7*(7), 628–636.

Buskila, A. A., Kannaiah, S., & Amster-Choder, O. (2014). RNA localization in bacteria. *RNA Biology*, *11*(8), 1051–1060.

Buszczak, M., Paterno, S., Lighthouse, D., Bachman, J., Planck, J., Owen, S., … Spradling, A. C. (2007). The carnegie protein trap library: a versatile tool for Drosophila developmental studies. *Genetics*, *175*(3), 1505–1531.

Buxbaum, A. R., Haimovich, G., & Singer, R. H. (2015). In the right place at the right time: visualizing and understanding mRNA localization. *Nature Reviews. Molecular Cell Biology*, *16*(2), 95–109.

Bzymek, M., & Lovett, S. T. (2001). Instability of repetitive DNA sequences: the role of replication in multiple mechanisms. *Proceedings of the National Academy of Sciences of the United States of America*, *98*(15), 8319–8325.

Cajigas, I. J., Tushev, G., Will, T. J., tom Dieck, S., Fuerst, N., & Schuman, E. M. (2012). The Local Transcriptome in the Synaptic Neuropil Revealed by Deep Sequencing and High-Resolution Imaging. *Neuron*, *74*(3), 453–466.

Candeias, M. M., Powell, D. J., Roubalova, E., Apcher, S., Bourougaa, K., Vojtesek, B., … Fåhraeus, R. (2006). Expression of p53 and p53/47 are controlled by alternative mechanisms of messenger RNA translation initiation. *Oncogene*, *25*(52), 6936–6947.

Cao, D., & Parker, R. (2003). Computational modeling and experimental analysis of nonsense-mediated decay in yeast. *Cell*, *113*(4), 533–545.

Carey, J., Cameron, V., de Haseth, P. L., & Uhlenbeck, O. C. (1983). Sequence-specific interaction of R17 coat protein with its ribonucleic acid binding site. *Biochemistry*, *22*(11), 2601–2610.

Carrera, P., Johnstone, O., Nakamura, A., Casanova, J., Jäckle, H., & Lasko, P. (2000). VASA mediates translation through interaction with a Drosophila yIF2 homolog. *Molecular Cell*, *5*(1), 181–187.

Carthew, R. W., & Sontheimer, E. J. (2009). Origins and Mechanisms of miRNAs and siRNAs. *Cell*, *136*(4), 642–655.

Castagnetti, S., & Ephrussi, A. (2003). Orb and a long poly(A) tail are required for efficient oskar translation at the posterior pole of the Drosophila oocyte. *Development (Cambridge, England)*, *130*(5), 835–843.

Catalanotto, C., Cogoni, C., & Zardo, G. (2016). MicroRNA in Control of Gene Expression: An Overview of Nuclear Functions. *International Journal of Molecular Sciences*, *17*(10).

Chan, A. P., Kloc, M., & Etkin, L. D. (1999). fatvg encodes a new localized RNA that uses a 25-nucleotide element (FVLE1) to localize to the vegetal cortex of Xenopus oocytes. *Development (Cambridge, England)*, *126*(22), 4943–4953.

Chang, H., Lim, J., Ha, M., & Kim, V. N. (2014). TAIL-seq: Genome-wide Determination of Poly(A) Tail Length and 3′ End Modifications. *Molecular Cell*, *53*(6), 1044–1052.

Chang, J. S., Tan, L., & Schedl, P. (1999). The Drosophila CPEB Homolog, Orb, Is Required for Oskar Protein Expression in Oocytes. *Developmental Biology*, *215*(1), 91–106.

Chang, J. S., Tan, L., Wolf, M. R., & Schedl, P. (2001). Functioning of the Drosophila orb gene in gurken mRNA localization and translation. *Development (Cambridge, England)*, *128*(16), 3169–3177.

Chang, Y.-F., Imam, J. S., & Wilkinson, M. F. (2007). The Nonsense-Mediated Decay RNA Surveillance Pathway. *Annual Review of Biochemistry*, *76*(1), 51–74.

Chao, J. A., Patskovsky, Y., Almo, S. C., & Singer, R. H. (2008). Structural basis for the coevolution of a viral RNA-protein complex. *Nature Structural & Molecular Biology*, *15*(1), 103–105.

Chao, J. A., Patskovsky, Y., Patel, V., Levy, M., Almo, S. C., & Singer, R. H. (2010). ZBP1 recognition of -actin zipcode induces RNA looping. *Genes & Development*, *24*(2), 148–158.

Chattopadhyay, S., Garcia-Mena, J., DeVito, J., Wolska, K., & Das, A. (1995). Bipartite function of a small RNA hairpin in transcription antitermination in bacteriophage lambda. *Proceedings of the National Academy of Sciences of the United States of America*, *92*(9), 4061–4065.

Chekulaeva, M., Hentze, M. W., & Ephrussi, A. (2006). Bruno Acts as a Dual Repressor of oskar Translation, Promoting mRNA Oligomerization and Formation of Silencing Particles. *Cell*, *124*(3), 521–533.

Chekulaeva, M., Mathys, H., Zipprich, J. T., Attig, J., Colic, M., Parker, R., & Filipowicz, W. (2011). miRNA repression involves GW182-mediated recruitment of CCR4–NOT through conserved W-containing motifs. *Nature Structural & Molecular Biology*, *18*(11), 1218–1226.

Chen, C.-Y. A., & Shyu, A.-B. (2003). Rapid deadenylation triggered by a nonsense codon precedes decay of the RNA body in a mammalian cytoplasmic nonsense-mediated decay pathway. *Molecular and Cellular Biology*, *23*(14), 4805–4813.

Chen, E., Sharma, M. R., Shi, X., Agrawal, R. K., & Joseph, S. (2014). Fragile X Mental Retardation Protein Regulates Translation by Binding Directly to the Ribosome. *Molecular Cell*, *54*(3), 407–417.

Chen, H.-C., & Cheng, S.-C. (2012). Functional roles of protein splicing factors. *Bioscience Reports*, *32*(4), 345–359.

Chen, Y., Boland, A., Kuzuoğlu-Öztürk, D., Bawankar, P., Loh, B., Chang, C.-T., … Izaurralde, E. (2014). A DDX6-CNOT1 Complex and W-Binding Pockets in CNOT9 Reveal Direct Links between miRNA Target Recognition and Silencing. *Molecular Cell*, *54*(5), 737–750.

Chen, Y., Pane, A., & Schüpbach, T. (2007). Cutoff and aubergine mutations result in retrotransposon upregulation and checkpoint activation in Drosophila. *Current Biology : CB*, *17*(7), 637–642.

Chi, S. W., Zang, J. B., Mele, A., & Darnell, R. B. (2009). Argonaute HITS-CLIP decodes microRNA–mRNA interaction maps. *Nature*, *460*(7254), 479–486.

Chicoine, J., Benoit, P., Gamberi, C., Paliouras, M., Simonelig, M., & Lasko, P. (2007). Bicaudal-C Recruits CCR4-NOT Deadenylase to Target mRNAs and Regulates Oogenesis, Cytoskeletal Organization, and Its Own Expression. *Developmental Cell*, *13*(5), 691–704.

Cho, H., Han, S., Choe, J., Park, S. G., Choi, S. S., & Kim, Y. K. (2013). SMG5–PNRC2 is functionally dominant compared with SMG5–SMG7 in mammalian nonsense-mediated mRNA decay. *Nucleic Acids Research*, *41*(2), 1319–1328.

Choudhury, S. R., Singh, A. K., McLeod, T., Blanchette, M., Jang, B., Badenhorst, P., … Brogna, S. (2016). Exon junction complex proteins bind nascent transcripts independently of pre-mRNA splicing in Drosophila melanogaster. *ELife*, *5*.

Chu, C., & Rana, T. M. (2006). Translation Repression in Human Cells by MicroRNA-Induced Gene Silencing Requires RCK/p54. *PLoS Biology*, *4*(7), e210.

Clark, A., Meignin, C., & Davis, I. (2007). A Dynein-dependent shortcut rapidly delivers axis determination transcripts into the Drosophila oocyte. *Development (Cambridge, England)*, *134*(10), 1955–1965.

Clark, I., Giniger, E., Ruohola-Baker, H., Jan, L. Y., & Jan, Y. N. (1994). Transient posterior localization of a kinesin fusion protein reflects anteroposterior polarity of the Drosophila oocyte. *Current Biology : CB*, *4*(4), 289–300.

Clouse, K. N., Ferguson, S. B., & Schüpbach, T. (2008). Squid, Cup, and PABP55B function together to regulate gurken translation in Drosophila. *Developmental Biology*, *313*(2), 713–724.

Clyne, P. J., Brotman, J. S., Sweeney, S. T., & Davis, G. (2003). Green fluorescent protein tagging Drosophila proteins at their native genomic loci with small P elements. *Genetics*, *165*(3), 1433–1441.

Coldwell, M. J., deSchoolmeester, M. L., Fraser, G. A., Pickering, B. M., Packham, G., & Willis, A. E. (2001). The p36 isoform of BAG-1 is translated by internal ribosome entry following heat shock. *Oncogene*, *20*(30), 4095–4100.

Collart, M. A. (2016). The Ccr4-Not complex is a key regulator of eukaryotic gene expression. *Wiley Interdisciplinary Reviews. RNA*, *7*(4), 438–454.

Collart, M. A., & Panasenko, O. O. (2012). The Ccr4--not complex. *Gene*, *492*(1), 42–53.

Colón-Ramos, D. A., Salisbury, J. L., Sanders, M. A., Shenoy, S. M., Singer, R. H., & García-Blanco, M. A. (2003). Asymmetric distribution of nuclear pore complexes and the cytoplasmic localization of beta2-tubulin mRNA in Chlamydomonas reinhardtii. *Developmental Cell*, *4*(6), 941–952.

Colón-Ramos, D. A., Shenvi, C. L., Weitzel, D. H., Gan, E. C., Matts, R., Cate, J., & Kornbluth, S. (2006). Direct ribosomal binding by a cellular inhibitor of translation. *Nature Structural & Molecular Biology*, *13*(2), 103–111.

Cooke, A., Prigge, A., & Wickens, M. (2010). Translational Repression by Deadenylases. *Journal of Biological Chemistry*, *285*(37), 28506–28513.

Coots, R. A., Liu, X.-M., Mao, Y., Dong, L., Zhou, J., Wan, J., … Qian, S.-B. (2017). m6A Facilitates eIF4F-Independent mRNA Translation. *Molecular Cell*, *68*(3), 504–514.e7.

Cordin, O., & Beggs, J. D. (2013). RNA helicases in splicing. *RNA Biology*, *10*(1), 83–95.

Cornelis, S., Bruynooghe, Y., Denecker, G., Van Huffel, S., Tinton, S., & Beyaert, R. (2000). Identification and characterization of a novel cell cycle-regulated internal ribosome entry site. *Molecular Cell*, *5*(4), 597–605.

Cougot, N., Babajko, S., & Séraphin, B. (2004). Cytoplasmic foci are sites of mRNA decay in human cells. *The Journal of Cell Biology*, *165*(1), 31–40.

Couttet, P., & Grange, T. (2004). Premature termination codons enhance mRNA decapping in human cells. *Nucleic Acids Research*, *32*(2), 488–494.

Couttet, P., Fromont-Racine, M., Steel, D., Pictet, R., & Grange, T. (1997). Messenger RNA deadenylylation precedes decapping in mammalian cells. *Proceedings of the National Academy of Sciences of the United States of America*, *94*(11), 5628–5633.

Covelo-Molares, H., Bartosovic, M., & Vanacova, S. (2018). RNA methylation in nuclear pre-mRNA processing. *Wiley Interdisciplinary Reviews: RNA*, e1489.

Cox, J., & Mann, M. (2008). MaxQuant enables high peptide identification rates, individualized p.p.b.-range mass accuracies and proteome-wide protein quantification. *Nature Biotechnology*, *26*(12), 1367–1372.

Cox, J., & Mann, M. (2011). Quantitative, High-Resolution Proteomics for Data-Driven Systems Biology. *Annual Review of Biochemistry*, *80*(1), 273–299.

Cox, J., Hein, M. Y., Luber, C. A., Paron, I., Nagaraj, N., & Mann, M. (2014). Accurate Proteome-wide Label-free Quantification by Delayed Normalization and Maximal Peptide Ratio Extraction, Termed MaxLFQ. *Molecular & Cellular Proteomics*, *13*(9), 2513–2526.

Crick F.H.C (1958). *Symp. Soc. Exp. Biol.* XII: 138-163

Crucs, S., Chatterjee, S., & Gavis, E. R. (2000). Overlapping but Distinct RNA Elements Control Repression and Activation of nanos Translation. *Molecular Cell*, *5*(3), 457–467.

Culbertson, M. R., Underbrink, K. M., & Fink, G. R. (1980). Frameshift suppression Saccharomyces cerevisiae. II. Genetic properties of group II suppressors. *Genetics*, *95*(4), 833–853.

da Costa, P. J., Menezes, J., & Romão, L. (2017). The role of alternative splicing coupled to nonsense-mediated mRNA decay in human disease. *The International Journal of Biochemistry & Cell Biology*, *91*, 168–175.

Dahanukar, A., & Wharton, R. P. (1996). The Nanos gradient in Drosophila embryos is generated by translational regulation. *Genes & Development*, *10*(20), 2610–2620.

Dahanukar, A., Walker, J. A., & Wharton, R. P. (1999). Smaug, a Novel RNA-Binding Protein that Operates a Translational Switch in Drosophila. *Molecular Cell*, *4*(2), 209–218.

Darnell, J. C., Van Driesche, S. J., Zhang, C., Hung, K. Y. S., Mele, A., Fraser, C. E., … Darnell, R. B. (2011). FMRP Stalls Ribosomal Translocation on mRNAs Linked to Synaptic Function and Autism. *Cell*, *146*(2), 247–261.

Darnell, J. E., Philipson, L., Wall, R., & Adesnik, M. (1971). Polyadenylic acid sequences: role in conversion of nuclear RNA into messenger RNA. *Science (New York, N.Y.)*, *174*(4008), 507–510.

Das, R., Zhou, Z., & Reed, R. (2000). Functional Association of U2 snRNP with the ATP-Independent Spliceosomal Complex E. *Molecular Cell*, *5*(5), 779–787.

Das, S., Sarkar, D., & Das, B. (2017). The interplay between transcription and mRNA degradation in Saccharomyces cerevisiae. *Microbial Cell*, *4*(7), 212–228.

Decker, C. J., & Parker, R. (2012). P-bodies and stress granules: possible roles in the control of translation and mRNA degradation. *Cold Spring Harbor Perspectives in Biology*, *4*(9), a012286.

Deckert, J., Hartmuth, K., Boehringer, D., Behzadnia, N., Will, C. L., Kastner, B., … Luhrmann, R. (2006). Protein Composition and Electron Microscopy Structure of Affinity-Purified Human Spliceosomal B Complexes Isolated under Physiological Conditions. *Molecular and Cellular Biology*, *26*(14), 5528–5543.

Dehghani, M., & Lasko, P. (2015). In vivo mapping of the functional regions of the DEAD-box helicase Vasa. *Biology Open*, *4*(4), 450–462.

Delanoue, R., Herpers, B., Soetaert, J., Davis, I., & Rabouille, C. (2007). Drosophila Squid/hnRNP helps Dyenin switch from a gurken mRNA transport motor to an ultrastrutural static anchor in sponge bodies. *Developmental Cell*, *13*(4), 523-538.

Delpy, L., Sirac, C., Magnoux, E., Duchez, S., & Cogne, M. (2004). RNA surveillance down-regulates expression of nonfunctional alleles and detects premature termination within the last exon. *Proceedings of the National Academy of Sciences*, *101*(19), 7375–7380.

Denning, G., Jamieson, L., Maquat, L. E., Thompson, E. A., & Fields, A. P. (2001). Cloning of a Novel Phosphatidylinositol Kinase-related Kinase. *Journal of Biological Chemistry*, *276*(25), 22709–22714.

Deshler, J. O., Highett, M. I., Abramson, T., & Schnapp, B. J. (1998). A highly conserved RNA-binding protein for cytoplasmic mRNA localization in vertebrates. *Current Biology*, *8*(9), 489–496.

Di Liegro, C. M., Schiera, G., & Di Liegro, I. (2014). Regulation of mRNA transport, localization and translation in the nervous system of mammals (Review). *International Journal of Molecular Medicine*, *33*(4), 747–762.

Diem, M. D., Chan, C. C., Younis, I., & Dreyfuss, G. (2007). PYM binds the cytoplasmic exon-junction complex and ribosomes to enhance translation of spliced mRNAs. *Nature Structural & Molecular Biology*, *14*(12), 1173–1179.

Dienstbier, M., Boehl, F., Li, X., & Bullock, S. L. (2009). Egalitarian is a selective RNA-binding protein linking mRNA localization signals to the dynein motor. *Genes & Development*, *23*(13), 1546–1558.

Dix, C. I., Soundararajan, H. C., Dzhindzhev, N. S., Begum, F., Suter, B., Ohkura, H., … Bullock, S. L. (2013). Lissencephaly-1 promotes the recruitment of dynein and dynactin to transported mRNAs. *The Journal of Cell Biology*, *202*(3), 479–494.

Djuranovic, S., Nahvi, A., & Green, R. (2012). miRNA- mediated gene silencing by translational repression followed by mRNA deadenylation and decay. *Science (New York, N.Y.)*, *336*(6078), 237–240.

Dolphin, C. T., & Hope, I. A. (2006). Caenorhabditis elegans reporter fusion genes generated by seamless modification of large genomic DNA clones. *Nucleic Acids Research*, *34*(9), e72–e72.

Dong, Y., Yang, J., Ye, W., Wang, Y., Ye, C., Weng, D., … Lei, Y. (2015). Isolation of Endogenously Assembled RNA-Protein Complexes Using Affinity Purification Based on Streptavidin Aptamer S1. *International Journal of Molecular Sciences*, *16*(9), 22456–22472.

Dostie, J., & Dreyfuss, G. (2002). Translation is required to remove Y14 from mRNAs in the cytoplasm. *Current Biology*, *12*(13), 1060–1067.

Doyle, M., & Kiebler, M. A. (2012). A zipcode unzipped. *Genes & Development*, *26*(2), 110–113.

Du, X., Wang, J., Zhu, H., Rinaldo, L., Lamar, K.-M., Palmenberg, A. C., … Gomez, C. M. (2013). Second Cistron in CACNA1A Gene Encodes a Transcription Factor Mediating Cerebellar Development and SCA6. *Cell*, *154*(1), 118–133.

Dunst, S., Kazimiers, T., von Zadow, F., Jambor, H., Sagner, A., Brankatschk, B., … Brankatschk, M. (2015). Endogenously Tagged Rab Proteins: A Resource to Study Membrane Trafficking in Drosophila. *Developmental Cell*, *33*(3), 351–365.

Dvinge, H. (2018). Regulation of alternative mRNA splicing: old players and new perspectives. *FEBS Letters*, *592*(17), 2987-3006.

Easow, G., Teleman, A. A., & Cohen, S. M. (2007). Isolation of microRNA targets by miRNP immunopurification. *RNA (New York, N.Y.)*, *13*(8), 1198–1204.

Eberl, H. C., Spruijt, C. G., Kelstrup, C. D., Vermeulen, M., & Mann, M. (2013). A map of general and specialized chromatin readers in mouse tissues generated by label-free interaction proteomics. *Molecular Cell*, *49*(2), 368–378.

Eberle, A. B., Lykke-Andersen, S., Mühlemann, O., & Jensen, T. H. (2009). SMG6 promotes endonucleolytic cleavage of nonsense mRNA in human cells. *Nature Structural & Molecular Biology*, *16*(1), 49–55.

Eberle, A. B., Stalder, L., Mathys, H., Orozco, R. Z., & Mühlemann, O. (2008). Posttranscriptional Gene Regulation by Spatial Rearrangement of the 3′ Untranslated Region. *PLoS Biology*, *6*(4), e92.

Ejsmont, R. K., Ahlfeld, P., Pozniakovsky, A., Stewart, A. F., Tomancak, P., & Sarov, M. (2011). Recombination-Mediated Genetic Engineering of Large Genomic DNA Transgenes. In *Methods in molecular biology (Clifton, N.J.)*, Vol. 772, 445–458.

Ejsmont, R. K., Sarov, M., Winkler, S., Lipinski, K. A., & Tomancak, P. (2009). A toolkit for high-throughput, cross-species gene engineering in Drosophila. *Nature Methods*, *6*(6), 435–437.

Elliott, M. H., Smith, D. S., Parker, C. E., & Borchers, C. (2009). Current trends in quantitative proteomics. *Journal of Mass Spectrometry*, *44*(12), 1637-60.

Emelyanov, A. V, Rabbani, J., Mehta, M., Vershilova, E., Keogh, M. C., & Fyodorov, D. V. (2014). Drosophila TAP/p32 is a core histone chaperone that cooperates with NAP-1, NLP, and nucleophosmin in sperm chromatin remodeling during fertilization. *Genes & Development*, *28*(18), 2027–2040.

Ephrussi, A., & Lehmann, R. (1992). Induction of germ cell formation by oskar. *Nature*, *358*(6385), 387–392.

Ephrussi, A., Dickinson, L. K., & Lehmann, R. (1991). oskar organizes the germ plasm and directs localization of the posterior determinant nanos. *Cell*, *66*(1), 37–50.

Erdélyi, M., Michon, A.-M., Guichet, A., Glotzer, J. B., & Ephrussi, A. (1995). Requirement for Drosophila cytoplasmic tropomyosin in oskar mRNA localization. *Nature*, *377*(6549), 524–527.

Eulalio, A., Behm-Ansmant, I., & Izaurralde, E. (2007a). P bodies: at the crossroads of post-transcriptional pathways. *Nature Reviews Molecular Cell Biology*, *8*(1), 9–22.

Eulalio, A., Behm-Ansmant, I., Schweizer, D., & Izaurralde, E. (2007b). P-body formation is a consequence, not the cause, of RNA-mediated gene silencing. *Molecular and Cellular Biology*, *27*(11), 3970–3981.

Eulalio, A., Huntzinger, E., & Izaurralde, E. (2008a). GW182 interaction with Argonaute is essential for miRNA-mediated translational repression and mRNA decay. *Nature Structural & Molecular Biology*, *15*(4), 346–353.

Eulalio, A., Huntzinger, E., & Izaurralde, E. (2008b). Getting to the root of miRNA-mediated gene silencing. *Cell*, *132*(1), 9–14.

Eulalio, A., Huntzinger, E., Nishihara, T., Rehwinkel, J., Fauser, M., & Izaurralde, E. (2009). Deadenylation is a widespread effect of miRNA regulation. *RNA*, *15*(1), 21–32.

Fabian, M. R., & Sonenberg, N. (2012). The mechanics of miRNA-mediated gene silencing: a look under the hood of miRISC. *Nature Structural & Molecular Biology*, *19*(6), 586–593.

Fabian, M. R., Cieplak, M. K., Frank, F., Morita, M., Green, J., Srikumar, T., … Sonenberg, N. (2011). miRNA-mediated deadenylation is orchestrated by GW182 through two conserved motifs that interact with CCR4–NOT. *Nature Structural & Molecular Biology*, *18*(11), 1211–1217.

Fabian, M. R., Mathonnet, G., Sundermeier, T., Mathys, H., Zipprich, J. T., Svitkin, Y. V., … Sonenberg, N. (2009). Mammalian miRNA RISC Recruits CAF1 and PABP to Affect PABP-Dependent Deadenylation. *Molecular Cell*, *35*(6), 868–880.

Fabian, M. R., Sonenberg, N., & Filipowicz, W. (2010). Regulation of mRNA Translation and Stability by microRNAs. *Annual Review of Biochemistry*, *79*(1), 351–379.

Fang, Z., & Rajewsky, N. (2011). The impact of miRNA target sites in coding sequences and in 3'UTRs. *PloS One*, *6*(3), e18067.

Ferraiuolo, M. A., Basak, S., Dostie, J., Murray, E. L., Schoenberg, D. R., & Sonenberg, N. (2005). A role for the eIF4E-binding protein 4E-T in P-body formation and mRNA decay. *The Journal of Cell Biology*, *170*(6), 913–924.

Ferrandon, D., Elphick, L., Nüsslein-Volhard, C., & St Johnston, D. (1994). Staufen protein associates with the 3'UTR of bicoid mRNA to form particles that move in a microtubule-dependent manner. *Cell*, *79*(7), 1221–1232.

Ferrandon, D., Koch, I., Westhof, E., & Nüsslein-Volhard, C. (1997). RNA-RNA interaction is required for the formation of specific bicoid mRNA 3' UTR-Staufen ribonucleoprotein particles. *The EMBO Journal, 16*(7), 1751–1758.

Filardo, P., & Ephrussi, A. (2003). Bruno regulates gurken during Drosophila oogenesis. *Mechanisms of Development*, *120*(3), 289–297.

Filipowicz, W., Bhattacharyya, S. N., & Sonenberg, N. (2008). Mechanisms of post-transcriptional regulation by microRNAs: are the answers in sight? *Nature Reviews Genetics*, *9*(2), 102–114.

Findley, S. D., Tamanaha, M., Clegg, N. J., & Ruohola-Baker, H. (2003). Maelstrom, a Drosophila spindle-class gene, encodes a protein that colocalizes with Vasa and RDE1/AGO1 homolog, Aubergine, in nuage. *Development (Cambridge, England)*, *130*(5), 859–871.

Foley, K., & Cooley, L. (1998). Apoptosis in late stage Drosophila nurse cells does not require genes within the H99 deficiency. *Development (Cambridge, England)*, *125*(6), 1075–1082.

Forrest, K. M., & Gavis, E. R. (2003). Live imaging of endogenous RNA reveals a diffusion and entrapment mechanism for nanos mRNA localization in Drosophila. *Current Biology*, *13*(14), 1159–1168.

Förstemann, K., Tomari, Y., Du, T., Vagin, V. V, Denli, A. M., Bratu, D. P., … Zamore, P. D. (2005). Normal microRNA Maturation and Germ-Line Stem Cell Maintenance Requires Loquacious, a Double-Stranded RNA-Binding Domain Protein. *PLoS Biology*, *3*(7), e236.

Frost, D. C., Greer, T., & Li, L. (2015). High-resolution enabled 12-plex DiLeu isobaric tags for quantitative proteomics. *Analytical Chemistry*, *87*(3), 1646–1654.

Fuchs, G., Diges, C., Kohlstaedt, L. A., Wehner, K. A., & Sarnow, P. (2011). Proteomic Analysis of Ribosomes: Translational Control of mRNA Populations by Glycogen Synthase GYS1. *Journal of Molecular Biology*, *410*(1), 118–130.

Fukaya, T., & Tomari, Y. (2011). PABP is not essential for microRNA-mediated translational repression and deadenylation *in vitro. The EMBO Journal*, *30*(24), 4998–5009.

Fukaya, T., & Tomari, Y. (2012). MicroRNAs Mediate Gene Silencing via Multiple Different Pathways in Drosophila. *Molecular Cell*, *48*(6), 825–836.

Fukaya, T., Iwakawa, H., & Tomari, Y. (2014). MicroRNAs Block Assembly of eIF4F Translation Initiation Complex in Drosophila. *Molecular Cell*, *56*(1), 67–78.

Fukunaga, R., & Zamore, P. D. (2012). Loquacious, a Dicer Partner Protein, Functions in Both the MicroRNA and siRNA Pathways. *The Enzymes*, *32*, 37–68.

Funakoshi, Y., Doi, Y., Hosoda, N., Uchida, N., Osawa, M., Shimada, I., … Hoshino, S. (2007). Mechanism of mRNA deadenylation: evidence for a molecular interplay between translation termination factor eRF3 and mRNA deadenylases. *Genes & Development*, *21*(23), 3135–3148.

Fusco, D., Accornero, N., Lavoie, B., Shenoy, S. M., Blanchard, J.-M., Singer, R. H., & Bertrand, E. (2003). Single mRNA molecules demonstrate probabilistic movement in living mammalian cells. *Current Biology*, *13*(2), 161–167.

Garcia, J. F., & Parker, R. (2015). MS2 coat proteins bound to yeast mRNAs block 5' to 3' degradation and trap mRNA decay products: implications for the localization of mRNAs by MS2-MCP system. *RNA*, *21*(8), 1393–1395.

Garcia, J. F., & Parker, R. (2016). Ubiquitous accumulation of 3′ mRNA decay fragments in *Saccharomyces cerevisiae* mRNAs with chromosomally integrated MS2 arrays. *RNA*, *22*(5), 657–659.

García-Mauriño, S. M., Rivero-Rodríguez, F., Velázquez-Cruz, A., Hernández-Vellisca, M., Díaz-Quintana, A., De la Rosa, M. A., & Díaz-Moreno, I. (2017). RNA Binding Protein Regulation and Cross-Talk in the Control of AU-rich mRNA Fate. *Frontiers in Molecular Biosciences*, *4* (71).

Garneau, N. L., Wilusz, J., & Wilusz, C. J. (2007). The highways and byways of mRNA decay. *Nature Reviews Molecular Cell Biology*, *8*(2), 113–126.

Gáspár, I., Sysoev, V., Komissarov, A., & Ephrussi, A. (2017). An RNA-binding atypical tropomyosin recruits kinesin-1 dynamically to oskar mRNPs. *The EMBO Journal*, *36*(3), 319–333.

Gatfield, D., & Izaurralde, E. (2004). Nonsense-mediated messenger RNA decay is initiated by endonucleolytic cleavage in Drosophila. *Nature*, *429*(6991), 575–578.

Gatfield, D., Unterholzner, L., Ciccarelli, F. D., Bork, P., & Izaurralde, E. (2003). Nonsense-mediated mRNA decay in Drosophila:at the intersection of the yeast and mammalian pathways. *The EMBO Journal*, *22*(15), 3960–3970.

Gautreau, D., Cote, C. A., & Mowry, K. L. (1997). Two copies of a subelement from the Vg1 RNA localization sequence are sufficient to direct vegetal localization in Xenopus oocytes. *Development (Cambridge, England)*, *124*(24), 5013–5020.

Gavis, E. R., & Lehmann, R. (1992). Localization of nanos RNA controls embryonic polarity. *Cell*, *71*(2), 301–313.

Gavis, E. R., Lunsford, L., Bergsten, S. E., & Lehmann, R. (1996). A conserved 90 nucleotide element mediates translational repression of nanos RNA. *Development (Cambridge, England)*, *122*(9), 2791–2800.

Gavis, E.R., Singer, R.H., Hüttelmaier, S. (2007). Localized translation through messenger RNA localization. Hershey, J.W.B., Mathews, M.B., Sonenberg, N. (Eds.), Translational Control in Biology and Medicine, Cold Spring Harbor Laboratory Press, Cold Spring Harbor, NY (2007), 687-717

Ge, H., & Manley, J. L. (1990). A protein factor, ASF, controls cell-specific alternative splicing of SV40 early pre-mRNA in vitro. *Cell*, *62*(1), 25–34.

Gebow, D., Miselis, N., & Liber, H. L. (2000). Homologous and nonhomologous recombination resulting in deletion: effects of p53 status, microhomology, and repetitive DNA length and orientation. *Molecular and Cellular Biology*, *20*(11), 4028–4035.

Gehring, N. H., Lamprinaki, S., Hentze, M. W., & Kulozik, A. E. (2009). The hierarchy of exon-junction complex assembly by the spliceosome explains key features of mammalian nonsense-mediated mRNA decay. *PLoS Biology*, *7*(5), e1000120.

Gehring, N. H., Lamprinaki, S., Kulozik, A. E., & Hentze, M. W. (2009). Disassembly of Exon Junction Complexes by PYM. *Cell*, *137*(3), 536–548.

Geissler, R., Simkin, A., Floss, D., Patel, R., Fogarty, E. A., Scheller, J., & Grimson, A. (2016). A widespread sequence-specific mRNA decay pathway mediated by hnRNPs A1 and A2/B1. *Genes & Development*, *30*(9), 1070–1085.

Geng, C., & Macdonald, P. M. (2006). Imp associates with squid and Hrp48 and contributes to localized expression of gurken in the oocyte. *Molecular and Cellular Biology*, *26*(24), 9508–9516.

Gerbracht, J. V, & Gehring, N. H. (2018). The exon junction complex: structural insights into a faithful companion of mammalian mRNPs. *Biochemical Society Transactions*, *46*(1), 153–161.

Ghosh, S., Marchand, V., Gáspár, I., & Ephrussi, A. (2012). Control of RNP motility and localization by a splicing-dependent structure in oskar mRNA. *Nature Structural & Molecular Biology*, *19*(4), 441–449.

Gibson, D. G., Young, L., Chuang, R.-Y., Venter, J. C., Hutchison, C. A., & Smith, H. O. (2009). Enzymatic assembly of DNA molecules up to several hundred kilobases. *Nature Methods*, *6*(5), 343–345.

Gilbert, W. V. (2011). Functional specialization of ribosomes? *Trends in Biochemical Sciences*, *36*(3), 127–132.

Gingras, A.-C., Raught, B., & Sonenberg, N. (1999). eIF4 Initiation Factors: Effectors of mRNA Recruitment to Ribosomes and Regulators of Translation. *Annual Review of Biochemistry*, *68*(1), 913–963.

Glisovic, T., Bachorik, J. L., Yong, J., & Dreyfuss, G. (2008). RNA-binding proteins and post-transcriptional gene regulation. *FEBS Letters*, *582*(14), 1977–1986.

Goldstrohm, A. C., Hook, B. A., Seay, D. J., & Wickens, M. (2006). PUF proteins bind Pop2p to regulate messenger RNAs. *Nature Structural & Molecular Biology*, *13*(6), 533–539.

Gong, C., Popp, M. W.-L., & Maquat, L. E. (2012). Biochemical analysis of long non-coding RNA-containing ribonucleoprotein complexes. *Methods*, *58*(2), 88–93.

Gonsalvez, G. B., Rajendra, T. K., Tian, L., & Matera, A. G. (2006). The Sm-Protein Methyltransferase, Dart5, Is Essential for Germ-Cell Specification and Maintenance. *Current Biology*, *16*(11), 1077–1089.

Gonsalvez, G. B., Rajendra, T. K., Wen, Y., Praveen, K., & Matera, A. G. (2010). Sm proteins specify germ cell fate by facilitating oskar mRNA localization. *Development (Cambridge, England)*, *137*(14), 2341–2351.

Goodrich, J. S., Clouse, K. N., & Schüpbach, T. (2004). Hrb27C, Sqd and Otu cooperatively regulate gurken RNA localization and mediate nurse cell chromosome dispersion in Drosophila oogenesis. *Development*, *131*(9), 1949–1958.

Gott, J. M., Wilhelm, L. J., & Uhlenbeck, O. C. (1991). RNA binding properties of the coat protein from bacteriophage GA. *Nucleic Acids Research*, *19.*

Götze, M., Dufourt, J., Ihling, C., Rammelt, C., Pierson, S., Sambrani, N., … Wahle, E. (2017). Translational repression of the *Drosophila nanos* mRNA involves the RNA helicase Belle and RNA coating by Me31B and Trailer hitch. *RNA*, *23*(10), 1552–1568.

Gramates, L. S., Marygold, S. J., Santos, G. dos, Urbano, J.-M., Antonazzo, G., Matthews, B. B., … Zhou, P. (2017). FlyBase at 25: looking to the future. *Nucleic Acids Research*, *45*(D1), D663–D671.

Granneman, S., Kudla, G., Petfalski, E., & Tollervey, D. (2009). Identification of protein binding sites on U3 snoRNA and pre-rRNA by UV cross-linking and high-throughput analysis of cDNAs. *Proceedings of the National Academy of Sciences*, *106*(24), 9613–9618.

Groth, A. C., Fish, M., Nusse, R., & Calos, M. P. (2004). Construction of transgenic Drosophila by using the site-specific integrase from phage phiC31. *Genetics*, *166*(4), 1775–1782.

Gu, W., Xu, Y., Xie, X., Wang, T., Ko, J.-H., & Zhou, T. (2014). The role of RNA structure at 5' untranslated region in microRNA-mediated gene regulation. *RNA (New York, N.Y.)*, *20*(9), 1369–1375.

Gumy, L. F., Yeo, G. S. H., Tung, Y.-C. L., Zivraj, K. H., Willis, D., Coppola, G., … Fawcett, J. W. (2011). Transcriptome analysis of embryonic and adult sensory axons reveals changes in mRNA repertoire localization. *RNA*, *17*(1), 85–98.

Gunkel, N., Yano, T., Markussen, F.-H., Olsen, L. C., & Ephrussi, A. (1998). Localization-dependent translation requires a functional interaction between the 5' and 3' ends of oskar mRNA. *Genes & Development*, *12*(11), 1652–1664.

Guo, H. (2018). Specialized ribosomes and the control of translation. *Biochemical Society Transactions*, *46(4),* 855-869.

Gustafson, E. A., & Wessel, G. M. (2010). Vasa genes: Emerging roles in the germ line and in multipotent cells. *BioEssays*, *32*(7), 626-637.

Gustafson, E. A., Yajima, M., Juliano, C. E., & Wessel, G. M. (2011). Post-translational regulation by gustavus contributes to selective Vasa protein accumulation in multipotent cells during embryogenesis. *Developmental Biology*, *349*(2), 440–450.

Gygi, S. P., Rist, B., Gerber, S. A., Turecek, F., Gelb, M. H., & Aebersold, R. (1999). Quantitative analysis of complex protein mixtures using isotope-coded affinity tags. *Nature Biotechnology*, *17*(10), 994–999.

Haag, C., Steuten, B., & Feldbrügge, M. (2015). Membrane-Coupled mRNA Trafficking in Fungi. *Annual Review of Microbiology*, *69*(1), 265–281.

Hachet, O., & Ephrussi, A. (2004). Splicing of oskar RNA in the nucleus is coupled to its cytoplasmic localization. *Nature*, *428*(6986), 959–963.

Hafner, M., Landthaler, M., Burger, L., Khorshid, M., Hausser, J., Berninger, P., … Tuschl, T. (2010). PAR-CliP - A Method to Identify Transcriptome-wide the Binding Sites of RNA Binding Proteins. *Journal of Visualized Experiments*, 41.

Haghighat, A., Mader, S., Pause, A., & Sonenberg, N. (1995). Repression of cap-dependent translation by 4E-binding protein 1: competition with p220 for binding to eukaryotic initiation factor-4E. *The EMBO Journal*, *14*(22), 5701–5709.

Haimovich, G., Zabezhinsky, D., Haas, B., Slobodin, B., Purushothaman, P., Fan, L., … Gerst, J. E. (2016). Use of the MS2 aptamer and coat protein for RNA localization in yeast: A response to "MS2 coat proteins bound to yeast mRNAs block 5' to 3' degradation and trap mRNA decay products: implications for the localization of mRNAs by MS2-MCP system". *RNA (New York, N.Y.)*, *22*(5), 660–666.

Halstead, J. M., Lionnet, T., Wilbertz, J. H., Wippich, F., Ephrussi, A., Singer, R. H., & Chao, J. A. (2015). Translation. An RNA biosensor for imaging the first round of translation from single cells to living animals. *Science (New York, N.Y.)*, *347*(6228), 1367–1671.

Hamilton, R. S., & Davis, I. (2011). Identifying and searching for conserved RNA localisation signals. *Methods in Molecular Biology (Clifton, N.J.)*, *714*, 447–466.

Hartmuth, K., Urlaub, H., Vornlocher, H.-P., Will, C. L., Gentzel, M., Wilm, M., & Luhrmann, R. (2002). Protein composition of human prespliceosomes isolated by a tobramycin affinity-selection method. *Proceedings of the National Academy of Sciences*, *99*(26), 16719–16724.

Harvey, R. F., Smith, T. S., Mulroney, T., Queiroz, R. M. L., Pizzinga, M., Dezi, V., … Willis, A. E. (2018). *Trans*-acting translational regulatory RNA binding proteins. *Wiley Interdisciplinary Reviews: RNA*, *9*(3), e1465.

Hase, M. E., Yalamanchili, P., & Visa, N. (2006). The *Drosophila* Heterogeneous Nuclear Ribonucleoprotein M Protein, HRP59, Regulates Alternative Splicing and Controls the Production of Its Own mRNA. *Journal of Biological Chemistry*, *281*(51), 39135–39141.

Hay, B., Ackerman, L., Barbel, S., Jan, L. Y., & Jan, Y. N. (1988a). Identification of a component of Drosophila polar granules. *Development*, *103*(4).

Hay, B., Jan, L. Y., & Jan, Y. N. (1988b). A protein component of Drosophila polar granules is encoded by vasa and has extensive sequence similarity to ATP-dependent helicases. *Cell*, *55*(4), 577–587.

Hay, B., Jan, L. Y., & Jan, Y. N. (1990). Localization of vasa, a component of Drosophila polar granules, in maternal-effect mutants that alter embryonic anteroposterior polarity. *Development (Cambridge, England)*, *109*(2), 425–433.

Hayashi, R., Handler, D., Ish-Horowicz, D., & Brennecke, J. (2014). The exon junction complex is required for definition and excision of neighboring introns in *Drosophila*. *Genes & Development*, *28*(16), 1772–1785.

He, F., Brown, A. H., & Jacobson, A. (1997). Upf1p, Nmd2p, and Upf3p are interacting components of the yeast nonsense-mediated mRNA decay pathway. *Molecular and Cellular Biology*, *17*(3), 1580–1594.

He, F., Li, X., Spatrick, P., Casillo, R., Dong, S., & Jacobson, A. (2003). Genome-wide analysis of mRNAs regulated by the nonsense-mediated and 5' to 3' mRNA decay pathways in yeast. *Molecular Cell*, *12*(6), 1439–1452.

He, F., Peltz, S. W., Donahue, J. L., Rosbash, M., & Jacobson, A. (1993). Stabilization and ribosome association of unspliced pre-mRNAs in a yeast upf1- mutant. *Proceedings of the National Academy of Sciences of the United States of America*, *90*(15), 7034–7038.

Heck, A. M., & Wilusz, J. (2018). The Interplay between the RNA Decay and Translation Machinery in Eukaryotes. *Cold Spring Harbor Perspectives in Biology*, *10*(5), a032839.

Hein, M. Y. Y., Hubner, N. C. C., Poser, I., Cox, J., Nagaraj, N., Toyoda, Y., … Mann, M. (2015). A Human Interactome in Three Quantitative Dimensions Organized by Stoichiometries and Abundances. *Cell*, *163*(3), 712–723.

Hellen, C. U. T., & Sarnow, P. (2001). Internal ribosome entry sites in eukaryotic mRNA molecules. *Genes & Development*, *15*(13), 1593–1612.

Hilliker, A. (2014). mRNA Localization and Localized Translation. In *Molecular Life Sciences* (pp. 1–3). New York, NY: Springer New York.

Hilliker, S., & Botstein, D. (1976). Specificity of genetic elements controlling regulation of early functions in temperate bacteriophages. *Journal of Molecular Biology*, *106*(3), 537–566.

Hinnebusch, A. G. (2014). The Scanning Mechanism of Eukaryotic Translation Initiation. *Annu. Rev. Biochem*, *83*, 779–812.

Hocine, S., Raymond, P., Zenklusen, D., Chao, J. A., & Singer, R. H. (2013). Single-molecule analysis of gene expression using two-color RNA labeling in live yeast. *Nature Methods*, *10*(2), 119–121.

Hönig, A., Auboeuf, D., Parker, M. M., O'Malley, B. W., & Berget, S. M. (2002). Regulation of alternative splicing by the ATP-dependent DEAD-box RNA helicase p72. *Molecular and Cellular Biology*, *22*(16), 5698–5707.

Hosoda, N., Kobayashi, T., Uchida, N., Funakoshi, Y., Kikuchi, Y., Hoshino, S., & Katada, T. (2003). Translation Termination Factor eRF3 Mediates mRNA Decay through the Regulation of Deadenylation. *Journal of Biological Chemistry*, *278*(40), 38287–38291.

House, A. E., & Lynch, K. W. (2008). Regulation of Alternative Splicing: More than Just the ABCs. *Journal of Biological Chemistry, 283*(3), 1217-21.

Houseley, J., & Tollervey, D. (2009). The Many Pathways of RNA Degradation. *Cell*, *136*(4), 763–776.

Hsu, J.-L., & Chen, S.-H. (2016). Stable isotope dimethyl labelling for quantitative proteomics and beyond. *Philosophical Transactions. Series A, Mathematical, Physical, and Engineering Sciences*, *374*(2079).

Hsu, J.-L., Huang, S.-Y., Chow, N.-H., & Chen, S.-H. (2003). Stable-Isotope Dimethyl Labeling for Quantitative Proteomics. *Analytical Chemistry*, *75*(24), 6843–6852.

Hu, W., Sweet, T. J., Chamnongpol, S., Baker, K. E., & Coller, J. (2009). Co-translational mRNA decay in Saccharomyces cerevisiae. *Nature*, *461*(7261), 225–229.

Huang, D. W., Sherman, B. T., & Lempicki, R. A. (2009a). Bioinformatics enrichment tools: paths toward the comprehensive functional analysis of large gene lists. *Nucleic Acids Research*, *37*(1), 1–13.

Huang, D. W., Sherman, B. T., & Lempicki, R. A. (2009b). Systematic and integrative analysis of large gene lists using DAVID bioinformatics resources. *Nature Protocols*, *4*(1), 44–57.

Hubner, N. C., Bird, A. W., Cox, J., Splettstoesser, B., Bandilla, P., Poser, I., … Mann, M. (2010). Quantitative proteomics combined with BAC TransgeneOmics reveals in vivo protein interactions. *The Journal of Cell Biology*, *189*(4), 739–754.

Hubstenberger, A., Courel, M., Bénard, M., Souquere, S., Ernoult-Lange, M., Chouaib, R., … Weil, D. (2017). P-Body Purification Reveals the Condensation of Repressed mRNA Regulons. *Molecular Cell*, *68*(1), 144–157.e5.

Huntzinger, E., Kashima, I., Fauser, M., Sauliere, J., & Izaurralde, E. (2008). SMG6 is the catalytic endonuclease that cleaves mRNAs containing nonsense codons in metazoan. *RNA*, *14*(12), 2609–2617.

Huntzinger, E., Kuzuoglu-Öztürk, D., Braun, J. E., Eulalio, A., Wohlbold, L., & Izaurralde, E. (2013). The interactions of GW182 proteins with PABP and deadenylases are required for both translational repression and degradation of miRNA targets. *Nucleic Acids Research*, *41*(2), 978–994.

Hurd, T. R., Herrmann, B., Sauerwald, J., Sanny, J., Grosch, M., & Lehmann, R. (2016). Long Oskar Controls Mitochondrial Inheritance in Drosophila melanogaster. *Developmental Cell*, *39*(5), 560–571.

Hutvágner, G., & Zamore, P. D. (2002). A microRNA in a multiple-turnover RNAi enzyme complex. *Science*, *297*(5589), 2056–2060.

Huynh, J.-R., Munro, T. P., Smith-Litière, K., Lepesant, J.-A., & Johnston, D. S. (2004). The Drosophila hnRNPA/B Homolog, Hrp48, Is Specifically Required for a Distinct Step in osk mRNA Localization. *Developmental Cell*, *6*(5), 625–635.

Igreja, C., & Izaurralde, E. (2011). CUP promotes deadenylation and inhibits decapping of mRNA targets. *Genes & Development*, *25*(18), 1955–1967.

Iioka, H., Loiselle, D., Haystead, T. A., & Macara, I. G. (2011). Efficient detection of RNA-protein interactions using tethered RNAs. *Nucleic Acids Research*, *39*(8), e53.

Irion, U., Adams, J., Chang, C.-W., & St Johnston, D. (2006). Miranda couples oskar mRNA/Staufen complexes to the bicoid mRNA localization pathway. *Developmental Biology*, *297*(2), 522–533.

Iwakawa, H.-O., & Tomari, Y. (2015). The Functions of MicroRNAs: mRNA Decay and Translational Repression. *Trends in Cell Biology*, *25*, 651–665.

Jackson, R. J., Hellen, C. U. T., & Pestova, T. V. (2010). The mechanism of eukaryotic translation initiation and principles of its regulation. *Nature Reviews Molecular Cell Biology*, *11*(2), 113–127.

Jain, R. A., & Gavis, E. R. (2008). The Drosophila hnRNP M homolog Rumpelstiltskin regulates nanos mRNA localization. *Development*, *135*(5), 973–982.

Jamar, N. H., Kritsiligkou, P., & Grant, C. M. (2018). Loss of mRNA surveillance pathways results in widespread protein aggregation. *Scientific Reports*, *8*(1), 3894.

Jambor, H., Brunel, C., & Ephrussi, A. (2011). Dimerization of oskar 3' UTRs promotes hitchhiking for RNA localization in the Drosophila oocyte. *RNA*, *17*(12), 2049–2057.

Jambor, H., Surendranath, V., Kalinka, A. T., Mejstrik, P., Saalfeld, S., & Tomancak, P. (2015). Systematic imaging reveals features and changing localization of mRNAs in Drosophila development. *ELife*, *4*.

Jang, S. K., Krausslich, H.-G., Nicklin, M. J. H., Duke, G. M., Palmenberg, A. C., & Wimmer, E. (1988). A segment of the 5' nontranslated region of encephalomyocarditis virus RNA directs internal entry of ribosomes during in vitro translation. *Journal of Virology*, *62*(8), 2636–2643.

Jankowsky, E., & Harris, M. E. (2015). Specificity and non-specificity in RNA–protein interactions. *Nature Reviews. Molecular Cell Biology*, *16*(9), 533-544.

Jansen, R.-P., & Niessing, D. (2012). Assembly of mRNA-protein complexes for directional mRNA transport in eukaryotes--an overview. *Current Protein & Peptide Science*, *13*(4), 284–293.

Januschke, J., Gervais, L., Gillet, L., Keryer, G., Bornens, M., & Guichet, A. (2006). The centrosome-nucleus complex and microtubule organization in the Drosophila oocyte. *Development*, *133*(1), 129–139.

Jaramillo, A. M., Weil, T. T., Goodhouse, J., Gavis, E. R., & Schupbach, T. (2008). The dynamics of fluorescently labeled endogenous gurken mRNA in Drosophila. *Journal of Cell Science*, *121*(6), 887–894.

Jeffery, W. R., Tomlinson, C. R., & Brodeur, R. D. (1983). Localization of actin messenger RNA during early ascidian development. *Developmental Biology*, *99*(2), 408–417.

Jenkins, V. K., Timmons, A. K., & McCall, K. (2013). Diversity of cell death pathways: insight from the fly ovary. *Trends in Cell Biology*, *23*(11), 567–574.

Jennings, B. H. (2011). Drosophila – a versatile model in biology & medicine. *Materials Today*, *14*(5), 190–195.

Jenny, A., Hachet, O., Závorszky, P., Cyrklaff, A., Weston, M. D. J., Johnston, D. S., … Ephrussi, A. (2006). A translation-independent role of oskar RNA in early Drosophila oogenesis. *Development (Cambridge, England)*, *133*(15), 2827–2833.

Jeske, M., Bordi, M., Glatt, S., Müller, S., Rybin, V., Müller, C. W., & Ephrussi, A. (2015). The Crystal Structure of the Drosophila Germline Inducer Oskar Identifies Two Domains with Distinct Vasa Helicase- and RNA-Binding Activities. *Cell Reports*, *12*(4), 587–598.

Jeske, M., Meyer, S., Temme, C., Freudenreich, D., & Wahle, E. (2006). Rapid ATP-dependent Deadenylation of *nanos* mRNA in a Cell-free System from *Drosophila* Embryos. *Journal of Biological Chemistry*, *281*(35), 25124–25133.

Jeske, M., Moritz, B., Anders, A., & Wahle, E. (2011). Smaug assembles an ATP-dependent stable complex repressing nanos mRNA translation at multiple levels. *The EMBO Journal*, *30*(1), 90–103.

Johansson, H. E., Liljas, L., & Uhlenbeck, O. C. (1997). RNA Recognition by the MS2 Phage Coat Protein. *Seminars in Virology*, *8*(3), 176–185.

Johnstone, O., & Lasko, P. (2001). Translational Regulation and RNA Localization in *Drosophila* Oocytes and Embryos. *Annual Review of Genetics*, *35*(1), 365–406.

Johnstone, O., & Lasko, P. (2004). Interaction with eIF5B is essential for Vasa function during development. *Development (Cambridge, England)*, *131*(17), 4167–4178.

Johnstone, O., Deuring, R., Bock, R., Linder, P., Fuller, M. T., & Lasko, P. (2005). Belle is a Drosophila DEAD-box protein required for viability and in the germ line. *Developmental Biology*, *277*(1), 92–101.

Jolles, B., Aliouat, A., Stierlé, V., Salhi, S., Jean-Jean, O., Jolles, B., … Jean-Jean, O. (2018). Translation termination-dependent deadenylation of MYC mRNA in human cells. *Oncotarget*, *9*(40), 26171–26182.

Jonas, S., & Izaurralde, E. (2015). Towards a molecular understanding of microRNA-mediated gene silencing. *Nature Reviews Genetics*, *16*(7), 421–433.

Jung, H., Yoon, B. C., & Holt, C. E. (2012). Axonal mRNA localization and local protein synthesis in nervous system assembly, maintenance and repair. *Nature Reviews. Neuroscience*, *13*(5), 308–324.

Jurica, M. S., Licklider, L. J., Gygi, S. R., Grigorieff, N., & Moore, M. J. (2002). Purification and characterization of native spliceosomes suitable for three-dimensional structural analysis. *RNA (New York, N.Y.)*, *8*(4), 426–439.

Kalifa, Y., Armenti, S. T., & Gavis, E. R. (2009). Glorund interactions in the regulation of gurken and oskar mRNAs. *Developmental Biology*, *326*(1), 68–74.

Kalifa, Y., Huang, T., Rosen, L. N., Chatterjee, S., & Gavis, E. R. (2006). Glorund, a Drosophila hnRNP F/H homolog, is an ovarian repressor of nanos translation. *Developmental Cell*, *10*(3), 291–301.

Kannaiah, S., & Amster-Choder, O. (2014). Protein targeting via mRNA in bacteria. *Biochimica et Biophysica Acta (BBA) - Molecular Cell Research*, *1843*(8), 1457–1465.

Karijolich, J., Kantartzis, A., & Yu, Y.-T. (2010). RNA modifications: a mechanism that modulates gene expression. *Methods in Molecular Biology (Clifton, N.J.)*, *629*, 1–19.

Katahira, J. (2015). Nuclear Export of Messenger RNA. *Genes*, *6*(2), 163–184.

Kaygun, H., & Marzluff, W. F. (2005). Regulated degradation of replication-dependent histone mRNAs requires both ATR and Upf1. *Nature Structural & Molecular Biology*, *12*(9), 794–800.

Kedersha, N., Stoecklin, G., Ayodele, M., Yacono, P., Lykke-Andersen, J., Fritzler, M. J., … Anderson, P. (2005). Stress granules and processing bodies are dynamically linked sites of mRNP remodeling. *The Journal of Cell Biology*, *169*(6), 871–884.

Keene, J. D., Komisarow, J. M., & Friedersdorf, M. B. (2006). RIP-Chip: the isolation and identification of mRNAs, microRNAs and protein components of ribonucleoprotein complexes from cell extracts. *Nature Protocols*, *1*(1), 302–307.

Kerényi, Z., Mérai, Z., Hiripi, L., Benkovics, A., Gyula, P., Lacomme, C., … Silhavy, D. (2008). Inter-kingdom conservation of mechanism of nonsense-mediated mRNA decay. *The EMBO Journal*, *27*(11), 1585–1595.

Kervestin, S., & Jacobson, A. (2012). NMD: a multifaceted response to premature translational termination. *Nature Reviews. Molecular Cell Biology*, *13*(11), 700–712.

Keryer-Bibens, C., Barreau, C., & Osborne, H. B. (2008). Tethering of proteins to RNAs by bacteriophage proteins. *Biology of the Cell*, *100*(2), 125–138.

Kieft, J. S., & Batey, R. T. (2004). A general method for rapid and nondenaturing purification of RNAs. *RNA (New York, N.Y.)*, *10*(6), 988–995.

Kim, Y. K., Furic, L., DesGroseillers, L., & Maquat, L. E. (2005). Mammalian Staufen1 Recruits Upf1 to Specific mRNA 3′UTRs so as to Elicit mRNA Decay. *Cell*, *120*(2), 195–208.

Kim-Ha, J., Kerr, K., & Macdonald, P. M. (1995). Translational regulation of oskar mRNA by bruno, an ovarian RNA-binding protein, is essential. *Cell*, *81*(3), 403–412.

Kim-Ha, J., Smith, J. L., & Macdonald, P. M. (1991). oskar mRNA is localized to the posterior pole of the Drosophila oocyte. *Cell*, *66*(1), 23–35.

Kim-Ha, J., Webster, P. J., Smith, J. L., & Macdonald, P. M. (1993). Multiple RNA regulatory elements mediate distinct steps in localization of oskar mRNA. *Development (Cambridge, England)*, *119*(1), 169–178.

King, M. Lou, Messitt, T. J., & Mowry, K. L. (2005). Putting RNAs in the right place at the right time: RNA localization in the frog oocyte. *Biology of the Cell*, *97*(1), 19–33.

Kistler, K. E., Trcek, T., Hurd, T. R., Chen, R., Liang, F.-X., Sall, J., … Lehmann, R. (2018). Phase transitioned nuclear Oskar promotes cell division of Drosophila primordial germ cells. *ELife*, *7*.

Kloc, M., Chan, A. P., Etkin, L. D., & Bilinski, S. (2001). Mitochondrial ribosomal RNA in the germinal granules in Xenopus embryos revisited. *Differentiation*, *67*(3), 80–83.

Kloosterman, W. P., Wienholds, E., Ketting, R. F., & Plasterk, R. H. A. (2004). Substrate requirements for let-7 function in the developing zebrafish embryo. *Nucleic Acids Research*, *32*(21), 6284–6291.

Komar, A. A., & Hatzoglou, M. (2005). Internal Ribosome Entry Sites in Cellular mRNAs: Mystery of Their Existence. *Journal of Biological Chemistry*, *280*(25), 23425–23428.

Konig, J., Zarnack, K., Rot, G., Curk, T., Kayikci, M., Zupan, B., … Ule, J. (2011). iCLIP - Transcriptome-wide Mapping of Protein-RNA Interactions with Individual Nucleotide Resolution. *Journal of Visualized Experiments*, 50, e2638.

Krainer, A. R., Conway, G. C., & Kozak, D. (1990). The essential pre-mRNA splicing factor SF2 influences 5' splice site selection by activating proximal sites. *Cell*, *62*(1), 35–42.

Kugler, J.-M., & Lasko, P. (2009). Localization, anchoring and translational control of oskar, gurken, bicoid and nanos mRNA during Drosophila oogenesis. *Fly*, *3*(1), 15–28.

Kugler, J.-M., Chicoine, J., & Lasko, P. (2009). Bicaudal-C associates with a Trailer Hitch/Me31B complex and is required for efficient Gurken secretion. *Developmental Biology*, *328*(1), 160–172.

Kugler, J.-M., Woo, J.-S., Oh, B.-H., & Lasko, P. (2010). Regulation of Drosophila Vasa In Vivo through Paralogous Cullin-RING E3 Ligase Specificity Receptors. *Molecular and Cellular Biology*, *30*(7), 1769–1782.

Kulkarni, M., Ozgur, S., & Stoecklin, G. (2010). On track with P-bodies. *Biochemical Society Transactions*, *38*(1), 242–251.

Łabno, A., Tomecki, R., & Dziembowski, A. (2016). Cytoplasmic RNA decay pathways - Enzymes and mechanisms. *Biochimica et Biophysica Acta (BBA) - Molecular Cell Research*, *1863*(12), 3125–3147.

Lange, S., Katayama, Y., Schmid, M., Burkacky, O., Bruchle, C., Lamb, D. C., & Jansen, R.-P. (2008). Simultaneous Transport of Different Localized mRNA Species Revealed by Live-Cell Imaging. *Traffic*, *9*(8), 1256–1267.

Lareau, L. F., Brooks, A. N., Soergel, D. A. W., Meng, Q., & Brenner, S. E. (2007a). The coupling of alternative splicing and nonsense-mediated mRNA decay. *Advances in Experimental Medicine and Biology*, *623*, 190–211.

Lareau, L. F., Inada, M., Green, R. E., Wengrod, J. C., & Brenner, S. E. (2007b). Unproductive splicing of SR genes associated with highly conserved and ultraconserved DNA elements. *Nature*, *446*(7138), 926–929.

Lasko, P. (2012). mRNA localization and translational control in Drosophila oogenesis. *Cold Spring Harbor Perspectives in Biology*, *4*(10), a012294.

Lasko, P. (2013). The DEAD-box helicase Vasa: Evidence for a multiplicity of functions in RNA processes and developmental biology. *Biochimica et Biophysica Acta (BBA) - Gene Regulatory Mechanisms*, *1829*(8), 810–816.

Lasko, P. F., & Ashburner, M. (1988). The product of the Drosophila gene vasa is very similar to eukaryotic initiation factor-4A. *Nature*, *335*(6191), 611–617.

Lasko, P. F., & Ashburner, M. (1990). Posterior localization of vasa protein correlates with, but is not sufficient for, pole cell development. *Genes & Development*, *4*(6), 905–921.

Le Hir, H., Gatfield, D., Izaurralde, E., & Moore, M. J. (2001). The exon-exon junction complex provides a binding platform for factors involved in mRNA export and nonsense-mediated mRNA decay. *The EMBO Journal*, *20*(17), 4987–4997.

Le Hir, H., Izaurralde, E., Maquat, L. E., & Moore, M. J. (2000). The spliceosome deposits multiple proteins 20-24 nucleotides upstream of mRNA exon-exon junctions. *The EMBO Journal*, *19*(24), 6860–6869.

LeBlanc, J. J., & Beemon, K. L. (2004). Unspliced Rous sarcoma virus genomic RNAs are translated and subjected to nonsense-mediated mRNA decay before packaging. *Journal of Virology*, *78*(10), 5139–5146.

Lécuyer, E., Parthasarathy, N., & Krause, H. M. (2008). Fluorescent In Situ Hybridization Protocols in Drosophila Embryos and Tissues. *Methods in Molecular Biology*, vol 420, 289-302. Humana Press.

Lécuyer, E., Yoshida, H., Parthasarathy, N., Alm, C., Babak, T., Cerovina, T., … Krause, H. M. (2007). Global Analysis of mRNA Localization Reveals a Prominent Role in Organizing Cellular Architecture and Function. *Cell*, *131*(1), 174–187.

LeCuyer, K. A., Behlen, L. S., & Uhlenbeck, O. C. (1995). Mutants of the Bacteriophage MS2 Coat Protein That Alter Its Cooperative Binding to RNA. *Biochemistry*, *34*(33), 10600–10606.

Lee, H. Y., Haurwitz, R. E., Apffel, A., Zhou, K., Smart, B., Wenger, C. D., … Doudna, J. A. (2013). RNA-protein analysis using a conditional CRISPR nuclease. *Proceedings of the National Academy of Sciences*, *110*(14), 5416–5421.

Lee, Y., & Rio, D. C. (2015). Mechanisms and Regulation of Alternative Pre-mRNA Splicing. *Annual Review of Biochemistry*, *84*, 291–323.

LeGendre, J. B., Campbell, Z. T., Kroll-Conner, P., Anderson, P., Kimble, J., & Wickens, M. (2013). RNA targets and specificity of Staufen, a double-stranded RNA-binding protein in Caenorhabditis elegans. *The Journal of Biological Chemistry*, *288*(4), 2532–2545.

Lehmann, R., & Nüsslein-Volhard, C. (1986). Abdominal segmentation, pole cell formation, and embryonic polarity require the localized activity of oskar, a maternal gene in Drosophila. *Cell*, *47*(1), 141–152.

Lehmann, R., & Nüsslein-Volhard, C. (1987). Involvement of the pumilio gene in the transport of an abdominal signal in the Drosophila embryo. *Nature*, *329*(6135), 167–170.

Lehmann, R., & Nusslein-Volhard, C. (1991). The maternal gene nanos has a central role in posterior pattern formation of the Drosophila embryo. *Development*, *112*(3).

Lejeune, F., Ishigaki, Y., Li, X., Maquat, L. E., Pouysségur, J., & Bensaude, O. (2002). The exon junction complex is detected on CBP80-bound but not eIF4E-bound mRNA in mammalian cells: dynamics of mRNP remodeling. *The EMBO Journal*, *21*(13), 3536–3545.

Lejeune, F., Li, X., & Maquat, L. E. (2003). Nonsense-mediated mRNA decay in mammalian cells involves decapping, deadenylating, and exonucleolytic activities. *Molecular Cell*, *12*(3), 675–687.

Lemaire, R., Prasad, J., Kashima, T., Gustafson, J., Manley, J. L., & Lafyatis, R. (2002). Stability of a PKCI-1-related mRNA is controlled by the splicing factor ASF/SF2: a novel function for SR proteins. *Genes & Development*, *16*(5), 594–607.

Lemieux, C., Marguerat, S., Lafontaine, J., Barbezier, N., Bähler, J., & Bachand, F. (2011). A Pre-mRNA degradation pathway that selectively targets intron-containing genes requires the nuclear poly(A)-binding protein. *Molecular Cell*, *44*(1), 108–119.

Leppek, K., & Stoecklin, G. (2014). An optimized streptavidin-binding RNA aptamer for purification of ribonucleoprotein complexes identifies novel ARE-binding proteins. *Nucleic Acids Research*, *42*(2), e13.

Leppek, K., Schott, J., Reitter, S., Poetz, F., Hammond, M. C., & Stoecklin, G. (2013). Roquin Promotes Constitutive mRNA Decay via a Conserved Class of Stem-Loop Recognition Motifs. *Cell*, *153*(4), 869–881.

Lev Maor, G., Yearim, A., & Ast, G. (2015). The alternative role of DNA methylation in splicing regulation. *Trends in Genetics*, *31*(5), 274–280.

Lewis, B. P., Burge, C. B., & Bartel, D. P. (2005). Conserved Seed Pairing, Often Flanked by Adenosines, Indicates that Thousands of Human Genes are MicroRNA Targets. *Cell*, *120*(1), 15–20.

Li, H., Han, J., Pan, J., Liu, T., Parker, C. E., & Borchers, C. H. (2017). Current trends in quantitative proteomics - an update. *Journal of Mass Spectrometry*, *52*(5), 319–341.

Li, J., Steen, H., & Gygi, S. P. (2003). Protein Profiling with Cleavable Isotope-coded Affinity Tag (cICAT) Reagents. *Molecular & Cellular Proteomics*, *2*(11), 1198–1204.

Li, S., & Mason, C. E. (2014). The Pivotal Regulatory Landscape of RNA Modifications. *Annual Review of Genomics and Human Genetics*, *15*(1), 127–150.

Li, Z., Adams, R. M., Chourey, K., Hurst, G. B., Hettich, R. L., & Pan, C. (2012). Systematic Comparison of Label-Free, Metabolic Labeling, and Isobaric Chemical Labeling for Quantitative Proteomics on LTQ Orbitrap Velos. *Journal of Proteome Research*, *11*(3), 1582–1590.

Liang, L., Diehl-Jones, W., & Lasko, P. (1994). Localization of vasa protein to the Drosophila pole plasm is independent of its RNA-binding and helicase activities. *Development*, *120*(5), 1201–1211.

Liao, G., Mingle, L., Van De Water, L., & Liu, G. (2015). Control of cell migration through mRNA localization and local translation. *Wiley Interdisciplinary Reviews. RNA*, *6*(1), 1–15.

Licatalosi, D. D., Mele, A., Fak, J. J., Ule, J., Kayikci, M., Chi, S. W., … Darnell, R. B. (2008). HITS-CLIP yields genome-wide insights into brain alternative RNA processing. *Nature*, *456*(7221), 464–469.

Lim, A. K., & Kai, T. (2007). Unique germ-line organelle, nuage, functions to repress selfish genetic elements in Drosophila melanogaster. *Proceedings of the National Academy of Sciences*, *104*(16), 6714–6719.

Lim, F., & Peabody, D. S. (1994). Mutations that increase the affinity of a translational repressor for RNA. *Nucleic Acids Research*, *22*(18), 3748–3752.

Lim, F., Downey, T. P., & Peabody, D. S. (2001). Translational repression and specific RNA binding by the coat protein of the Pseudomonas phage PP7. *The Journal of Biological Chemistry*, *276*(25), 22507–22513.

Lim, F., Spingola, M., & Peabody, D. S. (1996). The RNA-binding site of bacteriophage Qbeta coat protein. *The Journal of Biological Chemistry*, *271*(50), 31839–31845.

Lin, A. C., & Holt, C. E. (2007). Local translation and directional steering in axons. *The EMBO Journal*, *26*(16), 3729–3736.

Ling, S. H. M., Qamra, R., & Song, H. (2011). Structural and functional insights into eukaryotic mRNA decapping. *Wiley Interdisciplinary Reviews: RNA*, *2*(2), 193–208.

Lingner, J., & Cech, T. R. (1996). Purification of telomerase from Euplotes aediculatus: requirement of a primer 3' overhang. *Proceedings of the National Academy of Sciences of the United States of America*, *93*(20), 10712–10717.

Liu, N., Dansereau, D. A., & Lasko, P. (2003). Fat facets interacts with vasa in the Drosophila pole plasm and protects it from degradation. *Current Biology*, *13*(21), 1905–1909.

Loh, B., Jonas, S., & Izaurralde, E. (2013). The SMG5-SMG7 heterodimer directly recruits the CCR4-NOT deadenylase complex to mRNAs containing nonsense codons via interaction with POP2. *Genes & Development*, *27*(19), 2125–2138.

Long, R. M., Singer, R. H., Meng, X., Gonzalez, I., Nasmyth, K., & Jansen, R. P. (1997). Mating type switching in yeast controlled by asymmetric localization of ASH1 mRNA. *Science (New York, N.Y.)*, *277*(5324), 383–387.

Longman, D., Plasterk, R. H. A., Johnstone, I. L., & Caceres, J. F. (2007). Mechanistic insights and identification of two novel factors in the C. elegans NMD pathway. *Genes & Development*, *21*(9), 1075–1085.

Lovett, S. T. (2004). Encoded errors: mutations and rearrangements mediated by misalignment at repetitive DNA sequences. *Molecular Microbiology*, *52*(5), 1243–1253.

Lowary, P. T., & Uhlenbeck, O. C. (1987). An RNA mutation that increases the affinity of an RNA-protein interaction. *Nucleic Acids Research*, *15*(24), 10483–10493.

Lowe, N., Rees, J. S., Roote, J., Ryder, E., Armean, I. M., Johnson, G., … St Johnston, D. (2014). Analysis of the expression patterns, subcellular localisations and interaction partners of Drosophila proteins using a pigP protein trap library. *Development*, *141*(20), 3994–4005.

Luco, R. F., & Misteli, T. (2011). More than a splicing code: integrating the role of RNA, chromatin and non-coding RNA in alternative splicing regulation. *Current Opinion in Genetics & Development*, *21*(4), 366–372.

Lunde, B. M., Moore, C., & Varani, G. (2007). RNA-binding proteins: modular design for efficient function. *Nature Reviews Molecular Cell Biology, 8*(6), 479-490

Lykke-Andersen, J., Shu, M. D., & Steitz, J. A. (2000). Human Upf proteins target an mRNA for nonsense-mediated decay when bound downstream of a termination codon. *Cell*, *103*(7), 1121–1131.

Lykke-Andersen, S., & Jensen, T. H. (2015). Nonsense-mediated mRNA decay: an intricate machinery that shapes transcriptomes. *Nature Reviews Molecular Cell Biology*, *16*(11), 665–677.

Lytle, J. R., Yario, T. A., & Steitz, J. A. (2007). Target mRNAs are repressed as efficiently by microRNA-binding sites in the 5' UTR as in the 3' UTR. *Proceedings of the National Academy of Sciences*, *104*(23), 9667–9672.

Macdonald, P. M., & Kerr, K. (1997). Redundant RNA recognition events in bicoid mRNA localization. *RNA (New York, N.Y.)*, *3*(12), 1413–1420.

Macdonald, P. M., & Kerr, K. (1998). Mutational analysis of an RNA recognition element that mediates localization of bicoid mRNA. *Molecular and Cellular Biology*, *18*(7), 3788–3795.

MacDougall, N., Clark, A., MacDougall, E., & Davis, I. (2003). Drosophila gurken (TGFalpha) mRNA localizes as particles that move within the oocyte in two dynein-dependent steps. *Developmental Cell*, *4*(3), 307–319.

Mach, J. M., & Lehmann, R. (1997). An Egalitarian-BicaudalD complex is essential for oocyte specification and axis determination in Drosophila. *Genes & Development*, *11*(4), 423–435.

Mader, S., Lee, H., Pause, A., & Sonenberg, N. (1995). The translation initiation factor eIF-4E binds to a common motif shared by the translation factor eIF-4 gamma and the translational repressors 4E-binding proteins. *Molecular and Cellular Biology*, *15*(9), 4990–4997.

Mahowald, A. P. (2001). Assembly of the Drosophila germ plasm. *International Review of Cytology*, *203*, 187–213.

Makino, S., Mishima, Y., Inoue, K., & Inada, T. (2015). Roles of mRNA Fate Modulators Dhh1 and Pat1 in TNRC6-dependent Gene Silencing Recapitulated in Yeast. *Journal of Biological Chemistry, 290*(13), 8331-47.

Malone, C. D., Brennecke, J., Dus, M., Stark, A., McCombie, W. R., Sachidanandam, R., & Hannon, G. J. (2009). Specialized piRNA Pathways Act in Germline and Somatic Tissues of the Drosophila Ovary. *Cell*, *137*(3), 522–535.

Malone, C. D., Mestdagh, C., Akhtar, J., Kreim, N., Deinhard, P., Sachidanandam, R., … Roignant, J.-Y. (2014). The exon junction complex controls transposable element activity by ensuring faithful splicing of the *piwi* transcript. *Genes & Development*, *28*(16), 1786–1799.

Maniatis, T., & Reed, R. (2002). An extensive network of coupling among gene expression machines. *Nature*, *416*(6880), 499–506.

Manseau, L. J., & Schüpbach, T. (1989). Cappuccino and spire: two unique maternal-effect loci required for both the anteroposterior and dorsoventral patterns of the Drosophila embryo. *Genes & Development*, *3*(9), 1437–1452.

Marcotrigiano, J., Gingras, A. C., Sonenberg, N., & Burley, S. K. (1999). Cap-dependent translation initiation in eukaryotes is regulated by a molecular mimic of eIF4G. *Molecular Cell*, *3*(6), 707–716.

Marissen, W. E., Triyoso, D., Younan, P., & Lloyd, R. E. (2004). Degradation of poly(A)-binding protein in apoptotic cells and linkage to translation regulation. *Apoptosis*, *9*(1), 67–75.

Markussen, F. H., Michon, A. M., Breitwieser, W., & Ephrussi, A. (1995). Translational control of oskar generates short OSK, the isoform that induces pole plasma assembly. *Development (Cambridge, England)*, *121*(11), 3723–3732.

Martin, K. C., & Ephrussi, A. (2009). mRNA localization: gene expression in the spatial dimension. *Cell*, *136*(4), 719–730.

Mathews, M., Sonenberg, N., & Hershey, J. W. B. (2007). *Translational control in biology and medicine*. Cold Spring Harbor Laboratory Press.

Matsuda, D., Hosoda, N., Kim, Y. K., & Maquat, L. E. (2007). Failsafe nonsense-mediated mRNA decay does not detectably target eIF4E-bound mRNA. *Nature Structural & Molecular Biology*, *14*(10), 974–979.

Mauro, V. P., & Edelman, G. M. (2007). The Ribosome Filter Redux. *Cell Cycle*, *6*(18), 2246–2251.

Mauro, V. P., & Matsuda, D. (2016). Translation regulation by ribosomes: Increased complexity and expanded scope. *RNA Biology*, *13*(9), 748–755.

McDermott, S. M., Meignin, C., Rappsilber, J., & Davis, I. (2012). Drosophila Syncrip binds the gurken mRNA localisation signal and regulates localised transcripts during axis specification. *Biology Open*, *1*(5), 488–497.

McManus, C. J., & Graveley, B. R. (2011). RNA structure and the mechanisms of alternative splicing. *Current Opinion in Genetics & Development*, *21*(4), 373–379.

Meissner, F., & Mann, M. (2014). Quantitative shotgun proteomics: considerations for a high-quality workflow in immunology. *Nature Immunology*, *15*(2), 112–117.

Mellacheruvu, D., Wright, Z., Couzens, A. L., Lambert, J.-P., St-Denis, N. A., Li, T., … Nesvizhskii, A. I. (2013). The CRAPome: a contaminant repository for affinity purification–mass spectrometry data. *Nature Methods*, *10*(8), 730–736.

Mendez, R., & Richter, J. D. (2001). Translational control by CPEB: a means to the end. *Nature Reviews Molecular Cell Biology*, *2*(7), 521–529.

Metze, S., Herzog, V. A., Ruepp, M.-D., & Mühlemann, O. (2013). Comparison of EJC-enhanced and EJC-independent NMD in human cells reveals two partially redundant degradation pathways. *RNA (New York, N.Y.)*, *19*(10), 1432–1448.

Meyer, K. D., Patil, D. P., Zhou, J., Zinoviev, A., Skabkin, M. A., Elemento, O., … Jaffrey, S. R. (2015). 5′ UTR m6A Promotes Cap-Independent Translation. *Cell*, *163*(4), 999–1010.

Mhlanga, M. M., Bratu, D. P., Genovesio, A., Rybarska, A., Chenouard, N., Nehrbass, U., & Olivo-Marin, J.-C. (2009). In Vivo Colocalisation of oskar mRNA and Trans-Acting Proteins Revealed by Quantitative Imaging of the Drosophila Oocyte. *PLoS ONE*, *4*(7), e6241.

Micklem, D. R., Adams, J., Grünert, S., & St Johnston, D. (2000). Distinct roles of two conserved Staufen domains in oskar mRNA localization and translation. *The EMBO Journal*, *19*(6), 1366–1377.

Mili, S., Moissoglu, K., & Macara, I. G. (2008). Genome-wide screen reveals APC-associated RNAs enriched in cell protrusions. *Nature*, *453*(7191), 115–119.

Mingle, L. A., Okuhama, N. N., Shi, J., Singer, R. H., Condeelis, J., & Liu, G. (2005). Localization of all seven messenger RNAs for the actin-polymerization nucleator Arp2/3 complex in the protrusions of fibroblasts. *Journal of Cell Science*, *118*(Pt 11), 2425–2433.

Mishima, Y., Fukao, A., Kishimoto, T., Sakamoto, H., Fujiwara, T., & Inoue, K. (2012). Translational inhibition by deadenylation-independent mechanisms is central to microRNA-mediated silencing in zebrafish. *Proceedings of the National Academy of Sciences of the United States of America*, *109*(4), 1104–1109.

Mishima, Y., Giraldez, A. J., Takeda, Y., Fujiwara, T., Sakamoto, H., Schier, A. F., & Inoue, K. (2006). Differential Regulation of Germline mRNAs in Soma and Germ Cells by Zebrafish miR-430. *Current Biology*, *16*(21), 2135–2142.

Mitchell, P., & Tollervey, D. (2003). An NMD pathway in yeast involving accelerated deadenylation and exosome-mediated 3'-5' degradation. *Molecular Cell*, *11*(5), 1405–1413.

Moccia, R., Chen, D., Lyles, V., Kapuya, E., E, Y., Kalachikov, S., … Martin, K. C. (2003). An unbiased cDNA library prepared from isolated Aplysia sensory neuron processes is enriched for cytoskeletal and translational mRNAs. *The Journal of Neuroscience : The Official Journal of the Society for Neuroscience*, *23*(28), 9409–9417.

Molecular Cloning: A Laboratory Manual (Fourth edition) 2012 by Green, M.R. and Sambrook, J. Cold Spring Harbor Laboratory Press.

Montes, M., Becerra, S., Sánchez-Álvarez, M., & Suñé, C. (2012). Functional coupling of transcription and splicing. *Gene*, *501*(2), 104–117.

Morin, X., Daneman, R., Zavortink, M., & Chia, W. (2001). A protein trap strategy to detect GFP-tagged proteins expressed from their endogenous loci in Drosophila. *Proceedings of the National Academy of Sciences*, *98*(26), 15050–15055.

Morrison, M., Harris, K. S., & Roth, M. B. (1997). smg mutants affect the expression of alternatively spliced SR protein mRNAs in Caenorhabditis elegans. *Proceedings of the National Academy of Sciences of the United States of America*, *94*(18), 9782–9785.

Muench, D. G., Zhang, C., & Dahodwala, M. (2012). Control of cytoplasmic translation in plants. *Wiley Interdisciplinary Reviews: RNA*, *3*(2), 178–194.

Mühlemann, O. (2012). Intimate liaison with SR proteins brings exon junction complexes to unexpected places. *Nature Structural & Molecular Biology*, *19*(12), 1209–1211.

Muhlrad, D., & Parker, R. (1994). Premature translational termination triggers mRNA decapping. *Nature*, *370*(6490), 578–581.

Muhlrad, D., & Parker, R. (2005). The yeast EDC1 mRNA undergoes deadenylation-independent decapping stimulated by Not2p, Not4p, and Not5p. *The EMBO Journal*, *24*(5), 1033–1045.

Muhlrad, D., Decker, C. J., & Parker, R. (1994). Deadenylation of the unstable mRNA encoded by the yeast MFA2 gene leads to decapping followed by 5'-->3' digestion of the transcript. *Genes & Development*, *8*(7), 855–866.

Muslimov, I. A., Iacoangeli, A., Brosius, J., & Tiedge, H. (2006). Spatial codes in dendritic BC1 RNA. *The Journal of Cell Biology*, *175*(3), 427–439.

Muslimov, I. A., Patel, M. V, Rose, A., & Tiedge, H. (2011). Spatial code recognition in neuronal RNA targeting: role of RNA-hnRNP A2 interactions. *The Journal of Cell Biology*, *194*(3), 441–457.

Nagarkar-Jaiswal, S., DeLuca, S. Z., Lee, P.-T., Lin, W.-W., Pan, H., Zuo, Z., … Bellen, H. J. (2015). A genetic toolkit for tagging intronic MiMIC containing genes. *ELife*, *4*.

Nahnsen, S., Bielow, C., Reinert, K., & Kohlbacher, O. (2013). Tools for label-free peptide quantification. *Molecular & Cellular Proteomics*, *12*(3), 549–556.

Nakamura, A., Sato, K., & Hanyu-Nakamura, K. (2004). Drosophila cup is an eIF4E binding protein that associates with Bruno and regulates oskar mRNA translation in oogenesis. *Developmental Cell*, *6*(1), 69–78.

Nelson, M. R., Leidal, A. M., & Smibert, C. A. (2004). Drosophila Cup is an eIF4E-binding protein that functions in Smaug-mediated translational repression. *The EMBO Journal*, *23*(1), 150–159.

Ni, C.-Z., Syed, R., Kodandapani, R., Wickersham, J., Peabody, D. S., & Ely, K. R. (1995). Crystal structure of the MS2 coat protein dimer: implications for RNA binding and virus assembly. *Structure*, *3*(3), 255–263.

Nicholson, P., & Mühlemann, O. (2010). Cutting the nonsense: the degradation of PTC-containing mRNAs. *Biochemical Society Transactions*, *38*(6), 1615–1620.

Nicholson, P., Yepiskoposyan, H., Metze, S., Zamudio Orozco, R., Kleinschmidt, N., & Mühlemann, O. (2010). Nonsense-mediated mRNA decay in human cells: mechanistic insights, functions beyond quality control and the double-life of NMD factors. *Cellular and Molecular Life Sciences*, *67*(5), 677–700.

Nielsen, K. H., Chamieh, H., Andersen, C. B. F., Fredslund, F., Hamborg, K., Le Hir, H., & Andersen, G. R. (2009). Mechanism of ATP turnover inhibition in the EJC. *RNA (New York, N.Y.)*, *15*(1), 67–75.

Nishida, H., & Sawada, K. (2001). Macho-1 encodes a localized mRNA in ascidian eggs that specifies muscle fate during embryogenesis. *Nature*, *409*(6821), 724–729.

Nishihara, T., Zekri, L., Braun, J. E., & Izaurralde, E. (2013). miRISC recruits decapping factors to miRNA targets to enhance their degradation. *Nucleic Acids Research*, *41*(18), 8692–8705.

Norvell, A., Debec, A., Finch, D., Gibson, L., & Thoma, B. (2005). Squid is required for efficient posterior localization of oskar mRNA during Drosophila oogenesis. *Development Genes and Evolution*, *215*(7), 340–349.

Norvell, A., Kelley, R. L., Wehr, K., & Schüpbach, T. (1999). Specific isoforms of squid, a Drosophila hnRNP, perform distinct roles in Gurken localization during oogenesis. *Genes & Development*, *13*(7), 864–876.

Okada-Katsuhata, Y., Yamashita, A., Kutsuzawa, K., Izumi, N., Hirahara, F., & Ohno, S. (2012). N- and C-terminal Upf1 phosphorylations create binding platforms for SMG-6 and SMG-5:SMG-7 during NMD. *Nucleic Acids Research*, *40*(3), 1251–1266.

Okita, T. W., & Choi, S. B. (2002). mRNA localization in plants: targeting to the cell's cortical region and beyond. *Current Opinion in Plant Biology*, *5*(6), 553–559.

Oliveto, S., Mancino, M., Manfrini, N., & Biffo, S. (2017). Role of microRNAs in translation regulation and cancer. *World Journal of Biological Chemistry*, *8*(1), 45–56.

Ong, S.-E., Blagoev, B., Kratchmarova, I., Kristensen, D. B., Steen, H., Pandey, A., & Mann, M. (2002). Stable isotope labeling by amino acids in cell culture, SILAC, as a simple and accurate approach to expression proteomics. *Molecular & Cellular Proteomics : MCP*, *1*(5), 376–386.

Ottens, F., & Gehring, N. H. (2016). Physiological and pathophysiological role of nonsense-mediated mRNA decay. *Pflügers Archiv - European Journal of Physiology*, *468*(6), 1013–1028.

Ottone, C., Gigliotti, S., Giangrande, A., Graziani, F., & Verrotti di Pianella, A. (2012). The translational repressor Cup is required for germ cell development in Drosophila. *Journal of Cell Science*, *125*(13), 3114–3123.

Page, M. F., Carr, B., Anders, K. R., Grimson, A., & Anderson, P. (1999). SMG-2 is a phosphorylated protein required for mRNA surveillance in Caenorhabditis elegans and related to Upf1p of yeast. *Molecular and Cellular Biology*, *19*(9), 5943–5951.

Pal, M., Ishigaki, Y., Nagy, E., & Maquat, L. E. (2001). Evidence that phosphorylation of human Upfl protein varies with intracellular location and is mediated by a wortmannin-sensitive and rapamycin-sensitive PI 3-kinase-related kinase signaling pathway. *RNA (New York, N.Y.)*, *7*(1), 5–15.

Palacios, I. M., Gatfield, D., St Johnston, D., & Izaurralde, E. (2004). An eIF4AIII-containing complex required for mRNA localization and nonsense-mediated mRNA decay. *Nature*, *427*(6976), 753–757.

Palazzo, A. F., & Akef, A. (2012). Nuclear export as a key arbiter of "mRNA identity" in eukaryotes. *Biochimica et Biophysica Acta (BBA) - Gene Regulatory Mechanisms*, *1819*(6), 566–577.

Pane, A., Wehr, K., & Schüpbach, T. (2007). Zucchini and squash encode two putative nucleases required for rasiRNA production in the Drosophila germline. *Developmental Cell*, *12*(6), 851–862.

Paquin, N., & Chartrand, P. (2008). Local regulation of mRNA translation: new insights from the bud. *Trends in Cell Biology*, *18*(3), 105–111.

Park, J. W., Parisky, K., Celotto, A. M., Reenan, R. A., & Graveley, B. R. (2004). Identification of alternative splicing regulators by RNA interference in Drosophila. *Proceedings of the National Academy of Sciences*, *101*(45), 15974–15979.

Parker, R., & Sheth, U. (2007). P Bodies and the Control of mRNA Translation and Degradation. *Molecular Cell*, *25*(5), 635–646.

Patel, V. L., Mitra, S., Harris, R., Buxbaum, A. R., Lionnet, T., Brenowitz, M., … Chao, J. A. (2012). Spatial arrangement of an RNA zipcode identifies mRNAs under post-transcriptional control. *Genes & Development*, *26*(1), 43–53.

Patil, V. S., & Kai, T. (2010). Repression of Retroelements in Drosophila Germline via piRNA Pathway by the Tudor Domain Protein Tejas. *Current Biology*, *20*(8), 724–730.

Peabody, D. S. (1993). The RNA binding site of bacteriophage MS2 coat protein. *The EMBO Journal*, *12*(2), 595–600.

Pek, J. W., & Kai, T. (2011). A role for Vasa in regulating mitotic chromosome condensation in Drosophila. *Current Biology*, *21*(1), 39–44.

Pelletier, J., & Sonenberg, N. (1988). Internal initiation of translation of eukaryotic mRNA directed by a sequence derived from poliovirus RNA. *Nature*, *334*(6180), 320–325.

Peña, E., Heinlein, M., & Sambade, A. (2015). In Vivo RNA Labeling Using MS2. In *Methods in molecular biology (Clifton, N.J.)*, Vol. 1217, 329–341.

Pérez-Ortín, J. E., Alepuz, P., Chávez, S., & Choder, M. (2013). Eukaryotic mRNA Decay: Methodologies, Pathways, and Links to Other Stages of Gene Expression. *Journal of Molecular Biology*, *425*(20), 3750–3775.

Perrone-Bizzozero, N., & Bolognani, F. (2002). Role of HuD and other RNA-binding proteins in neural development and plasticity. *Journal of Neuroscience Research*, *68*(2), 121–126.

Piekna-Przybylska, D., Liu, B., & Fournier, M. J. (2007). The U1 snRNA Hairpin II as a RNA Affinity Tag for selecting snoRNP Complexes. *Methods in Enzymology*, *425*, 317–353.

Pillai, R. S., Bhattacharyya, S. N., Artus, C. G., Zoller, T., Cougot, N., Basyuk, E., … Filipowicz, W. (2005). Inhibition of translational initiation by Let-7 MicroRNA in human cells. *Science (New York, N.Y.)*, *309*(5740), 1573–1576.

Pinder, B. D., & Smibert, C. A. (2013). microRNA- independent recruitment of Argonaute 1 to nanos mRNA through the Smaug RNA-binding protein. *EMBO Reports*, *14*(1), 80–86.

Poon, M. M., Choi, S.-H., Jamieson, C. A. M., Geschwind, D. H., & Martin, K. C. (2006). Identification of Process-Localized mRNAs from Cultured Rodent Hippocampal Neurons. *Journal of Neuroscience*, *26*(51), 13390–13399.

Popp, M. W., & Maquat, L. E. (2016). Leading Edge Minireview Leveraging Rules of Nonsense-Mediated mRNA Decay for Genome Engineering and Personalized Medicine. *Cell, 165*(6), 1319-1322.

Poser, I., Sarov, M., Hutchins, J. R. A., Hériché, J.-K., Toyoda, Y., Pozniakovsky, A., … Hyman, A. A. (2008). BAC TransgeneOmics: a high-throughput method for exploration of protein function in mammals. *Nature Methods*, *5*(5), 409–415.

Proudfoot, N. J. (2003). Dawdling polymerases allow introns time to splice. *Nature Structural & Molecular Biology*, *10*(11), 876–878.

Puig, O., Caspary, F., Rigaut, G., Rutz, B., Bouveret, E., Bragado-Nilsson, E., … Séraphin, B. (2001). The Tandem Affinity Purification (TAP) Method: A General Procedure of Protein Complex Purification. *Methods*, *24*(3), 218–229.

Pyronnet, S., Imataka, H., Gingras, A. C., Fukunaga, R., Hunter, T., & Sonenberg, N. (1999). Human eukaryotic translation initiation factor 4G (eIF4G) recruits Mnk1 to phosphorylate eIF4E. *The EMBO Journal*, *18*(1), 270–279.

Quinones-Coello, A. T., Petrella, L. N., Ayers, K., Melillo, A., Mazzalupo, S., Hudson, A. M., … Cooley, L. (2006). Exploring Strategies for Protein Trapping in Drosophila. *Genetics*, *175*(3), 1089–1104.

Rajavel, K. S., & Neufeld, E. F. (2001). Nonsense-Mediated Decay of Human HEXA mRNA. *Molecular and Cellular Biology*, *21*(16), 5512–5519.

Raker, V. A., Plessel, G., & Lührmann, R. (1996). The snRNP core assembly pathway: identification of stable core protein heteromeric complexes and an snRNP subcore particle in vitro. *The EMBO Journal*, *15*(9), 2256–2269.

Ramanouskaya, T. V., & Grinev, V. V. (2017). The determinants of alternative RNA splicing in human cells. *Molecular Genetics and Genomics*, *292*(6), 1175–1195.

Ramos, A., Grünert, S., Adams, J., Micklem, D. R., Proctor, M. R., Freund, S., … Varani, G. (2000). RNA recognition by a Staufen double-stranded RNA-binding domain. *The EMBO Journal*, *19*(5), 997–1009.

Rauniyar, N., Yates, J. R., & III. (2014). Isobaric labeling-based relative quantification in shotgun proteomics. *Journal of Proteome Research*, *13*(12), 5293–5309.

Raz, E. (2000). The function and regulation of vasa-like genes in germ-cell development. *Genome Biology*, *1*(3), reviews1017.1- 1017.6.

Reiter, L. T., Potocki, L., Chien, S., Gribskov, M., & Bier, E. (2001). A systematic analysis of human disease-associated gene sequences in Drosophila melanogaster. *Genome Research*, *11*(6), 1114–1125.

Ren, X., Holsteens, K., Li, H., Sun, J., Zhang, Y., Liu, L.-P., … Ni, J.-Q. (2017). Genome editing in Drosophila melanogaster: from basic genome engineering to the multipurpose CRISPR-Cas9 system. *Science China Life Sciences*, *60*(5), 476–489.

Renault, A. D. (2012). vasa is expressed in somatic cells of the embryonic gonad in a sex-specific manner in Drosophila melanogaster. *Biology Open*, *1*(10), 1043–1048.

Ricci, E. P., Limousin, T., Soto-Rifo, R., Rubilar, P. S., Decimo, D., & Ohlmann, T. (2013). miRNA repression of translation in vitro takes place during 43S ribosomal scanning. *Nucleic Acids Research*, *41*(1), 586–598.

Richter, J. D., & Sonenberg, N. (2005). Regulation of cap-dependent translation by eIF4E inhibitory proteins. *Nature*, *433*(7025), 477–480.

Rigaut, G., Shevchenko, A., Rutz, B., Wilm, M., Mann, M., & Séraphin, B. (1999). A generic protein purification method for protein complex characterization and proteome exploration. *Nature Biotechnology*, *17*(10), 1030–1032.

Roignant, J.-Y., & Treisman, J. E. (2010). Exon Junction Complex Subunits Are Required to Splice Drosophila MAP Kinase, a Large Heterochromatic Gene. *Cell*, *143*(2), 238–250.

Romero-Barrios, N., Legascue, M. F., Benhamed, M., Ariel, F., & Crespi, M. (2018). Splicing regulation by long noncoding RNAs. *Nucleic Acids Research*, *46*(5), 2169–2184.

Rongo, C., Broihier, H. T., Moore, L., Van Doren, M., Forbes, A., & Lehmann, R. (1997). Germ plasm assembly and germ cell migration in Drosophila. *Cold Spring Harbor Symposia on Quantitative Biology*, *62*, 1–11.

Rongo, C., Gavis, E. R., & Lehmann, R. (1995). Localization of oskar RNA regulates oskar translation and requires Oskar protein. *Development (Cambridge, England)*, *121*(9), 2737–2746.

Ross, P. L., Huang, Y. N., Marchese, J. N., Williamson, B., Parker, K., Hattan, S., … Pappin, D. J. (2004). Multiplexed Protein Quantitation in *Saccharomyces cerevisiae* Using Amine-reactive Isobaric Tagging Reagents. *Molecular & Cellular Proteomics*, *3*(12), 1154–1169.

Rouault, T. A., Hentze, M. W., Haile, D. J., Harford, J. B., & Klausner, R. D. (1989). The iron-responsive element binding protein: a method for the affinity purification of a regulatory RNA-binding protein. *Proceedings of the National Academy of Sciences of the United States of America*, *86*(15), 5768–5772.

Rouget, C., Papin, C., Boureux, A., Meunier, A.-C., Franco, B., Robine, N., … Simonelig, M. (2010). Maternal mRNA deadenylation and decay by the piRNA pathway in the early Drosophila embryo. *Nature*, *467*(7319), 1128–1132.

Roundtree, I. A., Evans, M. E., Pan, T., & He, C. (2017). Dynamic RNA Modifications in Gene Expression Regulation. *Cell*, *169*, 1187–1200.

Roux, K. J., Kim, D. I., & Burke, B. (2013). BioID: A Screen for Protein-Protein Interactions. In *Current Protocols in Protein Science*, Vol. 74, 19.23.1-19.23.14. Hoboken, NJ, USA: John Wiley & Sons, Inc.

Ryazansky, S. S., Kotov, A. A., Kibanov, M. V., Akulenko, N. V., Korbut, A. P., Lavrov, S. A., … Olenina, L. V. (2016). RNA helicase Spn-E is required to maintain Aub and AGO3 protein levels for piRNA silencing in the germline of Drosophila. *European Journal of Cell Biology*, *95*(9), 311–322.

Ryder, P. V., & Lerit, D. A. (2018). RNA localization regulates diverse and dynamic cellular processes. *Traffic*, *19*(7), 496–502.

Saffman, E. E., Styhler, S., Rother, K., Li, W., Richard, S., & Lasko, P. (1998). Premature translation of oskar in oocytes lacking the RNA-binding protein bicaudal-C. *Molecular and Cellular Biology*, *18*(8), 4855–4862.

Said, N., Rieder, R., Hurwitz, R., Deckert, J., Urlaub, H., & Vogel, J. (2009). In vivo expression and purification of aptamer-tagged small RNA regulators. *Nucleic Acids Research*, *37*(20), e133.

Sakers, K., Lake, A. M., Khazanchi, R., Ouwenga, R., Vasek, M. J., Dani, A., & Dougherty, J. D. (2017). Astrocytes locally translate transcripts in their peripheral processes. *Proceedings of the National Academy of Sciences of the United States of America*, *114*(19), E3830–E3838.

Saltzman, A. L., Kim, Y. K., Pan, Q., Fagnani, M. M., Maquat, L. E., & Blencowe, B. J. (2008). Regulation of Multiple Core Spliceosomal Proteins by Alternative Splicing-Coupled Nonsense-Mediated mRNA Decay. *Molecular and Cellular Biology*, *28*(13), 4320–4330.

Sander, K., & Lehmann, R. (1988). Drosophila nurse cells produce a posterior signal required for embryonic segmentation and polarity. *Nature*, *335*(6185), 68–70.

Sarov, M., Barz, C., Jambor, H., Hein, M. Y., Schmied, C., Suchold, D., … Schnorrer, F. (2016). A genome-wide resource for the analysis of protein localisation in Drosophila. *ELife*, *5*.

Sarov, M., Murray, J. I., Schanze, K., Pozniakovski, A., Niu, W., Angermann, K., … Hyman, A. A. (2012). A Genome-Scale Resource for In Vivo Tag-Based Protein Function Exploration in C. elegans. *Cell*, *150*(4), 855–866.

Sarov, M., Schneider, S., Pozniakovski, A., Roguev, A., Ernst, S., Zhang, Y., … Stewart, A. F. (2006). A recombineering pipeline for functional genomics applied to Caenorhabditis elegans. *Nature Methods*, *3*(10), 839–844.

Saulière, J., Haque, N., Harms, S., Barbosa, I., Blanchette, M., & Le Hir, H. (2010). The exon junction complex differentially marks spliced junctions. *Nature Structural & Molecular Biology*, *17*(10), 1269–1271.

Saulière, J., Murigneux, V., Wang, Z., Marquenet, E., Barbosa, I., Le Tonquèze, O., … Le Hir, H. (2012). CLIP-seq of eIF4AIII reveals transcriptome-wide mapping of the human exon junction complex. *Nature Structural & Molecular Biology*, *19*(11), 1124–1131.

Saunders, C., & Cohen, R. S. (1999). The Role of Oocyte Transcription, the 5′UTR, and Translation Repression and Derepression in Drosophila gurken mRNA and Protein Localization. *Molecular Cell*, *3*(1), 43–54.

Scheper, G. C., & Proud, C. G. (2002). Does phosphorylation of the cap-binding protein eIF4E play a role in translation initiation? *Eur. J. Biochem.*, 269(22), 5350–5359.

Schindelin, J., Arganda-Carreras, I., Frise, E., Kaynig, V., Longair, M., Pietzsch, T., … Cardona, A. (2012). Fiji: an open-source platform for biological-image analysis. *Nature Methods*, *9*(7), 676–682.

Schisa, J. A. (2012). New insights into the regulation of RNP granule assembly in oocytes. *International Review of Cell and Molecular Biology*, *295*, 233–289.

Schoenberg, D. R. (2011). Mechanisms of endonuclease-mediated mRNA decay. *Wiley Interdisciplinary Reviews: RNA*, *2*(4), 582–600.

Schoenberg, D. R., & Maquat, L. E. (2012). Regulation of cytoplasmic mRNA decay. *Nature Reviews. Genetics*, *13*(4), 246–259.

Schopp, I. M., Amaya Ramirez, C. C., Debeljak, J., Kreibich, E., Skribbe, M., Wild, K., & Béthune, J. (2017). Split-BioID a conditional proteomics approach to monitor the composition of spatiotemporally defined protein complexes. *Nature Communications*, *8*(15690).

Schüpbach, T., & Wieschaus, E. (1986). Maternal-effect mutations altering the anterior-posterior pattern of the Drosophila embryo. *Roux's Archives of Developmental Biology*, *195*(5), 302–317.

Semotok, J. L., Cooperstock, R. L., Pinder, B. D., Vari, H. K., Lipshitz, H. D., & Smibert, C. A. (2005). Smaug Recruits the CCR4/POP2/NOT Deadenylase Complex to Trigger Maternal Transcript Localization in the Early Drosophila Embryo. *Current Biology*, *15*(4), 284–294.

Serin, G., Gersappe, A., Black, J. D., Aronoff, R., & Maquat, L. E. (2001). Identification and Characterization of Human Orthologues to Saccharomyces cerevisiae Upf2 Protein and Upf3 Protein (Caenorhabditis elegans SMG-4). *Molecular and Cellular Biology*, *21*(1), 209–223.

Shannon, P., Markiel, A., Ozier, O., Baliga, N. S., Wang, J. T., Ramage, D., … Ideker, T. (2003). Cytoscape: A Software Environment for Integrated Models of Biomolecular Interaction Networks. *Genome Research*, *13*(11), 2498–2504.

Sharma, S. (2008). Isolation of a Sequence-Specific RNA Binding Protein, Polypyrimidine Tract Binding Protein, Using RNA Affinity Chromatography. In *Methods in molecular biology (Clifton, N.J.)*, Vol. 488, 1–8.

Sharp, J. A., Plant, J. J., Ohsumi, T. K., Borowsky, M., & Blower, M. D. (2011). Functional analysis of the microtubule-interacting transcriptome. *Molecular Biology of the Cell*, *22*(22), 4312–4323.

Shatsky, I. N., Terenin, I. M., Smirnova, V. V., & Andreev, D. E. (2018). Cap-Independent Translation: What's in a Name? *Trends in Biochemical Sciences*, *43*(11), 882-895.

Shenoy, A., & Geiger, T. (2015). Super-SILAC: current trends and future perspectives. *Expert Review of Proteomics*, *12*(1), 13–19.

Sheth, U., & Parker, R. (2006). Targeting of aberrant mRNAs to cytoplasmic Processing bodies. *Cell*, *125*(6).

Shoemaker, C. J., & Green, R. (2012). Translation drives mRNA quality control. *Nature Structural & Molecular Biology*, *19*(6), 594–601.

Shveygert, M., Kaiser, C., Bradrick, S. S., & Gromeier, M. (2010). Regulation of eukaryotic initiation factor 4E (eIF4E) phosphorylation by mitogen-activated protein kinase occurs through modulation of Mnk1-eIF4G interaction. *Molecular and Cellular Biology*, *30*(21), 5160–5167.

Simon, B., Masiewicz, P., Ephrussi, A., & Carlomagno, T. (2015). The structure of the SOLE element of oskar mRNA. *RNA*, *21*(8), 1444–1453.

Simsek, D., Tiu, G. C., Flynn, R. A., Byeon, G. W., Leppek, K., Xu, A. F., … Barna, M. (2017). The Mammalian Ribo-interactome Reveals Ribosome Functional Diversity and Heterogeneity. *Cell*, *169*(6), 1051–1065.e18.

Singer-Krüger, B., & Jansen, R.-P. (2014). Here, there, everywhere. mRNA localization in budding yeast. *RNA Biology*, *11*(8), 1031–1039.

Singh, G., Kucukural, A., Cenik, C., Leszyk, J. D. D., Shaffer, S. A. A., Weng, Z., & Moore, M. J. J. (2012). The cellular EJC interactome reveals high-order mRNP structure and an EJC-SR protein nexus. *Cell*, *151*(4).

Singh, G., Rebbapragada, I., & Lykke-Andersen, J. (2008). A Competition between Stimulators and Antagonists of Upf Complex Recruitment Governs Human Nonsense-Mediated mRNA Decay. *PLoS Biology*, *6*(4), e111.

Sinsimer, K. S., Jain, R. A., Chatterjee, S., & Gavis, E. R. (2011). A late phase of germ plasm accumulation during Drosophila oogenesis requires lost and rumpelstiltskin. *Development (Cambridge, England)*, *138*(16), 3431–3440.

Sladewski, T. E., Billington, N., Ali, M. Y., Bookwalter, C. S., Lu, H., Krementsova, E. B., … Trybus, K. M. (2018). Recruitment of two dyneins to an mRNA-dependent Bicaudal D transport complex. *ELife*, *7*.

Slobodin, B., & Gerst, J. E. (2010). A novel mRNA affinity purification technique for the identification of interacting proteins and transcripts in ribonucleoprotein complexes. *RNA*, *16*(11), 2277–2290.

Smith, J. L., Wilson, J. E., & Macdonald, P. M. (1992). Overexpression of oskar directs ectopic activation of nanos and presumptive pole cell formation in Drosophila embryos. *Cell*, *70*(5), 849–859.

Smith, R. (2004). Moving Molecules: mRNA Trafficking in Mammalian Oligodendrocytes and Neurons. *The Neuroscientist*, *10*(6), 495–500.

Snee, M. J., & Macdonald, P. M. (2004). Live imaging of nuage and polar granules: evidence against a precursor-product relationship and a novel role for Oskar in stabilization of polar granule components. *Journal of Cell Science*, *117*(Pt 10), 2109–2120.

Snee, M. J., & Macdonald, P. M. (2009). Dynamic organization and plasticity of sponge bodies. *Developmental Dynamics : An Official Publication of the American Association of Anatomists*, *238*(4), 918–930.

Snee, M., Benz, D., Jen, J., & Macdonald, P. M. (2008). Two distinct domains of Bruno bind specifically to the oskar mRNA. *RNA Biology*, *5*(1), 1–9.

Spasic, M., Friedel, C. C., Schott, J., Kreth, J., Leppek, K., Hofmann, S., … Stoecklin, G. (2012). Genome-Wide Assessment of AU-Rich Elements by the AREScore Algorithm. *PLoS Genetics*, *8*(1), e1002433.

Spradling, A.C. (1993). Developmental genetics of oogenesis. In: Bate M, Martinez Arias A, editors. The Development of Drosophila melanogaster. New York: Cold Spring Harbor Laboratory Press. pp. 1–70.

Spriggs, K. A., Stoneley, M., Bushell, M., & Willis, A. E. (2008). Re-programming of translation following cell stress allows IRES-mediated translation to predominate. *Biology of the Cell*, *100*(1), 27–38.

Srisawat, C., & Engelke, D. R. (2001). Streptavidin aptamers: affinity tags for the study of RNAs and ribonucleoproteins. *RNA (New York, N.Y.)*, *7*(4), 632–641.

St Johnston, D. (2005). Moving messages: the intracellular localization of mRNAs. *Nature Reviews Molecular Cell Biology*, *6*(5), 363–375.

St Johnston, D., & Nüsslein-Volhard, C. (1992). The origin of pattern and polarity in the Drosophila embryo. *Cell*, *68*(2), 201–219.

St Johnston, D., Beuchle, D., & Nüsslein-Volhard, C. (1991). Staufen, a gene required to localize maternal RNAs in the Drosophila egg. *Cell*, *66*(1), 51–63.

St Johnston, D., Driever, W., Berleth, T., Richstein, S., & Nüsslein-Volhard, C. (1989). Multiple steps in the localization of bicoid RNA to the anterior pole of the Drosophila oocyte. *Development (Cambridge, England)*, *107 Suppl*, 13–19.

Stalder, L., & Mühlemann, O. (2009). Processing bodies are not required for mammalian nonsense-mediated mRNA decay. *RNA (New York, N.Y.)*, *15*(7), 1265–1273.

Standart, N., & Weil, D. (2018). P-Bodies: Cytosolic Droplets for Coordinated mRNA Storage. *Trends in Genetics*. *34*(8), 612-626.

Steckelberg, A.-L., Boehm, V., Gromadzka, A. M., & Gehring, N. H. (2012). CWC22 Connects Pre-mRNA Splicing and Exon Junction Complex Assembly. *Cell Reports*, *2*(3), 454–461.

Steinhauer, J., & Kalderon, D. (2006). Microtubule Polarity and Axis Formation in the Drosophila Oocyte. *Developmental Dynamics*, *235*, 1455–1468.

Styhler, S., Nakamura, A., & Lasko, P. (2002). VASA Localization Requires the SPRY-Domain and SOCS-Box Containing Protein, GUSTAVUS. *Developmental Cell*, *3*(6), 865–876.

Styhler, S., Nakamura, A., Swan, A., Suter, B., & Lasko, P. (1998). vasa is required for GURKEN accumulation in the oocyte, and is involved in oocyte differentiation and germline cyst development. *Development*, *125*(9).

Subtelny, A. O., Eichhorn, S. W., Chen, G. R., Sive, H., & Bartel, D. P. (2014). Poly(A)-tail profiling reveals an embryonic switch in translational control. *Nature*, *508*(7494), 66–71.

Supek, F., Bošnjak, M., Škunca, N., & Šmuc, T. (2011). REVIGO Summarizes and Visualizes Long Lists of Gene Ontology Terms. *PLoS ONE*, *6*(7), e21800.

Surabhi, S., Tripathi, B. K., Maurya, B., Bhaskar, P. K., Mukherjee, A., & Mutsuddi, M. (2015). Regulation of Notch Signaling by an Evolutionary Conserved DEAD Box RNA Helicase, Maheshvara in Drosophila melanogaster. *Genetics*, *201*(3), 1071–1085.

Sureau, A., Gattoni, R., Dooghe, Y., Stévenin, J., & Soret, J. (2001). SC35 autoregulates its expression by promoting splicing events that destabilize its mRNAs. *The EMBO Journal*, *20*(7), 1785–1796.

Suzuki, T., Tian, Q. B., Kuromitsu, J., Kawai, T., & Endo, S. (2007). Characterization of mRNA species that are associated with postsynaptic density fraction by gene chip microarray analysis. *Neuroscience Research*, *57*(1), 61–85.

Szklarczyk, D., Morris, J. H., Cook, H., Kuhn, M., Wyder, S., Simonovic, M., … von Mering, C. (2017). The STRING database in 2017: quality-controlled protein–protein association networks, made broadly accessible. *Nucleic Acids Research*, *45*(D1), D362–D368.

Tamayo, J. V, Teramoto, T., Chatterjee, S., Hall, T. M. T., & Gavis, E. R. (2017). The Drosophila hnRNP F/H Homolog Glorund Uses Two Distinct RNA-Binding Modes to Diversify Target Recognition. *Cell Reports*, *19*(1), 150–161.

Tange, T. Ø., Nott, A., & Moore, M. J. (2004). The ever-increasing complexities of the exon junction complex. *Current Opinion in Cell Biology*, *16*(3), 279–284.

Tange, T. O., Shibuya, T., Jurica, M. S., & Moore, M. J. (2005). Biochemical analysis of the EJC reveals two new factors and a stable tetrameric protein core. *RNA*, *11*(12), 1869–1883.

Taning, C. N. T., Andrade, E. C., Hunter, W. B., Christiaens, O., & Smagghe, G. (2016). Asian Citrus Psyllid RNAi Pathway – RNAi evidence. *Scientific Reports*, *6*(1), 38082.

Teixeira, D., Sheth, U., Valencia-Sanchez, M. A., Brengues, M., & Parker, R. (2005). Processing bodies require RNA for assembly and contain non translating mRNAs. *RNA*, *11*(4), 371-382.

Tetzlaff, M. T., Jäckle, H., & Pankratz, M. J. (1996). Lack of Drosophila cytoskeletal tropomyosin affects head morphogenesis and the accumulation of oskar mRNA required for germ cell formation. *The EMBO Journal*, *15*(6), 1247–1254.

Thio, G. L., Ray, R. P., Barcelo, G., & Schüpbach, T. (2000). Localization of gurken RNA in Drosophila Oogenesis Requires Elements in the 5′ and 3′ Regions of the Transcript. *Developmental Biology*, *221*(2), 435–446.

Thompson, A., Schäfer, J., Kuhn, K., Kienle, S., Schwarz, J., Schmidt, G., … Hamon, C. (2003). Tandem mass tags: A novel quantification strategy for comparative analysis of complex protein mixtures by MS/MS. *Analytical Chemistry*, *75*(8), 1895–1904.

Thompson, M. K., Rojas-Duran, M. F., Gangaramani, P., & Gilbert, W. V. (2016). The ribosomal protein Asc1/RACK1 is required for efficient translation of short mRNAs. *ELife*, *5*.

Thomsen, R., Pallesen, J., Daugaard, T. F., Børglum, A. D., & Nielsen, A. L. (2013). Genome wide assessment of mRNA in astrocyte protrusions by direct RNA sequencing reveals mRNA localization for the intermediate filament protein nestin. *Glia*, *61*(11), 1922–1937.

Thomson, T., Liu, N., Arkov, A., Lehmann, R., & Lasko, P. (2008). Isolation of new polar granule components in Drosophila reveals P body and ER associated proteins. *Mech Dev, 125*(9–10), 865-873

Tirronen, M., Lahti, V. P., Heino, T. I., & Roos, C. (1995). Two otu transcripts are selectively localised in Drosophila oogenesis by a mechanism that requires a function of the otu protein. *Mechanisms of Development*, *52*(1), 65–75.

Tolino, M., Köhrmann, M., & Kiebler, M. A. (2012). RNA-binding proteins involved in RNA localization and their implications in neuronal diseases. *European Journal of Neuroscience*, *35*(12), 1818–1836.

Tomancak, P., Guichet, A., Zavorszky, P., & Ephrussi, A. (1998). Oocyte polarity depends on regulation of gurken by Vasa. *Development*, Vol. 125.

Tomecki, R., & Dziembowski, A. (2010). Novel endoribonucleases as central players in various pathways of eukaryotic RNA metabolism. *RNA (New York, N.Y.)*, *16*(9), 1692–1724.

Tritschler, F., Braun, J. E., Motz, C., Igreja, C., Haas, G., Truffault, V., … Weichenrieder, O. (2009). DCP1 forms asymmetric trimers to assemble into active mRNA decapping complexes in metazoa. *Proceedings of the National Academy of Sciences*, *106*(51), 21591–21596.

Tsai, B. P., Wang, X., Huang, L., & Waterman, M. L. (2011). Quantitative Profiling of *In Vivo* -assembled RNA-Protein Complexes Using a Novel Integrated Proteomic Approach. *Molecular & Cellular Proteomics*, *10*(4), M110.007385.

Tucker, M., & Parker, R. (2000). Mechanisms and control of mRNA decapping in *Saccharomyces cerevisiae*. *Annual Review of Biochemistry*, *69*(1), 571–595.

Tucker, M., Staples, R. R., Valencia-Sanchez, M. A., Muhlrad, D., & Parker, R. (2002). Ccr4p is the catalytic subunit of a Ccr4p/Pop2p/Notp mRNA deadenylase complex in Saccharomyces cerevisiae. *The EMBO Journal*, *21*(6), 1427–1436.

Tucker, M., Valencia-Sanchez, M. A., Staples, R. R., Chen, J., Denis, C. L., & Parker, R. (2001). The Transcription Factor Associated Ccr4 and Caf1 Proteins Are Components of the Major Cytoplasmic mRNA Deadenylase in Saccharomyces cerevisiae. *Cell*, *104*(3), 377–386.

Tyanova, S., Temu, T., Sinitcyn, P., Carlson, A., Hein, M. Y., Geiger, T., … Cox, J. (2016). The Perseus computational platform for comprehensive analysis of (prote)omics data. *Nature Methods*, *13*(9), 731–740.

Ule, J., Jensen, K., Mele, A., & Darnell, R. B. (2005). CLIP: A method for identifying protein–RNA interaction sites in living cells. *Methods*, *37*(4), 376–386.

Urbanek, M. O., Galka-Marciniak, P., Olejniczak, M., & Krzyzosiak, W. J. (2014). RNA imaging in living cells - methods and applications. *RNA Biology*, *11*(8), 1083–1095.

Vagin, V. V, Klenov, M. S., Kalmykova, A. I., Stolyarenko, A. D., Kotelnikov, R. N., & Gvozdev, V. A. (2004). The RNA interference proteins and vasa locus are involved in the silencing of retrotransposons in the female germline of Drosophila melanogaster. *RNA Biology*, *1*(1), 54–58.

Vagner, S., Galy, B., & Pyronnet, S. (2001). Irresistible IRES: Attracting the translation machinery to internal ribosome entry sites. *EMBO Reports*, *2*(10), 893–898.

Vanzo, N. F., & Ephrussi, A. (2002). Oskar anchoring restricts pole plasm formation to the posterior of the Drosophila oocyte. *Development (Cambridge, England)*, *129*(15), 3705–3714.

Vasudevan, S., & Steitz, J. A. (2007). AU-Rich-Element-Mediated Upregulation of Translation by FXR1 and Argonaute 2. *Cell*, *128*(6), 1105–1118.

Veeranan-Karmegam, R., Boggupalli, D. P., Liu, G., & Gonsalvez, G. B. (2016). A new isoform of Drosophila non-muscle Tropomyosin 1 interacts with Kinesin-1 and functions in oskar mRNA localization. *Journal of Cell Science*, *129*(22), 4252–4264.

Velentzas, A. D., Anagnostopoulos, A. K., Velentzas, P. D., Mpakou, V. E., Sagioglou, N. E., Tsioka, M. M., … Stravopodis, D. J. (2015). Global Proteomic Profiling of Drosophila Ovary: A High-resolution, Unbiased, Accurate and Multifaceted Analysis. *Cancer Genomics & Proteomics*, *12*(6), 369–384.

Venken, K. J. T., Schulze, K. L., Haelterman, N. A., Pan, H., He, Y., Evans-Holm, M., … Bellen, H. J. (2011). MiMIC: a highly versatile transposon insertion resource for engineering Drosophila melanogaster genes. *Nature Methods*, *8*(9), 737–743.

Wagner, C., Palacios, I., Jaeger, L., St Johnston, D., Ehresmann, B., Ehresmann, C., & Brunel, C. (2001). Dimerization of the 3′UTR of bicoid mRNA involves a two-step mechanism. *Journal of Molecular Biology*, *313*(3), 511–524.

Walters, R., & Parker, R. (2014). Quality control: Is there quality control of localized mRNAs? *The Journal of Cell Biology*, *204*(6), 863–868.

Wang, C., & Lehmann, R. (1991). Nanos is the localized posterior determinant in Drosophila. *Cell*, *66*(4), 637–647.

Wang, C., Dickinson, L. K., & Lehmann, R. (1994). Genetics of nanos Localization in Drosophila. *Developmental Dynamics* (Vol. 199).

Wang, J., Vock, V. M., Li, S., Olivas, O. R., & Wilkinson, M. F. (2002). A Quality Control Pathway That Down-regulates Aberrant T-cell Receptor (TCR) Transcripts by a Mechanism Requiring UPF2 and Translation. *Journal of Biological Chemistry*, *277*(21), 18489–18493.

Wang, M., Ly, M., Lugowski, A., Laver, J. D., Lipshitz, H. D., Smibert, C. A., & Rissland, O. S. (2017). ME31B globally represses maternal mRNAs by two distinct mechanisms during the Drosophila maternal-to-zygotic transition. *ELife*, *6*.

Wang, S.-C., Hsu, H.-J., Lin, G., Wang, T.-F., Chang, C., & Lin, M.-D. (2015c). Germ plasm localisation of the HELICc of Vasa in Drosophila: analysis of domain sufficiency and amino acids critical for localisation. *Scientific Reports*, *5*(1), 14703.

Wang, X., Zhao, B. S., Roundtree, I. A., Lu, Z., Han, D., Ma, H., … He, C. (2015a). N6-methyladenosine Modulates Messenger RNA Translation Efficiency. *Cell*, *161*(6), 1388–1399.

Wang, Y., Liu, J., Huang, B. O., Xu, Y.-M., Li, J., Huang, L.-F., … Wang, X.-Z. (2015b). Mechanism of alternative splicing and its regulation. *Biomedical Reports*, *3*(2), 152–158.

Ward, A. M., Bidet, K., Yinglin, A., Ler, S. G., Hogue, K., Blackstock, W., … Garcia-Blanco, M. A. (2011). Quantitative mass spectrometry of DENV-2 RNA-interacting proteins reveals that the DEAD-box RNA helicase DDX6 binds the DB1 and DB2 3' UTR structures. *RNA Biology*, *8*(6), 1173–1186.

Webster, P. J., Liang, L., Berg, C. A., Lasko, P., & Macdonald, P. M. (1997). Translational repressor bruno plays multiple roles in development and is widely conserved. *Genes & Development*, *11*(19), 2510–2521.

Weil, T. T., Parton, R. M., Herpers, B., Soetaert, J., Veenendaal, T., Xanthakis, D., … Davis, I. (2012). Drosophila patterning is established by differential association of mRNAs with P bodies. *Nature Cell Biology*, *14*(12), 1305–1313.

Weingarten-Gabbay, S., Elias-Kirma, S., Nir, R., Gritsenko, A. A., Stern-Ginossar, N., Yakhini, Z., … Segal, E. (2016). Systematic discovery of cap-independent translation sequences in human and viral genomes.

Weis, B. L., Schleiff, E., & Zerges, W. (2013). Protein targeting to subcellular organelles via MRNA localization. *Biochimica et Biophysica Acta*, *1833*(2), 260–273.

Welch, E. M., & Jacobson, A. (1999). An internal open reading frame triggers nonsense-mediated decay of the yeast SPT10 mRNA. *The EMBO Journal*, *18*(21), 6134–6145.

Wellensiek, B. P., Larsen, A. C., Stephens, B., Kukurba, K., Waern, K., Briones, N., … Chaput, J. C. (2013). Genome-wide profiling of human cap-independent translation-enhancing elements. *Nature Methods*, *10*(8), 747–750.

Wen, J., & Brogna, S. (2010). Splicing-dependent NMD does not require the EJC in Schizosaccharomyces pombe. *The EMBO Journal*, *29*(9), 1537–1551.

Wharton, R. P., & Struhl, G. (1989). Structure of the Drosophila BicaudalD protein and its role in localizing the the posterior determinant nanos. *Cell*, *59*(5), 881–892.

Wheeler, E. C., Van Nostrand, E. L., & Yeo, G. W. (2018). Advances and challenges in the detection of transcriptome-wide protein-RNA interactions. *Wiley Interdisciplinary Reviews: RNA*, *9*(1), e1436.

Wickens, M., Bernstein, D. S., Kimble, J., & Parker, R. (2002). A PUF family portrait: 3′UTR regulation as a way of life. *Trends in Genetics*, *18*(3), 150–157.

Wilhelm, J. E., Buszczak, M., & Sayles, S. (2005). Efficient Protein Trafficking Requires Trailer Hitch, a Component of a Ribonucleoprotein Complex Localized to the ER in Drosophila. *Developmental Cell*, *9*(5), 675–685.

Wilhelm, J. E., Mansfield, J., Hom-Booher, N., Wang, S., Turck, C. W., Hazelrigg, T., & Vale, R. D. (2000). Isolation of a ribonucleoprotein complex involved in mRNA localization in Drosophila oocytes. *The Journal of Cell Biology*, *148*(3), 427–440.

Wilsch-Bräuninger, M., Schwarz, H., & Nüsslein-Volhard, C. (1997). A sponge-like structure involved in the association and transport of maternal products during Drosophila oogenesis. *The Journal of Cell Biology*, *139*(3), 817–829.

Wilusz, C. J., Wormington, M., & Peltz, S. W. (2001). The cap-to-tail guide to mRNA turnover. *Nature Reviews Molecular Cell Biology*, *2*(4), 237–246.

Wollerton, M. C., Gooding, C., Wagner, E. J., Garcia-Blanco, M. A., & Smith, C. W. J. (2004). Autoregulation of polypyrimidine tract binding protein by alternative splicing leading to nonsense-mediated decay. *Molecular Cell*, *13*(1), 91–100.

Wong, J. W. H., & Cagney, G. (2010). An Overview of Label-Free Quantitation Methods in Proteomics by Mass Spectrometry. *Methods Molecular Biology, 604*, 273–283.

Woodward, L. A., Mabin, J. W., Gangras, P., & Singh, G. (2017). The exon junction complex: a lifelong guardian of mRNA fate. *Wiley Interdisciplinary Reviews: RNA*, *8*(3), e1411.

Wreden, C., Verrotti, A. C., Schisa, J. A., Lieberfarb, M. E., & Strickland, S. (1997). Nanos and pumilio establish embryonic polarity in Drosophila by promoting posterior deadenylation of hunchback mRNA. *Development (Cambridge, England)*, *124*(15), 3015–3023.

Wu, B., Chao, J. A., & Singer, R. H. (2012). Fluorescence fluctuation spectroscopy enables quantitative imaging of single mRNAs in living cells. *Biophysical Journal*, *102*(12), 2936–2944.

Wu, B., Chen, J., & Singer, R. H. (2014). Background free imaging of single mRNAs in live cells using split fluorescent proteins. *Scientific Reports*, *4*.

Wu, B., Miskolci, V., Sato, H., Tutucci, E., Kenworthy, C. A., Donnelly, S. K., … Hodgson, L. (2015). Synonymous modification results in high-fidelity gene expression of repetitive protein and nucleotide sequences. *Genes & Development*, *29*(8), 876–886.

Wu, L., Fan, J., & Belasco, J. G. (2006). MicroRNAs direct rapid deadenylation of mRNA. *Proceedings of the National Academy of Sciences*, *103*(11), 4034–4039.

Wu, P.-H., Isaji, M., & Carthew, R. W. (2013). Functionally Diverse MicroRNA Effector Complexes Are Regulated by Extracellular Signaling. *Molecular Cell*, *52*(1), 113–123.

Wu, X., & Brewer, G. (2012). The regulation of mRNA stability in mammalian cells: 2.0. *Gene*, *500*(1), 10–21.

Xiang, F., Ye, H., Chen, R., Fu, Q., & Li, L. (2010). *N* , *N* -Dimethyl Leucines as Novel Isobaric Tandem Mass Tags for Quantitative Proteomics and Peptidomics. *Analytical Chemistry*, *82*(7), 2817–2825.

Xu, J., Ren, X., Sun, J., Wang, X., Qiao, H.-H., Xu, B.-W., … Ni, J.-Q. (2015). A Toolkit of CRISPR-Based Genome Editing Systems in Drosophila. *Journal of Genetics and Genomics*, *42*(4), 141–149.

Xue, S., & Barna, M. (2012). Specialized ribosomes: a new frontier in gene regulation and organismal biology. *Nature Reviews Molecular Cell Biology*, *13*(6), 355–369.

Xue, S., & Barna, M. (2015). *Cis* -regulatory RNA elements that regulate specialized ribosome activity. *RNA Biology*, *12*(10), 1083–1087.

Yamashita, A., Chang, T.-C., Yamashita, Y., Zhu, W., Zhong, Z., Chen, C.-Y. A., & Shyu, A.-B. (2005). Concerted action of poly(A) nucleases and decapping enzyme in mammalian mRNA turnover. *Nature Structural & Molecular Biology*, *12*(12), 1054–1063.

Yamashita, A., Ohnishi, T., Kashima, I., Taya, Y., & Ohno, S. (2001). Human SMG-1, a novel phosphatidylinositol 3-kinase-related protein kinase, associates with components of the mRNA surveillance complex and is involved in the regulation of nonsense-mediated mRNA decay. *Genes & Development*, *15*(17), 2215–2228.

Yang, N., Yu, Z., Hu, M., Wang, M., Lehmann, R., & Xu, R.-M. (2015). Structure of Drosophila Oskar reveals a novel RNA binding protein. *Proceedings of the National Academy of Sciences of the United States of America*, *112*(37), 11541–11546.

Yano, T., López de Quinto, S., Matsui, Y., Shevchenko, A., Shevchenko, A., & Ephrussi, A. (2004). Hrp48, a Drosophila hnRNPA/B homolog, binds and regulates translation of oskar mRNA. *Developmental Cell*, *6*(5), 637–648.

Yao, X., Freas, A., Ramirez, J., Demirev, P. A., & Fenselau, C. (2001). Proteolytic 18O labeling for comparative proteomics: model studies with two serotypes of adenovirus. *Analytical Chemistry, 73*(13), 2836–2842.

Yekta, S., Shih, I.-H., & Bartel, D. P. (2004). MicroRNA-directed cleavage of HOXB8 mRNA. *Science (New York, N.Y.)*, *304*(5670), 594–596.

Yisraeli, J. K. (2005). VICKZ proteins: a multi-talented family of regulatory RNA-binding proteins. *Biology of the Cell*, *97*(1), 87–96.

Yoon, J.-H., Srikantan, S., & Gorospe, M. (2012). MS2-TRAP (MS2-tagged RNA affinity purification): Tagging RNA to identify associated miRNAs. *Methods*, *58*(2), 81–87.

Yoon, J.-S., Mogilicherla, K., Gurusamy, D., Chen, X., Chereddy, S. C. R. R., & Palli, S. R. (2018). Double-stranded RNA binding protein, Staufen, is required for the initiation of RNAi in coleopteran insects. *Proceedings of the National Academy of Sciences of the United States of America*, *115*(33), 8334–8339.

Youngman, E. M., & Green, R. (2005). Affinity purification of in vivo-assembled ribosomes for in vitro biochemical analysis. *Methods*, *36*(3), 305–312.

Youngman, E. M., Brunelle, J. L., Kochaniak, A. B., & Green, R. (2004). The Active Site of the Ribosome Is Composed of Two Layers of Conserved Nucleotides with Distinct Roles in Peptide Bond Formation and Peptide Release. *Cell*, *117*(5), 589–599.

Zaessinger, S., Busseau, I., & Simonelig, M. (2006). Oskar allows nanos mRNA translation in Drosophila embryos by preventing its deadenylation by Smaug/CCR4. *Development*, *133*(22), 4573–4583.

Zekri, L., Huntzinger, E., Heimstädt, S., & Izaurralde, E. (2009). The silencing domain of GW182 interacts with PABPC1 to promote translational repression and degradation of microRNA targets and is required for target release. *Molecular and Cellular Biology*, *29*(23), 6220–6231.

Zekri, L., Kuzuoğlu-Öztürk, D., & Izaurralde, E. (2013). GW182 proteins cause PABP dissociation from silenced miRNA targets in the absence of deadenylation. *The EMBO Journal*, *32*(7), 1052–1065.

Zhang, J., Sun, X., Qian, Y., & Maquat, L. E. (1998a). Intron function in the nonsense-mediated decay of beta-globin mRNA: indications that pre-mRNA splicing in the nucleus can influence mRNA translation in the cytoplasm. *RNA (New York, N.Y.)*, *4*(7), 801–815.

Zhang, Y., Buchholz, F., Muyrers, J. P. P., & Stewart, A. F. (1998b). A new logic for DNA engineering using recombination in Escherichia coli. *Nature Genetics*, *20*(2), 123–128.

Zhang, Y., Nash, L., & Fisher, A. L. (2008). A simplified, robust and streamlined procedure for the production of C. elegans transgenes via recombineering. *BMC Developmental Biology*, *8*(1), 119.

Zhao, J., Ohsumi, T. K., Kung, J. T., Ogawa, Y., Grau, D. J., Sarma, K., … Lee, J. T. (2010). Genome-wide Identification of Polycomb-Associated RNAs by RIP-seq. *Molecular Cell*, *40*(6), 939–953.

Zheng, D., Ezzeddine, N., Chen, C.-Y. A., Zhu, W., He, X., & Shyu, A.-B. (2008). Deadenylation is prerequisite for P-body formation and mRNA decay in mammalian cells. *The Journal of Cell Biology*, *182*(1), 89–101.

Zhong, J., Zhang, T., & Bloch, L. (2006). Dendritic mRNAs encode diversified functionalities in hippocampal pyramidal neurons. *BMC Neuroscience*, *7*(1), 17.

Zhou, H., Ranish, J. A., Watts, J. D., & Aebersold, R. (2002). Quantitative proteome analysis by solid-phase isotope tagging and mass spectrometry. *Nature Biotechnology*, *20*(5), 512–515.

Zhou, Y., & King, M. Lou. (1996). RNA Transport to the Vegetal Cortex ofXenopusOocytes. *Developmental Biology*, *179*(1), 173–183.

Zhou, Z., Sim, J., Griffith, J., & Reed, R. (2002). Purification and electron microscopic visualization of functional human spliceosomes. *Proceedings of the National Academy of Sciences of the United States of America*, *99*(19), 12203–12207.

Zimyanin, V. L., Belaya, K., Pecreaux, J., Gilchrist, M. J., Clark, A., Davis, I., & St Johnston, D. (2008). In vivo imaging of oskar mRNA transport reveals the mechanism of posterior localization. *Cell*, *134*(5), 843–853.

Zivraj, K. H., Tung, Y. C. L., Piper, M., Gumy, L., Fawcett, J. W., Yeo, G. S. H., & Holt, C. E. (2010). Subcellular Profiling Reveals Distinct and Developmentally Regulated Repertoire of Growth Cone mRNAs. *Journal of Neuroscience*, *30*(46), 15464–15478.

7. Supplementary figures
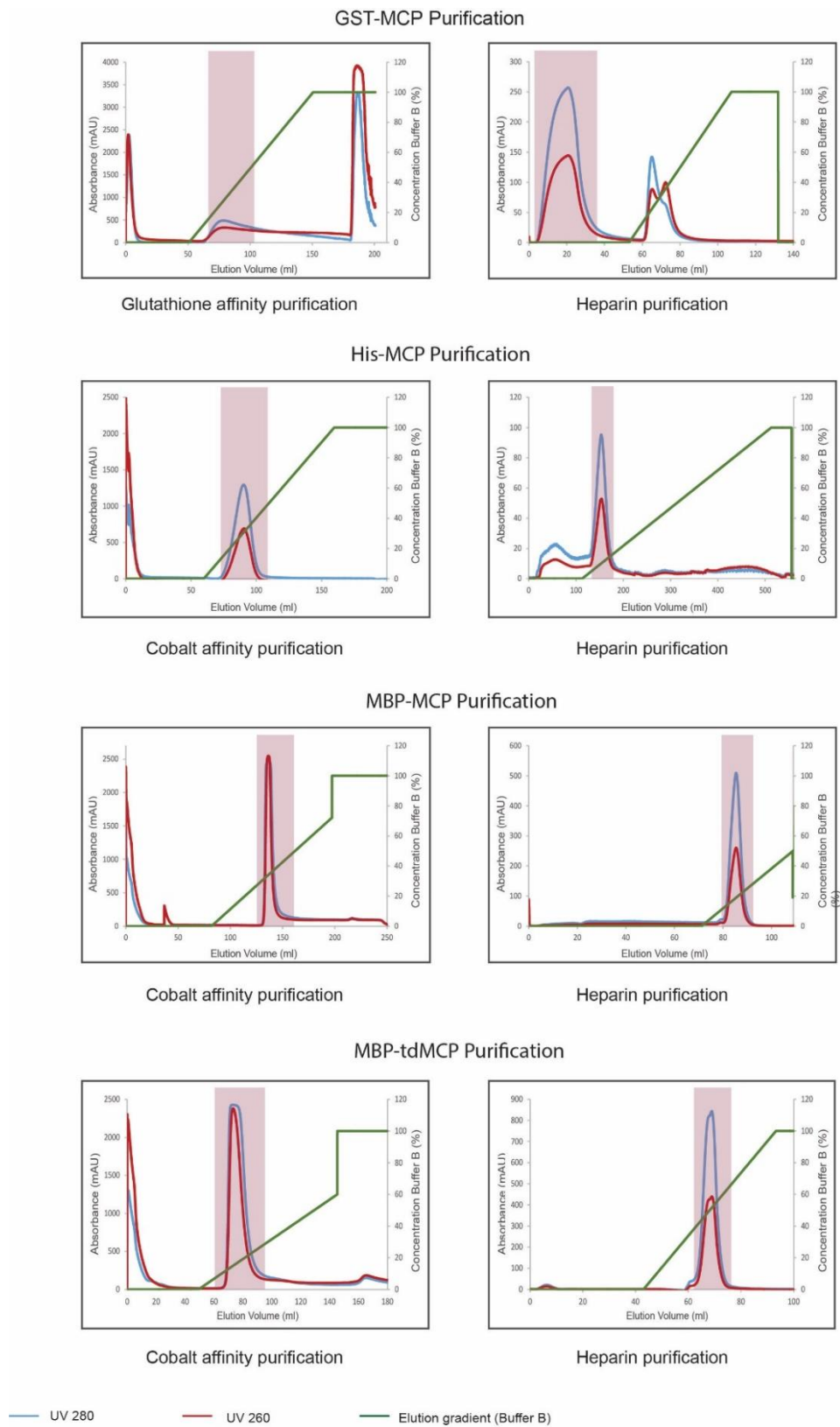
Supplementary Fig. 1. Chromatograms of affinity and heparin purification steps for differently tagged MCPs.

A)

MBP-MCP-*MS2* hairpin complex

B)

MBP-MCP-unrelated RNA hairpin complex
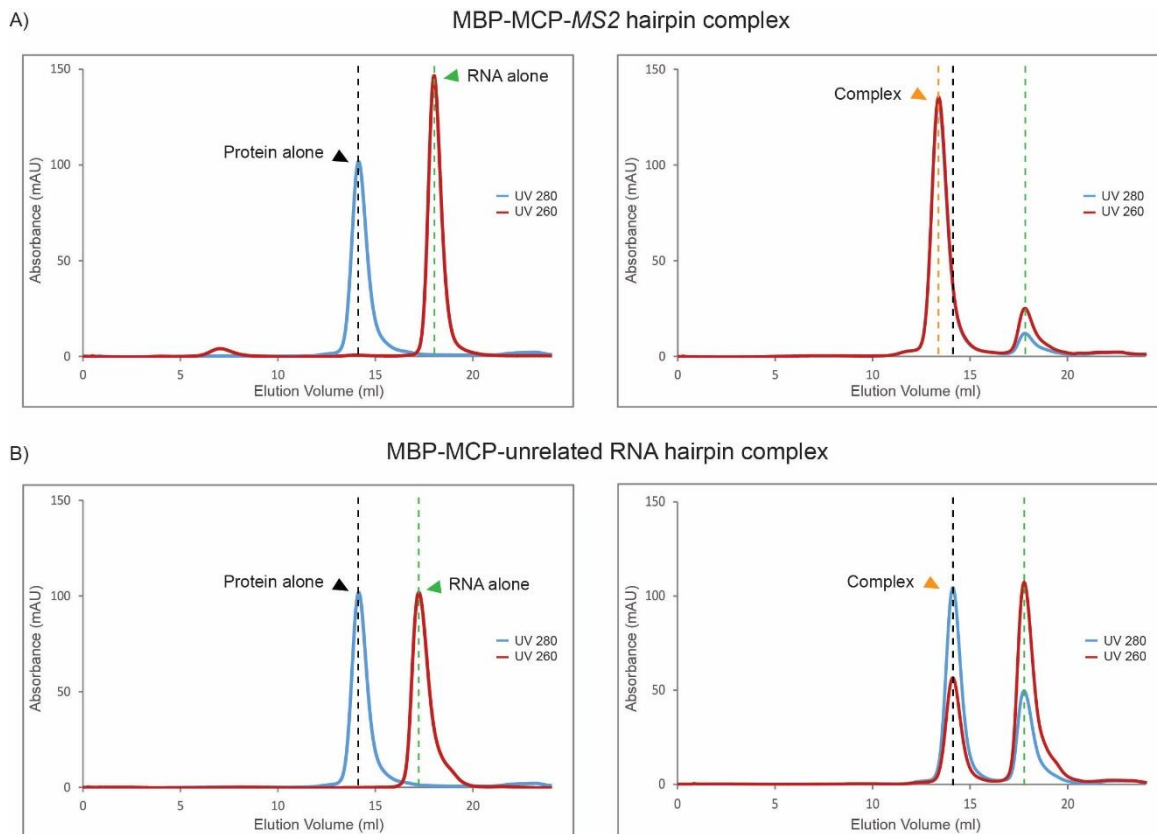
Supplementary Fig. 2. SEC profiles of the MBP-tagged MCP in complex with *MS2* hairpin (A) and with an unrelated RNA hairpin (B). Profiles for RNA and protein are shown on the left, while the RNA-protein complex is shown on the right. The elution profiles show UV absorption at 280nm (blue) and 260nm (red). Elution volume of the reference protein is marked by dotted black line; the reference RNA in dotted green line and the complex in dotted orange line.
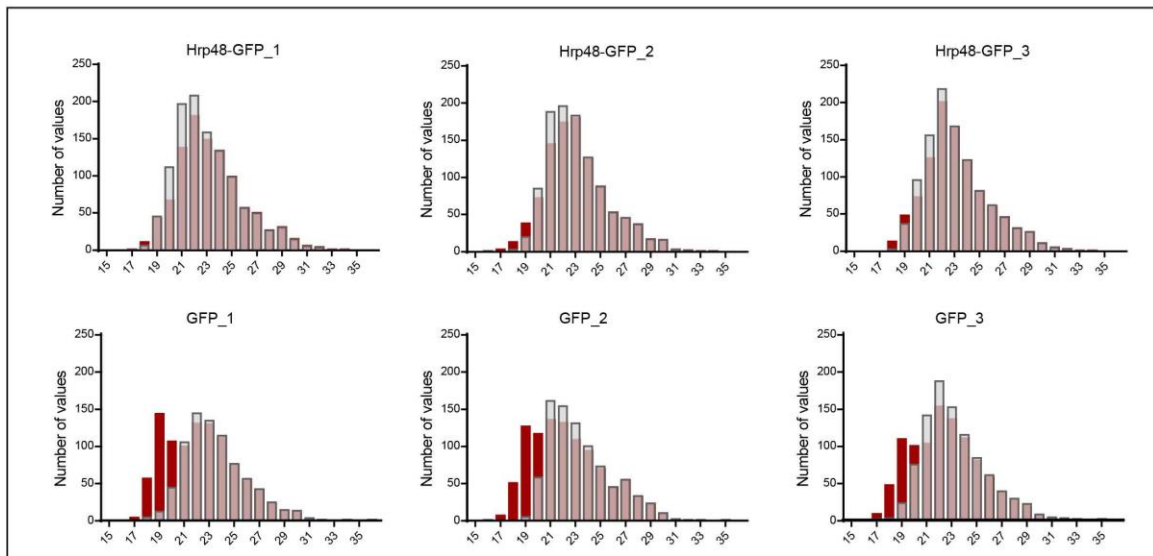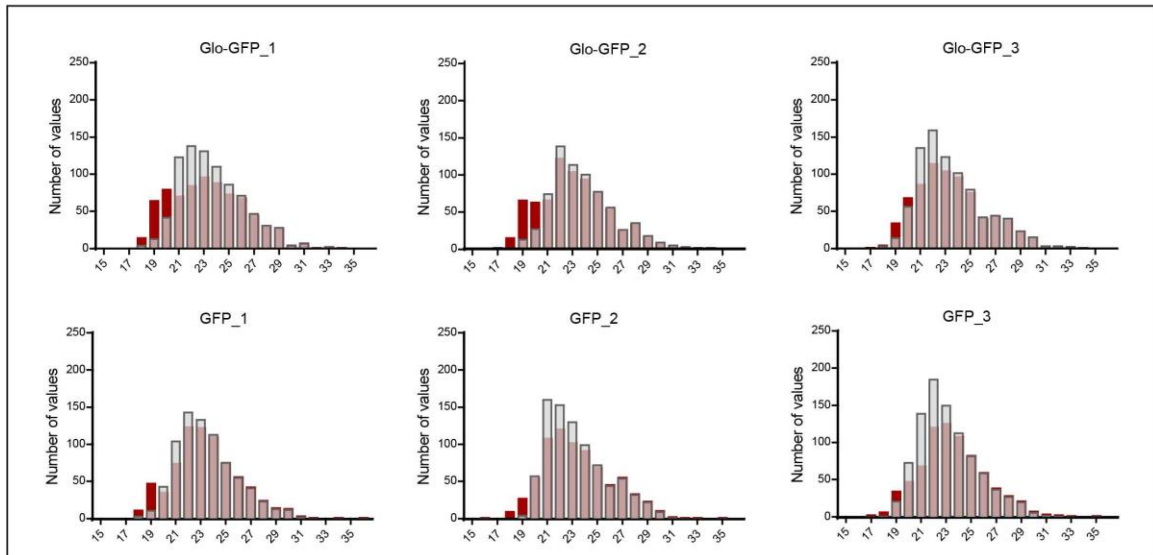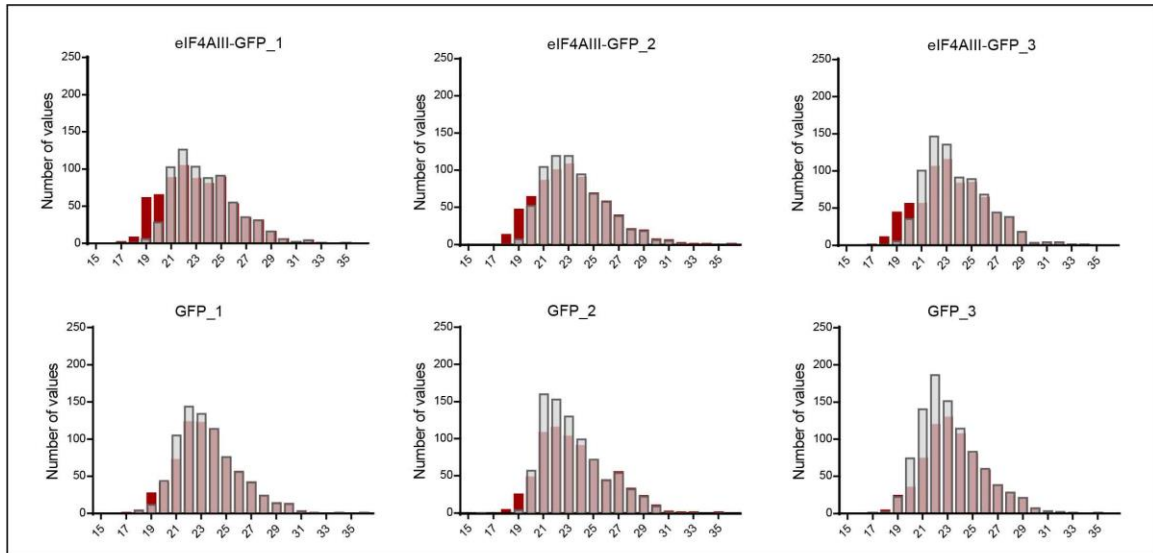
Log(2) Observed LFQ Intensity

Log(2) Calculated LFQ Intensity post-imputation
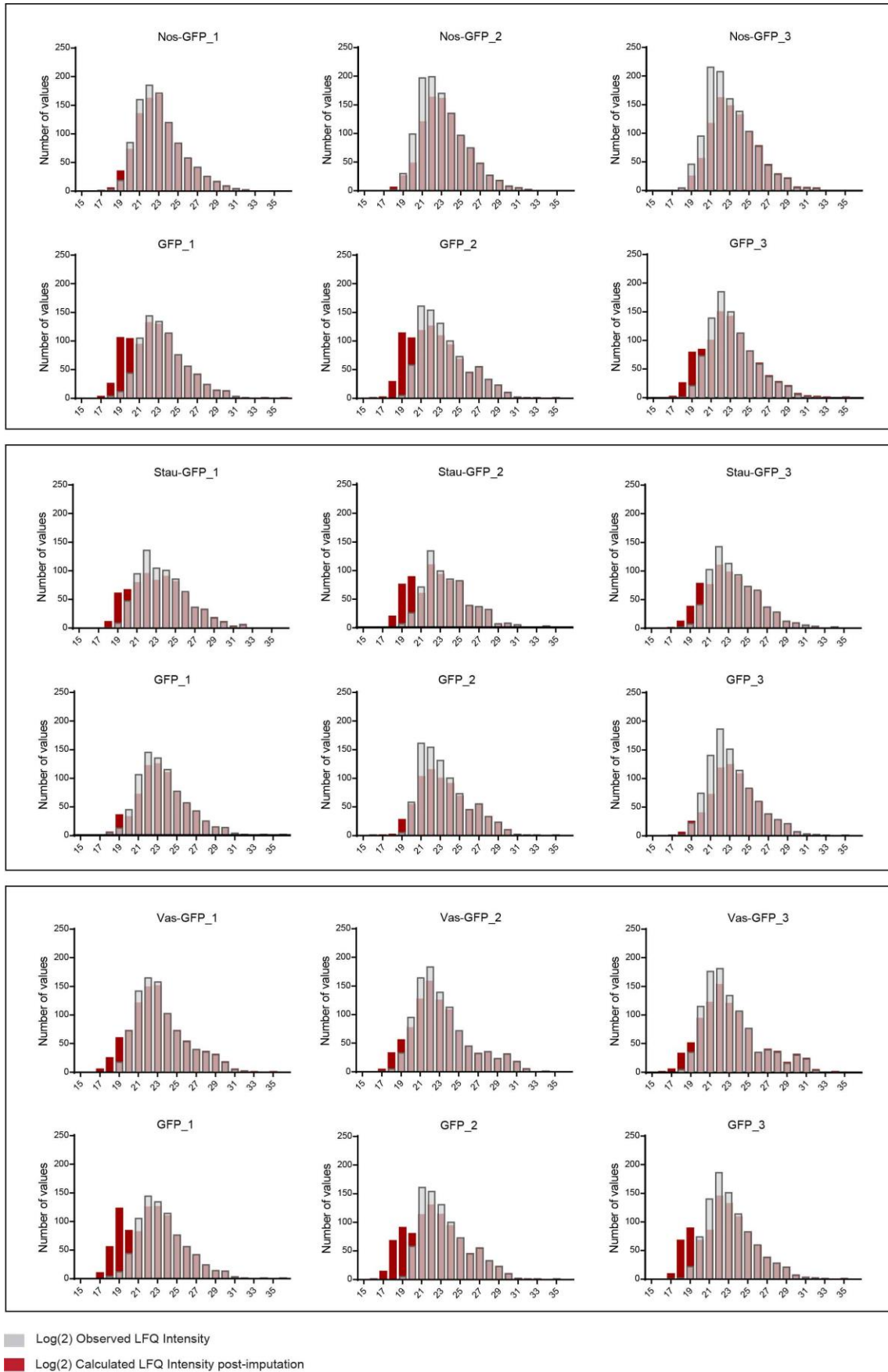
Supp Fig. 3 Overlay of frequency distribution of the logarithmized (Log2) LFQ intensities of all the proteins quantified in each IP, pre-imputation (highlighted in grey) and post-imputation (highlighted in

red). Imputation was done pairwise on each bait-control matrix. X axis represents the range of values; Y axis represents the number of values. To note that the imputed values occupy the low intensity range and generate a close to normal distribution that can be effectively used for further statistical calculations.
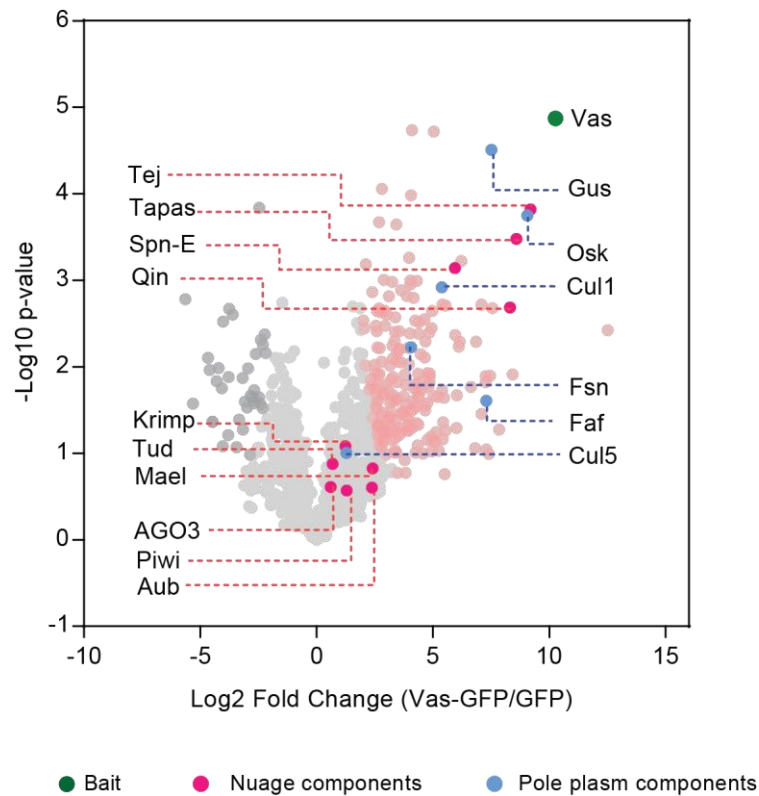
Supplementary Fig. 4. Scatter plot indicating components of functionally distinct pathways identified to be associated with Vas-GFP, in the label-free MS data. Each identified protein is represented as a dot in light grey; the bait is highlighted in green; significantly enriched proteins are highlighted in pink; proteins that associate in the nuage particles are highlighted in magenta; proteins involved in pole plasm assembly are highlighted in cyan; background binders are highlighted in dark grey. To note that many factors known to interact with Vas, such as Aub, are not highly enriched, suggesting transient or indirect association with Vas.
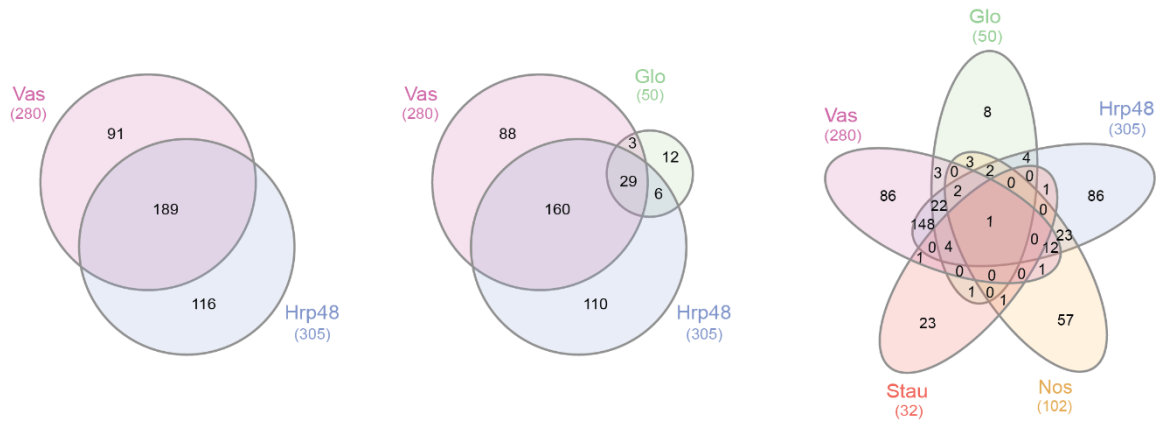
Supplementary Fig. 5. Venn representation of the proteins found common in different bait-associated complexes. Overlap between the proteomes found associated with Hrp48 and Vas are shown on the left; overlap between Hrp48, Glo and Vas are shown in the middle; overlap between Hrp48, Glo, Vas, Nos and Stau is shown on the right. The number of proteins analyzed in each case is shown in brackets.

8. Curriculum Vitae

PRASHALI BANSAL
01-02-1990 | Indian | prashali.90@gmail.com

EDUCATION	**GRADUATE STUDENT** MAX PLANCK INSTITUTE FOR DEVELOPMENTAL BIOLOGY, TÜBINGEN, GERMANY JANUARY 2014 – PRESENT
	INTEGRATED MASTER OF SCIENCE (HONS.) IN BIOLOGICAL SCIENCES BIRLA INSTITUTE OF TECHNOLOGY AND SCIENCE PILANI, PILANI, INDIA AUGUST 2008 – JUNE 2013
	BACHELOR OF PHARMACY (HONS.) BIRLA INSTITUTE OF TECHNOLOGY AND SCIENCE PILANI, PILANI, INDIA AUGUST 2008 – JUNE 2013
RESEARCH EXPERIENCE	**Biochemical and mass spectrometric analysis of interactions in *Drosophila* mRNA localization*.***
	Graduate student January 2014-Present Supervisor: Dr. Fulvia Bono, Max Planck Institute for Developmental Biology, Tübingen
	Protective role of RUNX3 against oncogene, YAP-induced metastasis.
	Research Assistant September- December 2013 Supervisor: Dr. Madhura Kulkarni (Ito Yoshiaki's lab), Cancer Science Institute, National University of Singapore, Singapore
	Identification of growth regulators in *Drosophila melanogaster.*
	Masters thesis July 2012- May 2013 Supervisor: Dr. Hugo Stocker, Institute of Molecular Systems Biology, ETH Zurich, Switzerland
	Cloning and characterization of *PP2C* like promoter from *Arabidopsis thaliana.*
	Undergraduate research project August 2011- May 2012 Supervisor: Dr. Rajesh Mehrotra, Department of Biological Sciences, Birla Institute of Technology and Science Pilani, India
PUBLICATIONS	Kullkarni M, Tan TZ, Syed Sulaiman NB, Lamar, JM, **Bansal P**, Cui J, Qiao Y, Ito Y. RUNX1 and RUNX3 protect against YAP-mediated EMT, stem-ness and other shorter survival outcomes in breast cancer. Oncotarget 9, 14175- 14192 (2018).
	Mehrotra R, Bhalothia P, **Bansal P**, Basantani MK, Bharti V, Mehrotra S. Abscisic acid and abiotic stress tolerance - different tiers of regulation. Journal of Plant Physiology 171, 486-496 (2014).

9.   Acknowledgements

discussions in and outside of the lab, not just limited to research. I would also like to mention Dr. Christian Feldhaus for his help with microscopy and Birgit Moldovan for the administrative help.

I am very thankful to all my friends here in Tübingen, Neel, Nidhi, Suryesh, Fabian, Ancilla and Agnes for all the joyous moments and memories. A special hug goes to Christiane, Florian, Aditi and Nishtha for being the support system during the toughest of times. A big shout out to the friends back home, Pallavi, Aashray, Swati, Vidushi, Nihar, Milan and Rahul for constantly encouraging me at every step. Ankit, I cannot thank you enough for always being there for me and believing in me, when I didn't. At last, but not the least, I could not have done this without the never-ending support of my family, Mom, Dad, Amma and Prachi.

I am extremely grateful to the Max Planck Society for giving me this opportunity. Working at the Max Planck Institute for Developmental Biology has been one of the most enriching and fulfilling experiences of my life.